Synthetic and Structure-Activity Studies of the 20S Proteasome Inhibitor Syringolin A

Dissertation

Von

M.Sc.-Chemiker

Jérôme Clerc

aus Rueil-Malmaison (Frankreich)

Synthetic and Structure-Activity Studies of the 20S Proteasome Inhibitor Syringolin A

Zur Erlangung des akademischen Grades eines
Doktors der Naturwissenschaften
(Dr. rer. nat.)
von der Fakultät für Chemie
der Universität Dortmund
angenomene

Dissertation

Von
M.Sc.-Chemiker
Jérôme Clerc
aus Rueil-Malmaison (Frankreich)

1. Gutachter: Prof. Dr. Herbert Waldmann
2. Gutachter: Prof. Dr. Mathias Christmann

Tag der mündlichen Prüfung: 16. April 2010

Die vorliegende Arbeit wurde in der Zeit von Oktober 2005 bis März 2010 am Chemical Genomics Centre der Max-Planck-Gesellschaft in Dortmund unter der Anleitung von Prof. Dr. Herbert Waldmann and Dr. Markus Kaiser durchgeführt.

À ma famille

et

Marlene

Table of contents

1. **Introduction** 1

2. **Background** 3

2.1. Natural products as starting structures for small molecule development 3
2.2. The ubiquitin-proteasome system and its modulation by proteasome inhibitors 4
2.3. The natural product syringolin A 7
2.4. Previous synthetic approaches to the synthesis of syrbactin-like macrocycles 11

3. **Aim of the project** 14

4. **Results and discussion** 16

4.1. Studies towards the total synthesis of syringolins 16
4.1.1. Synthesis of syringolin B (SylB) 16
4.1.2. Synthesis of syringolin A (SylA) 19
4.1.2.1. Macrolactamization pathway 19
4.1.2.1.1. Synthesis of the β,γ-dehydrolysine building block 20
4.1.2.1.2. Synthesis of the α,β-unsaturated building block 22
4.1.2.1.3. Macrolactamization studies 22
4.1.2.2. Metathesis pathway 23
4.1.2.2.1. First approach to employ RCM in syringolin macrocycle synthesis 24
4.1.2.2.2. RCM: second approach 26
4.1.2.2.3. Establishment of a more convergent route to SylA and analogues 29
4.1.2.2.4. Convergent synthesis of SylA and SylA isomers 34
4.1.2.3. Synthesis of a saturated SylA derivative 38
4.2. Chemical biology studies with syringolins 40
4.2.1. Synthesis and use of a rhodamine-tagged syringolin A derivative Rh-SylA 40
4.2.1.1. Synthesis of Rh-SylA 40
4.2.1.2. ABPP studies with Rh-SylA with mammalian cell lysates 41
4.2.1.3. The use of Rh-SylA for plant pathogen interaction studies 45
4.2.2. Structure-activity relationships of syringolins 45
4.2.2.1. Structural determinants of potency and subsite selectivity deduced from structural and biochemical studies 45
4.2.2.2. Synthesis of a lipophilic analogue 48
4.2.2.3. Synthesis of pegylated analogues 50
4.2.2.4. Synthesis of a SylA-GlbA hybrid 54
4.3. A bicyclic hydantoin as an activity-based probe: discovery of a new GAPC inhibitor . 56

5. **Summary and conclusions** 61

5.1. Summary and conclusions (English) 61
5.2. Zusammenfassung und Ausblick (German) 68
5.3. Résumé et conclusions (French) 75

6. Experimental Part 82

6.1. Materials, instruments and general methods for purification and analyses 82
6.2. Synthesis of syringolin B (SylB, **2**) 85
6.3. Synthesis of syringolin A (SylA, **1**) 95

7. References and Notes 167

8. Abbreviations 171

9. Curriculum Vitae 172

10. List of publications and patents 174

10.1. Publications 174
10.2. Patents 174

11. Acknowledgements 175

1. Introduction

In chemical biology, bioactive small molecules are applied to biological systems such as living cells for studying and manipulating biological processes.[1] Such a small molecule-based approach for studying biology has several advantages over more classical research strategies such as genetic knock-out studies: The biological effect induced by small molecule modulation is usually rapid and can be spatially and temporally controlled. It is often reversible and conditional as small molecule application can be initiated at any developmental stage of the studied biological system. Moreover, the observed biological effect is tunable by varying the concentration of the small molecule probe. Finally, small molecule probes can be tagged with additional functionalities that allow to accumulate further information in biological experiments. For example, the proper attachment of fluorophores on a bioactive small molecule targeting a protein of interest generates a probe that can directly be employed in imaging applications. Besides these straightforward experimental advantages, small molecule interference has at least one additional conceptual advantage over genetic manipulations. While gene mutations act on the gene-level, small molecules modulate the function of the gene products. Consequently, small molecules interfere at a much more sophisticated and biologically relevant level; accordingly, they are in contrast to genetic studies able to differentiate between different protein forms that result from the same gene, e.g. by alternative splicings or post-translational modifications.

Despite these huge advantages of small molecule manipulation of biological systems, the widespread use of chemical biology methods in biological research is limited by an inherent major disadvantage: In order to be feasible, such an approach requires the availability of suitable small molecules that induce a desired biological effect with high selectivity and potency. To date, only a limited number of proper small molecules for a restricted number of protein targets are though known.

To overcome this limitation, several concepts for identifying proper small molecules have evolved in the last years. Among them, high-throughput screening of compound collections to elucidate proper small molecule modulators is nowadays most regularly used. As a consequence, approaches for synthesizing ‘intelligent’ compound collections such as Biology-oriented synthesis (BIOS) or Diversity-oriented synthesis (DOS) have been devised to reduce compound synthesis and screening efforts.[2] In addition, more rational, structure-based approaches such as ‘virtual screening’ or fragment-based drug discovery are often employed.[3]

An alternative and in the past widely used method for identifying proper small molecules is the use of biologically active natural products as starting points for chemical probe synthesis.[4] In this work, such an approach has been followed with the aim to develop a small molecule for probing the plant immune system. To this end, a peptidic natural product named syringolin A was chosen as a target structure for small molecule development. Syringolin A was reported to induce a plant-protective effect *vs.* various plant pathogens upon application on plants. In contrast to most agrochemicals, this interesting effect however was not caused by an antimicrobial activity against the plant pathogens but by an apparent modulation of the plant immune system. The molecular target of syringolin A and a synthetic route to this natural product class though was unknown at the beginning of this work.

During the course of this PhD thesis, in which several chemical biology studies with syringolin A and derivatives thereof were performed, several unexpected findings either from the own research work or reported in literature, opened up possibilities for promising ‘side projects’ that were originally not even anticipated. Accordingly, the search for a suitable small molecule probe of the plant immune system ended up with an access to a promising new class of potent anti-cancer agents. Even more particular, the discovery of a new scaffold structure for covalently labelling glyceraldehyde-3-phosphate dehydrogenase has been accomplished. This work therefore gives a striking example on the unexpected but nevertheless promising results that can be achieved by basic science research.

2. Background

2.1. Natural products as starting structures for small molecule development

Since the first description of chemotherapeutic treatments, Nature has always played a prominent role for the identification of therapeutic agents.[5] In fact, in the beginning of commercial drug discovery, the vast majority of chemotherapeutics were derived from natural products. However, with the advance of high-throughput screenings (HTS) in the 1990's, natural products stepped out of the focus of the pharmaceutical industry, resulting in a significant decrease of natural product-based drugs released on the market.[6] The emergence and technological improvement of high-throughput screening (HTS) nowadays enables to test extremely large compound libraries and to evaluate their potency against various biological targets in a very small time frame. The build-up of these huge screening capacities however demanded the allocation of compound libraries of appropriate size. To overcome this bottleneck, combinatorial chemistry soared up to provide a facile and rapid access to drug-like screening libraries of simple compounds with a high diversity and in a low cost fashion.[7,8] Nevertheless, despite the big investment of the pharmaceutical industry and the generation of millions of compounds, it turned out that the biological relevance of combinatorial libraries was rather low, delivering only unexpected low numbers of lead structures suitable for further drug development.

These disappointing results led to a renaissance of natural products in drug discovery. This new awakened interest in natural products stem from their inherent biological relevance. As natural products are synthesized by living organisms to protect and defend themselves and are therefore the result of a long process of the natural selection, their chemical structures are biologically prevalidated for protein interactions. Moreover, their use is not restricted to their original biological function in the producing organism but can exert a biological effect also in other organisms. For example, large varieties of new scaffolds have been isolated from deep-sea organisms such as sponges or marine bacteria and are currently used to treat human pathologies and disorders.[9,10] Consequently, natural products are nowadays again in the focus of drug discovery efforts, either as 'direct' lead structures or as scaffolds for compound library synthesis as in Biology-oriented synthesis (BIOS).

While chemical biology approaches in mammalian cell studies are today well established, the use of small molecules in plant biology research is still in its infancy.[11] Only a limited number of compounds are used to date, although more-and-more small molecule studies have appeared in the last years. Of these probes, most are natural product-derived, exemplified by Brefeldin A that is used in plant vesicular transport studies or Concanamycin A or Bafilomycin A for elucidating the role of V-ATPases on plant cell tugor pressure.

2.2. The ubiquitin-proteasome system and its modulation by proteasome inhibitors

As described below, the syringolin natural products that are in the focus of this PhD work modulate the ubiquitin-proteasome system by inhibiting the eukaryotic 20S proteasome. For this reason, a short overview on the constitution and biological role of the ubiquitin-proteasome system is given.

Since its discovery in the late 1970’s, the ubiquitin-proteasome system (UPS) has been widely studied due to its direct involvement in almost all biological processes of living cells. It consists of several protein components that act in concert to achieve a regulated proteolysis of proteins. The significance of this degradation system is highlighted by the award of the Nobel Prize in Chemistry “for the discovery of ubiquitin-mediated protein degradation” to the UPS research pioneers Aaron Ciechanover, Avram Hershko and Irwin Rose in 2004.

One of the key player and name giving factors of the UPS is the protein ubiquitin. It is a small protein of about 8.5 kDa, highly-conserved in all eukaryotic species with a sequence similarity between the human and yeast variant of 96%. As indicated by its name, ubiquitin is ubiquitously expressed in all eukaryotes. In combination with the 26S proteasome and the ubiquitin-loading enzymes E1-E3, ubiquitin forms the ubiquitin-proteasome system which main function is the proteolysis of proteins which are destined for degradation and the cleavage of unfolded or misfolded proteins (Figure 1).[12,13,14] To this end, a cascade of enzymes known as E1, E2s and E3s tag such proteins with at least four ubiquitin units, thereby directing them to the proteasome which then acts as the proteolytic core system.

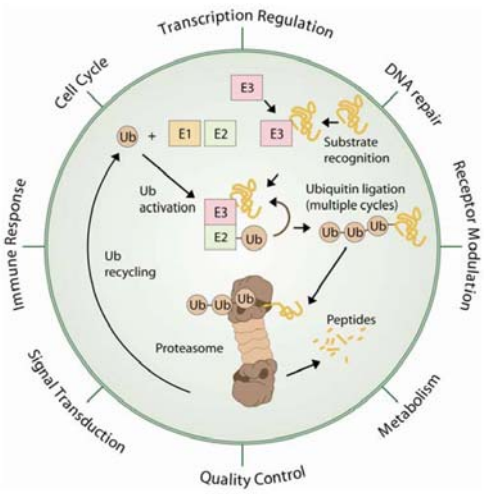
Transcription Regulation
DNA repair
Receptor Modulation
Metabolism
Quality Control
Signal Transduction
Immune Response
Cell Cycle
E3
Ub
+
E1
E2
E3
Substrate recognition
Ub activation
Ubiquitin ligation (multiple cycles)
E3
E2
Ub
Ub
Ub
Ub
Ub recycling
Ub
Ub
Ub
Peptides
Proteasome

Figure 1. Ubiquitin-mediated proteolysis and its relevance in different biological functions[15]

The 26S proteasome is a 2000 kDa complex of various proteins that can be classified into the 20S core particle structure and two 19S regulatory caps (Figure 2). The proteolysis occurs in the interior of the barrel-shaped 20S structure. The two 19S regulatory subunits overtake the recognition of the ubiquitin-tagged proteins, cleavage of the polyubiquitin chains, unfolding and translocation into the 20S proteasome. The 20S proteasome consists of four stacked ring systems that are arranged in a $\alpha_7\beta_7\beta_7\alpha_7$ manner. The α-subunits, in combination with the 19S subunits, regulate the access to the proteolytic sites which are located at the inner side of three of the seven β-subunits. The catalytic residue is a *N*-terminal threonine moiety which is situated at the β1-, β2-, β5-subunit.

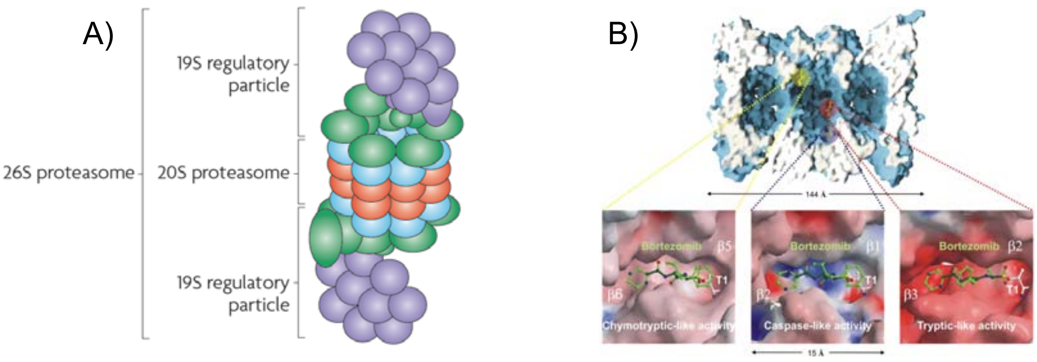
A)
26S proteasome
19S regulatory particle
20S proteasome
19S regulatory particle
B)
144 Å
Bortezomib
β5
T1
β6
Chymotryptic-like activity
Bortezomib
β1
T1
β2
Caspase-like activity
Bortezomib
β2
T1
β3
Tryptic-like activity
15 Å

Figure 2. A) Schematic diagram of the 26S proteasome.[16] B) Surface representation of the yeast 20S proteasome crystallized in the presence of bortezomib. The various proteolytic surfaces are marked by a specific color coding: blue = subunit β1; red = subunit β2; and yellow = subunit β5. The nucleophilic threonine (T1) and bortezomib are presented as a ball-and-stick model.[17]

The three different proteolytic sites of the 20S proteasome feature distinct substrate specificities. The β5-subunit shows a chymotrypsin-like activity which cleaves peptide bonds after hydrophobic residues (e.g. tyrosine, tryptophan, and phenylalanine); the β2-subunit exerts a trypsin-like site which cuts after basic residues (lysine and arginine) whereas the β1-subunit possesses a caspase-like activity resulting in preferential cleavage after acidic residues (aspartic acid, glutamic acid). Protein degradation by the proteasome normally results in peptide fragments with an average length of 7 to 9 amino acid residues which are either used for antigen presentation at MHC class I complexes or are further degraded by additional proteases to refill the amino acid pool for new protein synthesis.

Although the UPS has major implications in various cellular processes such as regulation of cell cycle, DNA repair, immune and inflammatory responses and cancer,[18,19,20,21,22,23,24] inhibition of the UPS has surprisingly emerged as a valuable approach for the development of novel anticancer therapies. In fact, the peptide boronic acid PS-341 (bortezomib) has recently been approved by the U.S. Food and Drug Administration for the treatment of relapsed and/or refractory multiple myeloma and is commercially available under its trade name Velcade ®.

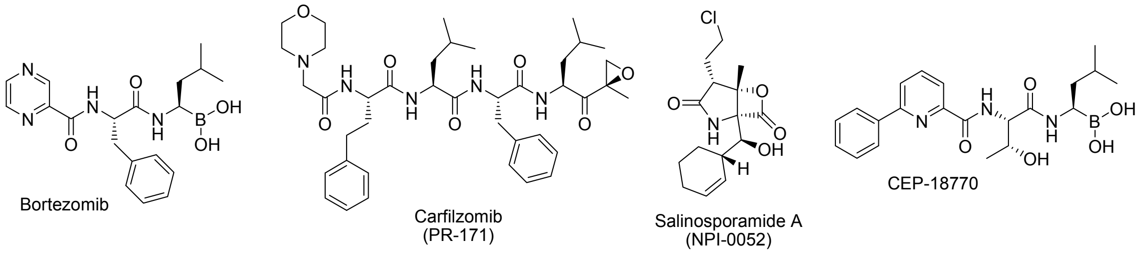

Bortezomib

Carfilzomib
(PR-171)

Salinosporamide A
(NPI-0052)

CEP-18770

Figure 3. Chemical structure of the marketed proteasome inhibitor Bortezomib and of the proteasome inhibitors currently evaluated in clinical trials.

Although the efficiency of Bortezomib in monotherapy has been considered as astonishing and exciting, side effects and resistances are frequently observed and combinations of bortezomib with other therapeutics are now under evaluation.[25] Consequently, three more proteasome inhibitors are currently evaluated in clinical trials, i.e. carfilzomib, NPI-0052 (also known as salinosporamide A) and CEP-18770 (Figure 3).[26,27,28]

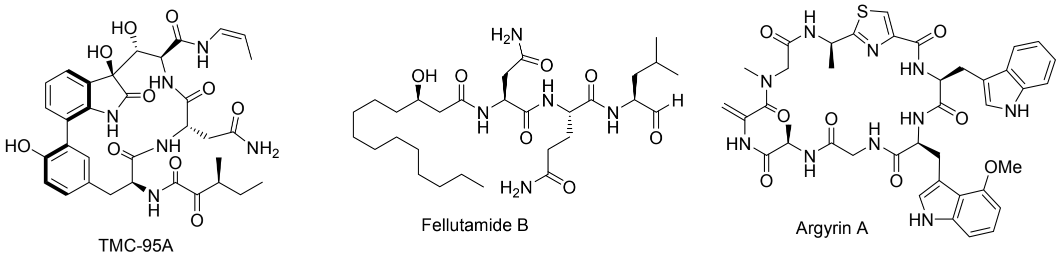

Figure 4. Recently discovered proteasome inhibitors from natural sources.

Despite these advanced clinical studies, alternative proteasome inhibitors are still urgently sought. Natural products have been an invaluable source for proteasome inhibitors, exemplified by the three natural products TMC-95A, fellutamide B or argyrin A (Figure 4) that have recently been disclosed.[29,30,31]

2.3. The natural product syringolin A

The peptidic small molecule syringolin A (SylA, **1**) (Figure 5) was isolated in 1998 from bacterial strains of *Pseudomonas syringae* pv. *syringae* (*Pss*). This plant pathogen causes the brown spot disease on various plant species. In 1999, syringolins B-F were subsequently reported as minor metabolites of *Pss*. SylA is biosynthesized by a mixed non-ribosomal peptide synthetase (NRPS) / polyketide synthetase (PKS) gene cluster exclusively under infection conditions. The syringolins (in particular syringolin B and E) have related chemical structures to another class of natural products known as glidobactins and cepafungins (Figure 5). The main structural differences between syringolins and glidobactins are an additional (*E*)-configured double bond in the syringolin A macrocycle and the presence of an exocyclic urea moiety in the syringolins while glidobactins feature a dipeptide residue.

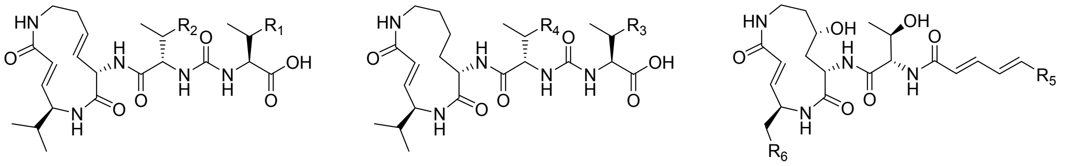

SylA, **1**: R_1= Me, R_2= Me
SylC: R_1= Me, R_2= Et
SylD: R_1= Et, R_2= Me
SylF: R_1= Et, R_2= Et

SylB, **2**: R_3= Me, R_4= Me
SylE: R_3= Et, R_4= Me

GlbA, **3** or Cepafungin II: R_5= $-(CH_2)_6CH_3$, R_6= H
GlbB: R_5= $-(CH_2)_2CH{=}CH(CH_2)_4CH_3$, R_6= H
GlbC: R_5= $-(CH_2)_8CH_3$, R_6= H
GlbD: R_5= $-(CH_2)_4CH(OH)CH_2CH_3$, R_6= H
GlbE: R_5= $-CH_2CH(OH)(CH_2)_4CH_3$, R_6= H
GlbF: R_5= $-(CH_2)_4CH_3$, R_6= H
GlbG: R_5= $-(CH_2)_6CH_3$, R_6= OH
Cepafungin I: R_5= $-(CH_2)_5CH(CH_3)_2$, R_6 = H
Cepafungin III: R_5= $-(CH_2)_3CH(CH_3)_2$, R_6 = H

Figure 5. Chemical structures of the major metabolite syringolin A of the syringolin family and the additional minor metabolites produced by *Pss*. The chiral centers of the amino acid residues were not assigned in the original structure elucidation and were elucidated only by our syntheses. For clarity, they have been added to this figure. In addition, the chemical structures of the structurally-related glidobactins and cepafungins are represented.

In the original structure elucidation of the syringolins, the chiral centers at the amino acids could not be elucidated. Although the analysis of the biosynthesis gene cluster suggested an overall (L)-configuration, definite prove of the stereochemistry was only achieved by chemical synthesis performed during this PhD project (see section 4.1.2.2.4 for details).

The interest to develop syringolin A into a small molecule probe for studying the plant immune system stemmed from a report in literature, in which the initiation of a plant immune response was described after application of syringolin A to non-host plants. Interestingly, while syringolin A application to healthy plants resulted in no evident phenotype, application of syringolin A to rice plants (*Oryza sativa*) infected with the blast fungus *Pyricularia oryzae* led to a plant protective and infection-counteractive plant immune reaction known as hypersensitive response. The same protective and curative properties of SylA were observed with wheat and powdery mildew as the plant infection.[32,33,34] In plant biology, compounds with such an immune-response promoting activity are generally referred to as elicitors. Most elicitors however are of high molecular weight, being whole proteins or large carbohydrate structures. Only a limited number of small molecule elicitors are known to date, thereby highlighting again the interesting biological activity of SylA.

In 2006, an interesting paper from the Bachmann group at the Hawaiian Cancer Center appeared; describing an anti-proliferative and apoptosis-inducing property of SylA in certain cancer cell lines were described.[35] However, no mode-of-action of SylA was mentioned.

During the course of this PhD thesis, Groll *et al.* then finally reported SylA's molecular target and biological function: SylA induces an irreversible inhibition of the eukaryotic 20S proteasome by a novel mechanism, thereby providing a previously unrecognized link of the plant immune response with the ubiquitin proteasome pathway. This inhibition facilitates infection of plants by a yet unknown mechanism, suggesting that SylA acts as a bacterial virulence factor.[36]

In addition, the authors disclosed that the structurally related natural product glidobactin A (GlbA, **3**) also potently inhibited the 20S proteasome.[37,38,39,40] Glidobactins have been isolated from *Polyangium brachysporum* and reported as antifungal compounds and antitumor antibiotics. *In vitro* testing of glidobactins (principally A, B and C) revealed a broad activity against clinically important pathogenic fungi such as *Candida albicans*, *Cryptococcus neoformans* or *Aspergillus fumigatus*, although their *in vivo* antifungal potency was considered as only marginal. More interestingly, a strong cytotoxicity was detected against various tumor cell lines. Subsequent studies with mice implanted with P388 leukemia revealed a dramatic prolongation of lifetime under glidobactin treatment.[41]

Biochemical inhibition assays were then used to evaluate the inhibition potency and subsite selectivity of SylA and GlbA (Table 1).

Table 1. Apparent K_i' values and rates of covalent inhibition ($k_{association}$) over inhibitor concentrations.

Inhibitor	Inhibited activity	K_i'	k_{assoc}, M^{-1} s^{-1}
SylA	Chymotrypsin-like	843 ± 8.4 nM (n = 3)	863 ± 106 (n = 6; 100 – 200 nM)
	Trypsin-like	6.7 ± 0.7 μM (n = 6)	94 ± 12 (n = 6; 150 – 600 nM)
	Caspase-like	n.d.[a]	6 ± 0.3 (n = 6; 20 – 40 μM)
GlbA	Chymotrypsin-like	49 ± 5.4 nM (n = 3)	3,377 ± 341 (n = 6; 40 – 60 nM)
	Trypsin-like	2.0 ± 0.6 μM (n = 6)	141 ± 21 (n = 6; 250 – 500 nM)
	Caspase-like	n.a.[b]	n.a.[b]

[a] n.d.: not determined. [b] n.a.: not active.

It turned out that both inhibitors acted in a non-competitive manner, suggesting an irreversible inhibition. SylA inhibited all three proteolytic activities, but with different potencies. While the chymotrypsin-like activity with a K_i' of 843 ± 8.4 nM was most potently inhibited, the trypsin-like activity was inhibited with a K_i' of 6.7 ± 0.7 μM, while no K_i' value for caspase-like inhibition could be quantified despite its apparent inhibition. In contrast, GlbA was much more potent in inhibiting the chymotrypsin-like activity with a K_i' of 49 ± 5.4 nM and the trypsin-like activity with a K_i' of 2.0 ± 0.6 μM while however the caspase-like activity was not inhibited at all in the concentration range tested.

Subsequent structural studies of the binding mode of SylA and GlbA to the yeast 20S proteasome confirmed the suggested irreversible binding mode (Figure 6). These studies revealed that the observed irreversible inhibition is indeed a result of a Michael-type addition of the threonine active site residue to the α,β-unsatured amide moiety of SylA and GlbA. Interestingly, these studies also validated the noticed subsite selectivity. While SylA binding was found in all three proteolytically active subsites, GlbA was only accommodated in the β2 and β5 subunits. Due to their similar binding mode, SylA and GlbA were grouped into a collective class of natural product, named syrbactins.

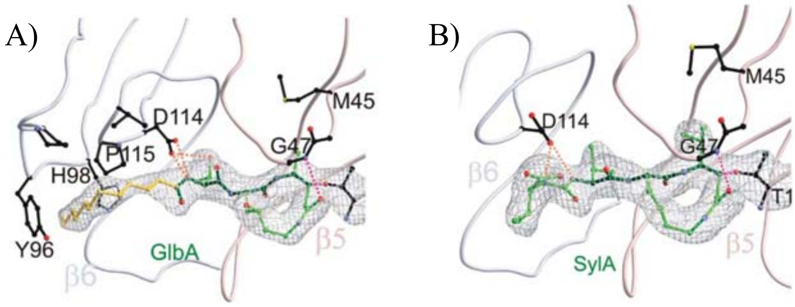

Figure 6. Stereo representation of the chymotryptic-like active site in complex with: A) GlbA and B) SylA. Magenta, covalent linkage of inhibitors with active site Thr1; dotted lines indicate hydrogen bonds. Black, residues performing specific interactions with SylA and GlbA.

Accordingly, the findings of Groll *et al.* also gave a mechanistic explanation to the previously observed anti-proliferative properties of SylA in cancer cells. As described in section 2.2, proteasome inhibitors are potential anticancer agents. Consequently, SylA and analogues thereof might represent promising new chemotherapeutics for the treatment of certain cancer types.

2.4. Previous synthetic approaches to the synthesis of syrbactin-like macrocycles

It has long been recognized that macrocyclic natural products often demonstrate high biological activities in conjunction with favorable pharmacological properties, turning them into interesting compounds for drug discovery efforts.[42] Their observed potent biological potencies seem to be to the consequences of different aspects. First, the entropic loss while forming the protein-ligand complex is dramatically reduced by using macrocyclic inhibitors, resulting in higher target affinity. Second, it has been shown that macrocyclic inhibitors are more selective than linear ligands due to a fixation of target-specific conformations. Third, the physicochemical properties of macrocycles such as cyclic peptide-like drugs have empirically been shown to be more appropriate for membrane passage than of related linear peptide-like candidates. Fourth, in the case of peptides, the proteolytic and metabolic stability of cyclopeptides is usually dramatically enhanced in comparison to linear ones.[43,44]

Despite the unambiguous potential of this class of natural products, their development into drugs was underexploited by the pharmaceutical industry for several reasons. One reason is that the molecular mass of these biologically active macrocycles often exceeds 500 Da; thereby violating the commonly adopted Lipinski's rule of 5 for evaluation of the druglikeness of small molecules. Additionally, macrocyclic compounds frequently display complex molecular architectures, thereby limiting their synthetic accessibility and discouraging a possible industrial development. With the advance of new synthetic methodologies for macrocyclization such as ring-closing metathesis,[45] multi-component reactions,[46] metal-templated chelation[47] or ring-closing-contraction sequences,[48] this chemistry-derived disadvantage however starts to vanish.

Accordingly, syringolins seem as attractive target molecules for drug discovery. They feature a highly rigid 12-membered macrocycle with two (*E*)-configured double bonds and two amide functionalities. Due to their limited flexibility, high affinity binding to the active subunit of the proteasome can be assumed which contributes to the observed potent inhibition. Additionally, syringolins possess a moderate number of stereocenters that are derived from amino acids and have a molecular mass close to 500 Da, suggesting favorable pharmacokinetic properties.

To date, only two chemical syntheses of syrbactins have been reported. While syringolins have not yet been prepared, two total syntheses of glidobactin A have been reported by Oka *et al.* in 1988 and the Schmidt group in 1992. In addition, different unfortunately unsuccessful approaches towards the synthesis of the glidobactin core structure were reported by the group of Hesse in 1991.[49,50,51] In all these syntheses, the macrocyclization proved as the most difficult step.

The first total synthesis performed by Oka *et al.* was based on successive peptide couplings (Scheme 1). In their approach, *erythro*-γ-hydroxy-(L)-lysine **5** was directly employed without any protective groups leading to poor yields of only 0.2% of Glidobactin for the overall synthesis after several purification rounds.

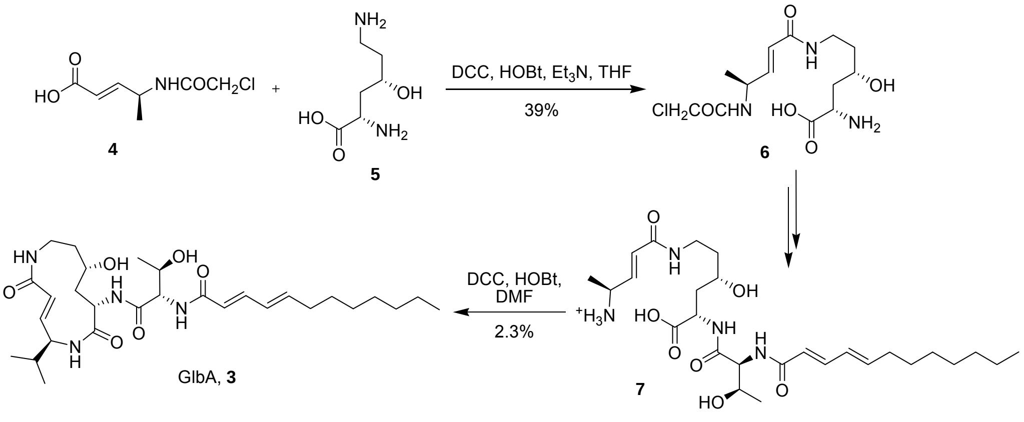
NHCOCH2Cl
HO
4
NH2
OH
NH2
5
DCC, HOBt, Et3N, THF
39%
ClH2COCHN
6
DCC, HOBt, DMF
2.3%
+H3N
7
GlbA, 3

Scheme 1. First total synthesis of Glidobactin A by Oka *et al.* in 1988.

In the total synthesis of the Schmidt group, *erythro*-γ-hydroxy-(L)-lysine was generated in an orthogonally protected form by starting from the chiral butanetriol **8** (Scheme 2). In order to obtain this intermediate, 13 synthetic steps were necessary. In contrast to the Oka strategy, the macrolactamization was however performed between the C-terminal end of the alanine derivative and the ε-amino group of the hydroxylysine analogue. This key step proceeded in a much better yield of 20%. The overall yield of the total synthesis of GlbA however was only 0.8% due to the required 19 steps.

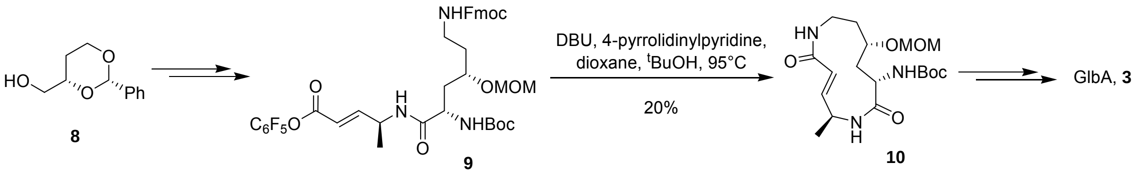
8
NHFmoc
OMOM
NHBoc
C6F5O
9
DBU, 4-pyrrolidinylpyridine, dioxane, tBuOH, 95°C
20%
10
GlbA, 3

Scheme 2. Second total synthesis of Glidobactin A by Schmidt *et al.* in 1992.

Synthetic studies to the synthesis of the glidobactin macrocycle were also reported by the group of Hesse (Scheme 3). In their work, a strategic reductive N-N bond cleavage of a bicyclic intermediate **13** was examined to install the desired 12-membered ring system. While model studies with simplified analogues led to promising results, the synthesis of GlbA macrocycle itself could not be accomplished.

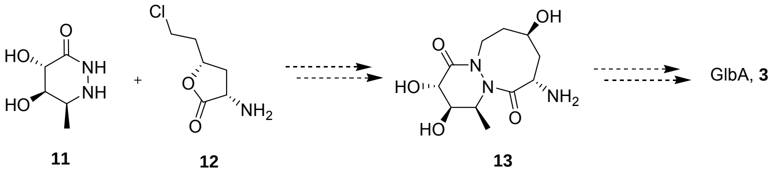

Scheme 3. Attempted synthesis of Glidobactin A macrocycle by Hesse in 1991.

In summary, an overall analysis of the so far achieved syntheses of Glidobactin A indicate that although these ring systems are synthetically accessible, they are obviously synthetically challenging as overall yields were always below 1%. In fact, the macrocyclizations proved as a very difficult step and could be obtained in the best case with only 20% yield, leaving plenty of space for an improvement of the synthesis by the employment of alternative synthetic methodologies.

3. Aim of the project

Due to the interesting biological properties of syringolin A in activating a plant immune response, the original aim of this PhD thesis was to develop syringolin A into a small molecule probe suitable for plant biology research. To achieve this, several different milestones were planned. First, a total synthesis of syringolin A was envisaged to obtain sufficient compound amounts to verify the literature-described biological effect. In addition, the synthetic route should also enable the generation of syringolin A derivatives that would then be employed for target identification, for example by pull-down experiments, capitalizing on the potentially reactive α,β-unsaturated Michael system. After this, an optimization of the biological properties of syringolin A to enhance its use as a chemical probe was envisaged.

However, as in parallel to the synthetic studies towards the synthesis of syringolin A, the elucidation of its target by Groll *et al.* appeared, the focus of the present work was partly shifted from target identification and development of a suitable probe for plant biology to the exploitation of the underlying structure-activity relationships of syringolins, thereby providing a rational basis for designing biologically more active and thus potentially better probes. To this end, the determinants of inhibition potency and subsite selectivity of syrbactins should become investigated. In addition, the selectivity of proteasome targeting by syringolins is an interesting question that was going to be explored in this PhD work.

To set this into practice, the first task was to achieve the first total synthesis of syringolin A (SylA). As however it was assumed that the syringolin A macrocycle due to its high ring strain was difficult to obtain, first a synthesis of syringolin B (SylB) was investigated. The employed synthetic route should then serve as a model system for the synthesis of syringolin A.

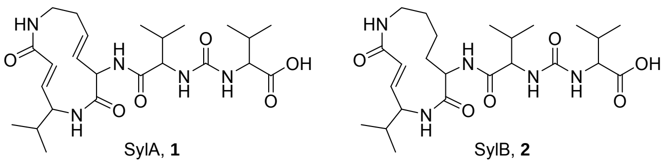

SylA, **1**

SylB, **2**

Figure 7. Chemical structures of the target molecules syringolin A and B. The configuration of the stereocenters was not known at the beginning of this PhD work.

Second, these chemical syntheses should be established in such a manner, that an unambiguous assignment of the chiral centers of syringolin A and B would become possible. To this end, several stereoisomers of SylA were identified as synthesis targets.

Third, an optimization of the inhibitory and pharmacokinetic properties of syringolins by derivatization was planned. Evaluation of these derivatives was envisaged by biochemical inhibition assays. Finally, the obtained inhibition data should allow the elucidation of the underlying structure-activity relationships of syringolins for proteasome inhibition and subsite selectivity.

Finally, the synthesis of a fluorescent probe of SylA was planned to obtain a potential probe for activity-based protein profiling (ABPP) of the proteasome, e.g. in plant-pathogen interactions. Moreover, this probe should have been employed to evaluate the selectivity of proteasome targeting by syringolins, thereby giving more insights into the potential of syringolins as anticancer agents.

Together, these studies should allow an in-depth investigation of the chemical biology and potential of syringolins as probes for plant biology research. Due to the potent anticancer effect of proteasome inhibitors, the findings of this PhD thesis however are not only relevant for organic chemistry and potentially plant biology, but might also have an impact on drug discovery.

4. Results and discussion

4.1. *Studies towards the total synthesis of syringolins*

Syringolin A (SylA) and syringolin B (SylB) are two metabolites extracted from *Pseudomonas syringae* pv. *syringae* (*Pss*) which feature many structural similarities. SylB differs from SylA only by the substitution of SylA's β,γ-dehydrolysine residue by a lysine moiety. For both natural products, the chirality of the stereocenters has not yet been assigned. However, an analysis of the gene cluster of SylA which does not contain any racemase domains suggest an all (L)-configuration of the chiral centers. To confirm this assumption, the total synthesis of syringolin A was required. As the synthesis of SylA however appeared challenging due to the ring strain of the core macrocycle, the study of its total synthesis started with the synthesis of a less strained model compound. Correspondingly, a prior total synthesis of SylB was considered as a good opportunity to establish a feasible methodology for macrocyclization that might prove useful also for the synthesis of syringolin A.

4.1.1. Synthesis of syringolin B (SylB)

As macrolactamization obviously represents the most challenging step in the synthesis of SylB, it was envisaged to perform it at a late stage of the synthesis (Scheme 4).

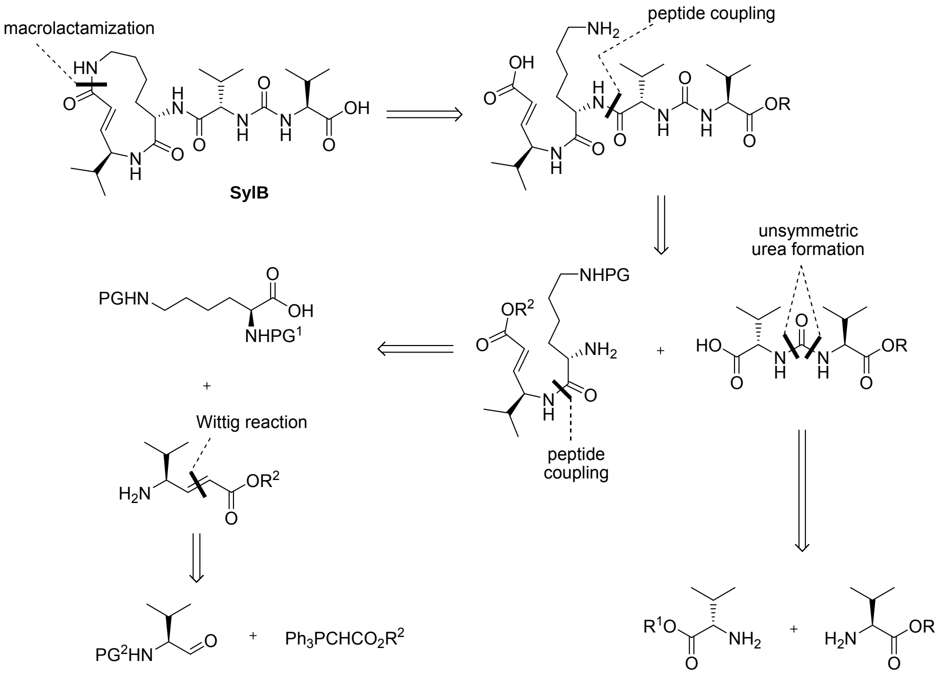

Scheme 4. Retrosynthetic pathway to SylB using a macrolactamization as a key step.

This disconnection then leads to a cyclization precursor that is easily accessible by straight-forward peptide synthesis, requiring only a careful protecting group strategy to allow regioselective cyclization. Further disconnections then results in building blocks which can be obtained by classical amino acid modifications. Noteworthy, this strategy does not involve the creation of chiral stereocenters; instead, the stereocenters are derived from the natural amino acids. Such an approach seemed as very practical for achieving the required determination of the configuration of the stereocenters of the natural SylB isomer, as all required amino acid starting materials were commercially available. In our first synthetic approach and in accordance with the reported biosynthesis,[52] all stereocenters were assumed as (L)-configured.

To put this retrosynthetic analysis into practice, the synthesis of SylB started with the preparation of the urea building block **18** (Scheme 5).

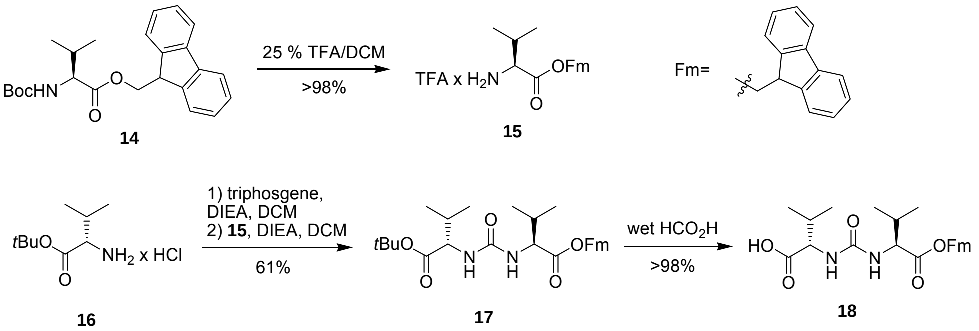

Scheme 5. Synthesis of the *N,N'*-unsymmetric urea **18**.

To this end, a fluorenylmethylester **15** of valine was prepared by Boc-deprotection of the valine derivative **14** that was synthesized according to the protocol of Bayer.[53] The *N,N'*-unsymmetrical urea side chain was then obtained following the procedure developed by Randad[54]. Thus, (L)-H-Val-O*t*Bu **16** and triphosgene were used to form *in situ* an isocyanate intermediate which was then further treated with the ammonium salt **15** to afford the urea **17**. Finally, deprotection of the *tert*-butyl ester group by acid treatment of **17** led to the desired urea building block **18**.

With the urea in hands, the synthesis was continued with the generation of the cyclization precursor (Scheme 6). Accordingly, (L)-Boc-valine methyl ester **19** was reduced to the corresponding aldehyde by DIBAL-H reduction, followed by a Wittig reaction to obtain the (*E*)-configured α,β-unsaturated derivative **20** in good yield. Selective cleavage of the Boc-protecting group and subsequent peptide coupling of a suitable protected lysine building block then yielded the dipeptide **21**.

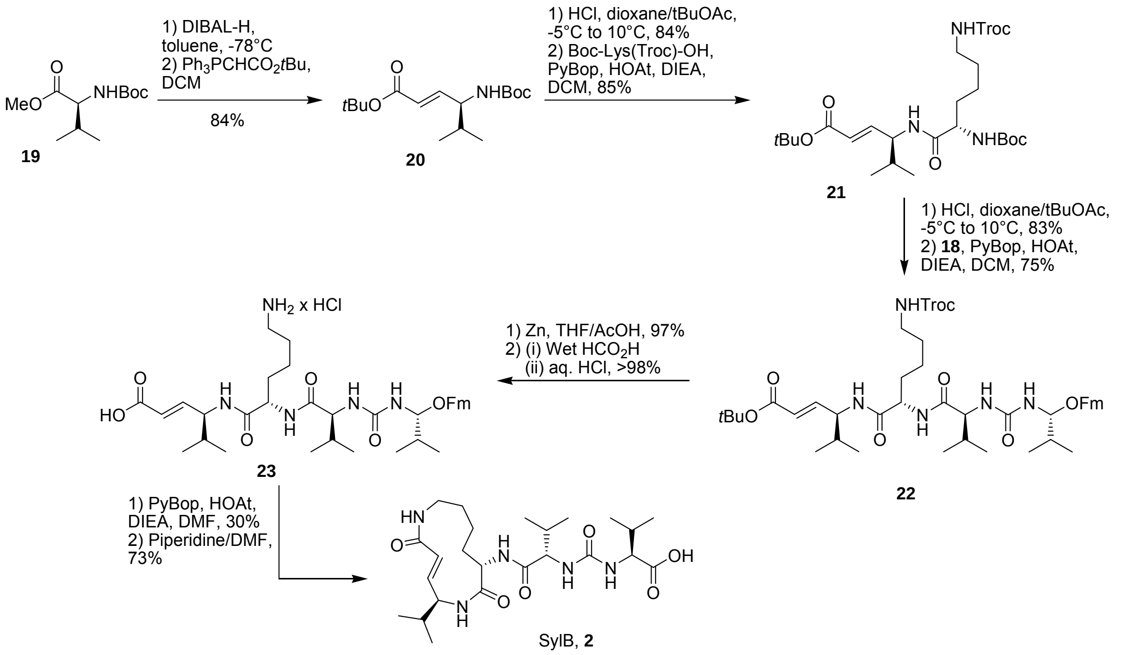
1) DIBAL-H, toluene, -78°C
2) Ph3PCHCO2tBu, DCM
84%
19
20
1) HCl, dioxane/tBuOAc, -5°C to 10°C, 84%
2) Boc-Lys(Troc)-OH, PyBop, HOAt, DIEA, DCM, 85%
21
1) HCl, dioxane/tBuOAc, -5°C to 10°C, 83%
2) 18, PyBop, HOAt, DIEA, DCM, 75%
22
1) Zn, THF/AcOH, 97%
2) (i) Wet HCO2H
(ii) aq. HCl, >98%
23
1) PyBop, HOAt, DIEA, DMF, 30%
2) Piperidine/DMF, 73%
SylB, 2

Scheme 6. Total synthesis of SylB by macrolactamization.

At this stage, the Boc-protecting group was cleaved with HCl in a mixture of dioxane and *tert*-BuOAc and coupled with the urea building block **18.** Selective deprotection of **22** by Troc cleavage with zinc in a mixture of THF and acetic acid, followed by acidic cleavage of the *tert*-butyl ester moiety led to the macrolactamization precursor **23**.

The subsequent key ring closure of **23** was achieved under high-dilution conditions with PyBop/HOAt as activating agents in DMF and produced the desired product in a satisfying yield of 30%. Final removal of the remaining fluorenylmethyl ester protecting group with piperidine in DMF afforded after reverse phase prep-HPLC purification SylB (**2**) in an overall yield of 7.8% in 9 steps. Satisfyingly, the NMR spectra of synthetic SylB and of a mixture of natural SylB isolated and synthetic SylB were almost completely identical. In addition, a coinjection experiment on a chiral HPLC system of synthetic SylB with natural SylB revealed no significant differences, thus verifying our initial stereochemical assignment of SylB.

4.1.2. Synthesis of syringolin A (SylA)

4.1.2.1. Macrolactamization pathway

After the success of the total synthesis of syringolin B as a model system for the elaboration of a syringolin collection, the application of the same strategy for the synthesis of syringolin A was undertaken. Consequently, a similar retrosynthetical pathway using however β,γ-dehydrolysine instead of the lysine residue was followed (Scheme 7). For establishing a synthesis route amenable for derivatization, an attachment of the exocyclic urea side chain was planned at a later stage of the synthesis. Thus, a synthesis of the macrocycle by macrolactamization followed by attachment of the exocyclic side chain was envisaged.

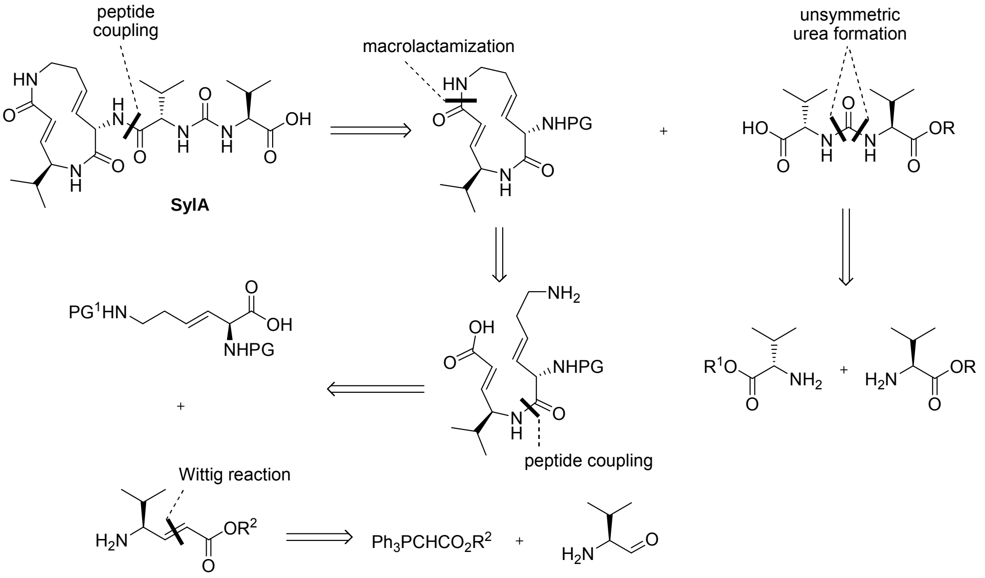
peptide coupling
macrolactamization
unsymmetric urea formation
SylA
HN
NHPG
HO
OR
OH
NH2
PG1HN
R1O
H2N
Wittig reaction
OR2
Ph3PCHCO2R2
peptide coupling

Scheme 7. Retrosynthetic pathway to SylA using a macrolactamization as a key step.

To date, a synthesis of β,γ-dehydrolysine has not yet been reported. Main difficulties of its synthesis are the required protecting group manipulations without isomerization of the deconjugated double bond into the chemically more stable conjugated form. Consequently, the use of strongly deprotonating agents such as bases might cause an unwanted shift of the double bond from the β,γ- to the α,β-position. Thus, to prevent the loss of the chiral information, it seemed advisable to use protecting groups which could be preferably cleaved with acidic conditions.

4.1.2.1.1. Synthesis of the β,γ-dehydrolysine building block

Several approaches for synthesis of the β,γ-dehydrolysine building block were attempted. First, Beaulieu's approach consisting of a Wittig reaction with a Garner aldehyde for the synthesis of β,γ-dehydro amino acids was followed. However, all our attempts to use this approach for the synthesis of β,γ-dehydrolysine failed. As a consequence, an alternative strategy was developed. For simplicity, again a synthetic approach in which the required (L)-configuration was 'pre-introduced' by relying on a chiral pool approach was chosen. Accordingly, a Garner aldehyde appeared as a promising starting point for generation of the required amino acid. Several strategies for the conversion of this aldehyde into the β,γ-dehydrolysine such as Julia olefination or Stille coupling[55] based approaches could be imagined to achieve the desired target structure. A Johnson-Claisen rearrangement-based methodology however would have the advantage to stereospecifically form the desired (*E*)-configuration and therefore was followed in this PhD thesis.

To this end, the vinylation of the (D)-Garner aldehyde **24** with vinyl magnesium bromide was performed with good yields on multigram scales to afford the vinyl alcohol **25** as a mixture of diastereomers.[56] Both isomers were then treated with triethyl orthoacetate under acidic catalysis and refluxed to yield a single product **27** with the desired double bond in the (*E*)-configuration (Scheme 8).[57]

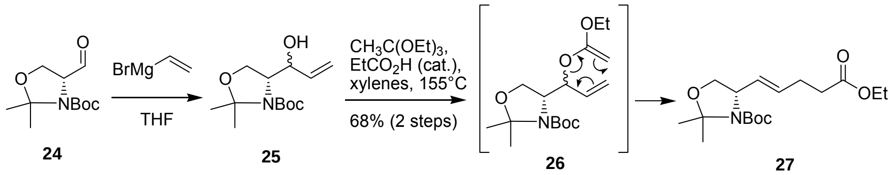

Scheme 8. Vinylation of Garner aldehyde and Johnson-Claisen rearrangement towards the synthesis of β,γ-dehydrolysine.

Mechanistically, the Johnson-Claisen rearrangement is a [3,3]-sigmatropic rearrangement involving a six-membered transition state with a delocalized electronic structure. Under the employed reaction conditions, the chair conformation is preferred, which can be adopted by two transition states **28** and **29** in regard to the mixture of isomers used. As shown in Scheme 9, the oxazolidine substituent due to its bulkiness can be assumed to preferentially adopt an equatorial position for both enantiomers. This arrangement results in *trans*-orientation of the vinylic proton and the chiral proton of the oxazolidine, leading to formation of the (*E*)-configured olefin.[58]

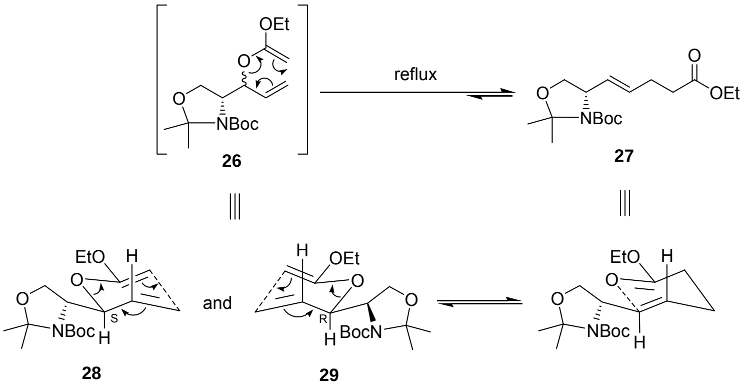

Scheme 9. Potential transition states involved during Johnson-Claisen rearrangement.

After establishment of the double bond, the terminal ethyl ester functionality was subsequently saponified to further react with diphenyl phosphoryl azide to undergo a modified Curtius rearrangement (Scheme 10).[59] After the rearrangement, the reaction was quenched with an excess of trichloroethanol enabling the formation of the desired intermediate **31** in high yields and in an orthogonally protected form.

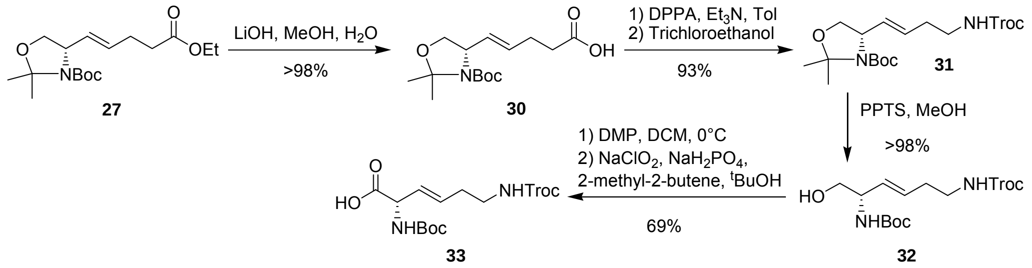

Scheme 10. Final steps towards the synthesis of the orthogonally protected β,γ-dehydrolysine building block **33**.

To complete the synthesis of **33**, first Jones oxidation of **31** with chromic acid in acetone was tested as it should enable the cleavage of the oxazolidine and the oxidation of the resulting primary alcohol to the desired carboxylic acid in one pot. Unfortunately, only poor yields of the desired β,γ-dehydrolysine were isolated by this method and led to the hypothesis that the intermediate aldehyde may be too sensitive for the rather harsh reaction conditions of a Jones oxidation. The reaction conditions were therefore changed: At first, the cleavage of the oxazolidine was realized by using a catalytic amount of *p*-toluene sulfonic acid in methanol under reflux. Then, the oxidation of the alcohol **32** was performed in two steps. First, the Dess-Martin periodinane was used to provide the unstable aldehyde which was immediately further oxidized to the corresponding carboxylic acid **33** using the Pinnick oxidation procedure.[60]

4.1.2.1.2. Synthesis of the α,β-unsaturated building block

The synthesis of the α,β-unsaturated building block as a methyl ester followed the same procedure as described in section 4.1.1 but employed (methoxycarbonylmethylene)-triphenylphosphorane as the ylide component in the Wittig reaction (Scheme 11).

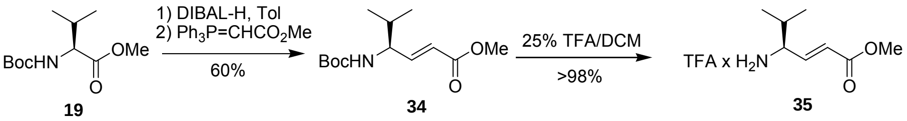
BocHN
OMe
O
19
1) DIBAL-H, Tol
2) Ph3P=CHCO2Me
60%
BocHN
OMe
O
34
25% TFA/DCM
>98%
TFA x H2N
OMe
O
35

Scheme 11. Synthesis of the α,β-unsaturated building block **35**.

The resulting α,β-unsaturated derivative **34** was then further Boc-deprotected with a mixture of trifluoroacetic acid in dichloromethane to afford the desired coupling partner **35**.

4.1.2.1.3. Macrolactamization studies

Finally, the two building blocks **33** and **35** were coupled, using general peptide coupling conditions to provide the intermediate **36**.

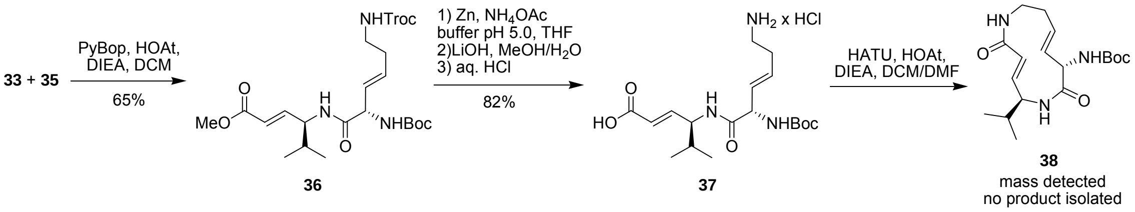
33 + 35
PyBop, HOAt,
DIEA, DCM
65%
NHTroc
MeO
O
H
N
NHBoc
O
36
1) Zn, NH4OAc
buffer pH 5.0, THF
2)LiOH, MeOH/H2O
3) aq. HCl
82%
NH2 x HCl
HO
O
H
N
NHBoc
O
37
HATU, HOAt,
DIEA, DCM/DMF
HN
O
NHBoc
N
H
O
38
mass detected
no product isolated

Scheme 12. Attempted synthesis of macrocycle **38** using a macrolactamization approach.

The selective deprotection of the Troc-group with zinc powder in buffer pH 5.0 followed by the saponification of the methyl ester cleanly provided the precursor for the macrolactamization in good yields.[61] Several strategies to perform macrolactamization have been reported in the literature. Among them, HATU/HOAt-mediated cyclization is nowadays one of the gold-standards, because it usually proceeds with low levels of racemization and can induce even cyclization of ring-strained macrocycles.

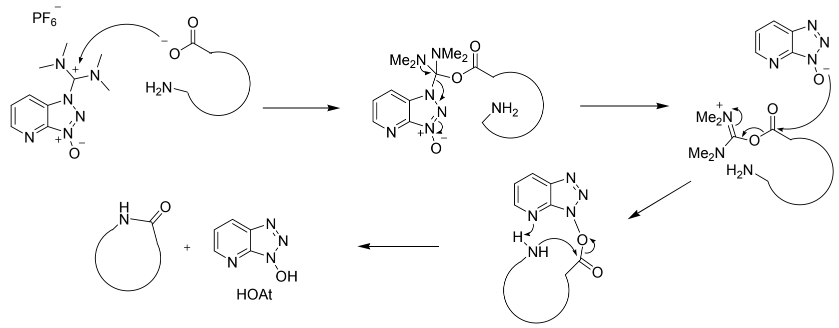

Scheme 13. Mechanism involved in the HATU-assisted macrolactamization.

It is assumed that the observed efficiency of HATU-assisted macrolactamizations results from a coordination of the nitrogen of the pyridine moiety with the free amine, thereby spatially arranging the C-terminally activated carboxylic acid in close distance to the amino nucleophile and consequently promoting the intramolecular coupling (Scheme 13). Unfortunately, all attempts to achieve the macrolactamization on a preparative scale failed, although the desired product could be detected in trace quantities by LC-MS analysis. Also other peptide coupling reagents and bases did not lead to better yields in the macrolactamization reaction. These negative findings then led to the decision to investigate alternative strategies for ring closure.

4.1.2.2. Metathesis pathway

Since the discovery of the metal-catalyzed ethylene polymerization by Karl Ziegler in the 1950’s and the mechanism theory formulated by Yves Chauvin in 1971, metathesis became an incontrovertible and powerful reaction in organic chemistry. During the last 20 years, with the development of efficient and stable catalysts by Grubbs and Schrock, this method has matured into a highly efficient approach to establish carbon-carbon bonds, whose significance is highlighted by the award of the Nobel Prize in Chemistry for Grubbs, Schrock and Chauvin in 2005. One prominent application of metathesis is to perform ring closures, commonly referred to as ring closure metathesis (RCM). RCM has nowadays proved its potential in numerous total syntheses of complex macrocyclic natural products due to its property to efficiently cyclize also highly-strained ring systems.[62] Consequently, its potential use for the synthesis of the macrocycle of syringolins was investigated.

4.1.2.2.1. First approach to employ RCM in syringolin macrocycle synthesis

Retrosynthetically, the desired macrocycle could be obtained by performing the RCM on the precursor **39** (if a Boc protecting group is installed). This compound features at its N-terminal end a vinyl glycine functionality, which is known to undergo under basic conditions, e.g. under peptide coupling conditions, isomerization to the conjugated α,β-unsaturated carbonyl derivative. In order to avoid this side reaction, a phenyl selenyl-based methodology was therefore designed, allowing the installation of the vinylglycine moiety just before the RCM. Further retrosynthetic disconnections led to three building blocks for establishing the macrocycle: 3-butenylamine (commercially available), a derivative of the building block **34** (synthesized previously) and the building block **40** which can be obtained by a procedure developed by Berkowitz[63]

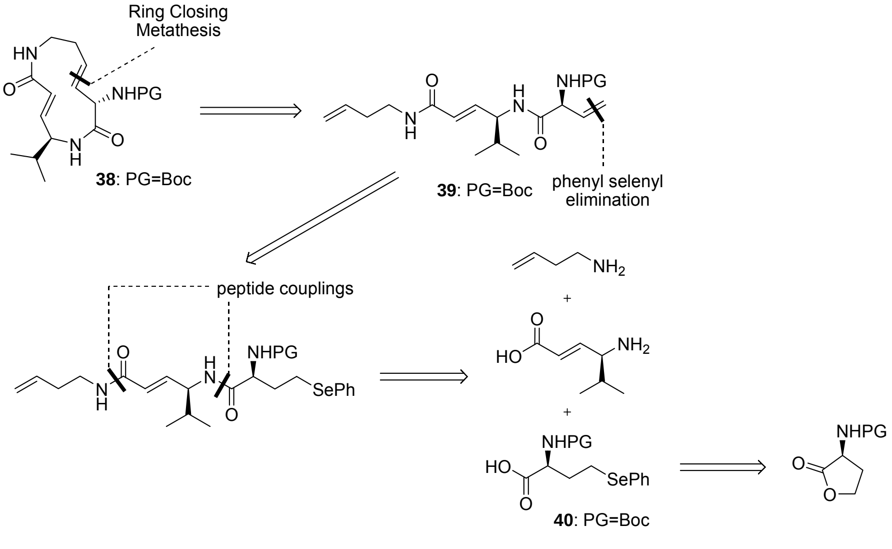
Ring Closing Metathesis
HN
O
NHPG
N H
O
38: PG=Boc
O
H N
NHPG
N H
O
39: PG=Boc
phenyl selenyl elimination
peptide couplings
O
H N
NHPG
N H
SePh
O
NH2
+
O
HO
NH2
+
NHPG
HO
SePh
O
40: PG=Boc
NHPG
O
O

Scheme 14. Retrosynthetic pathway to the protected SylA core macrocycle using a ring closing metathesis as a key step.

Thus, starting from (L)-homoserine and following the procedure of Berkowitz, the lactone **41** was synthesized and underwent a ring opening by addition of a phenyl selenyl anion to afford the desired carboxylic acid **40**. In parallel, the building block **34** was saponified, coupled to 3-butenylamine and Boc-deprotected to provide the ammonium salt **42**.

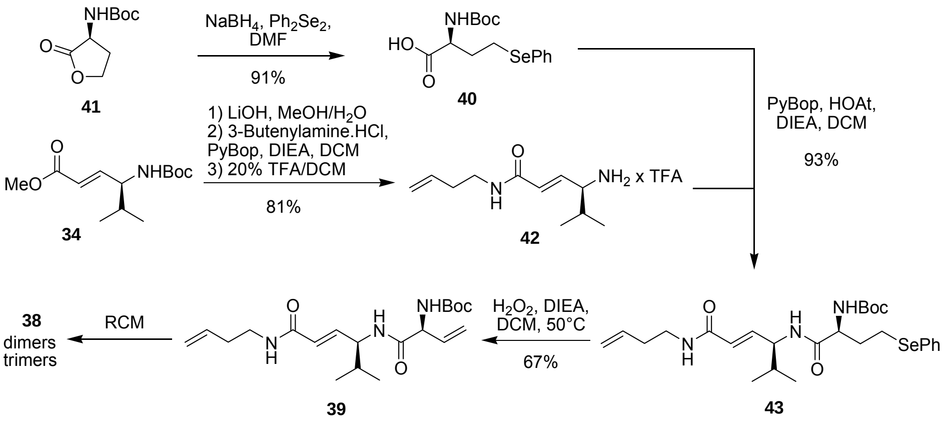
NaBH$_4$, Ph$_2$Se$_2$, DMF
91%
41
40
1) LiOH, MeOH/H$_2$O
2) 3-Butenylamine.HCl, PyBop, DIEA, DCM
3) 20% TFA/DCM
81%
34
42
PyBop, HOAt, DIEA, DCM
93%
38
dimers
trimers
RCM
H$_2$O$_2$, DIEA, DCM, 50°C
67%
39
43

Scheme 15. First attempted synthesis of macrocycle **38** using a ring closing metathesis approach.

Then, general coupling conditions were used to couple both compounds, thereby obtaining **43**. Subsequent one-pot oxidation/elimination of the phenyl selenyl group yielded the precursor **39** for the RCM in good yields.[64] Unfortunately, again as in the case of the macrolactamization, the critical key cyclization could not be achieved even after intensive screening of different Grubbs catalysts and reaction conditions. Instead, only dimers and trimers (opened and closed) besides several unidentifiable side products were detected by LC-MS analysis.

The failure of this RCM approach might be explainable by the overall structure of the precursor molecule (Figure 8). The double bonds as well as amide functionalities introduce rigidity and a structural pre-organization into the molecule that might prevent efficient pre-arrangement of the compound into a conformation that would allow the terminal olefins to undergo the RCM reaction.

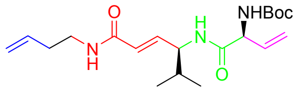

39

Figure 8. Chemical structure of the linear RCM precursor **39**. Functional groups that induce rigidity in the molecule by sp^2 hybridization are colored.

4.1.2.2.2. RCM: second approach

In order to introduce a different structural pre-arrangement into the RCM precursor, it was rationalized that a modification of the central (conjugated) double bond to a five-membered ring system by dihydroxylation and subsequent protection as an acetonide might lead to a more efficient RCM.

To set this into practice, the previously synthesized building block **34** was dihydroxylated with osmium tetroxide and NMO to yield to the diol **44** with a high diastereoselectivity (d.r. = 96%).[65] After formation of the acetonide, the ester moiety was saponified and derivatized with 3-butenylamine. Then, the amine moiety was selectively Boc-deprotected[66] and coupled with the building block **40**. Finally, oxidation and elimination of the phenyl selenyl group afforded the acetonide-modified precursor **47** for the RCM.

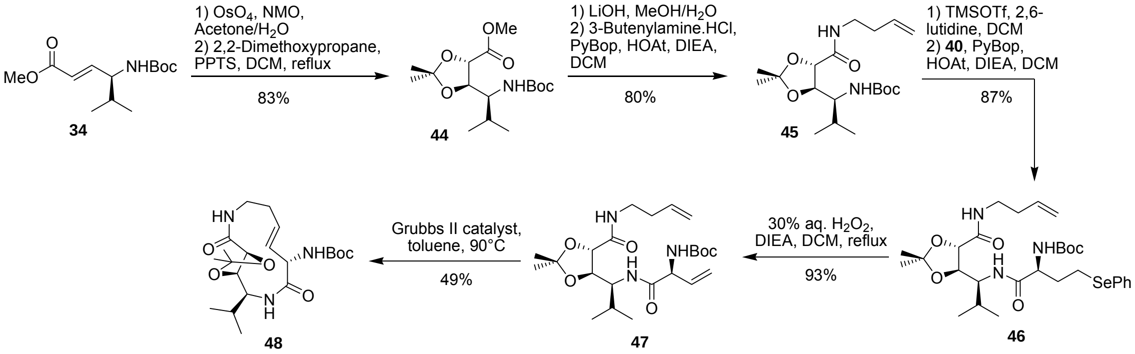
MeO
O
NHBoc
34
1) OsO_4, NMO, Acetone/H_2O
2) 2,2-Dimethoxypropane, PPTS, DCM, reflux
83%
OMe
O
O
O
NHBoc
44
1) LiOH, MeOH/H_2O
2) 3-Butenylamine.HCl, PyBop, HOAt, DIEA, DCM
80%
HN
O
NHBoc
45
1) TMSOTf, 2,6-lutidine, DCM
2) 40, PyBop, HOAt, DIEA, DCM
87%
NHBoc
H
N
SePh
46
30% aq. H_2O_2, DIEA, DCM, reflux
93%
47
Grubbs II catalyst, toluene, 90°C
49%
HN
NHBoc
N
H
48

Scheme 16. Synthesis of macrocycle **48** using a ring closing metathesis approach with an acetonide-modified precursor.

A subsequent screening for suitable catalysts and reaction conditions revealed that the commercially available Grubbs II catalyst enabled the ring closure in high yield but with a poor stereoselectivity. In fact, 42% of the desired (*E*)-isomer and 39% of the (*Z*)-isomer were isolated (Table 2).

Table 2. Reagents and conditions screened towards ring closing metathesis of **48**.

Entry	Catalysts	Selectivity (*E*:*Z*)	Rctn. Time [h]	Rctn. T [°C] and solvent	Yield 48 [%][b] (Conv. [%])[c]
1	Grubbs I	10:1	24	rt, DCM	n.i.[d] (25)
2	Grubbs II	1.1:1.0	24	rt, DCM	42 (95)
3	Grubbs II	3.1:1.0	20	110°C, toluene	39 (95)
4	Grubbs II	2.6:1.0	20	90°C, toluene	49 (95)
5	Grubbs-Hoveyda I	n.d.[a]	24	rt, DCM	n.i. [d] (5)
6	Grubbs-Hoveyda II	1.1:1.0	48	rt, DCM	22 (90)

[a] n.d.: not determined; [b] yield of (E)-isomer only; [c] determined by LC-MS; [d] n.i.: not isolated.

In contrast, the Grubbs I catalyst provided a remarkable stereoselectivity but enabled only a poor conversion to the desired product. The Grubbs-Hoveyda I catalyst was even less reactive and therefore no stereoselectivity could be determined. The Grubbs-Hoveyda II catalyst showed a similar selectivity than the Grubbs II catalyst but required a much longer reaction time to achieve the same level of conversion. Thus, further improvement of the reaction conditions were focussed on RCMs using the Grubbs II catalyst. As the desired (*E*)-configured product is assumed to be thermodynamically more stable than the (*Z*)-product, a variation of temperature might show beneficial effects on the selectivity. Effectively, if the reaction was performed at 110°C in toluene, an improvement of the selectivity by a factor 3 was observed. As a drawback however, side-products accumulated that led to a difficult purification, thereby decreasing the overall yield. It turned out that the "optimal" reaction conditions were 90°C in toluene, leading to a stereoselectivity of (2.6:1) and thus enabled a yield of 49% for the isolated (*E*)-isomer. Noteworthy, the reaction could be performed with similar yields also at a gram scale.

As the next step in the synthesis, a cleavage of the acetonide was anticipated. However, despite intense efforts, no reaction conditions could be found that allowed cleavage of the acetonide without Boc-deprotection. To overcome this problem, the synthetic route was changed, instead continuing with a selective Boc-group cleavage using TMSOTf in 2,6-lutidine/DCM (Scheme 17). The free amine was then coupled to the urea building block **49** (synthesis described in section 4.1.2.2.4.), yielding the intermediate **50**. At this stage then, the acetonide cleavage was performed using formic acid/methanol (3:2) under microwave conditions to obtain the corresponding diol.

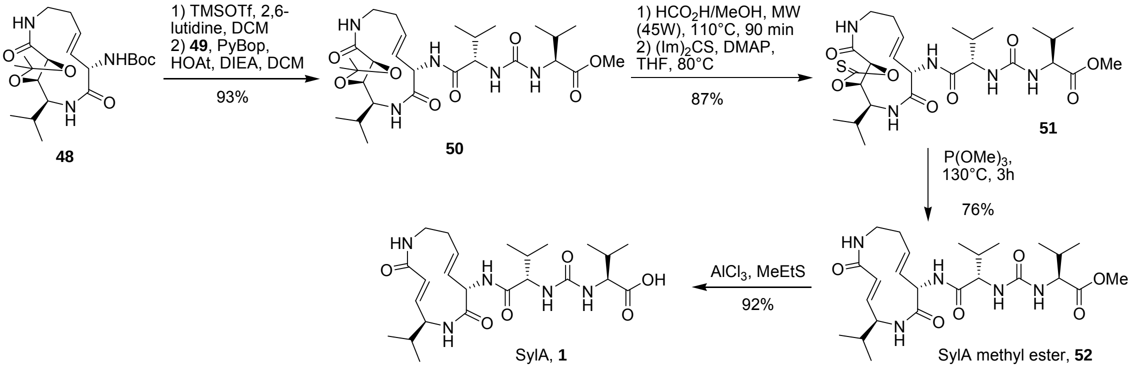
48
1) TMSOTf, 2,6-lutidine, DCM
2) 49, PyBop, HOAt, DIEA, DCM
93%
50
1) HCO2H/MeOH, MW (45W), 110°C, 90 min
2) (Im)2CS, DMAP, THF, 80°C
87%
51
P(OMe)3, 130°C, 3h
76%
SylA methyl ester, 52
AlCl3, MeEtS
92%
SylA, 1

Scheme 17. Final steps to the synthesis of SylA.

Restoration of the double bond was then envisaged by a Corey-Winter elimination. Consequently, the thiocarbonate **51** was formed by reflux of the diol in THF with 1,1'-thiocarbonyl diimidazole and DMAP, followed by treatment with trimethyl phosphite at 130°C to yield the methyl ester **52** of SylA.[67] Finally, the deprotection of the methyl ester was achieved using aluminium trichloride in methyl ethyl sulfide to afford the natural product SylA with an overall yield of 9.1% from **19** in 16 steps.[68]

Table 3. Apparent K_i' and k_{assoc} values for the chymotrypsin-, trypsin-, and caspase-like activity of human 20S proteasome of synthetic and natural SylA.

Inhibitor	**Inhibited activity**	K_i', nM	k_{assoc}, M^{-1} s^{-1}
Synthetic SylA	C-L	1,016 ± 179	828 ± 195 (n = 3; 100 – 200 nM)
	T-L	10,300 ± 1,400	83 ± 2.9 (n = 3; 1.25 – 5 μM)
	Cas-L	n.d.	15.8 ± 3.7 (n = 3; 20 – 40 μM)
Natural SylA	C-L	843 ± 8.4	863 ± 106 (n = 6; 100 – 200 nM)
	T-L	6,700 ± 700	94 ± 12 (n = 6; 150 – 600 nM)
	Cas-L	n.d.	6 ± 0.3 (n =6; 20 – 40 μM)

To verify that the synthesized SylA resembled the isolated SylA, thereby confirming our assumption that SylA indeed has an overall (L)-configuration, the NMR spectra of natural and synthetic SylA as well as a NMR spectrum of a mixture of both were compared and judged as equal. In addition, analysis with a chiral HPLC system was performed which also indicated identity. Finally, a biochemical inhibition assay was performed, revealing almost identical inhibition potencies (Table 3). These finding led to the conclusion that the synthetic SylA was indeed identical with natural SylA, thereby proving the original assignment of all stereocenters as (L).

4.1.2.2.3. Establishment of a more convergent route to SylA and analogues

Despite the successful total synthesis of SylA, an optimization of the overall route was investigated to enable a more facile generation of analogues of SylA. To this end, a modification of the synthesis pathway, consisting of the use of a Troc-protecting group at the intermediate **48** instead of the previously used Boc group was envisaged. This group exchange should then allow the chemoselective cleavage of the acetonide group, thereby allowing the synthesis of a fully functionalized macrocycle. With this macrocycle in hand, various exocyclic side chains could be coupled to the macrocycle, thereby enabling the facile generation of a SylA compound library.

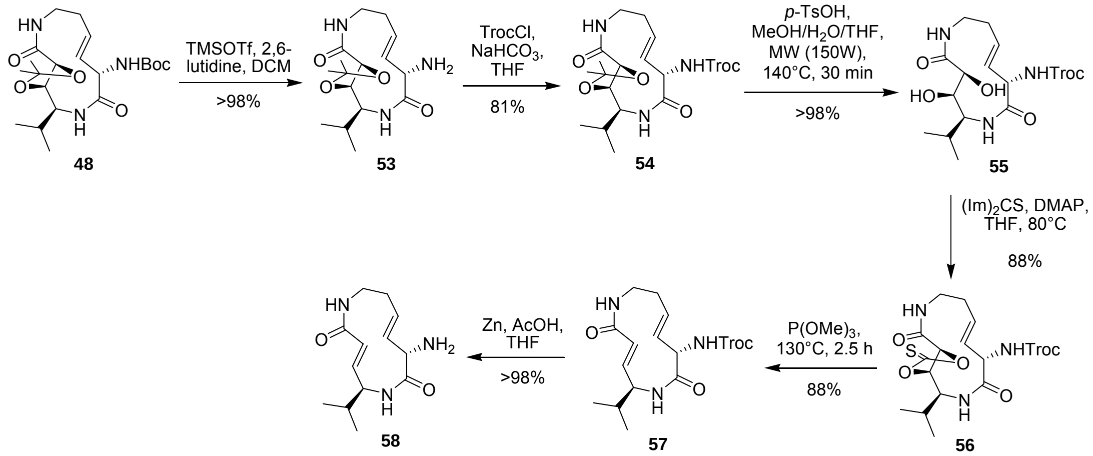

Scheme 18. Improvement of the synthesis of the SylA core macrocycle.

To put this into practice, the Boc-protecting group of **48** was cleaved with TMSOTf and 2,6-lutidine in DCM and immediately reprotected with Troc-Cl, leading to **54**. Acidic cleavage of the acetonide and reaction with 1,1’-thiocarbonyl diimidazole led to **56**, which upon Corey-Winter elimination with trimethyl phosphite and subsequent Troc cleavage with zinc in acetic acid/THF finally delivered the fully functionalized SylA macrocycle **58**. It is important to notify that the Corey-Winter reaction proved to be a critical step that required intensive effort for optimization. To this end, reaction conditions were modified to prevent the formation of side products. In order to gain an insight why these side products were formed, also additional studies were performed.

It turned out that in order to avoid the hydrolysis of the thiocarbonate **59** to the respective carbonate (Figure 9A), the reaction had to be carried out under strictly inert reaction conditions.[69] Second, LC-MS monitoring of the reaction revealed that the restored activated double bond was sensitive to the prolonged treatment of the molecule in trimethyl phosphite resulting in the formation of the phosphonate **60** (Figure 9B). These findings are in accordance with previous reports, describing that α,β-unsaturated carbonyls can behave as Michael acceptors towards nucleophilic attack of trialkyl phosphites.[70] In order to achieve optimal yields, the reaction time should not exceed more than 3 hours and only a minimum quantity of trimethyl phosphite should be used to promote the precipitation of the desired product and thus helping to direct the driving force of the reaction. Third, an unexpected cyclization could be revealed by the isolation of the bicycle **61** (arbitrarily called MRL) which was fully characterized by NMR and X-ray analysis (Figure 9C).

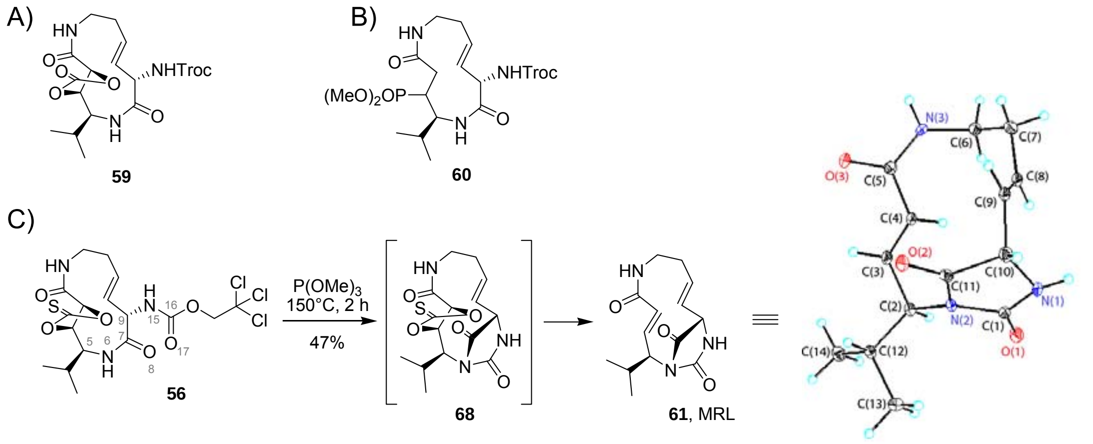

Figure 9. Structures of side-products **59**, **60** and **61**. A) carbonate side-product **59**; B) phosphonate side-product **60**; C) Synthesis and X-ray structure of the bicyclic side-product **61** (MRL).

The formation of this unusal side product was observed only while performing the reaction with a large quantity of trimethyl phosphite and at a temperature exceeding 150°C. The reaction consists of the liberation of a trichloroethanol moiety (Troc group) and the formation of the N_6-C_{16}(O) bond, thereby yielding a so-called hydantoin. Such a substitution of a Troc group by an amine has been reported before and has been for example used to create linear ureas. To accomplish these reactions, usually high reaction temperatures in solvents such as DMSO or THF are used.[71] Although no example of this reaction in an intramolecular fashion could be found in the literature, other carbamates were nevertheless reported to yield such hydantoins under basic treatment in protic solvents.[72] Moreover, such reactions were also observed in complex cyclic systems that contained a free amine and a carbamate-Cbz group as the active center for the intramolecular cyclization.[73] To explain the formation of the unexpected products in this example, the authors pinpointed the role of the base such as NaH or prolonged warming at high temperature (120°C).

Consequently, the mechanism for the formation of the compound **61** was investigated following two reaction parameters, (1) the temperature and (2) the basicity of trimethyl phosphite. Indeed, although the basicity of trimethyl phosphite has not been measured so far, Westheimer *et al.* have shown its potency to be hydrolyzed and therefore its capacity to accept protons.[74] Thus, the first approach to study the mechanism of this side-reaction consisted of dissolving compound **57** in xylenes and heating it up to 130°C for two hours and at 160 °C for further two hours. Subsequent LC-MS analyses proved that no product **61** was generated neither at 130°C nor 160°C, leading to the conclusion that the reaction is not purely thermic. To characterize the role of trimethyl phosphite as a base towards the generation of **61**, the compound **57** was treated with an excess of triethyl amine in xylenes at 130°C for two hours and at 160 °C for further two hours. Once again, no product was detected by LC-MS analysis which led to the hypothesis that the compound **57** might not be the precursor of the product **61**.

With the help of the software Chem 3D Ultra, MM2 energy minimizations were performed. These revealed a radical structural difference between compounds **57** and **56**. As shown in the figure 10, the orientation of the exocyclic N_{15}H-Troc group is dependent of the conformation of the nearby amide bond.

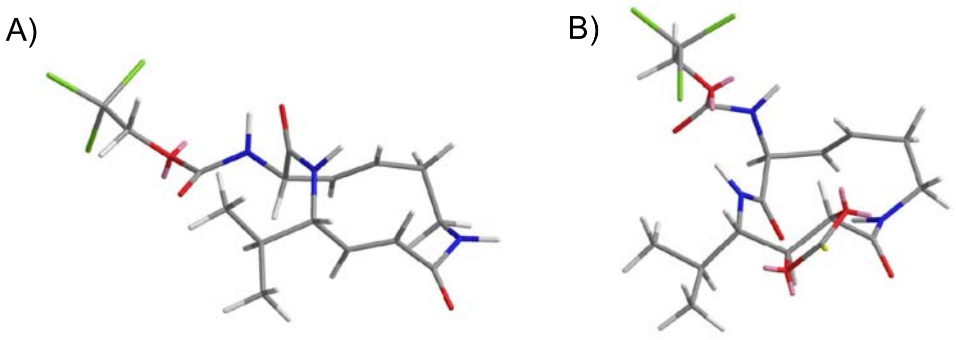

Figure 10. MM2 structure minimizations. A) compound **57** featuring two *cis* amide bonds; B) in contrast, compound **56** contains one *cis* and one *trans* amide bond.

Effectively, and in contrast to the first SylA published structure,[75] the presence of the two cyclic double bonds leads to an extreme rigid structure where both amide motifs seem to adopt a *cis* configuration to minimize the macrocyclic ring strain. Indeed, the N_{15}HTroc group assumes an equatorial position, leading to a dihedral angle close to 180° which does not allow a close proximity of the cyclic nitrogen (N_6H) and the carbamate. Exchange of the conjugated double bond by the thiocarbonate group however enables more flexibility in the ring structure and a *trans* configuration in one of the amide motives. With this configuration, the N_{15}HTroc group is placed in axial position and the resulting dihedral angle (close to 0°) indicates the overlapping of both C_9-N_{15} and C_7-N_6 bonds, an ideal arrangement for the cyclization leading to the formation of the hydantoin.

Unfortunately, due to limited time and starting material, this theory could not be verified with compound **56**. Instead, the close structural analogues **62** and **63** were used, originally prepared by Dipl.-Chem. Daniel Krahn, that differ from **56** and **57** just by the substitution of the isopropyl group with a methyl group. Treatment of compound **63** in xylenes at 130°C and 160°C for two hours with or without triethyl amine led the same result, i.e. no formation of the hydantoin derivative. However, if thiocarbonate **62** was treated under the same reaction conditions, the formation of the hydantoin **64** was observed for high reaction temperatures and promoted by the presence of triethyl amine (Scheme 19).

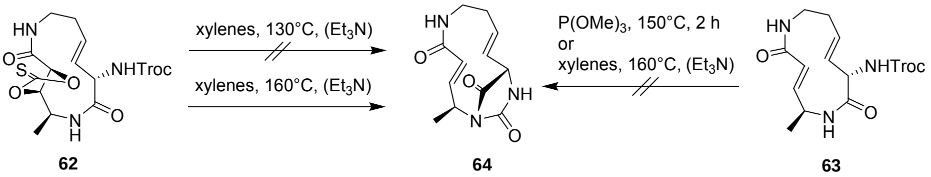

Scheme 19. Studies towards the formation of compound **64**.

Finally, to validate the importance of the ring conformation on hydantoin formation, the test procedure was applied also to compound **65**. Effectively, acetonide **65** has roughly a similar ring structure as **62** as revealed by MM2 energy minimizations and the exchange of the thiocarbonate moiety by an acetonide should reduce the possibilities of side reactions. Satisfyingly, the desired hydantoin **66** mass was detected by LC-MS analysis after treatment for two hours in xylenes at 160°C, but not at 130°C. If an excess of triethyl amine was used, the yield of the conversion increased significantly.

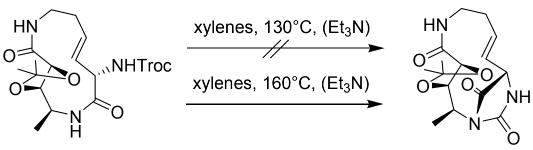

65 **66**

Scheme 20. Formation of the hydantoin **66** from the derivative **65** proved the importance of ring conformation on the cyclization efficiency.

From this study, several conclusions were made. First, the formation of the hydantoin is temperature dependent (> 130°C) and can be dramatically improved by the addition of base. Second, trimethyl phosphite did not specifically take part in the reaction mechanism but acted solely as a base. Third, this reaction is not limited to the thiocarbonate analogues but is dependent on the conformation of the macrolactam, thereby pre-organizing the reaction partners.

These findings might be explainable by two reaction mechanisms. In the first potential route, the cyclization could be activated by the deprotonation of the N_{15}-carbamate proton to form the isocyanate **67**, which could further react with the nucleophilic N_6-deprotonated amide to yield the desired hydantoin (Scheme 21, Path A). Then, the intermediate **68** could undergo the Corey-Winter degradation of the thiocarbonyl group to generate the conjugated double bond and compound **61**. Such a mechanism would be in accordance with the reaction mechanism described by Azad *et al.*.[71]

As an alternative, also a direct mechanism cannot be ruled out. Such a mechanism would then involve the direct cyclization of the N_6-deprotonated amide functionality by nucleophilic attack on the Troc-group (Scheme 21, Path B).

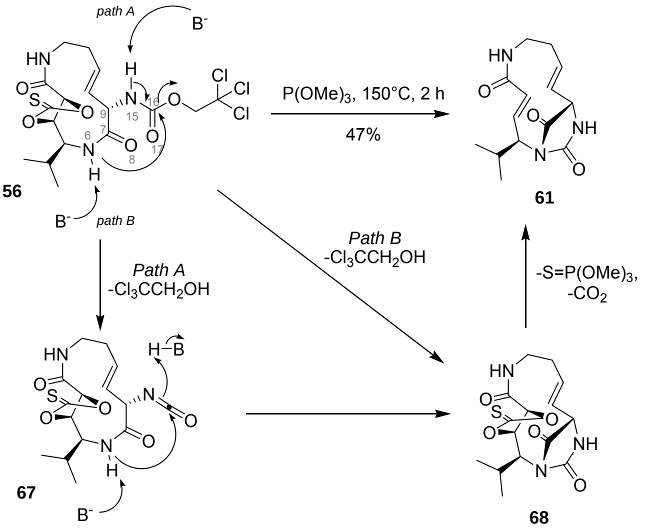

Scheme 21. Proposed reaction mechanisms in the formation of compound MRL (**61**).

In summary, these studies demonstrate that the Corey-Winter elimination to the SylA macrocycle is experimentally challenging, requiring a careful regulation of the reaction conditions. These studies furthermore show the difficulties associated in the synthesis of strained macrocycles.

4.1.2.2.4. Convergent synthesis of SylA and SylA isomers

With the SylA's core free amine **58** in hands, a variety of side-chains could now be attached to obtain SylA analogues. In order to gain an insight into the impact of the side-chain stereochemistry on the biological activity of the overall structure, all four urea isomers were coupled to the macrocycle. To this end, first all possible isomers of the urea side chain were synthesized.

Two procedures were used to generate these *N*,*N*'-unsymmetrical ureas. First, the reaction of the commercial isocyanate **69** with the (L)- or (D)-configured *tert*-butyl valine hydrochloride salts **16** and **72** generated ureas **70** and **73** which, after treatment with wet formic acid, afforded the acid **49** and **74** in excellent yields.

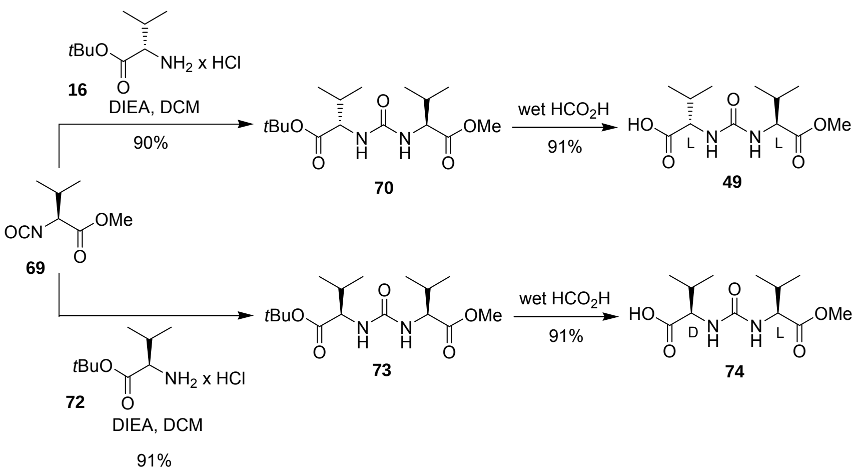

Scheme 22. Synthesis of exocyclic urea building blocks from commercial isocyanate.

Second, the procedure already employed for the synthesis of **17** in the section 4.1.1 provided the ureas **77** and **80** which were further treated with wet formic acid to cleave the *tert*-butyl group, thereby yielding acids **78** and **81**. It was however noted that if these reactions were performed on a larger scale, both the unwanted symmetrical and the desired unsymmetrical ureas were formed. Despite this drawback, no further optimization of the reaction was investigated as sufficient substance quantities could be generated by this procedure.

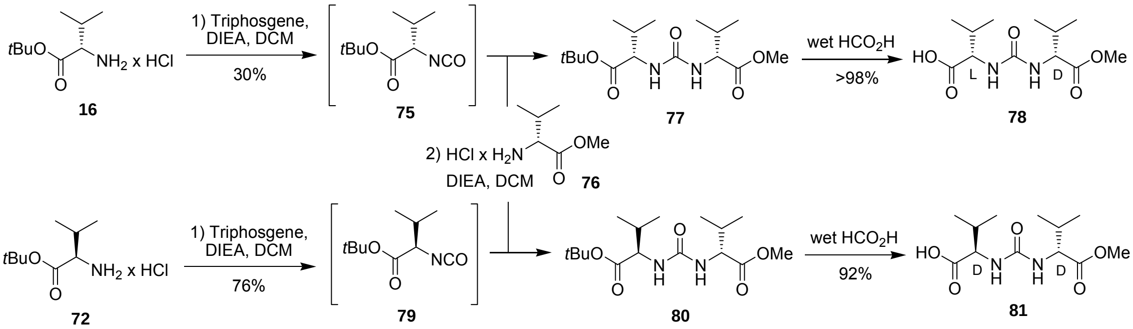

Scheme 23. Synthesis of exocyclic *N*,*N*'-unsymmetric urea building blocks.

The convergent syntheses of all four isomers was then completed by the coupling of the four different urea side chains to the fully functionalized SylA macrocycle **58**, followed by subsequent methyl ester cleavage with aluminium tribromide and tetrahydrothiophene to finally afford four SylA isomers (Table 4).

Table 4. Yields of SylA derivative syntheses of the last two steps.

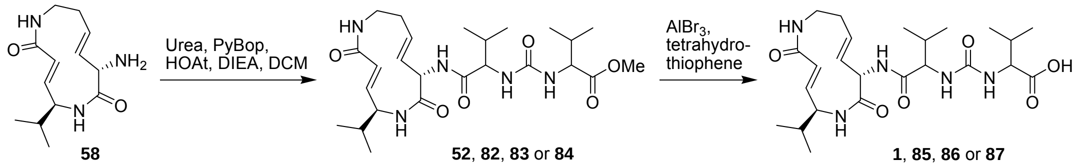

58 **52**, **82**, **83** or **84** **1**, **85**, **86** or **87**

Entry	Urea	Coupling prod. & yield	Deprotect. prod. & yield	Prod. structures
1	**49**	**52**, 95%	**1**, 84%	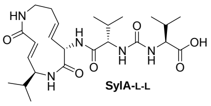 SylA-L-L
2	**78**	**82**, 87%	**85**, 93%	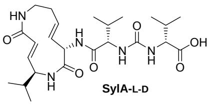 SylA-L-D
3	**74**	**83**, 76%	**86**, 53%	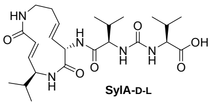 SylA-D-L
4	**81**	**84**, 68%	**87**, 68%	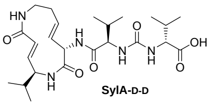 SylA-D-D

In order to get a first glimpse on the overall structural consequences of the side-chain configuration on the overall syringolin structure, the NMR spectra of the four SylA isomers were compared (Figure 11). It turned out that as expected the α-protons of the exocyclic valine residues but interestingly also the signals of the β-olefinic proton of the β,γ-unsaturated lysine were most sensitive to the stereochemical environment. As expected, all signals of the NMR spectrum of the all (L)-isomer **1** matched those of natural SylA. In contrast, the derivatives **86** and **87** which feature a (D)-valine residue adjacent to the macrocycle displayed a shift of ~ 0.48 ppm at the β-olefinic proton of the β,γ-unsaturated lysine (Figure 11A) indicating that this modification has a considerable effect on the overall arrangement of the molecule. The signals of the α-protons of the amino acid residues were also singular for each isomer, resulting in an individual pattern for all four isomers in the NMR spectra (Figure 11B).

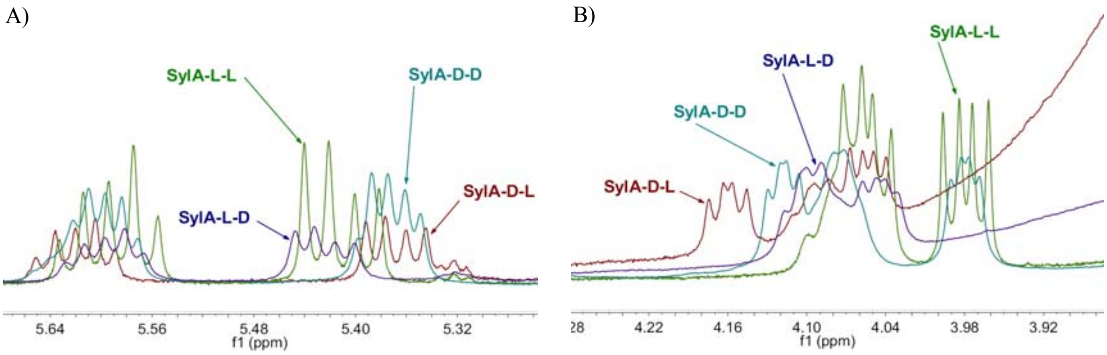

Figure 11. Overlay of the characteristic part of the ^{1}H-NMR spectra of **1** (SylA-L-L), **85** (SylA-L-D), **86** (SylA-D-L) and **87** (SylA-D-D). A) β-Olefinic proton of the β,γ-unsaturated lysine; B) α-protons of the amino acid residues.

Moreover, a subsequent biochemical evaluation of the inhibition potencies of these 4 isomers revealed that the configuration of the chiral centers of the side chain residues had a critical influence on the proteasome inhibition (Figure 12).

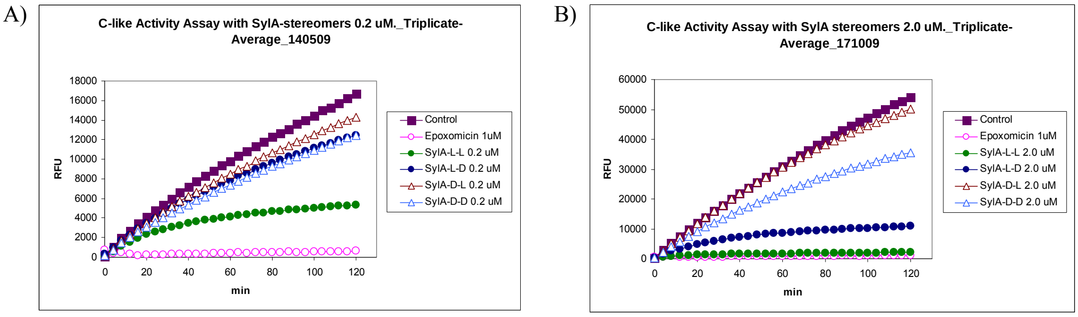

Figure 12. Biochemical inhibition assay for the chymotrypsin-like activity of the 20S proteasome. The inhibition is characterized by a lower fluorescence. A) Comparison of 4 isomers of SylA at the concentration of 0.2 μM; B) comparison of 4 isomers of SylA at the concentration of 2.0 μM.

Evaluation of the biochemical inhibition kinetics revealed that the natural SylA derivative is indeed the most potent inhibitor of all four isomers, displaying (as previously described) a K_i' of 1,016 ± 179 nM. SylA-L-D also proved as a potent inhibitor, despite being already 10-times less active for the inhibition of the chymotrypsin-like activity (11,117 ± 2,222 nM). In contrast, the derivative SylA-D-D was much less potent, displaying only a K_i' of 33,962 ± 11,317 nM, while SylA-D-L at the employed concentration ranges was completely inactive. These findings prove a critical influence of the stereochemistry on the inhibition potency.

4.1.2.3. Synthesis of a saturated SylA derivative

Finally, in order to obtain a probe that might serve as a negative control in biological assays and for confirming the X-ray derived inhibition mechanism, the synthesis of a SylA analogue without the conjugated double bond was undertaken.

As most of the building blocks were already prepared from previous synthetic trials, an RCM based route was investigated starting from the compound **34** (Scheme 24). After hydrogenation, saponification and coupling with 3-butenylamine, the intermediate **89** was formed and further Boc-deprotected and coupled to the building block **40**. The one-pot oxidation/elimination of the phenyl selenyl group then afforded compound **91** which under the elaborated RCM conditions yielded to the desired macrocycle. Compound **92** was Boc-deprotected and coupled with the building block **49** to yield **93**. Cleavage of the methyl ester group with aluminium trichloride and ethanethiol finally furnished the saturated SylA analogue **94** (SylA-Sat).

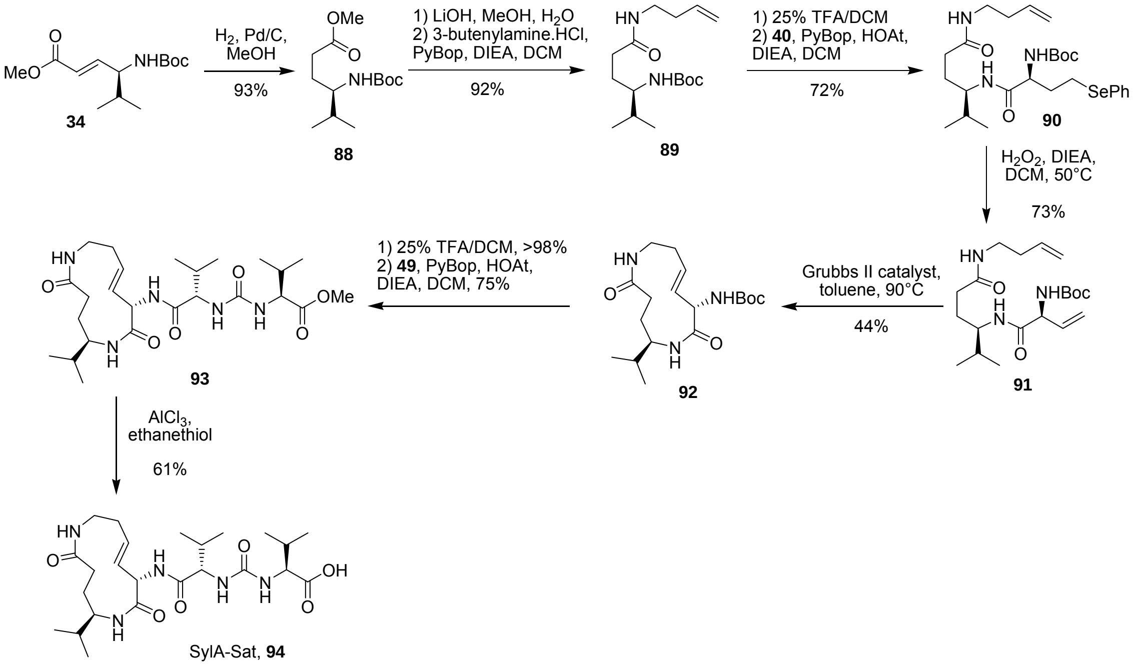
34
H2, Pd/C, MeOH
93%
88
1) LiOH, MeOH, H2O
2) 3-butenylamine.HCl, PyBop, DIEA, DCM
92%
89
1) 25% TFA/DCM
2) 40, PyBop, HOAt, DIEA, DCM
72%
90
H2O2, DIEA, DCM, 50°C
73%
91
Grubbs II catalyst, toluene, 90°C
44%
92
1) 25% TFA/DCM, >98%
2) 49, PyBop, HOAt, DIEA, DCM, 75%
93
AlCl3, ethanethiol
61%
SylA-Sat, 94

Scheme 24. Synthesis of a saturated SylA analogue (SylA-Sat, **94**) using ring closing metathesis.

As expected, the subsequent biochemical evaluation for proteasome inhibition of the chymotryptic activity by **94** demonstrated its inactivity, at least at a concentration of 100 μM. Further confirmation of this observation was provided by cellular labeling experiment of *Arabidopsis thaliana* extract (performed by collaborators in the van der Hoorn group). Thus, the saturated SylA derivative proved the proposed binding mode. Moreover, it represents a promising negative control for further biological experiments due to its structural similarity to natural SylA but completely distinct biological activity.

4.2. Chemical biology studies with syringolins

4.2.1. Synthesis and use of a rhodamine-tagged syringolin A derivative Rh-SylA

4.2.1.1. Synthesis of Rh-SylA

Activity-based protein profiling (ABPP) is a widely used method for determining the activity state of enzymes in complex proteomes *in vitro* and *in vivo*.[4] To this end, small molecules named activity base probes (ABPs) are applied to complex proteomes. These probes are based on irreversible inhibitors that covalently modify enzymes only in their active states. For visualization and target identification, ABPPs also contain a reporter group that is separated from the inhibitor by a linker region. As reporters, often biotin and/or rhodamine are used. As X-ray studies proved an irreversible inhibition of the proteasome by syringolin A, suitable derivatization of SylA should potentially lead to an ABP suitable for profiling proteasome activity. Moreover, such a probe could be used to elucidate the target selectivity of syringolins in complex proteomes.

To date, several proteasome-specific probes with different tag systems have already been reported.[76] In previous ABPP experiments, it turned out that fluorescently labeled ABPs are most versatile in biological applications. Therefore, the synthesis of a fluorescent SylA-based probe was envisaged. As a fluorescent tag, rhodamine was chosen as rhodamine-fluorescence can be straightforwardly detected and imaged in live cells as well as on SDS gels. To this end, the carboxyl group of SylA was chosen to be linked to the fluorophore as previous inhibition studies with SylA derivatives showed that this functional group is amenable to modification without significant loss of inhibitory potency.

Consequently, following the published procedure of Cravatt[77], the rhodamine-pentylamine hydrochloride salt **95** was synthesized and coupled to SylA to afford Rh-SylA (**96**) in a straight-forward manner.

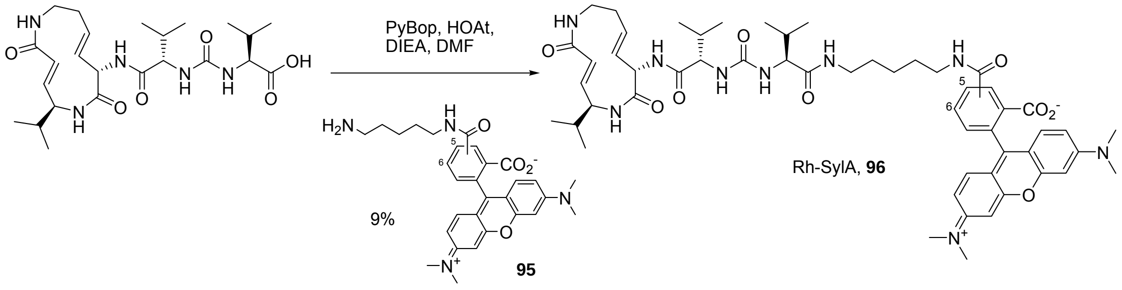

Scheme 25. Synthesis of the rhodamine-tagged SylA analogue Rh-SylA (**96**).

4.2.1.2. *ABPP studies with Rh-SylA with mammalian cell lysates*

With this probe in hand, the group of the Prof. Overkleeft performed labeling experiments with EL4 cell lysates. EL4 is a murine cell line that expresses both the constitutive as well as the immunoproteasome. Labeling of all proteasomal subunits by means of fluorescently tagged proteasome inhibitors has already shown the potential of this analytic strategy as depicted in figure 13.

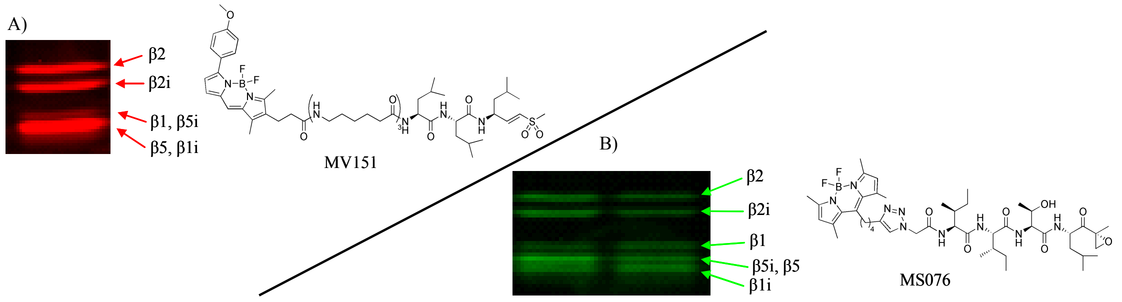

Figure 13. Magnification of in-gel fluorescence analyses showing labeled proteasome β subunits of murine EL4 cell lysates with fluorescent probes and the chemical structures of the used probes. A) Proteasome labeling pattern obtained by using the red fluorescent probe MV151 (λ_{ex}=523 nm, λ_{em}=580 nm). B) Proteasome labeling pattern obtained by using the green fluorescent probe MS076 (λ_{ex}=488 nm, λ_{em}=520 nm).

In order to gain insight into the covalent labeling specificity of Rh-SylA, a dilution series of Rh-SylA in the concentration range 10 nM to 10 μM was prepared and added to the EL4 cell lysate (20 mg per lane), incubated for 1 h at 37 °C and then analyzed by SDS-gels (Figure 14).

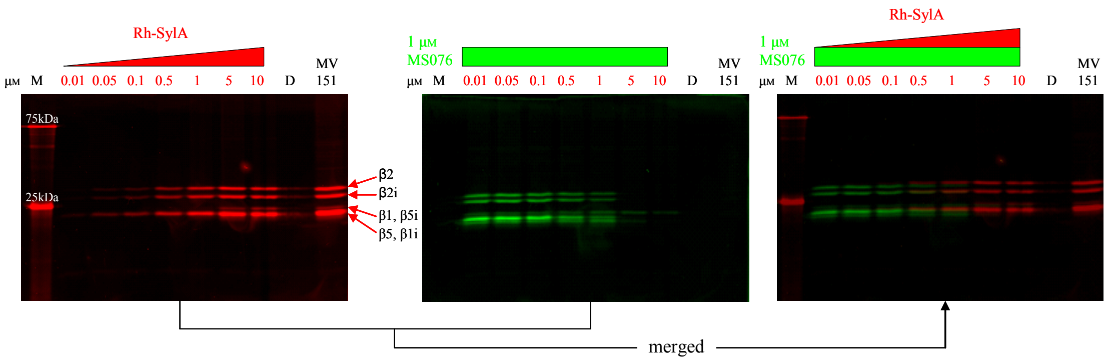

Figure 14. In-gel fluorescence analysis of Rh-SylA-labelled murine EL4 cell lysates in the presence and absence of known proteasome inhibitors or ABP. Concentration-dependent labelling of the proteasome by Rh-SylA. The left panel shows the red rhodamine channel, corresponding to Rh-SylA, the central panel corresponds to MS076 and the green BODIPY-FL channel, and the right panel is the merged image. Denatured (D) lysate and proteasome labelling with MV151 were used as negative and positive controls, respectively. M: protein molecular weight marker.

The left panel of Figure 14 shows the fluorescent signals resulting from rhodamine detection of Rh-SylA binding to proteins of the cell lysate. Labeling was detectable at a concentration of 50 nM Rh-SylA and increased gradually in a concentration-dependent manner until saturation was reached at around 5 µM. Already above 1 µM of Rh-SylA, four bands were visible. These bands corresponded to those obtained from profiling cell lysates with the known proteasome probe MV151. It is worth noting that Rh-SylA interfered with both the constitutive proteasome and the immunoproteasome catalytic β subunits. Moreover, the denatured control sample provided no labeling, indicating an activity-dependent labeling. Most strikingly however, no additional bands were detected in the gel, indicating a highly selective labeling of proteasome subunits by Rh-SylA.

To further characterize the potency and specificity of Rh-SylA, a second experiment was performed. To this end, again a dilution series of Rh-SylA was incubated with EL4 cell lysate for 1 h at 37 °C. Then, a 1 µM solution of MS076 that is tagged with a Bodipy fluorophore was added, incubated again for 1 h at 37 °C and then analyzed by SDS gel analysis. Importantly, the Bodipy and rhodamine fluorophore have different fluorescent properties, allowing a simultaneous detection on the gel depending on the emission and excitation wavelengths used during analysis.

As expected, MS076 fluorescence in this experiment decreased with increasing Rh-SylA concentration; this indicates competition between the two compounds for the same protein target, i.e. the proteasome β subunits. A more thorough analysis of the obtained gel revealed that Rh-SylA completely blocked the β2 and β2i subunits already at a concentration of 5 µM while a Rh-SylA concentration of 10 µM was necessary to fully inhibit the β1 subunit. From the merged picture of the green and red signal (Figure 14, right panel) the identity of Rh-SylA and MS076-labelled bands became apparent, although the Rh-SylA-labeled bands resolved at a slightly higher molecular weight than the MS076-labelled bands due to the higher molecular weight of Rh-SylA. This experiment clearly demonstrated that Rh-SylA is a potent and specific proteasome activity-based probe (ABP).

Next, the known proteasome inhibitors Ada-Ahx$_3$-L$_3$-VS and bortezomib were used to elucidate if Rh-SylA is a suitable ABP for further biological experiments (Figure 15).

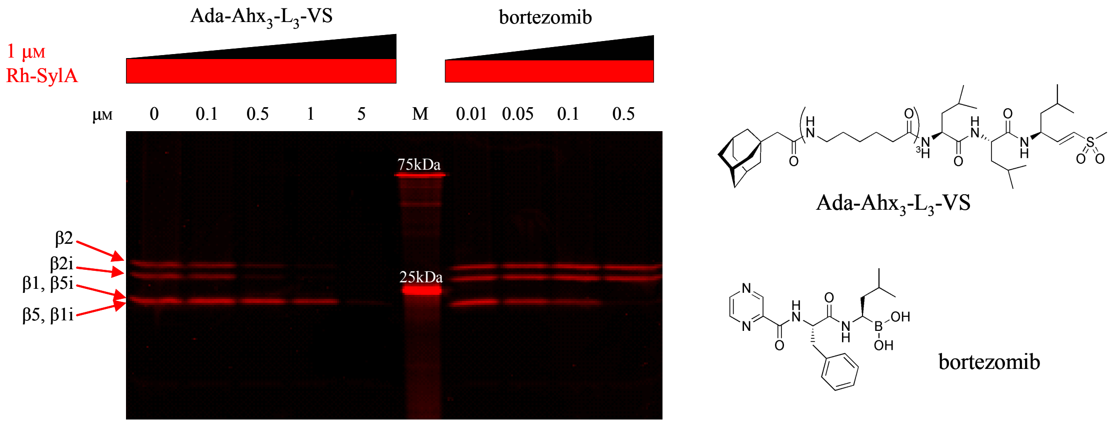

Figure 15. Competition assay with Rh-SylA (1 µM) in the presence of varying concentrations of the known proteasome inhibitors Ada-Ahx$_3$-L$_3$-VS and bortezomib.

To this end, protein (20 mg) from EL4 lysates were first incubated with increasing concentrations of competitors for 1 h at 37 °C and the residual proteasome activity was visualized by Rh-SylA. Figure 15 shows that Ada-Ahx$_3$-L$_3$-VS first bound to the β2 and β2i subunits and finally at a concentration of 5 µM, all proteasome subunits were fully blocked. In contrast, bortezomib efficiently blocked the constitutive and immuno-β1 and β5 subunits without inhibiting the β2 or β2i subunits.

Importantly, the observed difference in competition efficiency of Ada-Ahx$_3$-L$_3$-VS and bortezomib was in agreement with their known different inhibitory potency, indicating that Rh-SylA can indeed be used to evaluate inhibitors in complex proteomes.[78]

The group of Prof. Driessen then used Rh-SylA to evaluate its potential as an anticancer agent. To this end, protein (40 mg) from total cell lysates of parental and bortezomib-adapted HL60 (myeloid leukemia), ARH77 (plasmocytoid lymphoma) and AMO-1 (myeloma) cell lines were profiled for proteasome labeling with Rh-SylA (Figure 16).

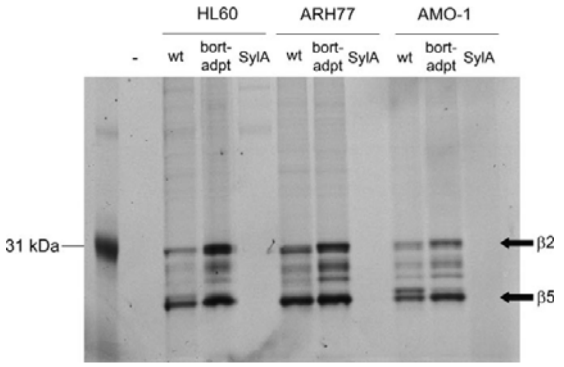

Figure 16. Profiling with Rh-SylA in wild-type (wt) and bortezomib-adapted (bort-adpt) HL60, ARH77 and AMO-1 leukemia cell lines. Unlabelled SylA (SylA) was used as negative control in all three wild-type cell lines.

These studies revealed that Rh-SylA also labeled and thus inhibited the proteasome in leukemic cell lines. Moreover, Rh-SylA also efficiently labeled proteasomal subunits in bortezomib-adapted cell lines in the presence of RhSylA concentrations usually used during therapeutic interventions. In accordance with the biochemical inhibition assays of SylA with human 20S proteasome and the EL4 profiling experiments, Rh-SylA thereby most efficiently bound to the β5 subunit, followed by the β2 subunit while binding to β1 was much weaker. Besides proteasome-derived bands, no further protein bands appeared; this again indicates selective labeling of the proteasome even in bortezomib-adapted cells.

The findings of both profiling experiments with mammalian cell lysates proved the high selectivity of Rh-SylA and thus SylA for the proteasome. No off-target labeling was detected in any of the performed experiments. Moreover, the studies with the leukemic cell lines revealed a promising biological activity of syringolins, i.e. their covalent reaction with proteasomes from bortezomib-adapted cell lines. These studies therefore indicated that syringolins might represent a lead structure capable of overcoming Bortezomib resistance resulting from proteasome mutation.

4.2.1.3. The use of Rh-SylA for plant pathogen interaction studies

The van der Hoorn group also used Rh-SylA in their studies of plant-pathogen interactions. As a prerequisite to elucidate the biological role of syringolins in these interactions, they determined the target of Rh-SylA in plants. As expected, their study with Rh-SylA proved selective targeting of the plant proteasome. Moreover, Rh-SylA can also be used as an ABP, demonstrated by their use of Rh-SylA to monitor the activity of the proteasome in *Nicothiana benthamiana*. Thus, labeling of the three proteasome subunits by Rh-SylA could be observed in *N. benthamiana* extracts and pre-incubation with SylA or proteasome inhibitor epoxomicin prevented this labeling, showing the competition between the inhibitors and the fluorescent probe. Future applications of Rh-SylA in plant-pathogen interaction studies are currently performed in their laboratory.

4.2.2. Structure-activity relationships of syringolins

4.2.2.1. Structural determinants of potency and subsite selectivity deduced from structural and biochemical studies

A thorough evaluation of the biochemical proteasome inhibition potencies of the synthesized analogues SylA and SylB as well as the published values for the natural product GlbA revealed several interesting points.

The most potent inhibitor of these three natural products is glidobactin A (GlbA, **3**), inhibiting the chymotryptic activity with a K_i' of 49 ± 5.4 nM and the tryptic activity with a K_i' of 2.0 ± 0.6 μM. Accordingly, GlbA is 15-fold more active than SylA for the chymotryptic and the tryptic activity (Table 5). In contrast, GlbA does not inhibit the caspase-like activity whereas SylA moderately affects this activity.

SylB however is ten-times less active than SylA, probably as a result of the lacking double bond in the lysine residue, thereby significantly reducing the macrocyclic ring strain that activates the α,β-unsaturated amide moiety for Michael-type additions. Alternatively, also different structural pre-organizations for an efficient nucleophilic attack of the proteasome active site residue might represent an explanation of the observed different activities. However, SylB shows a similar subsite selectivity as GlbA. While SylB addresses the chymotrypsin- and trypsin-like activity, no binding to the caspase-like subsite is observed.

Table 5. Apparent K_i' and k_{assoc} values for the chymotrypsin-, trypsin-, and caspase-like activity of human 20S proteasome.

Inhibitor	Inhibited activity	K_i', nM	k_{assoc}, M^{-1} s^{-1}
SylA	C-L	1,016 ± 179	828 ± 195 (n = 3; 100 – 200 nM)
	T-L	10,300 ± 1,400	83 ± 2.9 (n = 3; 1.25 – 5 μM)
	Cas-L	n.d.	15.8 ± 3.7 (n = 3; 20 – 40 μM)
SylB	C-L	7,778 ± 2,259	122 ± 31.7 (n = 3; 1.5 – 3.1 μM)
	T-L	107,800 ± 39,200	4.6 ± 0.7 (n = 3; 50 – 100 μM)
	Cas-L	n.a.	n.a.
GlbA	C-L	49 ± 5.4	3,377 ± 341 (n = 6; 40 – 60 nM)
	T-L	2,000 ± 600	141 ± 21 (n = 6; 250 – 500 nM)
	Cas-L	n.a.	n.a.
SylA methyl ester (52)	C-L	757 ± 148	1,925 ± 433 (n = 3; 100 – 200 nM)
	T-L	18,700 ± 500	186 ± 30 (n = 3; 1.25 – 2.5 μM)
	Cas-L	n.d.	10.2 ± 1.4 (n = 3; 25 – 50 μM)

The published co-crystallization experiments of SylA or GlbA with the yeast 20S proteasome revealed similar binding affinities: whereas in these structures SylA bound to all three catalytic subunits, GlbA occupied only the active site clefts of the chymotryptic and tryptic activities.[79] During the course of these studies, the group of Prof. Groll were also able to elucidate the complex structure of SylB:yeast 20S proteasome with the help of the synthesized SylB derivative (Figure 17A/B). This structural study revealed a surprising accordance with the structural studies from GlbA with the proteasome. Also SylB only accommodated the chymotrypsin- and trypsin-like subsites and thereby adopted a similar conformation as GlbA. In contrast, the conformation of SylA in complex with the proteasome is slightly different.

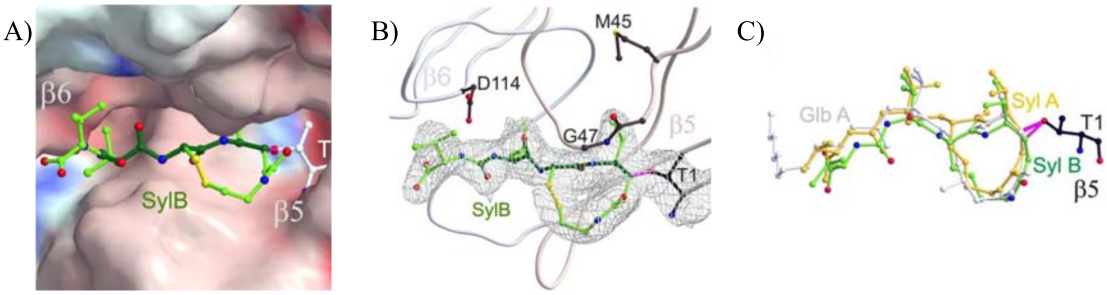

Figure 17. X-ray analysis of the complex of SylB and the 20S proteasome and comparison with other syrbactins. A) Electrostatic potential surface [contoured from +15 kT/e (intense blue) to -15 kT/e (intense red)] of SylB covalently bound to β5; B) Stereo representation of SylB bound to the chymotryptic like active site in complex with 20S proteasome (rose, subunit β5; gray, subunit β6); C) Structural superimposition of SylA (yellow), SylB (green), and GlbA (light gray).

The analysis of the biochemical inhibition potencies in conjunction with the structural data from co-crystalization experiments conjectured that the observed structural determinants of potency and subsite selectivity are a result of two main features:

First, as the X-ray analysis of SylB and GlbA revealed that the macrocyclic lactam moieties of SylB and GlbA adopt an almost identical binding mode (Figure 17C) and as no significant binding contribution is seen from the supplemental hydroxyl group at the lysine residue of GlbA, the exocyclic lipophilic alkyl chain seems to account mainly for the much higher potency of GlbA. In fact, the lipophilic chain shows well-defined electron density in the co-crystal structure of GlbA with the yeast 20S proteasome, which is in agreement with the tight binding to a distinct hydrophobic pocket. A similar hydrophobic pocket has been elucidated in the co-crystal structures of the yeast 20S proteasome with the proteasome inhibitor fetullamide B. As a consequence, these structures pinpoint that a lipophilic derivatization of syringolins at their N-terminal end should lead to significant higher inhibition potencies.

Second, the co-crystal structures of SylA, SylB, and GlbA with the yeast 20S proteasome provide also a possible explanation for the observed subsite selectivity. A structural superimposition of SylA bound to the β5 subunit with SylA bound to β1 reveals an identical binding conformation for SylA in both subsites (Figure 18).

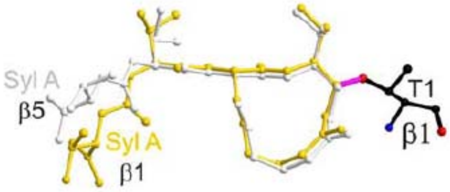

Figure 18. Structural superposition of SylA bound to subunit β5 with SylA bound to subunit β1. Both threonines are colored in black and the covalent bond between protein and inhibitor molecules is highlighted in magenta.

A docking of the structural conformation of SylB and GlbA bound to β5 into the β1 subunit, however, indicates a disturbed antiparallel β-sheet interaction, displacing the peptide backbone from the ideal alignment with the active site cleft and thereby significantly lowering binding affinity and thus subsite occupancy. Moreover, the similar conformation and subsite selectivity of SylB and GlbA in the co-crystal structures indicate that the structure of the different types of macrolactams is the driving factor in subsite selectivity. GlbA- and SylB-type macrocycles allow binding only to the chymotrypsin- and trypsin-like subsites while SylA enables binding to all three subsites.

With an established synthesis of the SylA macrocycle in hand, an experimental validation of these two hypotheses was started, aiming at the synthesis of N-terminally with lipophilic chains modified syringolins. A preliminary test was performed on the intermediate **52** (SylA methyl ester) to analyze the impact of the SylA free carboxylic acid moiety on proteasome inhibition. As expected from the X-ray analysis of SylA in complex with the yeast 20S proteasome, the free carboxylic acid moiety is not required for potent inhibition because both SylA and SylA methyl ester (**52**, Table 5) inhibit all proteolytic activities of the proteasome in a similar range.

4.2.2.2. Synthesis of a lipophilic analogue

The modified derivative with the N-terminal lipophilic group was designed in the following manner. First, as already mentioned in the section 4.1.2.2.4, modification of the P3 residue has been shown to have a strong impact on the overall biological activity of the molecule. Consequently, this valine residue was kept in the target molecule. Second, in order to make a direct comparison with natural SylA, also the urea functionality was maintained in the molecule and not an amide group as in GlbA.

Third, a lipophilic group was chosen that featured as many carbon atoms as the side chain of GlbA, however for ease of synthesis without double bonds.

To set this into practice, compound **48** from the previous synthesis (Section 4.1.2.2.2) was deprotected and coupled to Boc-(L)-valine to afford the intermediate **97** which after Boc-deprotection was treated with decyl isocyanate to obtain the compound **98**.

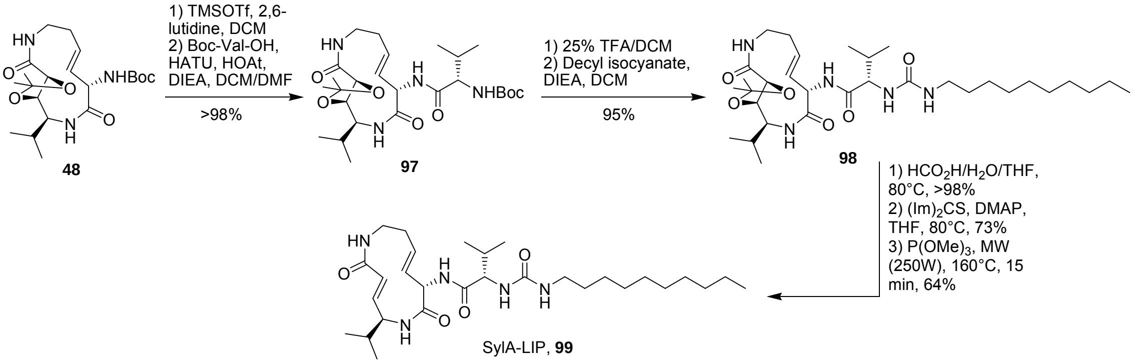
48
1) TMSOTf, 2,6-lutidine, DCM
2) Boc-Val-OH, HATU, HOAt, DIEA, DCM/DMF
>98%
97
1) 25% TFA/DCM
2) Decyl isocyanate, DIEA, DCM
95%
98
1) HCO2H/H2O/THF, 80°C, >98%
2) (Im)2CS, DMAP, THF, 80°C, 73%
3) P(OMe)3, MW (250W), 160°C, 15 min, 64%
SylA-LIP, 99

Scheme 26. Synthesis of the SylA lipophilic analogue SylA-LIP (**99**).

Accordingly, the desired lipophilic derivative **99** was obtained in only three steps in good yields (Scheme 26). Biochemical assay evaluation proved this derivative as the most potent inhibitor of the syrbactin derivatives synthesized so far, inhibiting the chymotryptic activity of the human 20S proteasome with a K_i' of 8.65 ± 1.33 nM, which is > 100-fold more potent than SylA and > 6-fold compared to GlbA (Table 6). Similar inhibition improvements were observed for the trypsin- (K_i' of 79.6 ± 29.3 nM) and for the caspase-like activity (K_i' of 943 ± 100 nM), ranking this derivative among the most potent proteasome inhibitors described so far. Importantly, the potent inhibition of the caspase-activity furthermore proved that SylA-type macrocycles allow inhibition of all three subsites.

Table 6. Apparent K_i' and k_{assoc} values for the chymotrypsin-, trypsin-, and caspase-like activity of human 20S proteasome.

Inhibitor	Inhibited activity	K_i', nM	k_{assoc}, M^{-1} s^{-1}
GlbA	C-L	49 ± 5.4	3,377 ± 341 (n = 6; 40 – 60 nM)
	T-L	2,000 ± 600	141 ± 21 (n = 6; 250 – 500 nM)
	Cas-L	n.a.	n.a.
SylA-LIP (99)	C-L	8.65 ± 1.33	40,477 ± 2,333 (n = 3; 6.3 – 12.5 nM)
	T-L	79.6 ± 29.3	7,947 ± 1,321 (n = 3; 31.3 – 62.5 nM)
	Cas-L	943 ± 100	n.d.

4.2.2.3. Synthesis of pegylated analogues

Despite its high biochemical activity, the introduction of the liphophilic side chain significantly increased the hydrophobicity of the molecule. An alternative approach which maintains the high affinity but which is better water soluble was sought. It was rationalized that pegylation instead of acylation with long hydrophobic alkyl chains might solve this problem. Effectively, the pegylation of small molecules is a common strategy to enhance the molecular mass or/and the solubility of active molecule and led to numerous drugs.[80] Consequently, a synthesis of two pegylated SylA-LIP analogues was undertaken.

In analogy to the structure of SylA-LIP, the analogue **108** (SylA-PEG1) was chosen as a target structure. In this compound, the PEG-linker has the same length as the liphophilic chain in SylA-LIP. In addition, a second derivative **109** (SylA-PEG2) was synthesized. This derivative resembles more to SylA, featuring the divaline urea moiety that however was elongated by a short PEG chain on its C-terminal end.

For their synthesis, first the required poly(ethylene oxide) amines **104** as well as **105** were prepared, thereby following the procedure described by Marks and coworkers (Scheme 27).[81] To this end, the corresponding PEG starting material **100** and **101** were converted into tosylates. Nucleophilic substitution with sodium azide in DMF, followed by Staudinger reduction then led to the desired amine **104** and **105**.

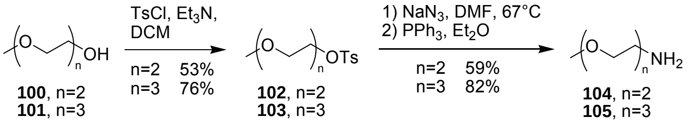
TsCl, Et3N, DCM
n=2 53%
n=3 76%
1) NaN3, DMF, 67°C
2) PPh3, Et2O
n=2 59%
n=3 82%
100, n=2
101, n=3
102, n=2
103, n=3
104, n=2
105, n=3

Scheme 27. Synthesis of two poly(ethylene oxide) amines, **104** and **105**.

The amine **105** was then converted into a PEG-succinimidyl carbamate derivative **106** upon treatment with *N,N*'-disuccinimidyl carbonate.[82] In parallel, SylA synthesis intermediate **58** was coupled to a Boc-(L)-valine residue and further Boc-deprotected to afford the ammonium salts **107** which were directly employed to react with the derivative **106** to obtain **108** (SylA-PEG1) in 68% yield (Scheme 28).

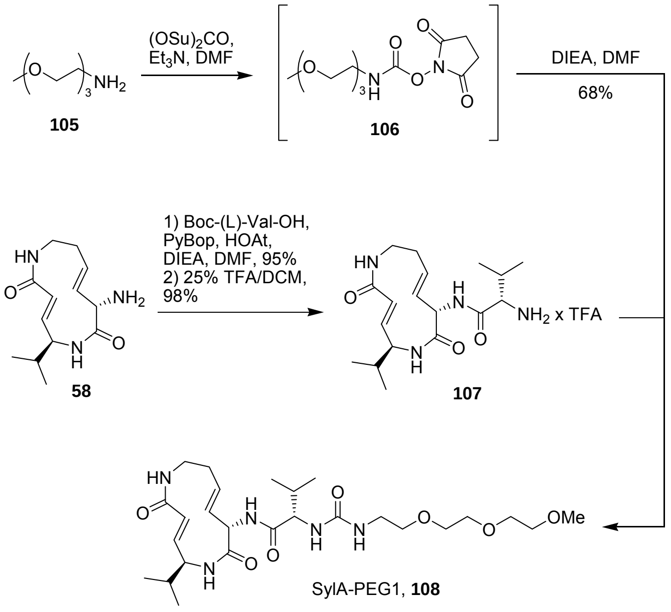
105
(OSu)2CO, Et3N, DMF
106
DIEA, DMF
68%
58
1) Boc-(L)-Val-OH, PyBop, HOAt, DIEA, DMF, 95%
2) 25% TFA/DCM, 98%
NH2 x TFA
107
SylA-PEG1, 108

Scheme 28. Synthesis of SylA analogue **108** (SylA-PEG1).

For the synthesis of SylA-PEG2, amine **104** was readily coupled to SylA to afford the PEG analogue **109** (SylA-PEG2) (Scheme 29).

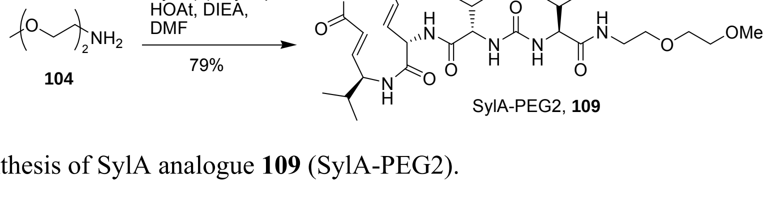
SylA (1), PyBop, HOAt, DIEA, DMF
79%
104
SylA-PEG2, 109

Scheme 29. Synthesis of SylA analogue **109** (SylA-PEG2).

The biological activities of these two new inhibitors were then analyzed in a biochemical inhibition assay. Disappointingly, both pegylated compounds did not fulfill the expectations. Although both molecules proved to be slightly more potent than SylA, their inhibition potencies were dramatically lower than those of SylA-LIP (Table 7). Indeed, SylA-PEG1 inhibited the chymotryptic activity of the proteasome with a K_i' of 586 ± 69 nM, while SylA-PEG2 inhibited the same activity with a K_i' of 401 ± 37 nM. Thus, both compounds are roughly 50-times less potent than SylA-LIP. This led to the conclusion that the hydrophobic alkyl chain cannot be replaced by the more hydrophilic PEG chains. Consequently, alternative strategies for obtaining high affinity but also water soluble SylA derivatives are required.

Table 7. Apparent K_i' values for the chymotrypsin-like activity of human 20S proteasome.

Inhibitor	**Inhibited activity**	**K_i', nM**
SylA-LIP **(99)**	C-L	8.65 ± 1.33
SylA-PEG1 **(108)**	C-L	586 ± 69
SylA-PEG2 **(109)**	C-L	401 ± 37

Complementary, these two new inhibitors were also tested in an *in vitro* labeling assay originally developed by the group of Renier van der Hoorn. In this assay, protein extracts of *Arabidopsis thaliana Col-0* in the presence of a sodium acetate buffer pH 7.0 and L-cystein (1 mM) were incubated with a concentration range of the inhibitor for 30 min and then treated with a fluorescent probe (MVB072, 1 μM) for 2 h, followed by analysis with SDS-PAGE gels. Fluorescently labeled proteins were visualized by in-gel fluorescence scanning. In the figure 19 are depicted the gel sections where the three catalytic activities of the proteasome (β2, β5 and β1 from up to down) are located by using MVB072 as a probe for the positive control. NPC (No Probe Control) lane is the negative control and proves the absence of fluorescence without probe. The inhibition of the proteasome subunits are characterized by a lower fluorescence.

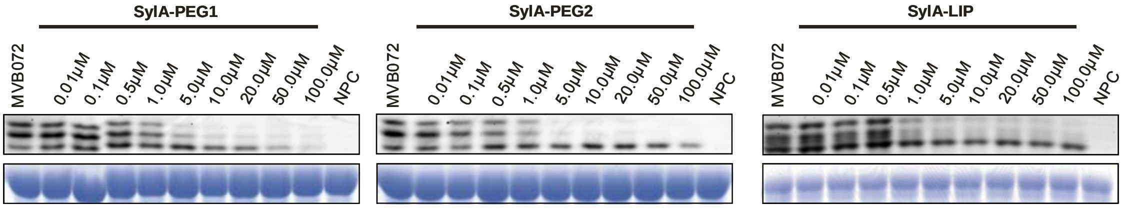

Figure 19. Competition assay on *Arabidopsis thaliana* extracts with MVB072 (1 μM) in the presence of varying concentrations of SylA-based proteasome inhibitors: SylA-PEG1 (Left panel); SylA-PEG2 (Center panel); SylA-LIP (right panel).

This assay revealed that SylA-PEG2 showed a complete inhibition of the β2 and β5 subunits at a concentration of 5 μM. The activity of SylA-PEG1 towards these two subunits was comparable and both molecules can be qualified as weak inhibitors of the β1 subunit, although SylA-PEG1 totally inhibited the β1 subunit at a concentration of 100 μM. To compare the potency of these two inhibitors with SylA-LIP, the same experiment was also performed with SylA-LIP. SylA-LIP already inhibited the β2 and β5 subunits at a concentration of 1 μM and showed a weak inhibition of the β1 subunit at 5 μM. Consequently, these experiments confirmed the results of the biochemical assay: Indeed, the newly synthesized pegylated analogues are less active than the lipidated analogue SylA-LIP which indicates that the linear carbon chain cannot be replaced by a polyethylene glycol chain. Obviously, and in agreement with the biochemical assay, lipophilic interactions between the ligand and this area of the binding pocket are necessary and therefore this structural determinant should be considered for the design of future analogues.

Additionally, a direct comparison of the two pegylated inhibitors confirmed previous conclusions. As SylA-PEG1 as well as SylA-PEG2 displayed almost similar inhibiton potency, the influence of a P4 residue on the overall inhibition is rather weak. Consequently, SylA based proteasome inhibitors can be shortened by this residue without significant loss of biological activity.

Although the biochemical and the plant cell assays were rather disappointing, the pegylated derivatives along with SylA-LIP were also tested in cell-based assay which was performed in the laboratory of Prof. Bachmann at the University of Hawaii. These assays revealed again SylA-LIP as the most potent inhibitor, whereas SylA-PEG1 and SylA-PEG2 were much less active.

4.2.2.4. Synthesis of a SylA-GlbA hybrid

The mimicry of structural features of GlbA already proved as a potent approach for obtaining SylA derivatives with improved inhibition potency. In order to fully evaluate the influence of the GlbA's exocyclic chain, the synthesis of a hybrid of both molecules was undertaken. For this purpose, an approach in which the macrocycle of SylA was coupled to the side chain of GlbA was developed (Scheme 30).

The synthesis started with the synthesis of the lipophilic acid moiety of GlbA. To this end, commercially available phophonate **110** was reacted with octanal in a Horner-Wittig-Emmons reaction, following essentially the procedure of Kishi.[83] The resulting ester **111** was then saponified with lithium hydroxide in a mixture of methanol, water and THF to yield the desired acid **112** (Scheme 30, entry 1).

With this building block in hand, the synthesis continued with a coupling of a protected threonine Boc-Thr(O^{t}Bu)-OH residue to the SylA macrocycle, thereby yielding intermediate **113.** Cleavage of the Boc- and *t*BuO-ester was then achieved with TFA in DCM, followed by coupling of the acid **112** to afford the analogue SylA-GlbA **114** (Scheme 30, entry 2).

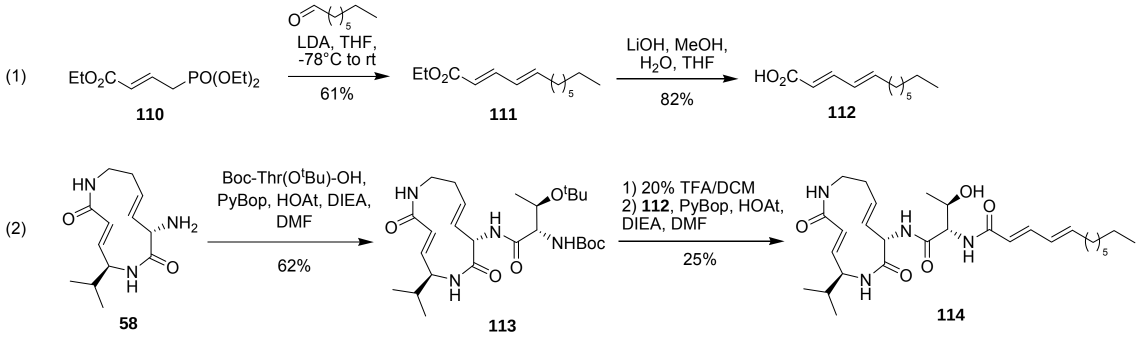

Scheme 30. (1) Synthesis of building block **112**; (2) Synthesis of SylA analogue **114** (SylA-GlbA).

After synthesis of SylA-GlbA, the activity of this new analogue was evaluated with the standard biochemical inhibition assay. Intriguingly, this derivative proved as potent as SylA-LIP (Table 8). Accordingly, SylA-GlbA is with a factor of 4 more potent than GlbA which indicated clearly that SylA's macrocycle probably as a result of its higher ring strain is more suitable for proteasome inhibition than the macrocycle of GlbA.

Table 8. Apparent K_i' and k_{assoc} values for the chymotrypsin-, trypsin-, and caspase-like activity of human 20S proteasome.

Inhibitor	Inhibited activity	K_i', nM
GlbA	C-L	49 ± 5.4
	T-L	2,000 ± 600
	Cas-L	n.a.
SylA-GlbA (114)	C-L	12.5 ± 1.6
	T-L	136.9 ± 12.4
	Cas-L	n.d.
SylA-LIP (99)	C-L	8.65 ± 1.33
	T-L	79.6 ± 29.3
	Cas-L	943 ± 100

Despite the obvious differences in the exocyclic chain of SylA-LIP and SylA-GlbA, the potency of both molecules is almost similar for the inhibition of the β2 and β5 catalytic subunits. This leads to three preliminary conclusions on structural determinants of the proteasome inhibition (1) the two unsaturations of the linear carbon chain of the SylA-GlbA analogue are not necessary to achieve potent inhibition as SylA-LIP does not contain them, (2) the urea functionality of SylA is also not required for potent inhibition as neither GlbA nor the SylA-GlbA hybrid does contain such a moiety, and (3) the exchange of the SylA's valine residue in P3 by a threonine residue does not play an important role to enhance the affinity of the inhibitor.

To complete the biological evaluation of this inhibitor, a preliminary cell-based assay has been undertaken by the Bachmann laboratory to evaluate its potential use. It revealed that SylA-GlbA appears much more potent than SylA-LIP in these assays, reaching the potency achieved with GlbA. These findings highlight that further syntheses of analogues of the SylA-GlbA type might lead to promising anticancer agents.

4.3. A bicyclic hydantoin as an activity-based probe: discovery of a new GAPC inhibitor

During the synthesis of SylA, an undesired bicyclic hydantoin derivative **61** (MRL) was formed (see section 4.1.2.2.3). It was furthermore shown that its formation was highly dependent on the employed reaction conditions. As this bicyclic hydantion compound interestingly consists of an unprecedented and rather complex scaffold that contains a potentially reactive α,β-unsaturated Michael system, a study of its potential targets in complex proteomes was started.

It was envisaged that activity-based protein profiling as in the case for syringolin A (see section 4.2.1.2) might enable the desired target identification. To this end, the conversion of the hydantoin into a probe by attachment of a suitable tag was required. As a tag, a terminal alkyne moiety was chosen, that can furthermore by derivatized in 'click-reactions' to easily attach other tags such as biotin or fluorophores.

The synthesis of a tagged version of biotin and rhodamine was therefore investigated and following an adaptation of Cravatt's protocol, [84] led to rhodamine-tagged azide **119** as well as biotin-tagged azide **121** in good yields (Scheme 31).

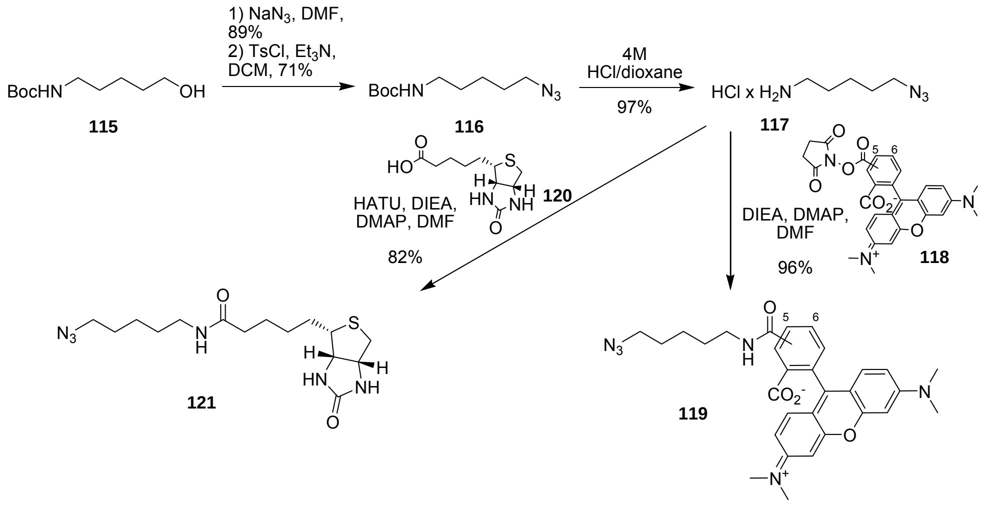
BocHN OH
115
1) NaN3, DMF, 89%
2) TsCl, Et3N, DCM, 71%
BocHN N3
116
4M HCl/dioxane
97%
HCl x H2N N3
117
HO
S
H
H
HN NH
O
120
HATU, DIEA, DMAP, DMF
82%
DIEA, DMAP, DMF
96%
118
N3 N H O S H H HN NH O
121
N3 N H O 5 6 CO2- N O N+
119

Scheme 31. Synthesis of rhodamine- and biotin-tagged azides **119** and **121**.

To introduce the orthogonal alkyne tag to the bicyclic hydantoin **61**, the NH proton of the hydantoin moiety was deprotonated with potassium carbonate in acetone and immediately alkylated with propargyl bromide to afford compound **122** (Scheme 32).[85]

Then, following the procedure of Fokin,[86] alkyne-tagged compound **122** was converted into a rhodamine-tagged derivative **124** by copper(I)-catalyzed 'click-reaction' with rhodamine-tagged azide **119**. Following the same procedure, also a biotin-tagged derivative **123** was generated. These probes were named as Rh-MRL and Biot-MRL, respectively.

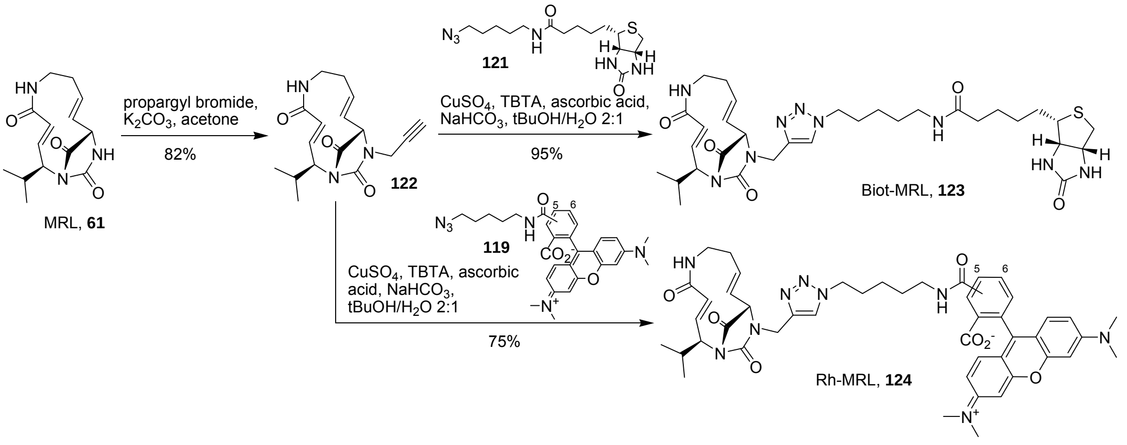
MRL, 61
propargyl bromide, K_2CO_3, acetone
82%
122
121
$CuSO_4$, TBTA, ascorbic acid, $NaHCO_3$, tBuOH/H_2O 2:1
95%
Biot-MRL, 123
119
$CuSO_4$, TBTA, ascorbic acid, $NaHCO_3$, tBuOH/H_2O 2:1
75%
Rh-MRL, 124

Scheme 32. Synthesis of the alkyne-tagged hydantoin **122** and the rhodamine- and biotin tagged probes **124** (Rh-MRL) and **123** (Biot-MRL), respectively.

With these probes in hand, protein extracts of *Arabidopsis thaliana Col-0* were incubated with the fluorescent probe **124** (Rh-MRL) for 2 h in the presence of (L)-cysteine (1 mM) and sodium acetate or Tris buffer in the pH range 3.5 to 10.5 in order to determine the physiological activity of the newly synthesized compound. SDS-PAGE gel analysis in conjunction with visualization by in-gel fluorescence scanning revealed an astonishingly specific binding of the probe **124** to a single target migrating around 43 kDa (Figure 20). Intriguingly, the labeling of the protein could be enhanced by increasing the pH of the buffer.

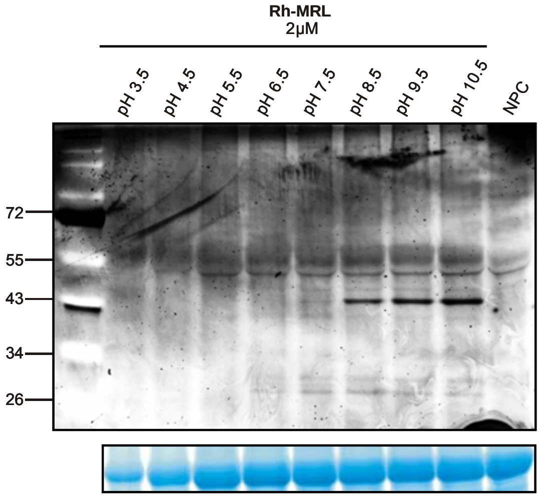
Rh-MRL
2µM
pH 3.5
pH 4.5
pH 5.5
pH 6.5
pH 7.5
pH 8.5
pH 9.5
pH 10.5
NPC
72
55
43
34
26

Figure 20. Labeling experiment of *Arabidopsis thaliana Col0* by activity-based probe **124** using a pH range 3.5 to 10.5. NPC: no probe control.

A subsequent concentration range experiment performed at pH 9.0 then demonstrated that Rh-MRL (**124**) labeling can be observed already at relatively low concentrations (1 µM). Furthermore, this experiment demonstrated again the specificity of the probe, as only one clear clear band at 43 kDa was visible at concentrations lower than 20 µM. If used at concentrations higher than 20 µM, the intensity of additionally appearing bands was much lower than the 43 kDa band. Surprisingly, as shown in lane 2 (Figure 21), this SylA-related compound did not target any of the 20S proteasome subunits, highlighting again the specificity of both scaffolds.

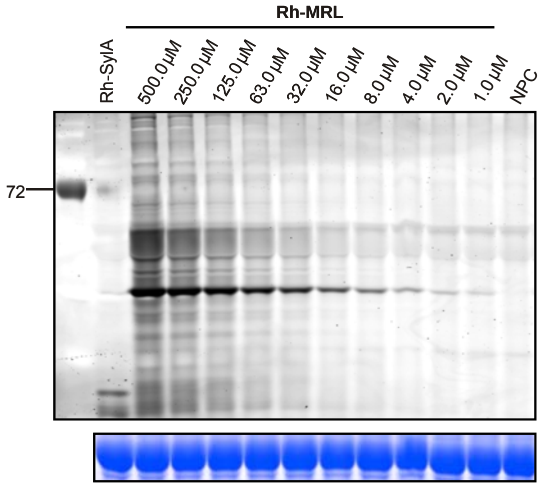
Rh-MRL
Rh-SylA
500.0µM
250.0µM
125.0µM
63.0µM
32.0µM
16.0µM
8.0µM
4.0µM
2.0µM
1.0µM
NPC
72

Figure 21. Labeling experiment of *Arabidopsis thaliana Col-0* by activity-based probe **124** using a concentration range of 1 µM to 500 µM. NPC: no probe control. Rh-SylA: labeling with Rh-SylA to localize 20S proteasome subunits.

After these promising results, Dr. Farnusch Kaschani from the van der Hoorn group performed a large scale labeling to identify the target of this class of compound by using the biotin-tagged derivative **123**. Following his reported procedure,[87] a concentrated cell culture protein extract of *Arabidopsis thaliana Col-0* was obtained and labeled with the fluorescent and biotinylated probes at pH 9. This led to the unambiguous identification of two glyceraldehyde-3-phosphate dehydrogenases C, GAPC-1 and GAPC-2, as the target of the bicyclic hydantoin probes.

The enzymes GAPC-1 and GAPC-2 are cytosolic highly conserved GAPDHs involved in the glycolysis and catalyze the conversion of glyceraldehyde-3-P to 1,3-bis-phosphoglycerate and belong to the family of glyceraldehyde-3-phosphate dehydrogenases (GAPDHs). All GAPDHs are photosynthetic enzymes that play an important role in the catalysis of the reductive step of the Calvin cycle by using either NADPH or NADH as coenzyme.[88] Recently, the generation of mutant lines of *Arabidopsis thaliana* revealed mitochondrial dysfunction and carbon flux modifications due to the lack of the gene encoding for the production of GAPC-1, leading to an alteration of plant and embryo development with decreased number of seeds.[89] This indicates that GAPC-1 is essential for normal fertility in *Arabidopsis* plants and that protein inhibition may lead to interesting properties in the field of plant protection.

On another hand, previous works on GAPDH inhibitors have reported the kinetics of inhibition by iodoacetate or again GAPDH as an off-target of the insulin mimic demethylasterriquinone B1.[90]

Inhibition of GAPDHs has also been reported as a chemotherapeutic approach for the treatment of the human diseases trypanosomiasis and leishmaniasis (Chagas's disease and sleeping sickness).[91] These parasitic infections are major health problems in several tropical and sub-tropical regions, affecting millions of people each year. Available drugs are becoming limited by suffering of poor efficacy, toxicity, resistance, and multiple side effects and therefore an urgent need emerged for the discovery of more effective and safer drugs. For these enzymes, the physiological pH of GAPDH activity was also determined. They are most active at basic pHs (7.5-9) as observed for GAPC labeling by Rh-MRL. Accordingly, Rh-MRL represents a highly potent lead structure for inhibiting GAPDHs. MRL-based compounds might therefore serve as a promising new class of chemotherapeutics for the treatment of serious human diseases although several additional studies for further verification are still necessary.

5. Summary and conclusions

5.1. *Summary and conclusions (English)*

In the last years, proteasome inhibitors have been investigated extensively due to their therapeutic anticancer potential. In fact, the first proteasome inhibitor Bortezomib has recently be approved by the FDA for treatment of relapsed and/or refractory multiple myeloma. Despite its success as an anticancer agent, Bortezomib therapy however is hampered by side effects and emerging drug resistance. Consequently, alternative lead structures with promising biological activities are still sought. As demonstrated during this PhD work, syringolin A (SylA), a 12-membered macrocyclic lactam isolated from strains of the plant pathogen *Pseudomonas syringae* pv. *syringae* (*Pss*), represents such a promising lead structure.

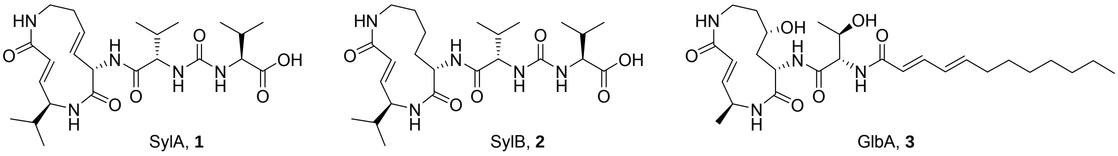

SylA, **1** SylB, **2** GlbA, **3**

Figure 22. The chemical structures of three members of the syrbactin natural product family: syringolin A (SylA, **1**), syringolin B (SylB, **2**) and glidobactin A (GlbA, **3**). All three compounds display potent proteasome inhibition activities.

During this PhD thesis, synthetic routes to members of the syrbactin family as well as to derivatives thereof have been developed. With the help of these compounds, structure-activity relationships for the inhibition of the eukaryotic proteasome by syringolins could be deduced. In addition, it could be shown that syringolins target the proteasome with a high selectivity even in complex proteomes. To reach these conclusions, several distinct subtasks were addressed within this PhD work:

At first, a total synthesis of SylB was achieved using a macrolactamization approach and employing starting materials from the natural chiral pool (valine and lysine derivatives). To complete the synthesis, careful orthogonal protection schemes were employed, enabling the synthesis of SylB in 9 steps starting from Boc-(L)-valine methyl ester with an overall yield of 7.8 % (Scheme 33). In addition to providing a model synthesis for syringolin A and to have access to an important syringolin derivative for structure-activity relationships, this synthesis also allowed the first elucidation of the configuration of all stereocenters of SylB.

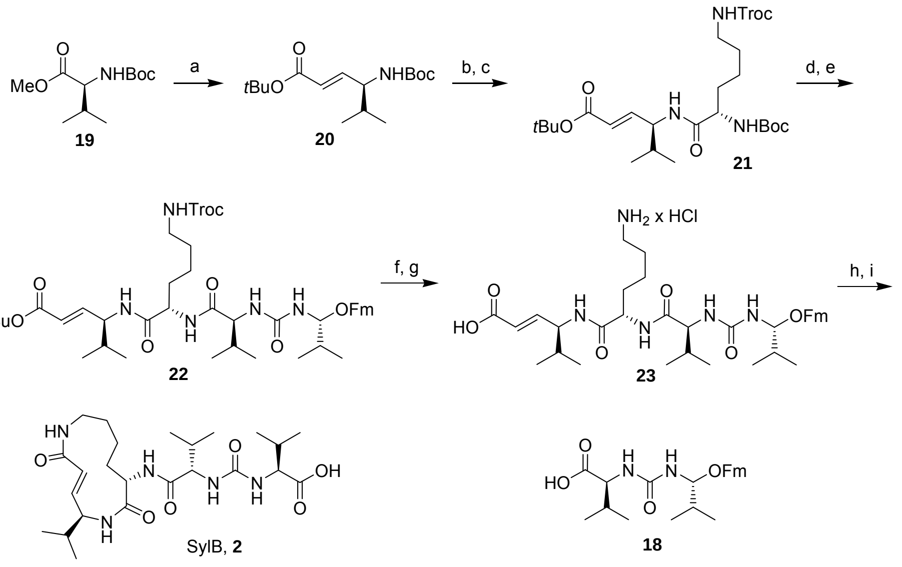

Scheme 33. Synthesis of syringolin B (SylB). Reagents and conditions: (a) (i) 1 M DIBAL-H/toluene (2 eq.), toluene, -78°C, 4 h; (ii) Ph_3PCHCO_2tBu (1.5 eq.), DCM, rt, 12 h, 84% (two steps); (b) 4 M HCl/dioxane, *t*BuOAc, 4 Å MS, -5 °C to 10 °C, overnight, 84%; (c) Boc-Lys(Troc)-OH (1.7 eq.), PyBop (3 eq.), HOAt (3 eq.), DIEA (6 eq.), DCM, 0 °C to rt, overnight, 85%; (d) 4 M HCl/dioxane, *t*BuOAc, 4 Å MS, -5 °C to 10 °C, overnight, 83%; (e) **18** (1.2 eq.), PyBop (1.5 eq.), HOAt (1.5 eq.), DIEA (3 eq.), DCM, 0 °C to rt, overnight, 75%; (f) Zn (150 eq.), THF/AcOH (1:1), 3 h, 97%; (g) (i) wet formic acid, overnight; (ii) aq. HCl, >98% (two steps); (h) PyBop (3 eq.), HOAt (3 eq.), DIEA (6 eq.), DMF, rt, 32 h, 30%; (i) piperidine/DMF (1:4), 73%.

Despite its success for the synthesis of SylB, the macrolactamization approach however unexpectedly failed for the total synthesis of SylA. Consequently, an alterative strategy was developed during this thesis. This led to a revised approach in which a ring closing metathesis (RCM) on a conformationally pre-organized linear precursor represented the key step (Scheme 34).

Accordingly, starting material **34** was first transformed into a 5-membered acetonide intermediate by dihydroxylation and acetonide formation. Subsequent iterative peptide couplings then led to an intermediate that cleanly underwent macrocyclization if the Grubbs 2nd generation catalyst was used.

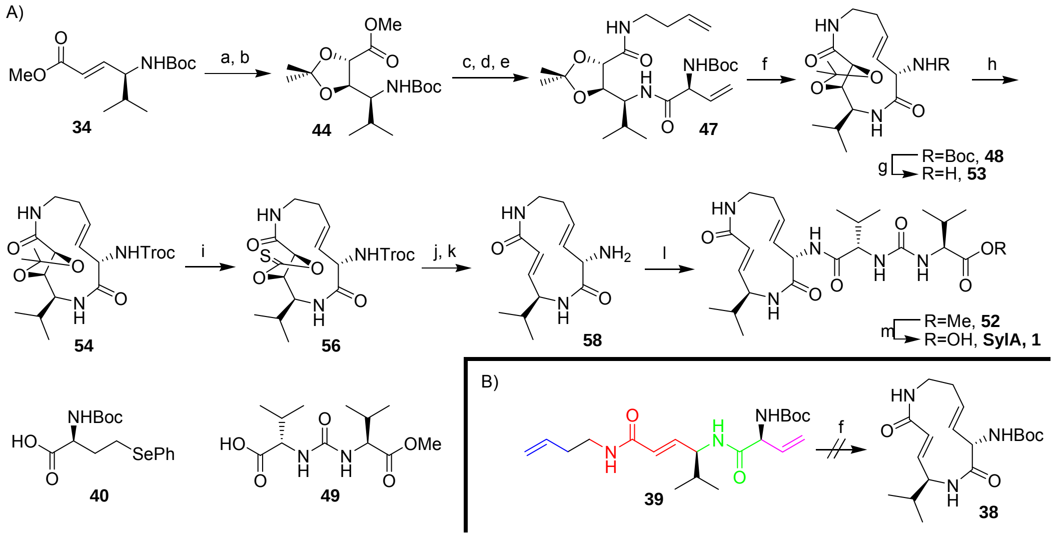

Scheme 34. A) Synthesis of syringolin A (SylA). Reagents and conditions: (a) OsO_4 (0.05 eq.), NMO (1.5 eq.), Ac_2O/H_2O (2:1), rt, 48 h, 85%; (b) 2,2-DMP (30 eq.), PPTS (0.05 eq.), DCM, 60°C, 5 h, >98%; (c) (i) 1 M aq. LiOH (3 eq.), $MeOH/H_2O$ (1:1), 0°C to rt over 30 min; (ii) 3-butenylamine hydrochloride (1.2 eq.), PyBop (1.5 eq.), HOAt (1.5 eq.), DIEA (2 eq.), DCM, 0°C to rt, overnight, 80% (two steps); (d) (i) 2,6-lutidine (2 eq.), TMSOTf (1.5 eq.), DCM, rt, 15 min; (ii) **40** (1.3 eq.), PyBop (1.5 eq.), HOAt (1.5 eq.), DIEA (2 eq.), DCM, 0°C to rt, overnight, 87% (two steps); (e) 30% aq. H_2O_2/DIEA (1:1), DCM, 50°C, 3 h, 93%; (f) Grubbs II catalyst (0.15 eq.), toluene, 90°C, 18 h, 49%; (g) 2,6-lutidine (2 eq.), TMSOTf (1.5 eq.), DCM, rt, 15 min; (h) 2,2,2-trichloroethyl chloroformate (1.1 eq.), $NaHCO_3$ (2 eq.), THF, 0°C to rt over 90 min, 81% (two steps); (i) (i) MW, 150W, 140°C, 30 min, *p*TsOH.H_2O (1 eq.), $MeOH/H_2O$/THF 2:2:1; (ii) $(Im)_2CS$ (10 eq.), DMAP (10 eq.), THF, 80 °C, overnight, 86% (two steps); (j) $P(OMe)_3$, 130°C, 2.5 h, 88%; (k) Zn (150 eq.), THF/AcOH (1:1), 3 h, >98%; (l) **49** (1.1 eq.), PyBop (1.2 eq.), HOAt (1.2 eq.), DIEA (2 eq.), DMF, 0°C to rt over 40 min, 95%; (m) $AlCl_3$ (8 eq.), methylethylsulfide, rt, 1 h, 92%. B) Attempted synthesis of the core macrocycle **38** using a RCM approach. The rigidity of the non-pre-organized precursor **39** is indicated by coloration of the different planar groups.

In a first synthetic approach to SylA, the exocyclic chain was directly attached to the Boc-deprotected derivative **48**, thereby completing the synthesis of SylA. However, this route was subsequently changed to a more convergent approach which facilitated derivative synthesis. In fact, preliminary biological studies indicated that modification of the exocyclic side chain can have dramatic influences on the overall activity. Consequently, a protecting group exchange at the stage of the ring-closed acetonide intermediate was performed which after acetonide-cleavage and Corey-Winter elimination afforded a fully functionalized SylA macrocycle. The corresponding free amine **58** was then coupled to several side chain residues to generate a small collection of derivatives (Figure 23) which were subsequently used to gain insights into the structure-activity relationships of syringolin-mediated proteasome inhibition. These studies for example led to a lipophilic SylA derivative (SylA-LIP) that proved as the most potent syringolin inhibitor known to date, being 100-times more potent than the natural product SylA.

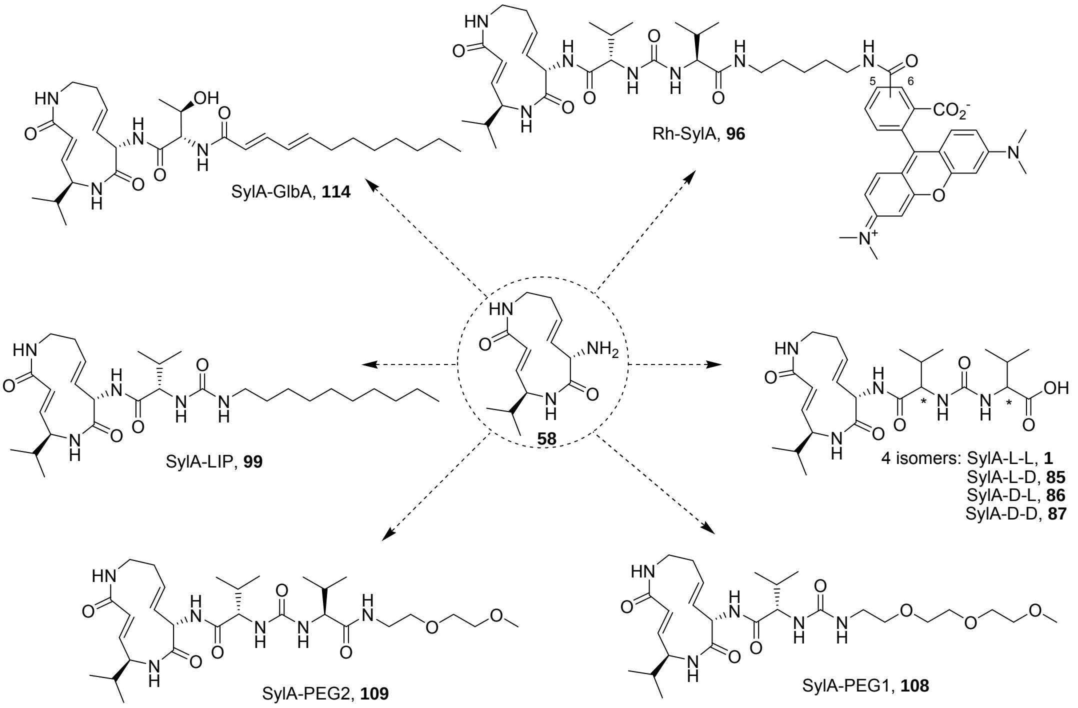

Figure 23. Chemical structures of synthesized SylA analogues by attaching different side chains to the fully functionalized SylA macrocycle.

The synthesized analogues have then been evaluated in diverse biological assays whose results are summarized in table 9.

In brief, these studies showed that release of macrocyclic ring strain and/or structural pre-organization are the driving force behind the potent proteasome inhibition observed with syringolins. This conclusion came from a comparison of the inhibition potencies of SylA and SylB. While structurally almost similar, SylB lacks the double bond of the dehydrolysine moiety, resulting in a much less ring-strained macrocycle that however is 10-times less active than the more ring-strained SylA.

In addition, studies with a lipophilic SylA derivative demonstrated that a lipophilic subsite exists in the 20S proteasome that can be addressed by appropriate derivatization of syringolins. These findings are in accordance with the higher inhibition potency of the syrbactin glidobactin A that seems to result from a binding of GlbA’s N-terminal lipophilic chain to this subpocket.

Finally, the studies revealed that syrbactins show pronounced proteasomal subsite selectivity. This selectivity seems to be directed by the constitution and therefore conformation of the macrocyclic ring system. However, future studies into this direction are still required to gain deeper insight into the underlying structure-activity relationships.

Table 9. Structure-activity relationship resulting from SylA-based analogues derived from different biological assays.

Compound	**Studied feature**[a]	**Analysis type**	**K_i' for inhibition of the chymotryptic activity [nM]**[b]	**Conclusions/Applications**
SylA: 4 isomers	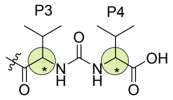	• NMR • Biochemical assay	L-L: 1,016 ± 179 L-D: 11,117 ± 2,222 D-L: >100,000 D-D: 33,962 ± 11,317	- all stereocenters of natural SylA are (L)-configured - dramatic loss of inhibition is observed if P3-amino acid's stereocenter is inversed to (D) - configuration of P4-amino acid has less influence on potency.
SylA-Sat	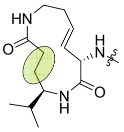	• Biochemical assay • ABPP competition assay with *Arabidopsis* cell lysates	n.a.[c]	- inhibition is extinguished if the double bond of the α,β-unsaturated amide is replaced by a CH_2-CH_2 moiety.
SylB	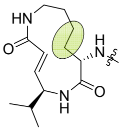	• Biochemical assay • X-ray	7,778 ± 2,259	- SylB's macrocycle adopts a similar conformation as GlbA in the binding pocket - reduced ring strain (in comparison to SylA) of the macrocycle leads to reduced activity.
SylA methyl ester	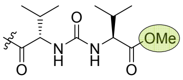	• Biochemical assay	757 ± 148	- terminal acid residue is not critical for inhibition.
Rh-SylA	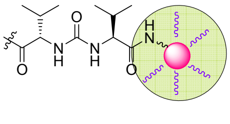	• ABPP competition assay with *Arabidopsis* cell lysates • ABPP competition assay with mammalian cell lysates	n.d.[d]	- can be used as an activity-based probe for profiling the 20S proteasome - studies of SylA in normal and bortezomib-resistant cancer cells.
SylA-LIP	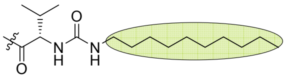	• Biochemical assay • Cellular assay in cancer cell lines	8.65 ± 1.33	- N-terminal lipophilic side chain significantly improves proteasome inhibition - promising influence on cell-based assay.
SylA-PEG1 **SylA-PEG2**	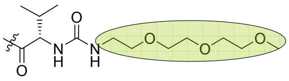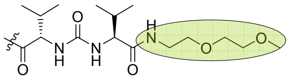	• Biochemical assay • Cellular assay in cancer cell lines • ABPP competition assay with *Arabidopsis* cell lysates	586 ± 69 401 ± 37	- long hydrophilic side chain does not improve SylA potency - lipophilicity is required for enhancing binding affinities - moderate influence in cell-based assay - P4 amino acid has only a weak influence on inhibition.

SylA-GlbA	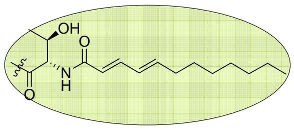	• Biochemical assay • Cellular assay in cancer cell lines	12.5 ± 1.6	- enhanced binding to subunits is only provided by the long lipophilic carbon chain - encouraging activity in cell-based assay.

[a] green circle denotes the part of the molecule that was modified from SylA's original structure. [b] *K*K_i': apparent constant of inhibiton of the chymotrypsin-like (C-L) activity of the human 20S proteasome determined with the biochemical assay and in triplicate (n=3). [c] n.a.: not active. [d] n.d.: not determined.

Finally, a fluorescent SylA derivative named Rh-SylA was used to determine the selectivity of SylA's binding to the proteasome. Surprisingly, these studies demonstrated a highly selective binding of SylA to the catalytically active proteasome subunits even in whole cell lysates. In addition, the same probe was used to evaluate SylA's potential to overcome Bortezomib's drug resistance. Encouragingly, these experiments showed that syringolins are still able to potently inhibit the eukaryotic proteasome in Bortezomib-adapted cells. These findings therefore further highlighted the promising properties of syringolins as anticancer agents. Moreover, this probe is now used by collaborators to further elucidate the biology of plant-pathogen interactions.

Finally, an alternative subproject evolved during this PhD thesis from an observed side-product in the total synthesis of SylA, occurring during the trimethyl phosphite mediated Corey-Winter elimination (Scheme 35). Optimization of the reaction conditions towards formation of the side product (arbitrarily called MRL) allowed synthesizing the probe in good yields. Preliminary studies were then performed for gaining a deeper insight into the mechanism of formation of this compound.

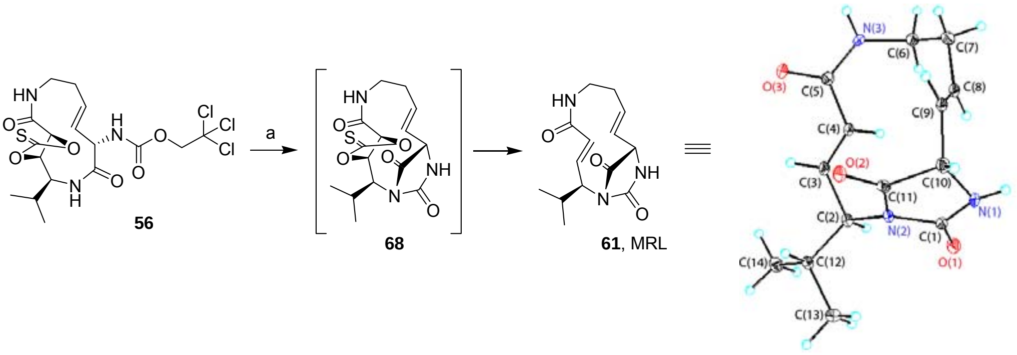

Scheme 35. Synthesis of MRL (**61**) from compound **56** and X-ray structure of MRL. Reagents and conditions: (a) P(OMe)$_3$, 150°C, 2 h, 47%.

After syntheses of fluorophor- or biotin-tagged derivatives, activity-based probe profiling (ABPP) was performed to elucidate the biological target of the hydantoin product. These studies revealed glyceraldehyde-3-phosphate-dehydrogenases (GADPHs) as their molecular targets which in whole cell lysates of *Arabidopsis thaliana* were covalently labeled in a highly selective manner. Moreover, a potent inhibition of yeast glyceraldehyde-3-phosphate dehydrogenases was also observed in biochemical assays, pinpointing towards a class-specific inhibition. As GAPDH inhibitors are considered as potential therapeutics against various diseases such as Chagas' disease or African sleeping sickness, these findings might indicate a possible medicinal relevance of this compound class. However, further studies are still required to fully evaluate all the potential of this new lead structure for GAPDH inhibition and its future application.

5.2. *Zusammenfassung und Ausblick (German)*

Proteasominhibitoren sind in den vergangenen Jahren in den Fokus des Interesses getreten, da sie großes therapeutisches Potential in der Krebstherapie zeigen. Der erste, von der FDA für den Menschen als Medikament zugelassene Proteasominhibitor ist Bortezomib, welcher Anwendung in der Therapierung von Plasmozytomen (multiples Myelom) findet. Die Behandlung mit Bortezomib ist allerdings durch eine Reihe an Nebenwirkungen und aufkommenden Resistenzen gekennzeichnet. Infolgedessen wird weiterhin nach neuen biologisch aktiven Substanzen gesucht, welche als verträglichere Medikamente in der Chemotherapie eingesetzt werden können. Wie in dieser Arbeit gezeigt wurde, besitzt Syringolin A (SylA), ein zwölfgliedriges makrozyklisches Lactam, welches aus dem Phytopatogen *Pseudomonas syringae* pv. *syringae* (*Pss*) isoliert wurde, eine vielversprechende Leitstruktur.

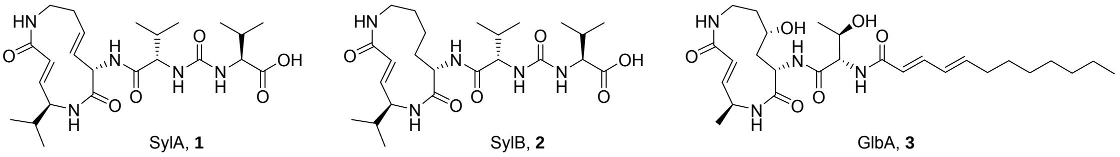

SylA, **1** SylB, **2** GlbA, **3**

Abbildung 24. Die chemischen Strukturen dreier Mitglieder der Syrbactin-Naturwirkstofffamilie: Syringolin A (SylA, **1**), Syringolin B (SylB, **2**) und Glidobactin (GlbA, **3**). Alle drei Verbindungen sind potente Proteasominhibitoren.

Während dieser Arbeit wurden Syntheserouten für verschiedene Mitglieder der Syrbactin-Familie und Derivate dieser entwickelt. Anhand dieser Verbindungen wurden Struktur-Aktivitätsbeziehungen für die Hemmung des eukaryotischen Proteasoms durch Syringoline aufgezeigt. Außerdem konnte gezeigt werden, dass Syringoline auch in komplexen Proteomen hochselektiv das Proteasom adressieren.

Zu Beginn wurde eine Totalsynthese von SylB, mit Substanzen aus dem natürlichen chiralem Pool (Valin und Lysin) entwickelt, welche als Schlüsselschritt eine Makrolactamisierung enthält. Um die erfolgreiche Synthese von SylB zu gewährleisten, wurden orthogonale Schutzgruppenstrategien etabliert, welche es erlaubten, SylB in neun Stufen ausgehend von Boc-(L)-Valinmethyester mit einer Gesamtausbeute von 7,8% darzustellen (Schema 36). Mit Hilfe dieser Syntheseroute war eine erstmalige Bestimmung aller Stereozentren von SylB möglich. Die Adaption dieser Synthesestrategie sollte dann den Zugang zu Syringolin A und weiteren wichtigen Syringolinderivaten ermöglichen.

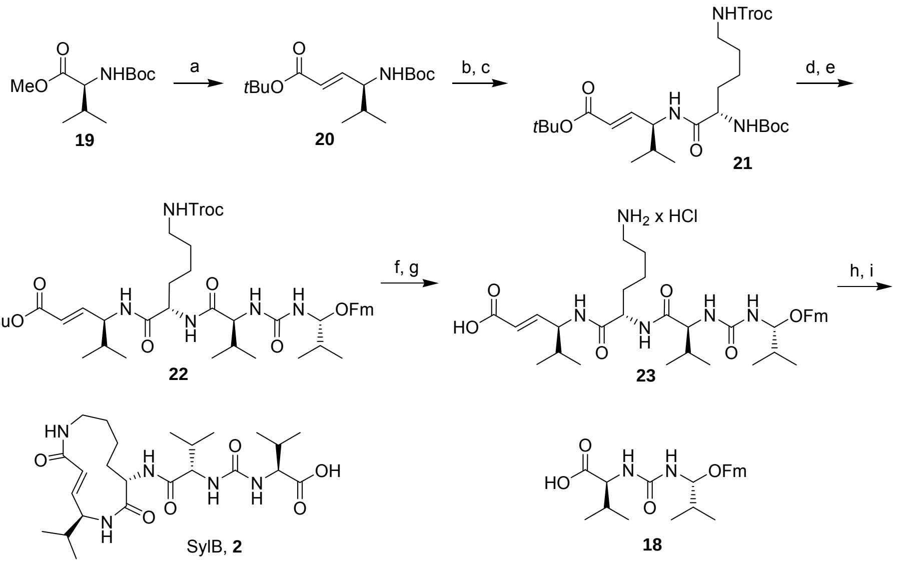

Schema 36. Synthese von Syringolin B (SylB). Reagenzien und Bedingungen: (a) (i) 1 M DIBAL-H/Toluol (2 eq.), Toluol, -78 °C, 4 h; (ii) Ph_3PCHCO_2*t*Bu (1,5 eq.), DCM, RT, 12 h, 84% (zwei Stufen); (b) 4 M HCl/Dioxan, *t*BuOAc, 4 Å MS, -5 °C bis 10 °C, über Nacht, 84%; (c) Boc-Lys(Troc)-OH (1,7 eq.), PyBop (3 eq.), HOAt (3 eq.), DIEA (6 eq.), DCM, 0 °C bis RT, über Nacht, 85%; (d) 4 M HCl/Dioxan, *t*BuOAc, 4 Å MS, -5 °C bis 10 °C, über Nacht, 83%; (e) **18** (1,2 eq.), PyBop (1,5 eq.), HOAt (1,5 eq.), DIEA (3 eq.), DCM, 0 °C bis RT, über Nacht, 75%; (f) Zn (150 eq.), THF/AcOH (1:1), 3 h, 97%; (g) (i) wässrige Ameisensäure, über Nacht; (ii) aq. HCl, >98% (zwei Stufen); (h) PyBop (3 eq.), HOAt (3 eq.), DIEA (6 eq.), DMF, RT, 32 h, 30%; (i) Piperidin/DMF (1:4), 73%.

Trotz der gelungenen Synthese von SylB führte die Makrolactamisierungsstrategie entgegen aller Erwartungen im Fall der Totalsynthese von SylA jedoch nicht zum Ziel. Daher wurde ein alternativer Weg für diese Synthese entwickelt. Die Schlüsselreaktion dieser alternativen verbesserten Route war eine Ringschlussmetathese mit einem konformationell-vororganisiertem, linearem Vorläufer (Schema 37).

Dementsprechend wurde das Ausgangsmaterial **34** zunächst durch Dihydroxylierung und anschließende Acetalisierung mit Aceton in ein fünfgliedriges, zyklisches Acetal transformiert. Zusätzliche iterative Peptidkupplungen führten zu einem linearen Intermediat, welches unter Verwendung des Grubbs-Katalysators (2. Generation) zyklisiert werden konnte.

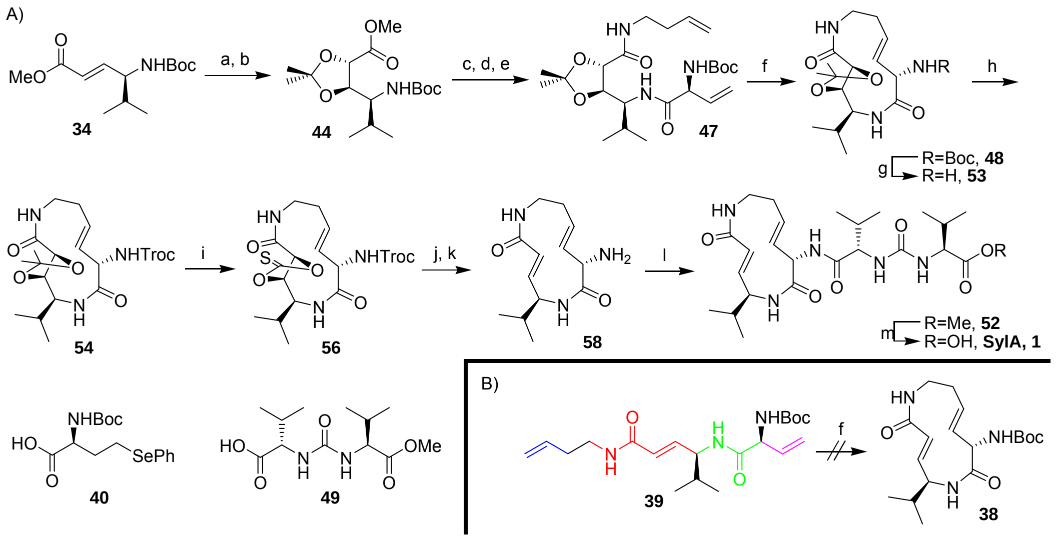

Schema 37. A) Synthese von Syringolin A (SylA). Reagenzien und Bedingungen: (a) OsO_4 (0,05 eq.), NMO (1,5 eq.), Ac_2O/H_2O (2:1), RT, 48 h, 85%; (b) 2,2-DMP (30 eq.), PPTS (0,05 eq.), DCM, 60 °C, 5 h, >98%; (c) (i) 1 M aq. LiOH (3 eq.), $MeOH/H_2O$ (1:1), 0 °C to RT über 30 min; (ii) 3-Butenylamin Hydrochlorid (1,2 eq.), PyBop (1,5 eq.), HOAt (1,5 eq.), DIEA (2 eq.), DCM, 0 °C bis RT, über Nacht, 80% (zwei Stufen); (d) (i) 2,6-Lutidin (2 eq.), TMSOTf (1,5 eq.), DCM, RT, 15 min; (ii) **40** (1,3 eq.), PyBop (1,5 eq.), HOAt (1,5 eq.), DIEA (2 eq.), DCM, 0 °C bis RT, über Nacht, 87% (zwei Stufen); (e) 30% aq. H_2O_2/DIEA (1:1), DCM, 50 °C, 3 h, 93%; (f) Grubbs II Katalysator (0,15 eq.), Toluol, 90 °C, 18 h, 49%; (g) 2,6-Lutidin (2 eq.), TMSOTf (1,5 eq.), DCM, RT, 15 min; (h) 2,2,2-Trichloroethylchloroformiat (1,1 eq.), $NaHCO_3$ (2 eq.), THF, 0 °C bis RT, 90 min, 81% (zwei Stufen); (i) (i) MW, 150 W, 140 °C, 30 min, *p*TsOH.H_2O (1 eq.), $MeOH/H_2O$/THF 2:2:1; (ii) $(Im)_2CS$ (10 eq.), DMAP (10 eq.), THF, 80 °C, über Nacht, 86% (zwei Stufen); (j) $P(OMe)_3$, 130 °C, 2.5 h, 88%; (k) Zn (150 eq.), THF/AcOH (1:1), 3 h, >98%; (l) **49** (1,1 eq.), PyBop (1,2 eq.), HOAt (1,2 eq.), DIEA (2 eq.), DMF, 0 °C bis RT, 40 min, 95%; (m) $AlCl_3$ (8 eq.), Methylethylsulfid, RT, 1 h, 92%. B) Versuchte Synthese des Makrozyklus **38** unter Verwendung der Ringschlussmetathese. Die einzelnen planaren Strukturelemente des nicht vororganisierten, linearen Vorläufers sind farblich hervorgehoben.

In einem ersten linearen, synthetischen Ansatz zur Darstellung von SylA wurde die exozyklische Seitenkette direkt an dem Boc-geschützte Derivat **48** aufgebaut. Dieser Weg wurde dann mit einer modifizierten Strategie, welche eine konvergentere und somit leichtere Synthese von SylA-Derivaten ermöglichte, ergänzt. Dies ist von Interesse, da erste biologische Studien zeigten, dass Modifikationen an der exozyklischen Seitenkette entscheidenden Einfluss auf die Gesamtaktivität der Syringoline haben. Folglich wurde zur Derivatisierung ein Schutzgruppenaustausch auf der Stufe des acetalgeschützten Makrozyklus vorgenommen. Aus diesem so erhaltenem Vorläufer wurde durch Entschützung des Diols und anschließender Corey-Winter Eliminierung ein vollständig funktionalisierter SylA-Makrozyklus erhalten. Das entsprechende freie Amin **58** wurde im Weiteren mit verschiedenen Seitenketten gekuppelt, um eine kleine Auswahl an Derivaten zu erhalten (Abbildung 25). Mit diesen wurden weitere Einblicke in die Struktur-Aktivitätsbeziehungen der Syringolin-vermittelten Proteasominhibierung erhalten. Auf diese Weise wurde z. B. ein lipophiles SylA-Derivat entwickelt, welcher bis heute der potenteste Inhibitor der Syringolinfamilie ist. Die Inhibierung des Proteasoms durch dieses hydrophobe SylA-Derivat ist dabei um das 100-fache stärker als die durch das natürliche SylA.

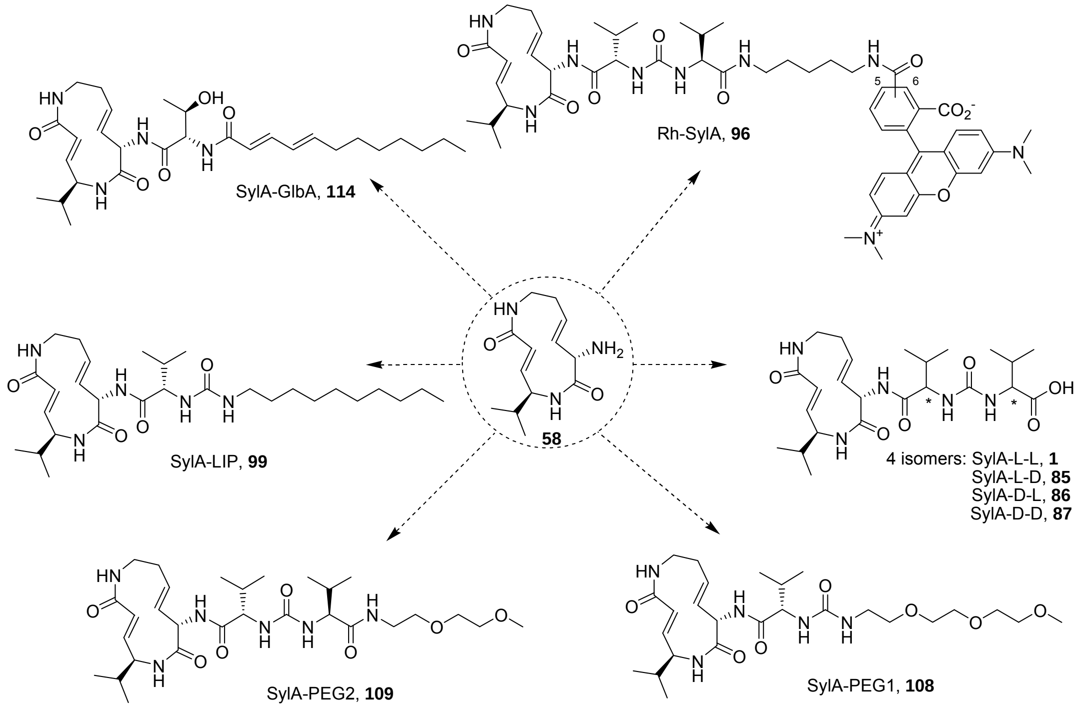

Abbildung 25. Chemische Strukturen verschiedener SylA-Analoga, dargestellt durch Kupplung verschiedener Seitenketten mit dem vollfunktionalisierten SylA-Makrozyklus.

Die dargestellten Analoga wurden in verschiedenen biologischen Assays evaluiert und die erhaltenen Ergebnisse stichpunktartig in Tabelle 10 aufgeführt.

Zusammenfassend zeigten diese Studien, dass die Freisetzung der makrozyklischen Ringspannung während der kovalenten Hemmung und/oder die strukturelle Vororganisierung die Triebkraft der beobachteten Proteasominhibition ist. Diese Schlussfolgerung resultiert aus dem Vergleich der Inhibierungspotenziale von SylA und SylB. Obwohl sich die Strukturen nur um eine endocyclische Doppelbindung (Dehydrolysin) unterscheiden, erhält man für den weniger gespannten Makrozyklus (SylB) eine 10-fach niedrigere Aktivität. Zusätzliche Studien mit dem lipophilen SylA-Derivat zeigten, dass eine hydrophobe Region im 20S Proteasom existiert, welche von entsprechenden, lipophilen Syringolinderivaten adressiert werden kann. Diese Ergebnisse sind im Einklang mit dem beobachteten, höheren

Inhibierungspotenzial des Syrbactins Glidobactin A, welches ebenfalls mit seiner lipophilen Seitenkette mit der hydrophoben Region des Proteasoms zu interagieren scheint. Diese Studien zeigten, dass Syrbactine an sich eine hohe Selektivität gegenüber der oben genannten proteasomalen hydrophoben Region aufweisen. Diese Selektivität beruht anscheinend auf der Konstitution und der Konformation des makrozyklischen Ringsystems. Weitere Untersuchungen sind nötig, um einen tieferen Einblick in die vorliegenden Struktur-Aktivitätsbeziehungen zu erhalten.

Tabelle 10. Struktur-Aktivitätsbeziehungen abgeleitet aus biologischen Untersuchungen auf der Basis von SylA Analoga.

Verbindung	**Untersuchte Eigenschaft[a]**	**Analyseart**	**K_i' für die Inhibierung der chymotryptischen Aktivität [nM][b]**	**Schlussfolgerungen/ Anwendungen**
SylA: 4 Isomer	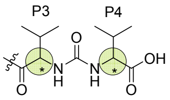	• NMR • Biochemische Analyse	L-L: 1,016 ± 179 L-D: 11,117 ± 2,222 D-L: >100,000 D-D: 33,962 ± 11,317	- Alle Stereozentren des natürlichen SylA sind (L)-konfiguriert - Deutlicher Verlust an Inhibierungspotential ist zu beobachten, wenn P3-Aminosäure inverses Stereozentrum (D) aufweist. - Konfiguration der P4-Aminosäure hat geringeren Einfluss auf das Inhibierungspotential.
SylA-Sat	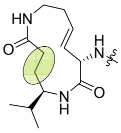	• Biochemische Analyse • ABPP-Kompetitions-Analyse mit *Arabidopsis* Zelllysaten	Nicht bestimmt	- Kein Inhibierungspotential mehr vorhanden, wenn α,β-ungesättigte Doppelbindung durch CH_2-CH_2 ersetzt wird.
SylB	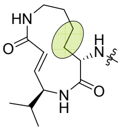	• Biochemische Analyse • Röntgenstruktur-analyse	7,778 ± 2,259	- Der SylB Makrrozyklus geht eine ähnliche Konformation wie GlbA in der Bindungstasche ein - Reduzierte Ringspannung (vgl. SylA) des Makrozyklus führt zu verringerter Aktivität.
SylA Methylester	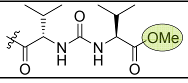	• Biochemische Analyse	757 ± 148	- Endständige Säurefunktion ist nicht essenziell für die Inhibierung.
Rh-SylA	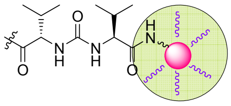	• ABPP-Kompetitions-Analyse mit *Arabidopsis* Zelllysaten • ABPP-Kompetitions-Analyse mit Säugetierzell-lysaten	Nicht analysiert	- Kann als ABPP-Sonde für das 20S Proteasom benutzt werden. - Studien von SylA in normalen und Bortezomib-resistenten Krebszellen.
SylA-LIP	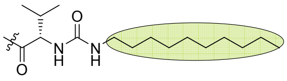	• Biochemische Analyse • Zellanalyse in Krebszelllinien	8.65 ± 1.33	- N-terminale, lipophile Seitenketten erhöhen die Proteasominhibierung signifikant - Vielversprechender Einfluss bei Zellanalysen

SylA-PEG1 **SylA-PEG2**	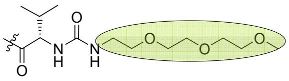 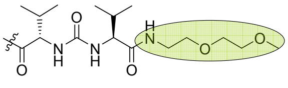	• Biochemische Analyse • Zellanalyse in Krebszelllinien • ABPP-Kompetitions-Analyse mit *Arabidopsis* Zelllysaten	586 ± 69 401 ± 37	- Lange hydrophile Seitenketten steigern nicht das Potential des SylAs - Lipophilität ist für die gesteigerte Bindungsaffinität erforderlich - Mäßiger Einfluss in Zellanalysen. - P4 Aminosäure hat nur geringen Einfluss auf die Inhibierung.
SylA-GlbA	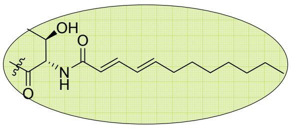	• Biochemische Analyse • Zellanalyse in Krebszelllinien	12.5 ± 1.6	- Gesteigerte Bindungsaffinität zu Untereinheiten ist nur durch lange lipophile Kohlenstoffketten gegeben. - Begünstigender Einfluss auf Zellanalysen.

[a] Der grau-grüne Kreis kennzeichnet die Unterschiede zur Struktur des Naturstoffes SylA. [b] K_i': Inhibitionskonstante der chymotrypsin-ähnlichen (C-L) Aktivität des menschlichen 20S Proteasoms, bestimmt durch biochemische Analysen (gemittelt aus drei Analysen n=3).

Ein fluoreszierendes SylA-Derivat (Rh-SylA) wurde zur Bestimmung der Bindungsselektivität von SylA in komplexen Proteomen verwendet. Überraschenderweise zeigten diese Studien eine hochselektive Bindung von SylA an die das 20S-Proteasom. Zusätzlich wurde diese chemische Sonde verwendet, um den Effekt von SylA auf Bortezomib-adaptierte Zellen zu evaluieren. Hierbei ergab sich, dass das eukaryotische Proteasom in bereits Bortezomib-adaptierten Zellen weiterhin durch Syringoline inhibiert werden kann. Dieser Befund zeigt auf, das Syringoline vielversprechende neue Therapeutika mit hohem Potential in der Krebsbekämpfung darstellen. Des Weiteren wird Rh-SylA zur Zeit von Kooperationspartnern verwendet, um die Biologie der Interaktionen von Phytopathogenen und Pflanzen weiter aufzuklären.

Ein weiteres Projekt entstand aus der biologsichen Evaluierung eines im Zuge der Totalsynthese von SylA während der Corey-Winter Eliminierung (Schema 38) auftretenden Nebenproduktes. Das hierbei gebildete Hydantoin (MRL) ließ sich isolieren und im Weiteren reproduzierbar synthetisieren.

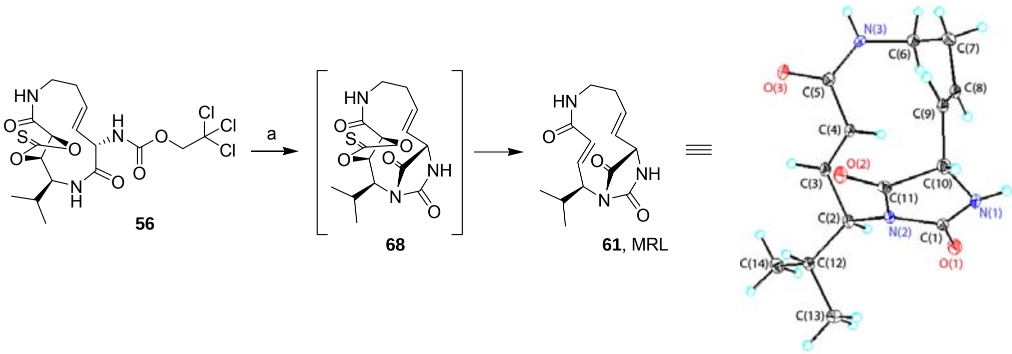

Schema. Synthese von MRL (**61**) ausgehend von **56** und Kristallstruktur von MRL. Reagenzien und Reaktionsbedingungen: (a) $P(OMe)_3$, 150 °C, 2 h, 47%.

Nach erfolgreicher Synthese der fluorophor- oder biotinmarkierten Derivate wurden aktivitätsbasierte Proteinprofilierungen (ABPP) durchgeführt, um potentielle biologische Zielproteine des Hydantoins zu identifizieren. Diese Studien ermittelten Glyceraldehyd-3-phosphat-dehydrogenasen (GADPHs) als molekulare Zielstrukturen, welche im komplexen Zelllysat von *Arabidopsis thaliana* selektiv von den Sonden kovalent modifiziert wurden. Des Weiteren wurde eine Inhibition der Hefe-Glyceraldehyd-3-phosphat-dehydrogenasen in biochemischen Analysen beobachtet, was auf eine klassenspezifische Inhibition hinweist. Möglicherweise ergeben sich so neue potentielle Therapeutika gegen verschiedene Krankheiten, die im Zusammenhang mit der Regulierung von GADPHs stehen, wie beispielsweise Chagas Krankheit (amerikanische Schlafkrankheit) oder der Afrikanischen Trypanosomiasis (afrikanische Schlafkrankheit). Letztendlich sind jedoch noch weitere Studien erforderlich, um das volle Potential dieser neuen Leitstruktur als GAPDH-Inhibitoren und ihre zukünftigen Anwendungsmöglichkeiten vollständig aufzuklären.

5.3. *Résumé et conclusions (French)*

Durant ces dernières années, les inhibiteurs de protéasome ont été largement étudiés pour leur propriété anticancéreuse. En effet, le premier inhibiteur de protéasome Bortézomib a récemment été approuvé par l'administration américaine des denrées alimentaires et des médicaments (FDA, Food and Drug Administration) pour le traitement du myélome multiple. Malgré le succès de cet agent anticancéreux, les thérapies à base de Bortézomib sont néanmoins sujettes à un grand nombre d'effets secondaires et à l'émergence de résistances. Par conséquence, il est primordial de rechercher de nouvelle structure moléculaire ayant la possibilité d'influencer des systèmes biologiques. Comme démontré dans cette thèse, syringoline A (SylA), un macrocycle lactamique à 12 atomes isolé de souches bactériennes de *Pseudomonas syringae* pv. *syringae* (*Pss*), représente ce genre de composé prometteur.

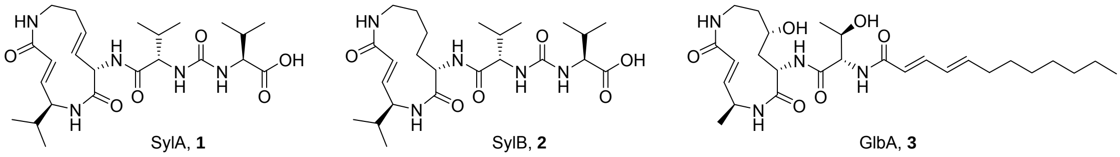

SylA, **1**   SylB, **2**   GlbA, **3**

Figure 26. Structures chimiques de trois membres de la famille de produits naturels appelés syrbactines: syringoline A (SylA, **1**), syringoline B (SylB, **2**) and glidobactine A (GlbA, **3**). Les trois composés exhibent une forte activité d'inhibition du protéasome.

Pendant cette thèse, différentes routes de synthèse de membres de la famille des syrbactines ont pu être développées. Avec l'aide de ces composés, des relations structure-activité envers l'inhibition du protéasome eukaryotique par les syringolines ont pu être estimées. De plus, il a été possible de démontrer que ces syringolines ciblent le protéasome de façon sélective même dans des protéomes complexes. Pour arriver à ces conclusions, plusieurs tâches distinctes ont dû être traitées durant cette thèse :

En premier temps, la synthèse totale de SylB a pu être accomplie par le biais d'une macrolactamisation et l'emploi de matériaux naturels du « pool » chiral (dérivés de valine et de lysine). Le succès de cette synthèse s'appuie sur la protection orthogonale de plusieurs groupements réactifs permettant finalement la synthèse de SylB en neuf étapes à partir de l'ester méthylique de la Boc-(L)-valine en un rendement final de 7.8 % (Schéma 39). Cette synthèse permet non seulement d'établir un model pour la synthèse de SylA et d'avoir accès à une importante syringoline pour la compréhension des relations structure-activité induis durant l'inhibition du protéasome mais elle permet également d'élucider la configuration de tous les stéréocentres de SylB.

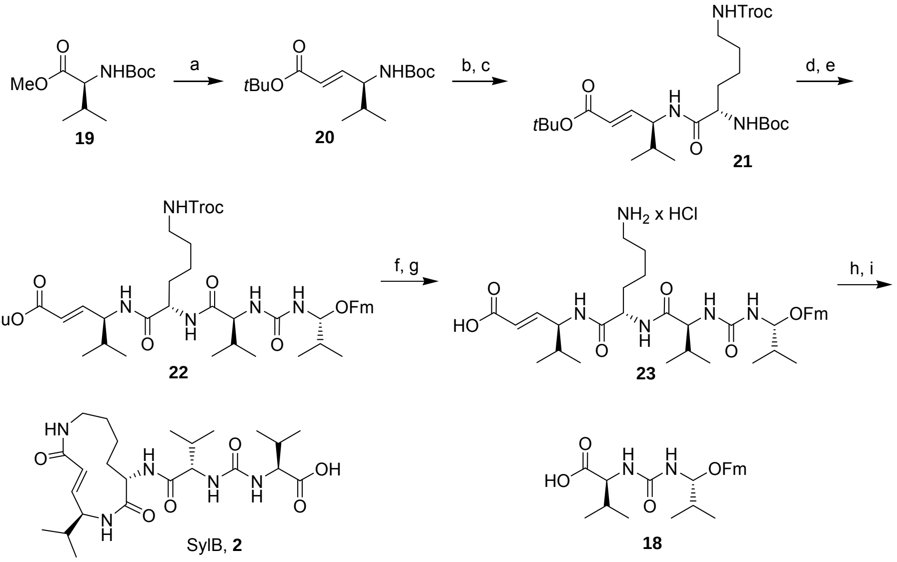

Schéma 39. Synthèse de la syringoline B (SylB). Réactifs et conditions: (a) (i) 1 M DIBAL-H/toluène (2 éq.), toluène, -78°C, 4 h; (ii) Ph_3PCHCO_2tBu (1,5 éq.), DCM, t.a., 12 h, 84% (deux étapes); (b) 4 M HCl/dioxane, *t*BuOAc, 4 Å MS, -5 °C to 10 °C, 8 h, 84%; (c) Boc-Lys(Troc)-OH (1,7 éq.), PyBop (3 éq.), HOAt (3 éq.), DIEA (6 éq.), DCM, 0 °C à t.a., 8 h, 85%; (d) 4 M HCl/dioxane, *t*BuOAc, 4 Å MS, -5 °C à 10 °C, 8 h, 83%; (e) **18** (1,2 éq.), PyBop (1,5 éq.), HOAt (1,5 éq.), DIEA (3 éq.), DCM, 0 °C à t.a., 8 h, 75%; (f) Zn (150 éq.), THF/AcOH (1:1), 3 h, 97%; (g) (i) acide formique humidifié, 8 h; (ii) aq. HCl, >98% (deux étapes); (h) PyBop (3 éq.), HOAt (3 éq.), DIEA (6 éq.), DMF, t.a., 32 h, 30%; (i) piperidine/DMF (1:4), 73%.

Malgré le succès de la synthèse de SylB, l'étape de macrocyclisation cependant échoua étonnement pour la synthèse de SylA. Par conséquent, une stratégie alternative a été développée durant cette thèse. Basée sur la métathèse cyclique d'oléfines intramoléculaire (RCM, Ring Closing Metathesis), cette nouvelle stratégie a dû néanmoins être modulé afin de pré-organiser le précurseur linéaire de cette étape clé de la synthèse (Schéma 40).

Ainsi, en utilisant le composé **34** comme matériau de départ, la pré-organisation strucutrelle a pu être effectué par osmylation et protection du diol sous la forme d'acétonide. Plusieurs couplages peptidiques ont permis ensuite d'aboutir à l'intermédiaire **47** qui, traité avec le catalyseur de Grubbs $2^{ème}$ génération, subi proprement la macrocyclisation.

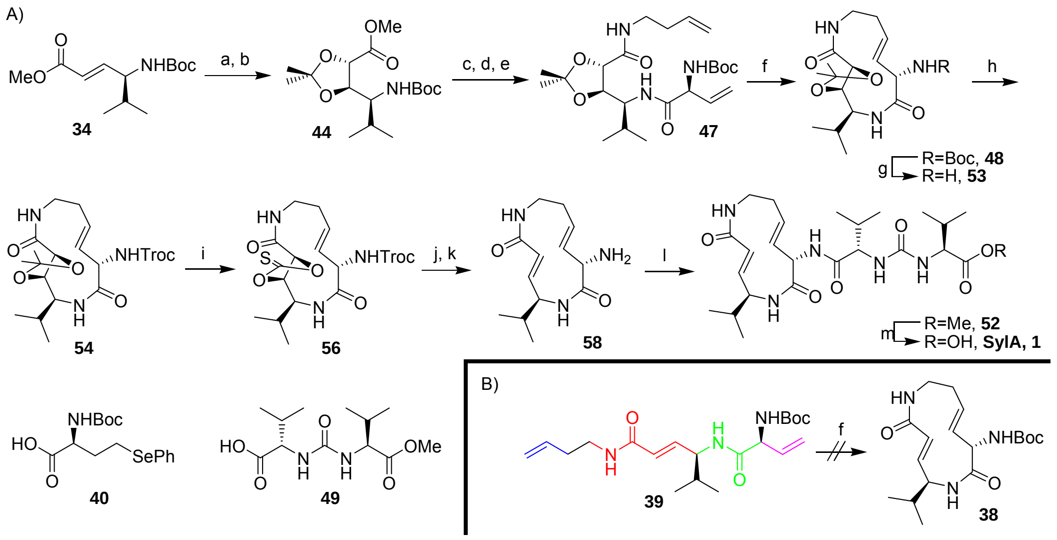

Schéma 40. A) Synthèse de la syringoline A (SylA). Réactifs et conditions: (a) OsO_4 (0,05 éq.), NMO (1,5 éq.), Ac_2O/H_2O (2:1), t.a., 48 h, 85%; (b) 2,2-DMP (30 éq.), PPTS (0,05 éq.), DCM, 60°C, 5 h, >98%; (c) (i) 1 M aq. LiOH (3 éq.), $MeOH/H_2O$ (1:1), 0°C à t.a. pendant 30 min; (ii) 3-butenylamine hydrochloride (1,2 éq.), PyBop (1,5 éq.), HOAt (1,5 éq.), DIEA (2 éq.), DCM, 0°C à t.a., 8 h, 80% (deux étapes); (d) (i) 2,6-lutidine (2 éq.), TMSOTf (1,5 éq.), DCM, t.a., 15 min; (ii) **40** (1,3 éq.), PyBop (1,5 éq.), HOAt (1,5 éq.), DIEA (2 éq.), DCM, 0°C à t.a., 8 h, 87% (deux étapes); (e) 30% aq. H_2O_2/DIEA (1:1), DCM, 50°C, 3 h, 93%; (f) catalyseur Grubbs II (0,15 éq.), toluène, 90°C, 18 h, 49%; (g) 2,6-lutidine (2 éq.), TMSOTf (1,5 éq.), DCM, t.a., 15 min; (h) 2,2,2-trichloroethyl chloroformate (1,1 éq.), $NaHCO_3$ (2 éq.), THF, 0°C à t.a. pendant 90 min, 81% (deux étapes); (i) (i) MW, 150W, 140°C, 30 min, *p*TsOH.H_2O (1 éq.), $MeOH/H_2O$/THF 2:2:1; (ii) $(Im)_2CS$ (10 éq.), DMAP (10 éq.), THF, 80 °C, 8 h, 86% (deux étapes); (j) $P(OMe)_3$, 130°C, 2.5 h, 88%; (k) Zn (150 éq.), THF/AcOH (1:1), 3 h, >98%; (l) **49** (1,1 éq.), PyBop (1,2 éq.), HOAt (1,2 éq.), DIEA (2 éq.), DMF, 0°C à t.a. pendant 40 min, 95%; (m) $AlCl_3$ (8 éq.), methylethylsulfide, t.a., 1 h, 92%. B) Tentative de synthèse du corps macrocyclique **38** de SylA par l'approche basique de la synthèse cyclique d'oléfines. La non-pré organization du précurseur **39** est représentée par la coloration de quatre motifs structuraux planaires.

Afin de compléter la synthèse de SylA, une première approche synthétique a tout d'abord consisté à attacher directement la chaîne exocyclique au dérivé **48** dont le groupement protecteur Boc avait été préalablement éliminé. Néanmoins, cette voix de synthèse a été par la suite modifiée par soucis de convergence et afin de faciliter la synthèse de dérivés. En effet, des études préliminaires ont indiqué l'influence considérable de la chaîne exocyclique sur le plan de l'activité globale des inhibiteurs. Ainsi, un échange de groupement protecteur (Boc → Troc) sur le composé **58** a pu permettre un clivage propre du groupement acétonide. Le diol résultant a été ensuite traité selon les conditions de la réaction d'élimination de Corey-Winter pour finallement former le macrocycle de SylA complètement fonctionnalisé. Enfin, une fois l'amine primaire restaurée, plusieurs chaînes exocycliques ont pu être attachées pour donner accès à une petite collection de dérivés (Figure 27). L'étude des relations structure-activité résultant de l'inhibition du protéasome par des syringolines ont ensuite procuré un grand nombre d'informations. Cette étude a notamment abouti à la découverte de l'inhibiteur syringoline le plus puissant découvert jusqu'à présent (Syl-LIP), révellant un potentiel cent fois supérieur au produit naturel SylA.

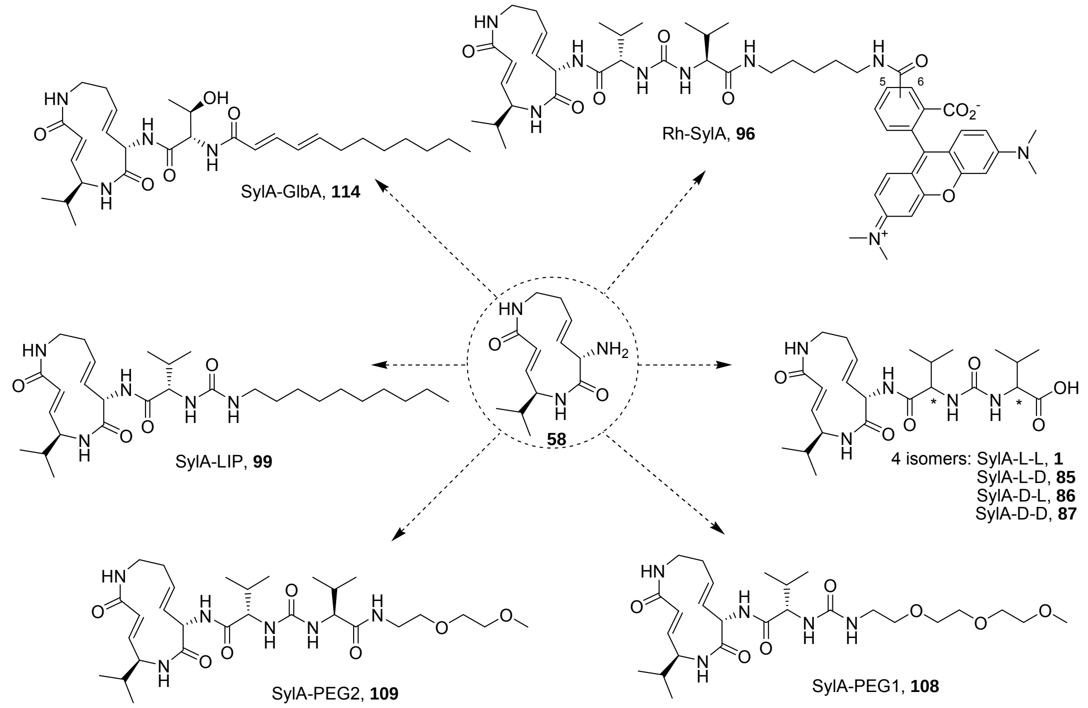

Figure 27. Structures chimiques d'analogues de SylA synthétisés par attachement de chaînes exocycliques au macrocycle fonctionnalisé de SylA.

Les analogues ainsi synthétisés ont ensuite été évalués à travers divers essais biologiques dont les résultats sont présentés dans le tableau 11.

En résumé, ces études montrent que la réduction de la tension macrocyclique et/ou la pré-organisation structurelle sont responsables du potentiel d'inhibition des syringolines sur le protéasome. Cette conclusion peut être argumentée par la comparaison des activités de SylA et SylB. En effet, bien que leurs structures soient très similaires, SylB ne présente qu'une seule oléfine dans son macrocycle impliquant une réduction dramatique de la tension cyclique qui se traduit par une activité dix fois inférieure à celle mesurée avec SylA.

Par ailleurs, les études portant sur le dérivé lipophile (SylA-LIP) a démontré qu'il existait une sous-unité lipophile proche du site actif du protéasome 20S. Cette découverte est en accord avec l’inhibition généralement supérieure mesurée avec l’inhibiteur glidobactine A (GlbA). Effectivement, l’activité de GlbA ne semble pas uniquement provenir du macrocyle mais bien plus du caractère lipophile porté par sa chaîne exocyclique. En effet, l’étude du complexe GlbA/protéasome au rayons X a révellé une très forte la sous-unité lipophilie du protéasome et la chaîne exocyclique de GlbA.

Tableau 11. Relation structure-activité résultant de différents essais biologiques pratiqués avec les analogues de SylA.

Composés	Motifs étudiés[a]	Type d’analyse	*K*i’ pour l’inhibition de l’activité chymotryptique [nM][b]	Conclusions/Applications
SylA: 4 isomères	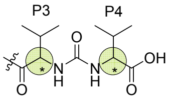	• RMN • Essai biochimique	L-L: 1,016 ± 179 L-D: 11,117 ± 2,222 D-L: >100,000 D-D: 33,962 ± 11,317	- la configuration naturele de tous les stéréocentres de SylA est (L) - observation d’une forte reduction de l’inhibition lorrsque le stéréocentre de l’acide aminé en P3 est inversé - la configuration de l’acide aminé en P4 a une influence moindre sur l’activité.
SylA-Sat	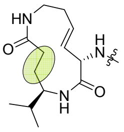	• Essai biochimique • Essai de compétition à partir d’extrait d’ *Arabidopsis*	n.a.[c]	- l’inhibition est anihilée lorsque la double liaison de l’amide α,β-insaturée est remplacée par le motif CH_2-CH_2.
SylB	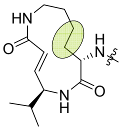	• Essai biochimique • Rayons X	7,778 ± 2,259	- le macrocycle de SylB adopte une conformation similaire à celle de GlbA dans la poche de fixation - réduction de la tension cyclique (en comparaison avec SylA) du macrocycle impliquant une réduction de l’activité.
Ester méthylique SylA	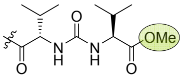	• Essai biochimique	757 ± 148	- le résidu acide terminal n’est pas un élément critique pour l’inhibition
Rh-SylA	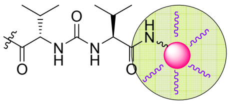	• Essai de compétition à partir d’extrait d’ *Arabidopsis* • Essai de compétition à partir de lysates de cellules de mammifère	n.d.[d]	- peut être utilisé entant qu’activity-based probe pour étudier le profil du protéasome 20S - études de SylA dans des cellules cancéreuses normales et adaptées à Bortézomib.
SylA-LIP	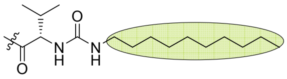	• Essai biochimique • Essai cellulaire à partir de cellules cancéreuses	8.65 ± 1.33	- la chaîne lipophile N-terminale améliore considérablement l’inhibition - influence prometteuse dans l’essai cellulaire.

SylA-PEG1 **SylA-PEG2**	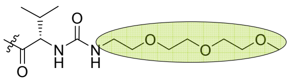 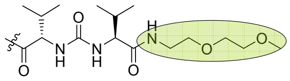	• Essai biochimique • Essai cellulaire à partir de cellules cancéreuses • Essai de compétition à partir d'extrait d' *Arabidopsis*	586 ± 69 401 ± 37	- longue chaîne hydrophile n'améliore pas l'activité - interactions lipophiles sont nécessaires pour augmenter l'affinité de fixation - influence modérée dans l'essai cellulaire - l'acide aminé en P4 a une faible influence sur l'inhibition.
SylA-GlbA	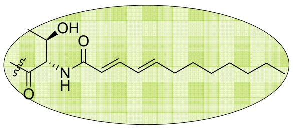	• Essai biochimique • Essai cellulaire à partir de cellules cancéreuses	12.5 ± 1.6	- l'amélioration de la fixation aux sous-unités est uniquement due à la longue chaîne carbonée lipophile - influence prometteuse dans l'essai cellulaire.

[a] cercle vert dénote la partie de la molécule qui a été modifiée en comparaison avec la structure naturelle de SylA. [b] K_i': constante apparente d'inhibition de l'activité chymotryptique (C-L, chymotrypsin-like) du protéasome 20S humain déterminée avec un essai biochimique, en triple (n=3). [c] n.a.: non actif. [d] n.d.: non déterminé.

Finalement, ces recherches ont démontré que les syrbactines présentent une sélectivité prononcée pour les différentes sous-unités du protéasome. Cette sélectivité semble être régie par la constitution et donc la conformation du système macrocyclique. Néanmoins, des études ultérieures dans cette direction devront être menées pour obtenir une meilleure connaissance de toutes les relations structure-activité impliquées. Enfin, le dérivé fluorescent de SylA nommé Rh-SylA a été utilisé pour déterminer la sélectivité de la fixation de SylA au protéasome. Il est surprenant de constater que cette étude a révélé une très forte sélectivité de SylA pour les sous-unités catalytiques du protéasome même dans des lysates entiers de cellules. De plus, la même substance a permis d'évaluer le potentiel de SylA dans des souches de cellules cancéreuses résistantes à Bortézomib. Ces découvertes surlignent l'aspect prometteur des syringolines entant qu'agents anticancéreux. Par ailleurs, cette molécule fluorescente est maintenant utilisée par nos collaborateurs pour aussi élucider des interactions biologiques entre plantes et pathogènes.

Pour conclure, un projet parallèle a éclot durant la synthèse totale de SylA en isolant un produit secondaire formé lors de la réaction de Corey-Winter et le traitement du thiocarbonate **56** avec la triméthyl phosphite (Schéma 41). L'optimisation des conditions de réaction afin de favoriser la formation de ce produit secondaire (arbitrairement appelé MRL) a pu aboutir à de bons rendements. Des études préalables sur le mécanisme de formation de ce composé présentant un motif hydantoïne ont déjà pu être mis à jour.

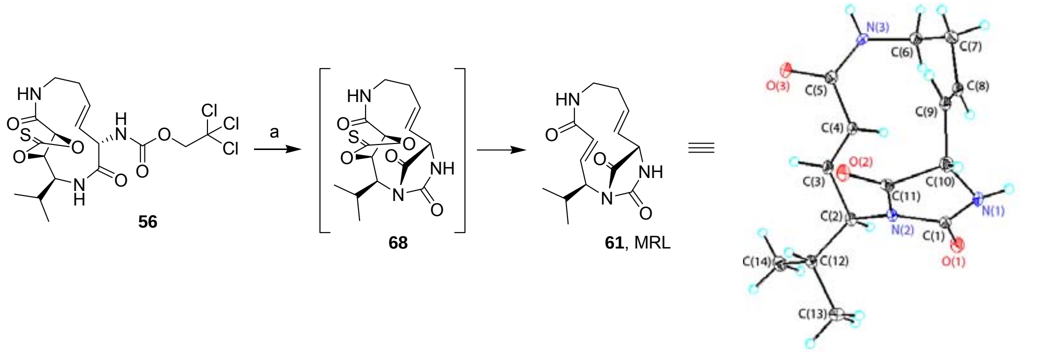

Schéma 41. Synthèse de MRL (**61**) à partir du composé **56** et structure aux rayons X de MRL. Réactifs et conditions: (a) $P(OMe)_3$, 150°C, 2 h, 47%.

L'élucidation de la cible biologique de cette hydantoïne bicyclique s'est ensuite appuyer sur l'utilisation de deux dérivés: l'un comportant un marquage fluorophore et l'autre un marquage biotine. Ainsi, la méthode communément appelée d'activity-based probe profiling (ABPP) permis de définir des glyceraldehyde-3-phosphate-dehydrogenases (GAPDHs) comme cible moléculaire de MRL à partir d'extraits d'*Arabidopsis thaliana*. La fixation de MRL sur ces GAPDHs s'est effectuée de manière covalente et extrêmement sélective. De plus, l'inhibition de GAPDHs a pu aussi être constatée en procédant à des essais biochimiques sur des levures, reflétant l'aspect spécifique de ce mode d'inhibition. Les inhibiteurs de GAPDHs sont actuellement considérés comme de possible agents thérapeutiques contre divers classes de maladies comme la maladie de Chagas ou la maladie du sommeil. Cette découverte révèle ainsi peut-être un intérêt médical à cette nouvelle classe de composés. Néanmoins, des études plus approfondies doivent être effectuées pour évaluer tout le potentiel de cette nouvelle structure sur l'inhibition des GAPDHs et sur un plan thérapeutique.

6. Experimental Part

6.1. Materials, instruments and general methods for purification and analyses

Reagents

The reagents were purchased from Acros Chimica, Aldrich, Avocado, Bachem, Fluka, J.T. Baker, Merck, Novabiochem, Riedel de Haen, Iris, Roth, or Sigma. Dry solvents were purchased as anhydrous reagents from commercial suppliers.

Thin layer chromatography (TLC)

TLC was carried out on Merck aluminium precoated silica gel plates (20 × 20 cm, 60F-254) using ultraviolet light irradiation at 254 nm or the following solutions of phosphomolybdic acid or potassium permanganate as developing agents.

Silica gel flash liquid chromatography

Purifications were performed using silica gel from J. T. Baker or Merck (particle size 40-60 µm) under approximately 0.5 bar pressure.

Reversed-phase liquid chromatography – electronspray ionization mass spectrometry (LC-MS)

LC-MS analyses were performed on an HPLC system from Agilent (1200 series) with a Eclipse XDB-C18, 5 µm (column dimensions: 150 × 4.60 mm) column from Agilent and a Thermo Finnigan LCQ Advantage Max ESI-Spectrometer and detection at 210 nm. Two linear gradients of solvent B (0.1% formic acid in acetonitrile) in solvent A (0.1% formic acid in water) were used at 1mL/min flow rate. Gradient 1: 0min/25%B → 1min/25%B → 10min/100%B → 12min/100%B → 15min/10%B. Gradient 2: 0min/10%B → 1min/10%B → 10min/100%B → 12min/100%B → 15min/10%B.

Chiral reversed-phase liquid chromatography

The chiral purity of syringolin A and B was checked with the chiral column Chiralcel® OD-R (column dimensions: 250 × 4.60 mm) from Daicel/Chiral Technologies.

Preparative reversed-phase high performance liquid chromatography (prep HPLC)

Purification of the compounds was performed on a Varian HPLC system (Pro Star 215) with a VP 250/21 Nucleosil C18PPN-column from Macherey-Nagel and detection at 210 nm. Linear gradients of solvent B (0.1% TFA in acetonitrile) in solvent A (0.1% TFA in water) were used at 25 mL/min flow rate.

Nuclear magnetic resonance spectroscopy (NMR)

Nuclear magnetic resonance (NMR) spectra were recorded on a Varian Mercury 400 system (400 MHz for ^{1}H- and 100 MHz for ^{13}C-NMR), a Bruker Avance DRX 500 system (500 MHz for ^{1}H- and 125 MHz for ^{13}C-NMR) or a Varian Unity Inova 600 system (600 MHz for ^{1}H- and 150 MHz for ^{13}C-NMR). ^{1}H NMR spectra are reported in the following manner: chemical shifts (δ) calculated with reference to solvent standards based on tetramethylsilane, multiplicity (s, singlet; d, doublet; t, triplet; sept, septuplet; dd, doublet of doublet; ddd, doublet of doublet of doublet; dt, doublet of triplet; td, triplet of doublet; dsept, doublet of septuplet; m, multiplet; br, broad signal), coupling constants (J) in Hertz (Hz), and number of protons (H).

High resolution mass spectrometry (HRMS)

HRMS measurements were performed on a LC-HR/ESI-FTMS machine from Thermo Electron Corporation.

Microwave-assisted reactions (MW)

The microwave-assisted reactions were conducted using a focused microwave unit (Discover® Reactor from CEM Corporation). The instrument consists of a continuous focused microwave power delivery system with operator-selectable power output from 0 - 300 W. In all experiments, the microwave power was held constant to ensure reproducibility. Reactions were performed in 10-mL glass vessels, which were sealed with a septum and locked into a pressure device, which controlled the pressure in the reaction vessel (maximum 10 bars). The specified reaction time corresponds to the total irradiation time. The temperature was monitored by an infrared temperature sensor positioned below the reaction vessel. The indicated temperature correlates with the maximum temperature reached during each experiment.

MM2 energy minimization:

MM2 energy minimizations were performed using the software Chem 3D Ultra version 8.0. The minimization run was configured to a minimum RMS Gradient of 0.100 and each interaction was displayed.

Proteasome inhibition: biochemical assay

Proteasome inhibition assays with human erythrocyte 20S proteasome (AK-740, Biomol) were performed at 37 °C in 100 μL reaction volumes containing 2 $\mu g.ml^{-1}$ 20S proteasome and 100 μM of substrate Suc-LLVY-AMC for assaying the chymotrypsin-like activity. Fluorescence was monitored with a Safire^2 plate reader (Tecan) equipped with 360nm excitation and 460nm emission filters. Fluorescence values (RFU) measured in proteasome inhibition assays were plotted versus time (t). The fluorescence data were fitted by the least squares method using SigmaPlot version 10.0 software (Systat Software) to the equation $f=f_0+v_st+[(v_i-v_s)/k_{obs}][1-\exp(-k_{obs}t)]$, where v_i and v_s are initial and final velocities, respectively, and k_{obs} is the pseudo-first-order association rate constant (Meng, L. H.; Mohan, R.; Kwok, B. H. B.; Elofsson, M.; Sin, N. and Crews, C. M. *Proc. Natl. Acad. Sci. USA* **1999**, *96*, 10403–10408; Fenteany, G.; Standaert, R. F.; Lane, W. S.; Choi, S.; Corey, E. J. and Schreiber, S. L. *Science* **1995**, *268*, 726–731.). Fittings with R^2 values > 0.99 were usually obtained. Where possible, apparent K_i' values were determined by plotting v_i against the inhibitor concentration ([I]). Using SigmaPlot, the data were fitted to the hyperbolic equation $v_i=c+[v_0/(K_i'+[I])]$, where v_0 is the velocity of the control. Usually, R^2 values > 0.98 were obtained. Triplicate of the testing of each molecules were performed on the chymotrypsin-like activity to afford the apparent constants of inhibition.

6.2. *Synthesis of syringolin B (SylB, 2)*

Synthesis of 4*S*-*tert*-Butoxycarbonylamino-5-methyl-hex-2*E*-enoic acid *tert*-butyl ester, 20:

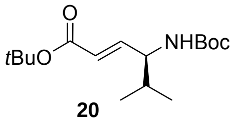

20

N-(*tert*-Butoxycarbonyl)-(L)-valine methyl ester **19** (500 mg, 2.16 mmol, 1 eq.) was dissolved in toluene (22 mL) under argon in a 100 mL flame-dried flask. The solution was cooled to -78 °C and a 1 M solution of DIBAL-H in toluene (4.4 mL, 4.32 mmol, 2 eq.) was slowly added over 2 hours. After further 2 hours of stirring, the mixture was quenched with a 1.2 M solution of potassium sodium tartrate (25 mL) and vigorously stirred at room temperature for further 2 hours. The resulting mixture was extracted with dichloromethane and the organic layers were dried with Na_2SO_4. The solution was filtered and concentrated to give *N*-(*tert*-butoxycarbonyl)-(L)-valinal which was directly used in the next step without further purification.

Crude *N*-(*tert*-butoxycarbonyl)-(L)-valinal was dissolved in dichloromethane (22 mL) and (*tert*-butoxycarbonylmethylene)triphenylphosphorane (1.21 g, 3.24 mmol, 1.5 eq.) was added in one portion. After 12 hours of stirring the mixture was concentrated and purified by flash column chromatography (10% ethyl acetate in cyclohexane) to afford **20**.

Yield: 466 mg (1.81 mmol, 84%) as colorless crystals.

TLC (15% ethyl acetate in cyclohexane)**:** $R_f = 0.49$.

HPLC (gradient 1): $t_R = 10.77$ min.

^{1}H NMR (400 MHz, $CDCl_3$): δ 6.73 (dd, J = 15.6, 5.6 Hz, 1 H), 5.82 (dd, J = 15.6, 1.6 Hz, 1 H), 4.55 (br s, 1 H), 4.15 (br s, 1 H), 1.79-1.88 (m, 1 H), 1.47 (s, 9 H), 1.43 (s, 9 H), 0.92 (d, J = 6.8 Hz, 3 H), 0.89 (d, J = 6.8 Hz, 3 H).

^{13}C NMR (100 MHz, $CDCl_3$): δ 165.66, 155.45, 146.10, 123.30, 80.50, 79.65, 56.66, 32.40, 28.44, 28.20, 18.94, 18.05.

HRMS (ESI): *m/z* calcd for $C_{16}H_{29}O_4NH^+$ $[M + H]^+$ 300.2169, found 300.2171.

Synthesis of Boc-Lys(Troc)-OH:

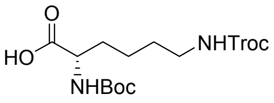

Boc-Lys(Troc)-OH

Boc-(L)-Lys-OH (3.00 g, 12.18 mmol, 1 eq.) and Na_2CO_3 (1.30 g, 12.18 mmol, 1 eq.) were dissolved in water/dioxane/acetonitrile (19:14:12, 450 mL) in a 1 L flask. The solution was cooled to 0 °C and a solution of 2,2,2-trichloroethyl chloroformate (1.8 mL, 13.40 mmol, 1.1 eq.) in dioxane (160 mL) was slowly added. The resulting mixture was stirred overnight at room temperature, concentrated to dryness and redissolved in a saturated aqueous solution of ammonium chloride. Crude product was extracted from the aqueous phase with dichloromethane (3 × 200 mL), dried over Na_2SO_4, filtered and evaporated to dryness. The crude product was purified by flash column chromatography (dichloromethane/methanol/acetic acid = 38:1:1) to afford Boc-(L)-Lys(Troc)-OH.

Yield: 4.19 g (9.91 mmol, 82%) as a colorless solid.
TLC (methanol/acetic acid/dichloromethane = 1:1:38)**:** $R_f = 0.30$.
HPLC (gradient 2): $t_R = 9.11$ min.
^{1}H NMR (400 MHz, $CDCl_3$): δ 5.10 (br s, 1 H), 4.72 (d, J = 1.6 Hz, 2 H), 4.31 (br s, 1 H), 3.26 (t, J = 6.4 Hz, 1 H), 3.24 (t, J = 6.8 Hz, 1 H), 1.80-1.93 (m, 1 H), 1.66-1.78 (m, 1 H), 1.53-1.64 (m, 2 H), 1.45-1.50 (m, 2 H), 1.45 (s, 9 H).
^{13}C NMR (100 MHz, $CDCl_3$): δ 177.24, 155.83, 154.92, 95.66, 80.27, 74.51, 53.13, 40.80, 31.97, 29.07, 28.32, 22.32.
HRMS (ESI): *m/z* calcd for $C_{14}H_{23}O_6N_2Cl_3H^+$ $[M + H]^+$ 421.0695, found 421.0695.

Synthesis of 4*S*-Amino-5-methyl-hex-2*E*-enoic acid *tert*-butyl ester, 125:

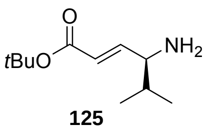

125

20 (1.07 g, 3.57 mmol, 1 eq.) was dissolved under argon in *tert*-butyl acetate (12 mL, dried over 4 Å molecular sieves) in a 100 mL flame-dried flask. The resulting solution was cooled to -5 °C, a 4 M solution of HCl in dioxane (12 mL) was slowly added and the resulting mixture was stirred overnight at 10 °C. Evaporation to dryness provided the crude hydrogenchloride salt which was subsequently recrystallized in cyclohexane. The crystals were filtered and washed with small portions of cyclohexane, redissolved in saturated Na_2CO_3 solution and the free amine was extracted from the aqueous phase with dichloromethane. The organic layer was dried over Na_2SO_4, filtered and concentrated to dryness to give the pure deprotected **125.**

Yield: 596 mg (2.99 mmol, 84%) as a colorless oil.
TLC (7% methanol in dichloromethane)**:** $R_f = 0.33$.
HPLC (gradient 2): $t_R = 5.86$ min.
^{1}**H NMR** (400 MHz, $CDCl_3$): δ 6.79 (dd, J = 15.6, 6.8 Hz, 1 H), 5.82 (dd, J = 15.6, 1.6 Hz, 1 H), 3.22 (ddd, J = 6.8, 5.6, 1.2 Hz, 1 H), 1.66-1.75 (m, 1 H), 1.46 (s, 9 H), 1.30 (br s, 2 H), 0.91 (d, J = 6.8 Hz, 3 H), 0.90 (d, J = 6.8 Hz, 3 H).
^{13}**C NMR** (100 MHz, $CDCl_3$): δ 166.02, 150.00, 122.52, 80.31, 58.46, 33.69, 28.21, 18.85, 18.28.
HRMS (ESI): *m/z* calcd for $C_{11}H_{21}O_2NH^+$ $[M + H]^+$ 200.1645, found 200.1644.

Synthesis of 4*S*-[2*S*-*tert*-Butoxycarbonylamino-6-(2,2,2-trichloro-ethoxycarbonylamino)-hexanoylamino]-5-methyl-hex-2*E*-enoic acid *tert*-butyl ester, 21:

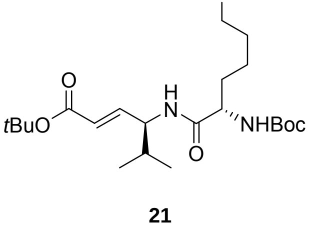

21

125 (484 mg, 2.43 mmol, 1 eq.) was dissolved in dichloromethane (2 mL) in a 25 mL flask and cooled to 0 °C. A solution of **Boc-Lys(Troc)-OH** (1.74 g, 4.13 mmol, 1.7 eq.), PyBop (3.80 g, 7.30 mmol, 3 eq.), HOAt (994 mg, 7.30 mmol, 3 eq.) and *N*,*N*-

diisopropylethylamine (2.65 mL, 14.60 mmol, 6 eq.) in dichloromethane (8 mL) was added and stirred overnight at room temperature. After evaporation to dryness, the crude product was purified by flash column chromatography (30% ethyl acetate in cyclohexane) to yield **21**.

Yield: 1.25 g (2.07 mmol, 85%) as a colorless solid.
TLC (30% ethyl acetate in cyclohexane)**:** $R_f = 0.23$.
HPLC (gradient 2): $t_R = 11.35$ min.
^{1}H NMR (400 MHz, $CDCl_3$): δ 6.72 (dd, J = 15.6, 5.6 Hz, 1 H), 6.66 (br s, 1 H), 5.78 (dd, J = 15.6, 1.6 Hz, 1 H), 5.46 (br s, 1 H), 5.32 (br s, 1 H), 4.70 (d, J = 12.0 Hz, 1 H), 4.65 (d, J = 12.0 Hz, 1 H), 4.42-4.48 (m, 1 H), 4.03 (br s, 1 H), 3.19 (t, J = 6.8 Hz, 1 H), 3.18 (t, J = 6.8 Hz, 1 H), 1.76-1.87 (m, 2 H), 1.57-1.66 (m, 1 H), 1.49-1.57 (m, 2 H), 1.43 (s, 9 H), 1.40 (s, 9 H), 0.87 (d, J = 6.8 Hz, 3 H), 0.85 (d, J = 6.8 Hz, 3 H).
^{13}C NMR (100 MHz, $CDCl_3$): δ 171.86, 165.52, 156.06, 154.85, 145.45, 123.39, 95.72, 80.58, 80.19, 74.43, 54.99, 54.55, 40.61, 32.12, 31.08, 29.32, 28.34, 28.12, 22.67, 18.97, 17.98.
HRMS (ESI): *m/z* calcd for $C_{25}H_{42}O_7N_3{}^{35}Cl_3H^+$ $[M + H]^+$ 602.2161, found 602.2160 and calcd for $C_{25}H_{42}O_7N_3{}^{37}Cl_3H^+$ $[M + H]^+$ 604.2132, found 604.2130.

Synthesis of 4*S*-[2*S*-Amino-6-(2,2,2-trichloro-ethoxycarbonylamino)-hexanoylamino]-5-methyl-hex-2*E*-enoic acid *tert*-butyl ester, 126:

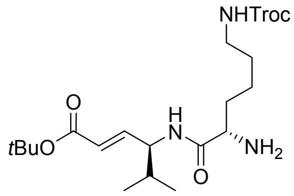

126

21 (935 mg, 1.55 mmol, 1 eq.) was dissolved under argon in *tert*-butyl acetate (12 mL, dried over 4 Å molecular sieves) in a 100 mL flame-dried flask and cooled to -5 °C. A solution of 4 M HCl in dioxane (12 mL) was slowly added and stirred overnight at 10 °C. The resulting mixture was evaporated to dryness and recrystallized in cyclohexane. The crystals were filtered, washed with small portions of cyclohexane and redissolved in saturated aqueous Na_2CO_3 solution. The free amine was extracted from the aqueous phase with ethyl acetate (3 × 50 mL), dried over Na_2SO_4, filtered and concentrated to dryness to give **126**.

Yield: 628 mg (1.29 mmol, 83%) as a colorless oil.
TLC (7% methanol in dichloromethane)**:** $R_f = 0.33$.
HPLC (gradient 2): $t_R = 7.56$ min.
^{1}H NMR (400 MHz, $CDCl_3$): δ 7.57 (d, J = 9.6 Hz, 1 H), 6.75 (dd, J = 15.6, 5.6 Hz, 1 H), 5.77 (dd, J = 15.6, 1.6 Hz, 1 H), 5.20 (br s, 1 H), 4.70 (s, 2 H), 4.42-4.48 (m, 1 H), 3.41 (dd, J = 8.0, 4.4 Hz, 1 H), 3.24 (t, J = 6.8 Hz, 1 H), 3.23 (t, J = 6.4 Hz, 1 H), 1.80-1.92 (m, 4 H), 1.52-1.63 (m, 3 H), 1.46 (s, 9 H), 1.39-1.47 (m, 2 H), 0.92 (d, J = 6.8 Hz, 3 H), 0.91 (d, J = 6.8 Hz, 3 H).
^{13}C NMR (100 MHz, $CDCl_3$): δ 174.38, 165.64, 154.76, 145.57, 123.48, 95.77, 80.63, 74.52, 55.10, 54.68, 40.92, 34.61, 32.16, 29.59, 28.19, 22.80, 19.08, 18.16.
HRMS (ESI): *m/z* calcd for $C_{20}H_{34}O_5N_3Cl_3H^+$ $[M + H]^+$ 502.1637, found 502.1633.

Synthesis of 2*S*-Amino-3-methyl-butyric acid 9*H*-fluoren-9-ylmethyl ester trifluoroacetic salts, 15:

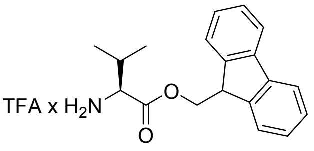

15

14 (3.96 g, 10.0 mmol, 1 eq., prepared according to Henkel B *et al* (1997) *Liebigs Annalen/Receuil* 10:2161-2168) was dissolved in dichloromethane (75 mL) in a 250 mL flask and trifluoroacetic acid (25 mL) was slowly added. The mixture was stirred for 30 minutes, followed by evaporation to dryness. Addition of toluene and re-evaporation to dryness yielded **15**.

Yield: 4.10 g **(**10.0 mmol, >98%) as a colorless solid.
TLC (60% ethyl acetate in cyclohexane)**:** $R_f = 0.17$.
HPLC (gradient 2): $t_R = 7.09$ min.
^{1}H NMR (400 MHz, $CDCl_3$): δ 7.73 (d, J = 6.0 Hz, 1 H), 7.71 (d, J = 5.6 Hz, 1 H), 7.51 (dd, J = 8.0, 0.8 Hz, 1 H), 7.49 (dd, J = 7.2, 0.8 Hz, 1 H), 7.38 (t, J = 7.6 Hz, 1 H), 7.35 (t, J = 8.0 Hz, 1 H), 7.28 (td, J = 7.6, 1.2 Hz, 1 H), 7.26 (td, J = 7.6, 1.2 Hz, 1 H),

4.61 (dd, J = 10.8, 6.0 Hz, 1 H), 4.51 (dd, J = 10.8, 5.6 Hz, 1 H), 4.16 (dd, J = 6.0, 5.6 Hz, 1 H), 3.76 (d, J = 4.0 Hz, 1 H), 2.08-2.17 (m, 1 H), 0.87 (d, J = 6.8 Hz , 3 H), 0.79 (d, J = 6.8 Hz , 3 H).

^{13}C NMR (100 MHz, $CDCl_3$): δ 169.22, 143.21, 142.86, 141.52, 141.40, 128.12, 128.06, 127.38, 127.34, 124.73, 120.16, 67.72, 58.48, 46.70, 29.66, 17.47, 17.46.

HRMS (ESI): *m/z* calcd for $C_{19}H_{21}O_2NH^+$ $[M + H]^+$ 296.1645, found 296.1646.

Synthesis of 2*S*-{3-[1*S*-(9*H*-Fluoren-9-ylmethoxycarbonyl)-2-methyl-propyl]-ureido}-3-methyl-butyric acid *tert*-butyl ester, 17:

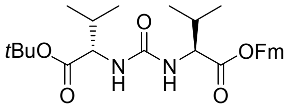

17

Triphosgene (110 mg, 0.37 mmol, 1.11 eq.) was dissolved under argon in dichloromethane (2 mL) in a 25 mL flame-dried flask and a solution of commercially available (L)-valine *tert*-butylester hydrochloride **16** (210 mg, 1.00 mmol, 1.00 eq.) and *N*,*N*-diisopropylethylamine (385 µL, 2.20 mmol, 2.20 eq.) in dichloromethane (3.5 mL) was added over 30 minutes. The mixture was stirred for further five minutes, then a mixture of **15** (410 mg, 1.00 mmol, 1.00 eq.) and *N*,*N*-diisopropylethylamine (385 µL, 2.20 mmol, 2.20 eq.) in dichloromethane (2.0 mL) was added in one portion. The resulting mixture was stirred for 10 minutes, concentrated to dryness; the residue was redissolved in ethyl acetate and successively washed with a 10% aq. $KHSO_4$ solution, a 5% aq. $NaHCO_3$ solution and with brine. The organic layer was dried over Na_2SO_4, filtered and evaporated to dryness. The resulting crude product was purified by flash column chromatography (15% ethyl acetate in cyclohexane) to afford **17**.

Yield: 299 mg (0.61 mmol, 61%) as colorless crystals.

TLC (15% ethyl acetate in cyclohexane)**:** $R_f = 0.16$.

HPLC (gradient 1): $t_R = 11.55$ min.

^{1}H NMR (400 MHz, $CDCl_3$): δ 7.75 (d, J = 7.2 Hz, 1 H), 7.74 (d, J = 7.2 Hz, 1 H), 7.61 (dd, J = 7.2, 0.8 Hz, 1 H), 7.59 (dd, J = 7.2, 0.8 Hz, 1 H), 7.39 (t, J = 7.2 Hz, 1 H), 7.37 (t, J = 7.2 Hz, 1 H), 7.30 (td, J = 7.2, 1.2 Hz, 1 H), 7.28 (td, J = 7.2, 1.2 Hz, 1 H), 5.40 (br s, 2 H), 4.47-4.53 (m, 3 H), 4.31-4.35 (m, 1 H), 4.20 (dd, J = 6.8, 6.4 Hz, 1H), 1.99-2.14 (m, 2 H), 1.46 (s, 9 H), 0.92 (d, J = 6.8 Hz, 3 H), 0.90 (d, J = 6.8 Hz, 3 H), 0.84 (d, J = 6.8 Hz, 3 H), 0.76 (d, J = 6.8 Hz, 3 H).

^{13}C NMR (100 MHz, $CDCl_3$): δ 173.65, 172.54, 157.53, 143.71, 143.53, 141.39, 141.35, 127.85, 127.22, 127.19, 125.09, 125.07, 120.02, 120.00, 81.72, 66.94, 58.37, 58.14, 46.86, 31.69, 31.47, 28.13, 19.11, 19.05, 17.63.

HRMS (ESI): *m/z* calcd for $C_{29}H_{38}O_5N_2H^+$ $[M + H]^+$ 495.2854, found 495.2846.

Synthesis of 2*S*-{3-[1*S*-(9*H*-Fluoren-9-ylmethoxycarbonyl)-2-methyl-propyl]-ureido}-3-methyl-butyric acid, 18:

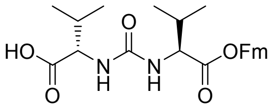

18

17 (299 mg, 0.61 mmol) was dissolved in formic acid (4 mL) in a 25 mL flask. Some drops of water were added and the mixture was stirred overnight. Evaporation to dryness, addition of toluene and re-evaporation yielded **18**.

Yield: 262 mg (0.60 mmol, >98%) as a colorless solid.

TLC (methanol/acetic acid/dichloromethane = 1:1:38)**:** $R_f = 0.26$.

HPLC (gradient 2): $t_R = 9.99$ min.

^{1}H NMR (400 MHz, $CDCl_3$): δ 11.00 (br s, 1 H), 7.73 (d, J = 7.2 Hz, 1 H), 7.72 (d, J = 7.6 Hz, 1 H), 7.59 (d, J = 7.2 Hz, 1 H), 7.57 (d, J = 7.2 Hz, 1 H), 7.38 (t, J = 7.2 Hz, 1 H), 7.36 (t, J = 7.2 Hz, 1 H), 7.29 (td, J = 7.2, 1.2 Hz, 1 H), 7.27 (td, J = 7.2, 1.2 Hz, 1 H), 5.94 (br s, 2 H), 4.50 (dd, J = 10.8, 6.8 Hz, 1 H), 4.45-4.48 (m, 1 H), 4.44 (dd, J = 10.8, 6.4 Hz, 1 H), 4.38-4.42 (m, 1 H), 4.19 (dd, J = 6.8, 6.4 Hz, 1 H), 2.12-2.21 (m, 1 H), 1.98-2.06 (m, 1 H), 0.95 (d, J = 7.2 Hz, 3 H), 0.89 (d, J = 7.2 Hz, 3 H), 0.87 (d, J = 7.2 Hz, 3 H), 0.73 (d, J = 7.2 Hz, 3 H).

^{13}C NMR (100 MHz, $CDCl_3$): δ 176.91, 173.77, 158.27, 143.53, 143.36, 141.34, 141.28, 127.85, 127.19, 127.16, 124.99, 120.00, 119.99, 67.07, 58.34, 58.24, 46.74, 31.35, 31.05, 19.02, 18.92, 17.63, 17.47.

HRMS (ESI): *m/z* calcd for $C_{25}H_{30}O_5N_2H^+$ $[M + H]^+$ 439.2228, found 439.2224.

Synthesis of 4*S*-[2*S*-(2*S*-{3-[1*S*-(9*H*-Fluoren-9-ylmethoxycarbonyl)-2-methyl-propyl]-ureido}-3-methyl-butyrylamino)-6-(2,2,2-trichloro-ethoxycarbonylamino)-hexanoylamino]-5-methyl-hex-2*E*-enoic acid *tert*-butyl ester, 22:

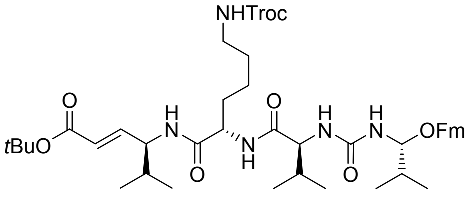

22

126 (29 mg, 58 µmol, 1 eq.) was dissolved in dichloromethane (1 mL) in a 10 mL flask and cooled to 0 °C. A solution of **18** (31 mg, 69 µmol, 1.2 eq.), PyBop (46 mg, 87 µmol, 1.5 eq.), HOAt (12 mg, 87 µmol, 1.5 eq.) and *N*,*N*-diisopropylethylamine (32 µL, 180 µmol, 3 eq.) in dichloromethane (1 mL) were added and the resulting mixture was stirred overnight at room temperature. After evaporation, the crude product was purified by flash column chromatography (60% ethyl acetate in cyclohexane) to yield **22**.

Yield: 40 mg (43 µmol, 75%) as a colorless solid.
TLC (60% ethyl acetate in cyclohexane)**:** $R_f = 0.35$.
HPLC (gradient 2): $t_R = 11.33$ min.
^{1}H NMR (400 MHz, d^6-DMSO): δ 7.95 (d, J = 8.0 Hz, 1 H), 7.89 (d, J = 7.6 Hz, 1 H), 7.87 (d, J = 7.6 Hz, 1 H), 7.86 (d, J = 9.6 Hz, 1 H), 7.71 (d, J = 8.0 Hz, 1 H), 7.68 (d, J = 7.6 Hz, 1 H), 7.62-7.66 (m, 1 H), 7.42 (t, J = 7.2 Hz, 1 H), 7.41 (t, J = 7.2 Hz, 1 H), 7.33 (td, J = 6.0, 0.8 Hz, 1 H), 7.31 (td, J = 6.0, 1.2 Hz, 1 H), 6.70 (dd, J = 15.6, 5.6 Hz, 1 H), 6.46 (d, J = 8.8 Hz, 1 H), 6.30 (d, J = 8.8 Hz, 1 H), 5.75 (dd, J = 15.6, 1.6 Hz, 1 H), 4.77 (s, 2 H), 4.52 (dd, J = 10.8, 6.4 Hz, 1 H), 4.39 (dd, J = 10.8, 6.4 Hz, 1 H), 4.21-4.30 (m, 2 H), 4.23 (dd, J = 6.4, 6.4 Hz, 1 H), 4.00-4.07 (m, 2 H), 2.99 (t, J = 6.8 Hz, 1 H), 2.98 (t, J = 6.4 Hz, 1 H), 1.86-1.95 (m, 1 H), 1.74-1.86 (m, 2 H), 1.49-1.65 (m, 2 H), 1.37-1.46 (m, 2 H), 1.42 (s, 9 H), 1.16-1.33 (m, 2 H), 0.80-0.90 (m, 9 H), 0.77 (d, J = 6.8 Hz, 3 H), 0.76 (d, J = 6.8 Hz , 3 H), 0.67 (d, J = 7.2 Hz, 3 H).
^{13}C NMR (150 MHz, d^6-DMSO): δ 172.43, 171.60, 171.19, 164.79, 157.59, 154.28, 146.74, 143.60, 143.50, 140.76, 140.73, 127.67, 127.59, 127.11, 127.02, 125.07, 122.32, 122.26, 120.03, 96.31, 79.80, 73.25, 65.47, 57.76, 57.64, 54.57, 52.70, 46.38,

40.35, 31.51, 31.13, 30.13, 28.87, 27.67, 22.68, 19.20, 18.99, 18.94, 18.19, 17.51, 17.49.

HRMS (ESI): *m/z* calcd for $C_{45}H_{62}O_9N_5{}^{35}Cl_3H^+$ $[M + H]^+$ 922.3686, found 922.3698 and calcd for $C_{45}H_{62}O_9N_5{}^{37}Cl_3H^+$ $[M + H]^+$ 924.3656, found 924.3673.

Synthesis of 4*S*-[6-Amino-2*S*-(2*S*-{3-[1*S*-(9*H*-fluoren-9-ylmethoxycarbonyl)-2-methyl-propyl]-ureido}-3-methyl-butyrylamino)-hexanoylamino]-5-methyl-hex-2*E*-enoic acid hydrochloride, 23:

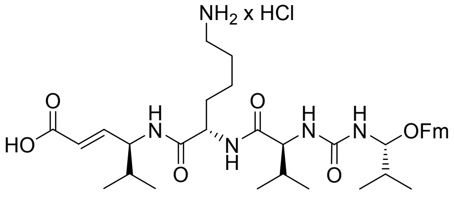

23

22 (60 mg, 65 µmol, 1 eq.) was dissolved in tetrahydrofurane (2 mL) in a 10 mL flask. Acetic acid was added (2 mL), followed by zinc powder (638 mg, 9.76 mmol, 150 eq.) which was added in portions over 30 minutes. After 3 hours of vigorous stirring, the mixture was filtered over a small plug of Celite and washed with ethyl acetate. After evaporation to dryness, 47 mg (63 µmol, 97%) of the deprotected amine was obtained which was used in the next step without further purification.

The cleaved intermediate (47 mg, 63 µmol) was dissolved in formic acid (4 mL) in a 10 mL flask and some drops of water were added. The resulting mixture was stirred overnight, concentrated to dryness, redissolved in diluted aq. HCl and re-evaporated to dryness. Addition of toluene and concentration to dryness yielded **23**.

Yield: 45 mg (62 µmol, >98%) as a colorless solid.

HPLC (gradient 2): $t_R = 7.75$ min.

^{1}H NMR (400 MHz, d^6-DMSO): δ 8.24 (s, 1 H), 7.98 (d, J = 8.0 Hz, 1 H), 7.92 (d, J = 9.2 Hz, 1 H), 7.89 (d, J = 7.6 Hz, 1 H), 7.88 (d, J = 7.6 Hz, 1 H), 7.71 (d, J = 7.2 Hz, 1 H), 7.68 (d, J = 7.6 Hz, 1 H), 7.42 (t, J = 7.2 Hz, 1 H), 7.41 (t, J = 7.6 Hz, 1 H), 7.28-7.36 (m, 2 H), 6.60 (dd, J = 15.6, 5.6 Hz, 1 H), 6.47 (d, J = 9.2 Hz, 1 H), 6.31 (d, J = 8.8 Hz, 1 H), 5.76 (dd, J = 15.6, 2.4 Hz, 1 H), 4.54 (dd, J = 10.8, 6.4 Hz, 1 H), 4.39 (dd, J = 10.8, 6.4 Hz, 1 H), 4.21-4.32 (m, 2 H), 4.23 (dd, J = 6.4, 6.4 Hz, 1 H), 4.05

(dd, J = 8.4, 5.2 Hz, 1 H), 4.00 (dd, J = 8.8, 4.8 Hz, 1H), 3.40 (br s, ~5H), 2.73 (t, J = 7.6 Hz, 2 H), 1.86-1.95 (m, 1 H), 1.72-1.84 (m, 2 H), 1.47-1.67 (m, 4 H), 1.20-1.34 (m, 2 H), 0.80-0.86 (m, 9 H), 0.77 (d, J = 6.8 Hz, 3 H), 0.75 (d, J = 6.8 Hz, 3 H), 0.66 (d, J = 7.2 Hz, 3 H).

^{13}C NMR (100 MHz, d^6-DMSO): δ 172.43, 171.67, 171.00, 165.39, 157.63, 143.61, 143.50, 140.78, 140.75, 128.89, 127.09, 125.09, 125.04, 121.34, 120.04, 119.99, 65.46, 57.74, 57.54, 54.67, 52.43, 46.37, 44.28, 31.60, 31.35, 31.19, 30.14, 22.35, 19.22, 19.00, 18.97, 18.26, 17.49, 17.47.

HRMS (ESI): *m/z* calcd for $C_{38}H_{53}O_7N_5H^+$ $[M + H]^+$ 692.4018, found 692.4016.

Synthesis of syringolin B, 2:

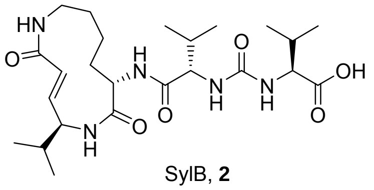

SylB, **2**

PyBop (339 mg, 651 µmol, 3 eq.), HOAt (89 mg, 651 µmol, 3 eq.) and *N*,*N*-diisopropylethylamine (114 µL, 651 µmol, 3 eq.) were dissolved under argon in dimethylformamide (114 mL) in a 500 mL flame-dried flask. A solution of **23** (150 mg, 217 µmol, 1 eq.) and *N*,*N*-diisopropylethylamine (114 µL, 651 µmol, 3 eq.) in *N*,*N*-dimethylformamide (58 mL) was slowly added over 8 hours with a syringe pump and stirred for further 24 hours. The reaction was quenched by addition of a 20% aq. citric acid solution and extracted with ethyl acetate. The organic layers were washed with water (2 × 50 mL) and dried over Na_2SO_4, filtered and evaporated to dryness. The remaining residue was purified by flash column chromatography (4% methanol in ethyl acetate) to yield 44 mg (65 µmol, 30%) of the cyclized product.

The cyclized product (7.70 mg, 11.4 µmol, 1 eq.) was dissolved in *N*,*N*-dimethylformamide (800 µL) in a 10 mL flask and piperidine (200 µL) was added. The mixture was stirred for one hour and then evaporated to dryness. The remaining residue was purified by preparative HPLC (0min/10%B → 10min/10%B → 30min/30%B → 50min/60%B → 60min/100%B → 80min/100%B) to yield syringolin B (SylB, **2**).

Yield: 4.11 mg (8.3 µmol, 73%) as a colorless powder.

TLC (2% acetic acid + 15 % methanol in dichloromethane)**:** $R_f = 0.40$.

HPLC (gradient 2): $t_R = 6.12$ min.

^{1}H NMR (600 MHz, d^6-DMSO): δ 12.44 (br s, 1H), 8.26 (d, J = 7.8 Hz, 1 H), 7.63 (d, J = 7.8 Hz, 1 H), 7.37 (dd, J = 7.2, 7.2 Hz, 1 H), 6.77 (dd, J = 15.6, 4.8 Hz, 1 H), 6.33 (d, J = 8.4 Hz, 1 H), 6.32 (d, J = 8.4 Hz, 1 H), 6.21 (d, J = 15.6 Hz, 1 H), 4.55-4.60 (m, 1 H), 4.08-4.13 (m, 1 H), 4.03 (dd, J = 8.4, 4.8 Hz, 1 H), 3.99 (dd, J = 9.0, 4.8 Hz, 1H), 3.23-3.32 (m, 2H), 2.91-2.98 (m, 1 H), 2.03-2.10 (m, 1 H), 1.94-2.02 (m, 2 H), 1.73-1.80 (m, 1 H), 1.58-1.65 (m, 1 H), 1.40-1.46 (m, 1 H), 1.21-1.33 (m, 2 H), 0.95 (d, J = 6.6 Hz, 3 H), 0.92 (d, J = 6.6 Hz , 3 H), 0.86 (d, J = 6.6 Hz, 3 H), 0.84 (d, J = 7.2 Hz, 3 H), 0.83 (d, J = 6.6 Hz, 3 H), 0.78 (d, J = 6.6 Hz, 3 H).

^{13}C NMR (125 MHz, d^6-DMSO): δ 173.97, 171.22, 170.82, 165.87, 157.75, 144.85, 119.79, 57.87, 57.53, 56.00, 51.33, 38.03, 31.13, 30.53, 30.29, 30.19, 29.88, 19.86, 19.26, 19.16, 17.61, 17.38.

HRMS (ESI): *m/z* calcd for $C_{24}H_{41}O_6N_5H^+$ $[M + H]^+$ 496.3130, found 496.3123.

6.3. *Synthesis of syringolin A (SylA, 1)*

Synthesis of 4*R*-(1-Hydroxy-allyl)-2,2-dimethyl-oxazolidine-3-carboxylic acid *tert*-butyl ester, 25:

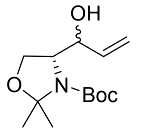

25

(D)-Garner aldehyde 24 (5.07 g, 22.12 mmol, 1 eq.) was dissolved in tetrahydrofurane (210 mL) in a 500 mL flame-dried flask and a solution of vinylmagnesium bromide (67 mL, 66.36 mmol, 3 eq.) in tetrahydrofurane (1.0 M) was added over 30 minutes at -78 °C under argon. The mixture was slowly allowed to warm to room temperature over two hours. The reaction was quenched upon addition of a saturated aq. NH_4Cl solution and extracted twice with diethyl ether. The combined organic layers were washed with brine, dried over Na_2SO_4, filtered and concentrated to dryness. The crude product was purified by flash column chromatography (10% ethyl acetate in cyclohexane) to afford **25**. The inseparable mixture of diastereomers was used in the next step without further purification.

Yield: 4.29 g (16.67 mmol, 75%) as a colorless oil.
TLC (15% ethyl acetate in cyclohexane)**:** $R_f = 0.11$.
HPLC (gradient 2): $t_R = 5.96$ min.
HRMS (ESI): *m/z* calcd for $C_{13}H_{23}O_4NH^+$ $[M + H]^+$ 258.1700, found 258.1700.

Synthesis of 4*S*-(4-Ethoxycarbonyl-but-1*E*-enyl)-2,2-dimethyl-oxazolidine-3-carboxylic acid *tert*-butyl ester, 27:

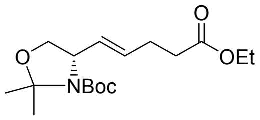

27

The mixture of vinylic alcohols **25** (4.12 g, 16.65 mmol, 1 eq.) was dissolved in xylenes (150 mL) in a 500 mL flame-dried flask under argon. Triethyl orthoacetate (29 mL, 150 mmol, 9 eq.) and propionic acid (250 µL, 3.33 mmol, 0.2 eq.) were added and the mixture was heated at reflux (155 °C) for 24 hours. After evaporation *in vacuo*, the residue was dissolved in ethyl acetate and the resulting solution washed twice with brine. The organic layer was dried over Na_2SO_4, filtered and concentrated to dryness. The crude product was purified by flash column chromatography (15% ethyl acetate in cyclohexane) to afford **27**.

Yield: 4.89 g (14.94 mmol, 90%) as a colorless oil.
TLC (15% ethyl acetate in cyclohexane)**:** $R_f = 0.39$.
HPLC (gradient 2): $t_R = 7.42$ min.
^{1}H NMR (400 MHz, $CDCl_3$): δ 5.56 (br s, 1 H), 5.47 (dd, J = 15.2, 7.5 Hz, 1 H), 4.20 (br s, 1 H), 4.11 (q, J = 7.1 Hz, 2 H), 3.99 (dd, J = 8.8, 6.1 Hz, 1 H), 3.68 (dd, J = 8.8, 2.2 Hz, 1 H), 2.31-2.39 (m, 4 H), 1.57 (br s, 3 H), 1.48 (s, 3 H), 1.42 (br s, 9 H), 1.24 (t, J = 7.1 Hz, 3 H).
^{13}C NMR (100 MHz, $CDCl_3$): δ 172.92, 151.98, 130.38, 93.88, 79.47, 68.45, 60.40, 59.08, 33.98, 28.52, 27.46, 26.69, 23.80, 14.30.

HRMS (ESI): *m/z* calcd for $C_{17}H_{29}O_5NH^+$ $[M + H]^+$ 328.2119, found 328.2119.

Synthesis of 4*S*-(4-Carboxy-but-1*E*-enyl)-2,2-dimethyl-oxazolidine-3-carboxylic acid *tert*-butyl ester, 30:

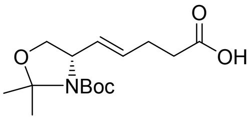

30

27 (4.89 g, 14.94 mmol, 1 eq.) was dissolved in a mixture methanol/water (3:1, 100 mL) in a 250 mL flask and a solution of lithium hydroxide (1.88 g, 41.36 mmol, 3 eq.) in water (1.0 M., 45 mL) was added slowly at 0 °C. The mixture allowed warming at room temperature for 2 hours. After concentration *in vacuo* the residue was dissolved in ethyl acetate and the organic layer was washed with a 10% aq. $KHSO_4$ solution (final pH <3). The aqueous layer was extracted with ethyl acetate and the combined organic layers were washed with brine, dried over Na_2SO_4, filtered and concentrated to dryness to afford **30**.

Yield: 4.38 g (14.64 mmol, 98%) as a colorless solid.
TLC (2% acetic acid + 30% ethyl acetate in cyclohexane)**:** $R_f = 0.41$.
HPLC (gradient 2): $t_R = 6.12$ min.
^{1}H NMR (400 MHz, $CDCl_3$): δ 9.94 (br s, 1 H), 5.58 (br s, 1 H), 5.47 (dd, J = 15.3, 7.4 Hz, 1 H), 4.14-4.40 (br s, 1 H), 3.98 (dd, J = 8.8, 6.1 Hz, 1 H), 3.67 (dd, J = 8.8, 2.1 Hz, 1 H), 2.30-2.43 (m, 4 H), 1.56 (br s, 3 H), 1.47 (s, 3 H), 1.40 (br s, 9 H).
^{13}C NMR (100 MHz, $CDCl_3$): δ 178.44, 152.00, 130.59, 130.08, 93.93, 79.63, 68.35, 59.02, 33.64, 28.46, 27.10, 26.66, 23.72.
HRMS (ESI): *m/z* calcd for $C_{15}H_{25}O_5NH^+$ $[M + H]^+$ 300.1806, found 300.1806.

Synthesis of 2,2-Dimethyl-4*S*-[4-(2,2,2-trichloro-ethoxycarbonylamino)-but-1*E*-enyl]-oxazolidine-3-carboxylic acid *tert*-butyl ester, 31:

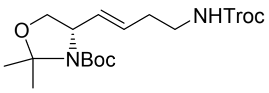

31

30 (3.50 g, 11.69 mmol, 1 eq.) was dissolved in toluene (120 mL) in a 250 mL flame-dried flask under argon. Triethylamine (1.95 mL, 14.03 mmol, 1.2 eq.) and diphenyl phosphoryl azide (2.52 mL, 11.69 mmol, 1 eq.) were added and the mixture was stirred for 30 minutes at room temperature and at reflux (120 °C) for 4 hours. After cooling the reaction to 50 °C, trichloroethanol (3.36 mL, 35.07 mmol, 3 eq.) was added and the mixture was refluxed overnight. The reaction was quenched upon addition of a saturated aq. $NaHCO_3$ solution and extracted with diethyl ether. The combined organic layers were dried over Na_2SO_4, filtered and concentrated to dryness. The crude product was purified by flash column chromatography (15% ethyl acetate in cyclohexane) to afford **31**.

Yield: 4.84 g (10.87 mmol, 93%) as a colorless solid.
TLC (15% ethyl acetate in cyclohexane)**:** $R_f = 0.19$.
HPLC (gradient 2): $t_R = 11.52$ min.
^{1}H NMR (400 MHz, d^6-DMSO): δ 7.66 (br s, 1 H), 5.42-5.54 (m, 2 H), 4.77 (s, 2 H), 4.19 (br s, 1 H), 3.97 (dd, J = 8.8, 6.1 Hz, 1 H), 3.64 (dd, J = 8.8, 2.1 Hz, 1 H), 3.03-3.10 (m, 2 H), 2.14-2.22 (m, 2 H), 1.49 (s, 3 H), 1.41 (s, 3 H), 1.37 (br s, 9 H).
^{13}C NMR (100 MHz, d^6-DMSO): δ 154.27, 151.08, 130.89, 128.26, 96.24, 92.82, 78.53, 73.30, 67.65, 58.45, 40.29, 31.70, 28.00, 26.32, 23.44.
HRMS (ESI): *m/z* calcd for $C_{17}H_{27}O_5N_2{}^{35}Cl_3H^+$ $[M + H]^+$ 445.1058, found 445.1058 and calcd for $C_{17}H_{27}O_5N_2{}^{35}Cl_2{}^{37}ClH^+$ $[M + H]^+$ 447.1029, found 447.1026.

Synthesis of (5*S*-*tert*-Butoxycarbonylamino-6-hydroxy-hex-3*E*-enyl)-carbamic acid 2,2,2-trichloro-ethyl ester, 32:

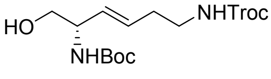

32

31 (1.34 g, 3.00 mmol, 1 eq.) was dissolved in methanol (120 mL) in a 250 mL flask. Pyridinium *p*-toluenesulfonate (151 mg, 0.60 mmol, 0.2 eq.) was added and the mixture was stirred at reflux (70 °C) overnight. The reaction was filtered over a plug of silica and the plug was washed with diethyl ether. Concentration to dryness afforded **32**.

Yield: 1.19 g (2.94 mmol, 98%) as a colorless oil.
TLC (60% ethyl acetate in cyclohexane)**:** $R_f = 0.42$.
HPLC (gradient 2): $t_R = 9.16$ min.
^{1}H NMR (400 MHz, $CDCl_3$): δ 5.63 (dt, J = 15.5, 7.4 Hz, 1 H), 5.49 (dd, J = 15.6, 5.8 Hz, 1 H), 5.30 (br s, 1 H), 4.97 (d, J = 7.7 Hz, 1 H), 4.72 (d, J = 12.0 Hz, 1 H), 4.69 (d, J = 12.1 Hz, 1 H), 4.16 (br s, 1 H), 3.66 (dd, J = 11.0, 4.3 Hz, 1 H), 3.60 (dd, J = 11.1, 5.3 Hz, 1 H), 3.25-3.32 (m, 2 H), 2.64 (br s, 1 H), 2.23-2.32 (m, 2 H), 1.44 (s, 9 H).
^{13}C NMR (100 MHz, $CDCl_3$): δ 155.99, 154.86, 130.51, 129.03, 95.73, 79.90, 74.55, 65.25, 54.19, 40.62, 32.79, 28.47.
HRMS (ESI): *m/z* calcd for $C_{14}H_{23}O_5N_2{}^{35}Cl_3H^+$ $[M + H]^+$ 405.0745, found 405.0744 and calcd for $C_{14}H_{23}O_5N_2{}^{35}Cl_2{}^{37}ClH^+$ $[M + H]^+$ 407.0716, found 407.0712.

Synthesis of 2*S*-*tert*-Butoxycarbonylamino-6-(2,2,2-trichloro-ethoxycarbonylamino)-hex-3*E*-enoic acid, 33:

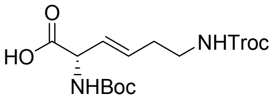

33

32 (777 mg, 1.92 mmol, 1 eq.) was dissolved in dichloromethane (10 mL) in a 25 mL flame-dried flask under argon at 0 °C. A solution of Dess-Martin periodinane in dichloromethane (15% wt, 7.95 mL, 3.83 mmol, 2 eq.) was added and the mixture was stirred for 2 hours at 0 °C. The reaction was filtrated over a plug of silica and the plug was washed with a mixture ethyl acetate/cyclohexane (1:1). Concentration to dryness afforded the air sensitive aldehyde which was used in the next step without further purification.

The crude aldehyde was diluted in a mixture of *tert*-butanol / 2-methyl-2-butene (3:1, 40mL) and the resulting solution was cooled to 0 °C. A solution of sodium chlorite (1.2 mg, 13.41 mmol, 7eq.) and sodium phosphate monobasic (1.1 mg, 7.66 mmol, 4 eq.) in water (10 mL) was slowly added and the reaction was stirred for 30 minutes at room temperature. The mixture was diluted with water and extracted with *tert*-butylmethyl ether. The combined organic layers were dried over Na_2SO_4, filtered and concentrated to dryness. The crude product was purified by flash column chromatography (0.2% acetic acid + 2% methanol in dichloromethane) to afford **33**.

Yield: 554 mg (1.32 mmol, 69%) as a colorless solid.
TLC (0.5% acetic acid + 3% methanol in dichloromethane)**:** $R_f = 0.15$.
HPLC (gradient 2): $t_R = 6.64$ min.
^{1}H NMR (400 MHz, $CD_3OD/CDCl_3$ = 1:9): δ 5.67 (dtd, J = 15.6, 6.8, 1.1 Hz, 1 H), 5.52 (dd, J = 15.5, 6.0 Hz, 1 H), 4.65-4.68 (m, 1 H), 4.64 (s, 2 H), 3.12-3.26 (m, 2 H), 2.18-2.26 (m, 2 H), 1.37 (s, 9 H).
^{13}C NMR (100 MHz, $CD_3OD/CDCl_3$ = 1:9): δ 172.79, 155.49, 155.00, 130.35, 127.31, 95.65, 80.20, 74.39, 55.18, 40.19, 32.28, 28.19.
HRMS (ESI): *m/z* calcd for $C_{14}H_{21}O_6N_2{}^{35}Cl_3H^+$ $[M + H]^+$ 419.0538, found 419.0538 and calcd for $C_{14}H_{21}O_6N_2{}^{35}Cl_2{}^{37}ClH^+$ $[M + H]^+$ 421.0509, found 421.0508.

Synthesis of 4*S*-*tert*-Butoxycarbonylamino-5-methyl-hex-2*E*-enoic acid methyl ester, 34:

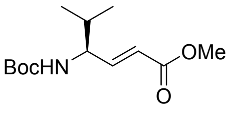

34

N-(*tert*-Butoxycarbonyl)-(L)-valine methyl ester **19** (5.64 g, 24.39 mmol, 1 eq.) was dissolved under argon in toluene (245 mL) in a 500 mL flame-dried flask. The solution was cooled to -78 °C and a 1 M solution of DIBAL-H in toluene (49 mL, 48.78 mmol, 2 eq.) was slowly added over 2 hours. After stirring for further 2 hours, the mixture was quenched with a 1.2 M solution of potassium sodium tartrate (150 mL) and stirred vigorously at room temperature for 2 hours. The resulting solution was extracted with dichloromethane and the organic layers were dried over Na_2SO_4, filtered and concentrated to dryness to give *N*-(*tert*-butoxycarbonyl)-(L)-valinal which was directly used in the next step without further purification.

Crude *N*-(*tert*-butoxycarbonyl)-(L)-valinal was dissolved in dichloromethane (245 mL) and (methoxycarbonylmethylene)triphenylphosphorane (9.38 g, 28.05 mmol, 1.15 eq.) was added in one portion. After stirring for 12 hours, the mixture was successively washed with a 10% aq. $KHSO_4$ solution, a 5% aq. $NaHCO_3$ solution and with brine. The organic layer was dried over Na_2SO_4, filtered and evaporated to dryness. The resulting crude product was purified by flash column chromatography (10% ethyl acetate in cyclohexane) to afford **34**.

Yield: 3.78 g (14.69 mmol, 60%) as colorless crystals.

TLC (15% ethyl acetate in cyclohexane)**:** $R_f = 0.31$.

HPLC (gradient 1): $t_R = 8.93$ min.

^{1}H NMR (400 MHz, $CDCl_3$): δ 6.86 (dd, J = 15.6, 5.6 Hz, 1 H), 5.92 (dd, J = 15.6, 1.6 Hz, 1 H), 4.50-4.62 (m, 1 H), 4.11-4.23 (m, 1 H), 3.73 (s, 3 H), 1.80-1.91 (m, 1 H), 1.44 (s, 9 H), 0.93 (d, J = 6.8 Hz, 3 H), 0.90 (d, J = 6.8 Hz, 3 H).

^{13}C NMR (100 MHz, $CDCl_3$): δ 166.75, 155.42, 147.74, 121.19, 79.78, 56.79, 51.66, 32.32, 28.44, 18.92, 18.10.

HRMS (ESI): *m/z* calcd for $C_{13}H_{23}O_4NH^+$ $[M + H]^+$ 258.1700, found 258.1702.

Synthesis of 4*S*-Amino-5-methyl-hex-2*E*-enoic acid methyl ester trifluoroacetic salts, 35:

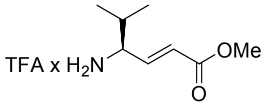

35

34 (100 mg, 389 μmol, 1 eq.) was dissolved in a mixture trifluoroacetic acid/dichloromethane (1:3, 2 mL) in a 10 mL flask. After 30 minutes, the mixture was evaporated to dryness and co-evaporated with toluene to afford **35**.

Yield: 104 mg (381 μmol, 98%) as a colorless solid.

TLC (2% triethylamine + 48% ethyl acetate in cyclohexane)**:** $R_f = 0.24$.

HPLC (gradient 2): $t_R = 3.29$ min.

^{1}H NMR (400 MHz, $CDCl_3$): δ 8.32 (br s, 2 H), 6.84 (dd, J = 15.9, 8.1 Hz, 1 H), 6.08 (d, J = 15.9 Hz, 1 H), 3.75 (s, 3 H), 3.62-3.68 (m, 1 H), 2.05-2.15 (m, 1 H), 1.04 (d, J = 6.8 Hz, 3 H), 0.98 (d, J = 6.8 Hz, 3 H).

^{13}C NMR (100 MHz, $CDCl_3$): δ 166.07, 140.41, 125.78, 58.19, 52.13, 31.14, 18.67, 17.39.

HRMS (ESI): *m/z* calcd for $C_8H_{15}O_2NH^+$ $[M + H]^+$ 158.1176, found 158.1170.

Synthesis of 4*S*-[2*S*-*tert*-Butoxycarbonylamino-6-(2,2,2-trichloro-ethoxycarbonylamino)-hex-3*E*-enoylamino]-5-methyl-hex-2*E*-enoic acid methyl ester, 36:

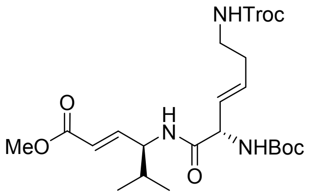

36

35 (49 mg, 182 µmol, 1.2 eq.), **33** (64 mg, 152 µmol, 1 eq.), PyBop (119 mg, 228 µmol, 1.5 eq.) and HOAt (31 mg, 228 µmol, 1.5 eq.) were dissolved in dichloromethane (2.0 mL) in a 10 mL flask. The solution was cooled to 0 °C and *N*,*N*-diisopropylethylamine (53 µL, 304 µmol, 2.0 eq.) was added. The reaction was stirred at room temperature overnight. After dilution with dichloromethane the mixture was washed with a 20% aq. citric acid solution and the organic layer was dried over Na_2SO_4, filtered and concentrated to dryness. The crude product was purified by flash column chromatography (35% ethyl acetate in cyclohexane) to afford **36**.

Yield: 55 mg (99 µmol, 65%) as a colorless solid.

TLC (40% ethyl acetate in cyclohexane)**:** $R_f = 0.35$.

HPLC (gradient 2): $t_R = 7.56$ min.

^{1}H NMR (400 MHz, $CDCl_3$): δ 6.87 (dd, J = 15.7, 5.6 Hz, 1 H), 6.36 (d, J = 7.6 Hz, 1 H), 5.88 (dd, J = 15.7, 1.6 Hz, 1 H), 5.80 (dt, J = 15.6, 6.4 Hz, 1 H), 5.60 (dd, J = 15.6, 7.3 Hz, 1 H), 5.33-5.45 (m, 2 H), 4.72 (d, J = 12.2 Hz, 1 H), 4.68 (d, J = 12.2 Hz, 1 H), 4.58 (t, J = 6.3 Hz, 1 H), 4.43-4.50 (m, 1 H), 3.72 (s, 3 H), 3.27-3.34 (m, 2 H), 2.28-

2.35 (m, 2 H), 1.84-1.94 (m, 1 H), 1.44 (s, 9 H), 0.93 (d, J = 6.7 Hz, 3 H), 0.91 (d, J = 6.6 Hz, 3 H).

^{13}C NMR (100 MHz, $CDCl_3$): δ 169.98, 166.60, 155.56, 154.90, 146.72, 132.16, 128.52, 121.58, 95.73, 80.44, 74.50, 56.81, 55.61, 51.73, 40.69, 32.81, 32.10, 28.39, 19.03, 18.25.

HRMS (ESI): *m/z* calcd for $C_{22}H_{34}O_7N_3{}^{35}Cl_3H^+$ $[M + H]^+$ 558.1535, found 558.1532 and calcd for $C_{22}H_{34}O_7N_3{}^{35}Cl_2{}^{37}ClH^+$ $[M + H]^+$ 560.1506, found 560.1502.

Synthesis of 4*S*-(6-Amino-2*S*-*tert*-butoxycarbonylamino-hex-3*E*-enoylamino)-5-methyl-hex-2*E*-enoic acid, 37:

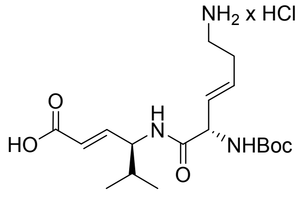

37

36 (34 mg, 61 µmol, 1 eq.) was dissolved in tetrahydrofurane (2.5 mL) in a 10 mL flask. A NH_4OAc buffer solution (1 M, pH 5.0, 0.5 mL) was added, followed by zinc powder (599 mg, 9.15 mmol, 150 eq.) which was added in portions over 30 minutes. After 3 hours of vigorous stirring, the mixture was filtered over a small plug of Celite ® and washed with ethyl acetate. After evaporation to dryness, the deprotected amine was used in the next step without further purification (intermediate characterization: TLC (2% acetic acid + 5% methanol in dichloromethane): Rf = 0.23; HPLC (gradient 2): t_R = 6.38 min; HRMS (ESI): *m/z* calcd for $C_{19}H_{33}O_5N_3H^+$ $[M + H]^+$ 384.2493, found 384.2497).

The cleaved intermediate was dissolved in a mixture methanol/water (3:1, 0.9 mL) in a 10 mL flask. A solution of lithium hydroxide (5.1 mg, 122 µmol, 2 eq.) in water (0.7 mL) was added dropwise at 0 °C and the resulting mixture was allowed to stir at room temperature for 30 minutes. After concentration to dryness, the residue was redissolved in diluted aq. HCl and re-evaporated to dryness. Addition of toluene and concentration to dryness yielded **37**.

Yield: 20 mg (50 µmol, 82%) as a colorless solid.

HPLC (gradient 2): t_R = 6.01 min.

^{1}H NMR (400 MHz, $CD_3OD/CDCl_3$ = 1:4): δ 6.77 (ddd, J = 15.4, 5.4, 1.7 Hz, 1 H), 5.78 (d, J = 15.5 Hz, 1 H), 5.58-5.63 (m, 2 H), 4.55-4.62 (m, 1 H), 4.30 (dd, J = 5.7, 5.7 Hz, 1 H), 2.85-2.99 (m, 2 H), 2.31-2.42 (m, 2 H), 1.75-1.86 (m, 1 H), 1.37 (s, 9 H), 0.86 (d, J = 7.0 Hz, 3 H), 0.84 (d, J = 7.2 Hz, 3 H).

^{13}C NMR (100 MHz, $CD_3OD/CDCl_3$ = 1:4): δ 171.01, 168.22, 146.77, 130.14, 128.03, 121.88, 80.49, 56.29, 55.69, 38.47, 31.89, 29.90, 28.11, 18.86, 17.97.

HRMS (ESI): *m/z* calcd for $C_{18}H_{31}O_5N_3H^+$ $[M + H]^+$ 370.2337, found 370.2337.

Synthesis of 2*S*-*tert*-Butoxycarbonylamino-4-phenylselanyl-butyric acid, 40:

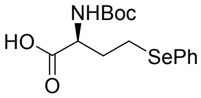

40

Sodium borohydride (125 mg, 3.3 mmol, 4.4 eq.) was disposed under argon in a 100 mL flame dried flask. A solution of diphenyl diselenide (937 mg, 3.0 mmol, 1 eq.) in *N*,*N*-dimethylformamide (20 mL) was added, followed by addition of a solution of Boc-homoserine lactone **41** (603 mg, 3.0 mmol, 1 eq.) in *N*,*N*-dimethylformamide (20 mL). The resulting mixture was heated to 100 °C for 90 minutes. After cooling to 0 °C, methanol (5 mL) was added and the mixture was stirred for an hour. The solvents were removed *in vacuo* and the remaining residue was partitioned between diethyl ether (150 mL) and 100 mM NaOAc buffer (pH 5.0). The aqueous layer was extracted twice more with diethyl ether (150 mL). The combined organic layers were dried over Na_2SO_4, filtered and concentrated. The crude product was purified by flash column chromatography (40% ethyl acetate in cyclohexane) to afford **40**.

Yield: 973 mg (2.72 mmol, 91%) as a colorless solid.

TLC (2% acetic acid + 58% ethyl acetate in cyclohexane)**:** R_f = 0.56.

HPLC (gradient 2): t_R = 9.54 min.

^{1}H NMR (400 MHz, $CDCl_3$): δ 9.20 (br s, 1 H), 7.48-7.52 (m, 2 H), 7.23-7.28 (m, 3 H), 5.07 (d, J = 6.4 Hz, 1 H), 4.35 (br s, 1 H), 2.93 (t, J = 8.0 Hz, 2 H), 2.16-2.32 (m, 1 H), 1.98-2.15 (m, 1 H), 1.44 (s, 9 H).

^{13}C NMR (100 MHz, $CDCl_3$): δ 176.32, 155.68, 133.04, 129.54, 129.24, 127.26, 80.56, 53.56, 33.23, 28.38, 23.21.
HRMS (ESI): *m/z* calcd for $C_{15}H_{21}O_4N^{80}SeH^+$ $[M + H]^+$ 360.0709, found 360.0710 and calcd for $C_{15}H_{21}O_4N^{78}SeH^+$ $[M + H]^+$ 358.0716, found 358.0719.

Synthesis of 4*S*-*tert*-Butoxycarbonylamino-5-methyl-hex-2*E*-enoic acid, 127:

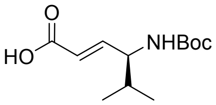

127

In a 250 mL flask was dissolved **34** (2.45 g, 9.52 mmol, 1 eq.) in a mixture methanol/water (3:1, 60 mL) and a 1 M solution of lithium hydroxide (2.4 g, 57.12 mmol, 6 eq.) was added dropwise at 0 °C. The resulting mixture was allowed to stir at room temperature for 30 minutes and concentrated to dryness. A biphasic mixture was obtained after dissolution between ethyl acetate (100 mL) and a 10% aq. $KHSO_4$ solution (100 mL). The aqueous layer was extracted with ethyl acetate and the combined organic layers were dried with brine (50 mL) and over Na_2SO_4, filtered and concentrated to dryness to afford **127**.

Yield: 2.30 g (9.46 mmol, 99%) as a colorless solid.
TLC (2% acetic acid + 50% ethyl acetate in cyclohexane)**:** $R_f = 0.57$.
HPLC (gradient 2): $t_R = 8.35$ min.
^{1}H NMR (400 MHz, $CDCl_3$): δ 11.20 (br s, ~1 H), 6.97 (dd, J = 15.5, 4.7 Hz, 1 H), 5.93 (dd, J = 15.7, 1.7 Hz, 1 H), 4.50-4.66 (br s, 1 H), 4.15-4.29 (br s, 1 H), 1.82-1.95 (m, 1 H), 1.45 (s, 9 H), 0.95 (d, J = 6.8 Hz, 3 H), 0.93 (d, J = 6.9, 3 H).
^{13}C NMR (100 MHz, $CDCl_3$): δ 170.90, 155.47, 150.06, 120.91, 79.99, 56.81, 32.33, 28.45, 18.96, 18.11.
HRMS (ESI): *m/z* calcd for $C_{12}H_{21}O_4NH^+$ $[M + H]^+$ 244.1543, found 244.1545.

Synthesis of (3-But-3*E*-enylcarbamoyl-1*S*-isopropyl-allyl)-carbamic acid *tert*-butyl ester, 128:

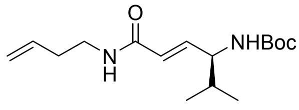

128

127 (649 mg, 2.67 mmol, 1 eq.), 3-butenylamine hydrochloride (317 mg, 2.94 mmol, 1.1 eq.), PyBop (1.53 g, 2.94 mmol, 1.1 eq.) were dissolved in dichloromethane (4 mL) in a 25 mL flask. The solution was cooled to 0 °C and *N*,*N*-diisopropylethylamine (1.39 mL, 8.00 mmol, 3 eq.) was added. The reaction was stirred overnight at room temperature, quenched by addition of a 20% aq. citric acid solution and extracted with chloroform (3 × 50 mL). The combined organic layers were dried over Na_2SO_4, filtered and concentrated to dryness. The crude product was purified by flash column chromatography (50% ethyl acetate in cyclohexane) to afford **128**.

Yield: 658 mg (2.22 mmol, 83%) as a colorless solid.
TLC (70% ethyl acetate in cyclohexane)**:** $R_f = 0.65$.
HPLC (gradient 2): $t_R = 8.99$ min.
^{1}H NMR (500 MHz, $CDCl_3$): δ 6.69 (dd, J = 15.0, 6.1 Hz, 1 H), 5.85 (d, J = 15.2 Hz, 1 H), 5.76 (ddt, J = 17.1, 10.2, 6.8 Hz, 1 H), 5.64 (br s, 1 H), 5.06-5.13 (m, 2 H), 4.59 (d, J = 8.6 Hz, 1 H), 4.09 (d, J = 6.5 Hz, 1 H), 3.36-3.42 (m, 2 H), 2.25-2.31 (m, 2 H), 1.77-1.87 (m, 1 H), 1.43 (s, 9 H), 0.91 (d, J = 7.2 Hz, 3 H), 0.90 (d, J = 7.8 Hz, 3 H).
^{13}C NMR (125 MHz, $CDCl_3$): δ 165.34, 155.48, 142.80, 135.27, 124.19, 117.39, 79.64, 56.97, 38.55, 33.72, 32.39, 28.45, 18.91, 18.20.
HRMS (ESI): *m/z* calcd for $C_{16}H_{28}O_3N_2H^+$ $[M + H]^+$ 297.2173, found 297.2174.

Synthesis of 4*S*-Amino-5-methyl-hex-2*E*-enoic acid but-3-enylamide trifluoroacetic salts, 42:

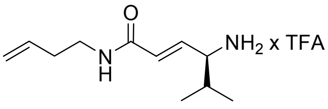

42

128 (2.11 g, 7.10 mmol, 1 eq.) was dissolved in a mixture trifluoroacetic acid/dichloromethane (1:4, 70 mL) in a 100 mL flask. After 30 minutes, the mixture was concentrated to dryness and co-evaporated with toluene to afford **42**.

Yield: 2.16 g (6.96 mmol, >98%) as a colorless solid.
TLC (2.5% triethylamine + 8% methanol in dichloromethane)**:** $R_f = 0.53$.
HPLC (gradient 2): $t_R = 4.61$ min.
^{1}H NMR (500 MHz, $CDCl_3$): δ 6.69 (dd, J = 15.5, 8.7 Hz, 1 H), 6.62-6.66 (m, 1 H), 6.17 (d, J = 15.5 Hz, 1 H), 5.73 (ddt, J = 16.5, 10.7, 6.8 Hz, 1 H), 5.07-5.12 (m, 2 H), 3.66 (br s, 1 H), 3.30-3.43 (m, 2 H), 2.25-2.31 (m, 2 H), 2.02-2.12 (m, 1 H), 1.03 (d, J = 6.8 Hz, 3 H), 0.96 (d, J = 6.8 Hz, 3 H).
^{13}C NMR (125 MHz, $CDCl_3$): δ 165.76, 136.81, 134.36, 128.58, 117.76, 58.88, 39.33, 33.09, 31.06, 18.44, 17.49.
HRMS (ESI): *m/z* calcd for $C_{11}H_{20}ON_2H^+$ $[M + H]^+$ 197.1648, found 197.1647.

Synthesis of [1*S*-(3-But-3*E*-enylcarbamoyl-1*S*-isopropyl-allylcarbamoyl)-3-phenylselanyl-propyl]-carbamic acid *tert*-butyl ester, 43:

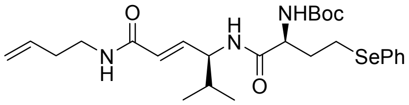

43

40 (1.23 g, 3.42 mmol, 1 eq.), **42** (1.06 g, 3.42 mmol, 1 eq.), PyBop (1.80 g, 3.46 mmol, 1.01 eq.) and HOAt (471 mg, 3.46 mmol, 1.01 eq.) were dissolved in dichloromethane (20 mL) in a 100 mL flask. The solution was cooled to 0 °C and *N*,*N*-diisopropylethylamine (1.60 mL, 9.24 mmol, 2.7 eq.) was added. The reaction was stirred overnight at room temperature, quenched by addition of a 20% aq. citric acid solution and extracted with chloroform (3 × 50 mL). The combined organic layers were dried over Na_2SO_4, filtered and concentrated to dryness. The crude product was purified by flash column chromatography (4% methanol in dichloromethane) to afford **43**.

Yield: 1.71 g (3.18 mmol, 93%) as a colorless solid.

TLC (8% methanol in dichloromethane)**:** $R_f = 0.69$.

HPLC (gradient 2): $t_R = 10.29$ min.

^{1}H NMR (400 MHz, d^6-DMSO): δ 7.99 (t, J = 5.6 Hz, 1 H), 7.82 (d, J = 8.5 Hz, 1 H), 7.41-7.45 (m, 2 H), 7.22-7.30 (m, 3 H), 7.02 (d, J = 8.1 Hz, 1 H), 6.50 (dd, J = 15.4, 7.4 Hz, 1 H), 5.90 (d, J = 15.3 Hz, 1 H), 5.77 (ddt, J = 17.0, 10.3, 6.7 Hz, 1 H), 5.04 (dd, J = 17.3, 1.8 Hz, 1 H), 4.99 (d, J = 10.3 Hz, 1 H), 4.12-4.19 (m, 1 H), 4.02-4.10 (m, 1 H), 3.10-3.23 (m, 2 H), 2.83-2.94 (m, 2 H), 2.13-2.21 (m, 2 H), 1.88-1.97 (m, 2 H), 1.71-1.79 (m, 1 H), 1.37 (s, 9 H), 0.84 (d, J = 7.1 Hz, 3 H), 0.82 (d, J = 7.1 Hz, 3 H).

^{13}C NMR (100 MHz, d^6-DMSO): δ 170.79, 164.43, 155.32, 140.57, 135.94, 131.09, 130.03, 129.17, 126.40, 125.02, 116.19, 78.13, 55.11, 54.47, 38.01, 33.38, 31.61, 28.10, 25.82, 22.77, 18.92, 18.33.

HRMS (ESI): *m/z* calcd for $C_{26}H_{39}O_4N_3SeH^+$ $[M + H]^+$ 538.2179, found 538.2171.

Synthesis of [1*S*-(3-But-3*E*-enylcarbamoyl-1*S*-isopropyl-allylcarbamoyl)-allyl]-carbamic acid *tert*-butyl ester, 39:

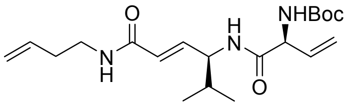

39

43 (508 mg, 947 µmol, 1 eq.) was dissolved in dichloromethane (50 mL) in a 100 mL flask. Hydrogen peroxide (30% in water, 2.5 mL) and *N*,*N*-diisopropylethylamine (2.5 mL) were added and the resulting mixture was heated to 50 °C for 3 hours. The reaction was quenched by addition of a saturated aq. $CuSO_4$ solution. Addition of ethyl acetate (50 mL) and a 10% aq. $KHSO_4$ solution (50 mL) generated a biphasic mixture which was separated in a funnel. The organic phase was washed with a 5% aq. $NaHCO_3$ solution (50 mL) and brine (50 mL), dried over Na_2SO_4, filtered and concentrated to dryness. The crude product was purified by flash column chromatography (70% ethyl acetate in cyclohexane) to afford **39**.

Yield: 241 mg (635 µmol, 67%) as a colorless solid.

TLC (70% ethyl acetate in cyclohexane)**:** $R_f = 0.42$.

HPLC (gradient 2): $t_R = 8.59$ min.

^{1}H NMR (400 MHz, CDCl$_3$): δ 6.77 (br s, 1 H), 6.69 (dd, J = 15.2, 6.6 Hz, 1 H), 6.10 (br s, 1 H), 5.91 (d, J = 15.2 Hz, 1 H), 5.84-5.96 (m, 1 H), 5.75 (ddt, J = 17.1, 10.3, 6.8 Hz, 1 H), 5.56 (d, J = 7.2 Hz, 1 H), 5.33 (d, J = 17.1 Hz, 1 H), 5.24 (d, J = 10.3 Hz, 1 H), 5.02-5.11 (m, 2 H), 4.69 (br s, 1 H), 4.35-4.43 (m, 1 H), 3.32-3.38 (m, 2 H), 2.23-2.30 (m, 2 H), 1.79-1.89 (m, 1 H), 1.42 (s, 9 H), 0.89 (d, J = 6.8 Hz, 6 H).
^{13}C NMR (100 MHz, CDCl$_3$): δ 169.88, 165.35, 155.52, 141.55, 135.22, 133.94, 124.98, 117.96, 117.18, 80.28, 57.20, 55.84, 38.70, 33.70, 32.16, 28.39, 19.00, 18.38.
HRMS (ESI): *m/z* calcd for $C_{20}H_{33}O_4N_3H^+$ $[M + H]^+$ 380.2544, found 380.2545.

Synthesis of 4*S*-*tert*-Butoxycarbonylamino-2*S*,3*R*-dihydroxy-5-methyl-hexanoic acid methyl ester, 129:

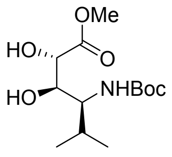

129

34 (643 mg, 2.50 mmol, 1 eq.) was dissolved in acetone/water (2:1, 22.5 mL) in a 100 mL flask. 4-Methylmorpholine *N*-oxide (440 mg, 3.75 mmol, 1.5 eq.) and osmium tetroxide solution (4% wt/H$_2$O, 764 µL, 125 µmol, 0.05 eq.) were added consecutively. The flask was flushed with argon and the reaction was stirred for 2 days. The reaction was quenched by addition of a saturated aq. NaHSO$_3$ solution and the acetone was evaporated *in vacuo*. Ethyl acetate and further water were added, separated in a funnel, and the organic layer was dried over Na$_2$SO$_4$, filtered over Celite and concentrated to dryness to give a crude mixture of diastereoisomers. **129** was obtained by recrystallization from cyclohexane to yield 583 mg (2.00 mmol, 80 %) of a pure single diastereoisomer **129** as colorless crystals. The residual mixture was then purified by flash column chromatography (70% diethyl ether in petroleum ether) to afford another 38 mg (0.13 mmol, 5%) of **129** as colorless crystals.

Yield: 621 mg (2.13 mmol, 85%) as a colorless solid.
TLC (70% diethyl ether in petroleum ether)**:** $R_f = 0.23$.
HPLC (gradient 2): $t_R = 7.55$ min.

^{1}H NMR (400 MHz, $CDCl_3$): δ 4.78 (d, J = 10.0 Hz, 1 H), 4.32 (br s, 1 H), 4.01 (br s, 1 H), 3.81-3.86 (m, 1 H), 3.81 (s, 3 H), 3.52-3.59 (m, 1 H), 2.59 (br s, 1 H), 2.08-2.18 (m, 1 H), 1.43 (s, 9 H), 0.98 (d, J = 6.8 Hz, 3 H), 0.91 (d, J = 6.8 Hz, 3 H).

^{13}C NMR (100 MHz, $CDCl_3$): δ 173.04, 157.49, 80.36, 72.16, 71.17, 57.35, 52.73, 28.38, 27.99, 20.11, 16.67.

HRMS (ESI): *m/z* calcd for $C_{13}H_{25}O_6NH^+$ $[M + H]^+$ 292.1755, found 292.1757.

Synthesis of 5*R*-(1*S*-*tert*-Butoxycarbonylamino-2-methyl-propyl)-2,2-dimethyl-[1,3]dioxolane-4*S*-carboxylic acid methyl ester, 44:

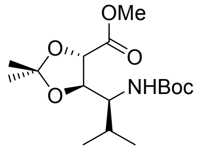

44

129 (3.53 g, 12.12 mmol, 1 eq.) was dissolved in dichloromethane (45 mL) in a 250 mL flame-dried flask and 2,2-dimethoxypropane (45 mL, 364.00 mmol, 30 eq.) and pyridinium *p*-toluenesulfonate (153 mg, 0.61 mmol, 0.05 eq.) were added. The flask was flushed with argon and the solution was heated to reflux for 5 hours. After evaporation to dryness, the desired product **44** was obtained.

Yield: 3.93 g (11.88 mmol, >98%) as a colorless solid.

TLC (15% ethyl acetate in cyclohexane)**:** $R_f = 0.26$.

HPLC (gradient 1): $t_R = 9.78$ min.

^{1}H NMR (400 MHz, $CDCl_3$): δ 4.46 (d, J = 6.0 Hz, 1 H), 4.41-4.45 (m, 1 H), 4.11 (dd, J = 9.2, 6.4 Hz, 1 H), 3.76 (s, 3 H), 3.69-3.76 (m, 1 H), 2.09 (septd, J = 6.8, 3.6 Hz, 1 H), 1.44 (s, 3 H), 1.42 (s, 9 H), 1.41 (s, 3 H), 0.94 (d, J = 6.8 Hz, 3 H), 0.86 (d, J = 6.8 Hz, 3 H).

^{13}C NMR (100 MHz, $CDCl_3$): δ 171.87, 156.07, 111.88, 79.50, 77.97, 57.50, 52.47, 28.52, 28.39, 27.23, 26.02, 19.83, 15.70.

HRMS (ESI): *m/z* calcd for $C_{16}H_{29}O_6NH^+$ $[M + H]^+$ 332.2068, found 332.2069.

Synthesis of 5*R*-(1*S*-*tert*-Butoxycarbonylamino-2-methyl-propyl)-2,2-dimethyl-[1,3]dioxolane-4*S*-carboxylic acid, 130:

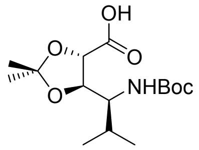

130

44 (1.40 g, 4.23 mmol, 1 eq.) was dissolved in methanol/water (1:1, 20 mL) in a 50 mL flask and a 1 M aq. lithium hydroxide solution (13 mL, 533 mg, 12.69 mmol, 3 eq.) was added at 0 °C. The mixture was stirred for further 30 min at room temperature. After evaporation of the methanol, a 20% aq. citric acid solution was added to acidify the reaction mixture. Extraction with dichloromethane (3 × 50 mL), drying over Na_2SO_4, filtering and concentration to dryness yielded **130**.

Yield: 1.31 g (4.15 mmol, >98%) as a white powder.
TLC (methanol/acetic acid/dichloromethane = 1:1:38)**:** $R_f = 0.33$.
HPLC (gradient 2): $t_R = 9.05$ min.
^{1}H NMR (500 MHz, CD_3OD): δ 4.23 (dd, J = 7.5, 5.5 Hz, 1 H), 4.14 (d, J = 5.5 Hz, 1 H), 3.54 (dd, J = 8.0, 4.5 Hz, 1 H), 1.97-2.05 (m, 1 H), 1.43 (s, 9 H), 1.40 (s, 3 H), 1.38 (s, 3 H), 0.94 (d, J = 7.0 Hz, 3 H), 0.89 (d, J = 7.0 Hz, 3 H).
^{13}C NMR (125 MHz, CD_3OD): δ 178.61, 158.72, 111.38, 80.72, 80.34, 79.98, 59.62, 30.54, 28.79, 27.86, 26.72, 20.49, 17.31.
HRMS (ESI): *m/z* calcd for $C_{15}H_{27}O_6NH^+$ $[M + H]^+$ 318.1911, found 318.1913.

Synthesis of [1*S*-(5*R*-But-3-enylcarbamoyl-2,2-dimethyl-[1,3]dioxolan-4*S*-yl)-2-methyl-propyl]-carbamic acid *tert*-butyl ester, 45:

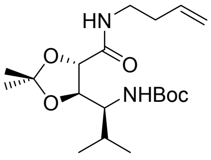

45

130 (1.33 g, 4.20 mmol, 1 eq.), 3-butenylamine hydrochloride (0.54 g, 5.10 mmol, 1.2 eq.), HOAt (858 mg, 6.30 mmol, 1.5 eq.) and PyBop (3.28 g, 6.30 mmol, 1.5 eq.) were dissolved in dichloromethane (5 mL) in a 10 mL flask. *N*,*N*-Diisopropylethylamine (1.46 mL, 8.40 mmol, 2 eq.) was added at 0 °C and the resulting mixture was stirred overnight at room temperature. The reaction was stopped by quenching with a 20% aq. citric acid solution and **45** was extracted from the mixture with chloroform (3 × 50 mL). The combined organic layers were dried over Na_2SO_4, filtered and concentrated to dryness. The crude product was purified by flash column chromatography (20% ethyl acetate in cyclohexane) to afford **45**.

Yield: 1.27 g (3.43 mmol, 82%) as a colorless solid.
TLC (30% ethyl acetate in cyclohexane)**:** $R_f = 0.49$.
HPLC (gradient 2): $t_R = 10.79$ min.
^{1}H NMR (400 MHz, $CDCl_3$): δ 6.63 (br s, 1 H), 5.75 (ddt, J = 17.2, 10.4, 6.8 Hz, 1 H), 5.19 (d, J = 9.2 Hz, 1 H), 5.06-5.13 (m, 2 H), 4.30 (d, J = 6.0 Hz, 1 H), 4.06 (dd, J = 9.2, 6.0 Hz, 1 H), 3.64-3.73 (m, 1 H), 3.37-3.46 (m, 1 H), 3.24-3.33 (m, 1 H), 2.24-2.31 (m, 2 H), 2.01-2.11 (m, 1 H), 1.45 (s, 3 H), 1.43 (s, 9 H), 1.36 (s, 3 H), 0.96 (d, J = 7.2 Hz, 3 H), 0.87 (d, J = 7.2 Hz, 3 H).
^{13}C NMR (100 MHz, $CDCl_3$): δ 171.40, 156.60, 135.05, 117.49, 111.36, 79.17, 78.36, 58.11, 37.99, 33.77, 29.59, 28.47, 27.28, 26.32, 19.81, 16.25.
HRMS (ESI): *m/z* calcd for $C_{19}H_{34}O_5N_2H^+$ $[M + H]^+$ 371.2541, found 371.2540.

Synthesis of 5*R*-(1*S*-Amino-2-methyl-propyl)-2,2-dimethyl-[1,3]dioxolane-4*S*-carboxylic acid but-3-enylamide, 131:

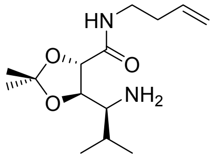

131

45 (710 mg, 1.92 mmol, 1 eq.) was dissolved under argon in dichloromethane (2 mL) in a 10 mL flame-dried flask. 2,6-Lutidine (446 µL, 3.84 mmol, 2 eq.) and trimethylsilyl trifluoro methanesulfonate (522 µL, 2.88 mmol, 1.5 eq.) were added and the resulting mixture was stirred for further 15 minutes. The reaction was quenched upon addition of a saturated aq. NH_4Cl solution. The pH of the water phase was adjusted to 9 by addition of a 2 M aq. NaOH solution and was extracted with dichloromethane. The combined organic layers were washed with brine, dried over Na_2SO_4, filtered and concentrated to dryness, yielding the desired product **131**.

Yield: 508 mg (1.88 mmol, >98%) as a white powder.
TLC (7% methanol in dichloromethane)**:** $R_f = 0.38$.
HPLC (gradient 2): $t_R = 5.88$ min.
^{1}H NMR (400 MHz, $CDCl_3$): δ 6.83 (br s, 1 H), 5.75 (ddt, J = 17.2, 10.0, 6.8 Hz, 1 H), 5.06-5.13 (m, 2 H), 4.34 (d, J = 6.8 Hz, 1 H), 3.99 (dd, J = 7.6, 6.8 Hz, 1 H), 3.27-3.43 (m, 2 H), 2.95 (br s, 2 H), 2.85 (dd, J = 7.6, 4.4 Hz, 1 H), 2.24-2.31 (m, 2 H), 2.06 (septd, J = 6.8, 4.4 Hz, 1 H), 1.44 (s, 3 H), 1.37 (s, 3 H), 1.02 (d, J = 7.2 Hz, 3 H), 0.92 (d, J = 6.8 Hz, 3 H).
^{13}C NMR (100 MHz, $CDCl_3$): δ 171.27, 135.10, 117.47, 110.29, 80.35, 78.77, 59.17, 37.99, 33.71, 29.07, 27.04, 25.88, 19.87, 16.03.
HRMS (ESI): *m/z* calcd for $C_{14}H_{26}O_3N_2H^+$ $[M + H]^+$ 271.2016, found 271.2017.

Synthesis of {1*S*-[1*S*-(5*R*-But-3-enylcarbamoyl-2,2-dimethyl-[1,3]dioxolan-4*S*-yl)-2-methyl-propylcarbamoyl]-3-phenylselanyl-propyl}-carbamic acid *tert*-butyl ester, 46:

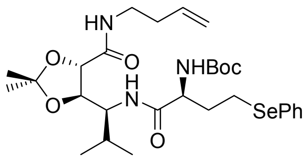

46

131 (512 mg, 1.90 mmol, 1 eq.), **40** (878 mg, 2.45 mmol, 1.3 eq.), PyBop (1.48 g, 2.85 mmol, 1.5 eq.) and HOAt (388 mg, 2.85 mmol, 1.5 eq.) were dissolved in dichloromethane (10 mL) in a 25 mL flask. The solution was cooled to 0 °C and *N*,*N*-diisopropylethylamine (662 μL, 3.80 mmol, 2 eq.) was added. The reaction was stirred overnight at room temperature, quenched by addition of a 20% aq. citric acid solution and extracted with chloroform (3 × 50 mL). The combined organic layers were dried over Na_2SO_4, filtered and concentrated to dryness. The crude product was purified by flash column chromatography (20% ethyl acetate in cyclohexane) to afford **46**.

Yield: 1.03 g (1.69 mmol, 89%) as a colorless solid.

TLC (25% ethyl acetate in cyclohexane)**:** $R_f = 0.27$.

HPLC (gradient 2): $t_R = 11.68$ min.

^{1}H NMR (400 MHz, $CDCl_3$): δ 7.42-7.46 (m, 2 H), 7.17-7.23 (m, 3 H), 6.97 (d, J = 8.4 Hz, 1 H), 6.64 (t, J = 5.6 Hz, 1 H), 5.72 (ddt, J = 17.6, 9.6, 6.8 Hz, 1 H), 5.19 (d, J = 8.0 Hz, 1 H), 5.04-5.10 (m, 2 H), 4.16-4.25 (m, 1 H), 4.10 (d, J = 6.8 Hz, 1 H), 4.03 (dd, J = 8.8, 6.8 Hz, 1 H), 3.96 (ddd, J = 8.8, 3.6, 3.6 Hz, 1 H), 3.33-3.42 (m, 1 H), 3.17-3.26 (m, 1 H), 2.83-2.90 (m, 2 H), 2.16-2.28 (m, 3 H), 2.07 (septd, J = 6.8, 3.6 Hz, 1 H), 1.91-2.00 (m, 1 H), 1.42 (s, 3 H), 1.40 (s, 9 H), 1.33 (s, 3 H), 0.90 (d, J = 6.8 Hz, 3 H), 0.87 (d, J = 7.2 Hz, 3 H).

^{13}C NMR (100 MHz, $CDCl_3$): δ 171.58, 171.15, 155.38, 134.87, 132.51, 130.08, 129.01, 126.79, 117.49, 111.29, 79.76, 78.41, 78.24, 56.85, 54.96, 37.90, 33.64, 32.98, 29.90, 28.33, 26.95, 25.88, 23.22, 19.57, 16.40.

HRMS (ESI): *m/z* calcd for $C_{29}H_{45}O_6N_3{}^{80}SeH^+$ $[M + H]^+$ 612.2546, found 612.2543 and calcd for $C_{29}H_{45}O_6N_3{}^{78}SeH^+$ $[M + H]^+$ 610.2554, found 610.2558.

Synthesis of {1*S*-[1*S*-(5*R*-But-3-enylcarbamoyl-2,2-dimethyl-[1,3]dioxolan-4*S*-yl)-2-methyl-propylcarbamoyl]-allyl}-carbamic acid *tert*-butyl ester, 47:

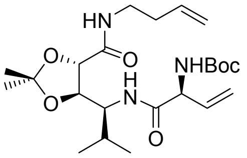

47

46 (925 mg, 2.04 mmol) was dissolved in dichloromethane (85 mL) in a 250 mL flask. Hydrogen peroxide (30% in water, 10 mL) and *N*,*N*-diisopropylethylamine (10 mL) were added and the resulting mixture was heated to 50 °C for 3 hours. The reaction was quenched by addition of a saturated aq. $CuSO_4$ solution. Addition of ethyl acetate (50 mL) and a 10% aq. $KHSO_4$ solution (50 mL) generated a biphasic mixture which was separated in a funnel. The organic phase was washed with a 5% aq. $NaHCO_3$ solution (50 mL) and brine (50 mL), dried over Na_2SO_4, filtered and concentrated to dryness. The crude product was purified by flash column chromatography (20% ethyl acetate in cyclohexane) to afford **47**.

Yield: 861 mg (1.90 mmol, 93%) as a colorless solid.
TLC (25% ethyl acetate in cyclohexane)**:** $R_f = 0.16$.
HPLC (gradient 2): $t_R = 10.27$ min.
^{1}H NMR (400 MHz, $CDCl_3$): δ 6.95 (d, J = 8.8 Hz, 1 H), 6.67 (t, J = 5.6 Hz, 1 H), 5.93 (ddd, J = 17.2, 10.4, 6.4 Hz, 1 H), 5.76 (ddt, J = 17.6, 9.6, 6.8 Hz, 1 H), 5.49 (br s, 1 H), 5.38 (ddd, J = 17.2, 1.2, 1.2 Hz, 1 H), 5.23 (ddd, J = 10.4, 1.2, 1.2 Hz, 1 H), 5.08-5.14 (m, 2 H), 4.67 (br s, 1 H), 4.15 (d, J = 6.4 Hz, 1 H), 4.06 (dd, J = 9.2, 6.8 Hz, 1 H), 3.98 (ddd, J = 9.2, 3.6, 3.6 Hz, 1 H), 3.36-3.45 (m, 1 H), 3.25-3.34 (m, 1 H), 2.25-2.31 (m, 2 H), 2.09 (septd, J = 6.8, 3.6 Hz, 1 H), 1.45 (s, 3 H), 1.44 (s, 9 H), 1.36 (s, 3 H), 0.94 (d, J = 7.2 Hz, 3 H), 0.90 (d, J = 7.2 Hz, 3 H).
^{13}C NMR (100 MHz, $CDCl_3$): δ 171.31, 170.21, 155.08, 134.78, 134.20, 117.41, 117.22, 111.33, 79.61, 78.45, 78.02, 57.51, 56.89, 37.90, 33.59, 30.03, 28.29, 26.90, 25.82, 19.50, 16.49.
HRMS (ESI): *m/z* calcd for $C_{23}H_{39}O_6N_3H^+$ $[M + H]^+$ 454.2912, found 454.2906.

Synthesis of compound 48:

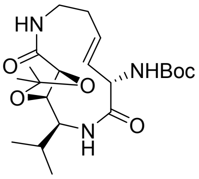

48

47 (737 mg, 1.620 mmol, 1 eq.) was dissolved under argon in toluene (800 mL) in a 1 L flame-dried flask and heated to 90 °C. A solution of Grubbs' 2nd generation catalyst (207 mg, 0.243 mmol, 0.15 eq.) in toluene (25 mL) was added over 8 hours with a syringe pump to the preheated mixture. The resulting solution was stirred for further 10 hours at 90 °C. After concentration to dryness, the crude product was purified by flash column chromatography (50% ethyl acetate in cyclohexane) to afford **48** as a light brown solid. The product was pure enough to be used in the next step without further purification. Nevertheless, a second flash column chromatography can be performed to completely eliminate the remaining traces of ruthenium residues.

Yield: 335 mg (0.787 mmol, 49%) as a colorless solid.
TLC (60% ethyl acetate in cyclohexane)**:** $R_f = 0.29$.
HPLC (gradient 2): $t_R = 8.56$ min.
^{1}H NMR (400 MHz, $CDCl_3$): δ 5.63-5.77 (m, 2 H), 5.47-5.55 (m, 2 H), 5.12 (ddd, J = 15.2, 10.0, 0.8 Hz, 1 H), 4.46 (dd, J = 10.0, 8.4 Hz, 1 H), 4.34 (t, J = 8.0 Hz, 1 H), 3.83-3.95 (m, 2 H), 3.68 (d, J = 8.0 Hz, 1 H), 2.82-2.90 (m, 1 H), 2.36-2.44 (m, 1 H), 1.98-2.04 (m, 1 H), 1.83-1.94 (m, 1 H), 1.36 (s, 9 H), 1.34 (s, 3 H), 1.33 (s, 3 H), 0.88 (d, J = 6.8 Hz, 3 H), 0.86 (d, J = 6.8 Hz, 3 H).
^{13}C NMR (100 MHz, $CDCl_3$): δ 170.86, 169.67, 154.82, 131.54, 130.49, 111.65, 79.93, 79.81, 76.14, 58.04, 56.71, 37.07, 34.62, 30.09, 28.43, 26.90, 26.27, 19.75, 15.98.
HRMS (ESI): *m/z* calcd for $C_{21}H_{35}O_6N_3H^+$ $[M + H]^+$ 426.2599, found 426.2596.

Synthesis of 53:

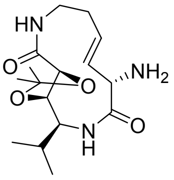

53

48 (295 mg, 0.69 mmol, 1 eq.) was dissolved in dichloromethane (4 mL) under argon in a 10 mL flame-dried flask. 2,6-Lutidine (161 µL, 1.38 mmol, 2 eq.) and trimethylsilyl trifluoro methanesulfonate (188 µL, 1.04 mmol, 1.5 eq.) were added at room temperature and the resulting mixture was stirred for 15 minutes. Addition of a saturated aq. NH_4Cl solution quenched the reaction. The pH was adjusted to 9 by addition of a 2 M NaOH solution and the desired product was extracted from the water phase with dichloromethane. The combined organic layers were washed with brine, dried over Na_2SO_4, filtered and concentrated to dryness to yield **53**.

Yield: 221 mg (0.68 mmol, 98 %) as a colorless solid.
TLC (15% methanol in dichloromethane)**:** $R_f = 0.20$.

HPLC (gradient 2): t_R = 6.18 min.

^{1}H NMR (400 MHz, CD_3OD): δ 5.58 (ddd, J = 15.2, 10.8, 4.0 Hz, 1 H), 5.31 (ddd, J = 15.2, 9.2, 0.8 Hz, 1 H), 4.43 (dd, J = 10.4, 8.0 Hz, 1 H), 3.95 (dd, J = 10.4, 3.6 Hz, 1 H), 3.86 (d, J = 9.2 Hz, 1 H), 3.84 (d, J = 8.0 Hz, 1 H), 3.79-3.88 (m, 1 H), 2.88 (ddd, J = 13.2, 5.2, 1.6 Hz, 1 H), 2.32-2.38 (m, 1 H), 1.98-2.13 (m, 2 H), 1.40 (s, 3 H), 1.39 (s, 3 H), 0.93 (d, J = 6.8 Hz, 6 H).

^{13}C NMR (100 MHz, CD_3OD): δ 176.23, 170.80, 136.34, 130.29, 111.99, 81.71, 78.22, 58.80, 57.56, 37.46, 33.98, 31.02, 27.14, 26.48, 20.12, 16.23.

HRMS (ESI): *m/z* calcd for $C_{16}H_{27}O_4N_3H^+$ $[M + H]^+$ 326.2074, found 326.2074.

Synthesis of compound 50:

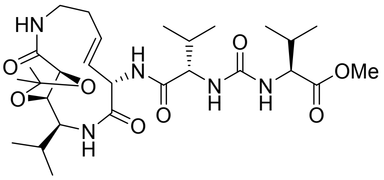

50

53 (161 mg, 495 µmol, 1 eq.), **49** (190 mg, 693 µmol, 1.4 eq.), PyBop (387 mg, 743 µmol, 1.5 eq.) and HOAt (102 mg, 743 µmol, 1.5 eq.) were dissolved in dichloromethane (10 mL) in a 50 mL flask. The solution was cooled to 0 °C and *N*,*N*-diisopropylethylamine (173 µL, 990 µmol, 2 eq.) was added. The reaction was stirred overnight at room temperature, was diluted with methanol/dichloromethane (1:9, 25 mL) and then washed with a 20% aq. citric acid solution and a 5% aq. $NaHCO_3$ solution. The organic layer was dried over Na_2SO_4, filtered and concentrated to dryness. The crude product was purified by flash column chromatography (5% methanol in ethyl acetate) to yield **50**.

Yield: 273 mg (469 mmol, 95%) as a colorless solid.

TLC (5% methanol in ethyl acetate)**:** R_f = 0.67.

HPLC (gradient 2): t_R = 8.07 min.

^{1}H NMR (400 MHz, $CD_3OD/CDCl_3$ = 1:1): δ 8.25 (d, J = 6.0 Hz, 1 H), 8.02 (d, J = 8.4 Hz, 1 H), 7.49 (d, J = 10.4 Hz, 1 H), 6.52 (d, J = 9.2 Hz, 1 H), 6.47 (d, J = 8.8 Hz, 1 H), 5.65 (ddd, J = 14.8, 11.2, 4.0 Hz, 1 H), 5.41 (dd, J = 15.2, 10.0, 1 H), 4.92 (dd, J =

9.2, 6.8 Hz, 1 H), 4.41 (dd, J = 10.0, 7.6 Hz, 1 H), 4.25-4.30 (m, 1 H), 4.08-4.14 (m, 1 H), 3.94 (ddd, J = 10.0, 10.0, 3.2 Hz, 1 H), 3.84-3.90 (m, 1 H), 3.82 (d, J = 8.0 Hz, 1 H), 3.73 (s, 3 H), 2.85-2.92 (m, 1 H), 2.31-2.38 (m, 1 H), 1.94-2.12 (m, 4 H), 1.41 (s, 3 H), 1.38 (s, 3 H), 0.83-0.94 (m, 18 H).

^{13}C NMR (100 MHz, $CD_3OD/CDCl_3$ = 1:1): δ 174.14, 172.90, 172.84, 169.72, 158.95, 131.85, 130.01, 111.04, 80.72, 77.21, 58.63, 58.30, 56.94, 56.38, 51.83, 36.54, 32.91, 32.16, 31.20, 29.75, 26.46, 25.74, 19.45, 18.91, 18.85, 17.57, 17.38, 15.34.

HRMS (ESI): *m/z* calcd for $C_{28}H_{47}O_8N_5H^+$ $[M + H]^+$ 582.3497, found 582.3494.

Synthesis of compound 51

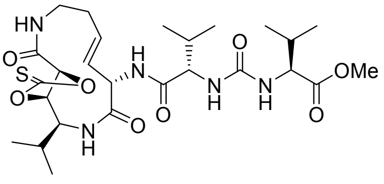

51

In a 10 mL vessel was placed **50** (5 mg, 8.6 μmol), formic acid/methanol (6:4, 5 mL) and a magnetic stirring bar. The vessel was sealed with a septum, placed into the MW cavity, and locked with the pressure device. Constant microwave irradiation of 45 W as well as a simultaneous air-cooling (300 kPa, 45 Psi) were used during the entire reaction time (90 min, 110 °C, resulting reaction pressure 6 bar). After cooling to room temperature, the solvent was removed under reduced pressure to afford 4.5 mg (8.4 μmol, >98%) of the dihydroxyl intermediate as a colorless solid. The product was pure enough to be used in the next step without further purification (intermediate characterization: HPLC (gradient 2): t_R = 6.49 min; HRMS (ESI): *m/z* calcd for $C_{25}H_{43}O_8N_5H^+$ $[M + H]^+$ 542.3184, found 542.3179).

After performing this reaction several times, all product fractions were pooled and the resulting residue of the dihydroxyl derivative (92 mg, 170 μmol, 1 eq.) was dissolved under argon in tetrahydrofurane (50 mL) in a 100 mL flame-dried flask. To this solution was added thiocarbonyl diimidazole (303 mg, 1.70 mmol, 10 eq.) and 4-(dimethylamino)pyridine (208 mg, 1.70 mmol, 10 eq.). The resulting reaction mixture was heated to 80 °C and stirred at this temperature overnight. After recooling to room temperature, a small portion of silica gel was added and the solvent was removed under vacuo. The adsorbed crude product was purified by flash column chromatography (4% methanol in dichloromethane) to yield **51**.

Yield: 88 mg (151 μmol, 89%) as a colorless solid.
TLC (6% methanol in dichloromethane)**:** $R_f = 0.32$.
HPLC (gradient 2): $t_R = 8.38$ min.
^{1}H NMR (400 MHz, $CD_3OD/CDCl_3 = 1:4$): δ 8.30 (d, J = 9.6 Hz, 1 H), 8.20-8.25 (m, 1 H), 7.72 (d, J = 9.1 Hz, 1 H), 5.58 (ddd, J = 15.5, 11.5, 4.2 Hz, 1 H), 5.39 (dd, J = 15.5, 9.4, 1 H), 5.07 (dd, J = 10.2, 10.2 Hz, 1 H), 4.85-4.92 (m, 1 H), 4.62 (d, J = 9.6 Hz, 1 H), 4.30 (d, J = 4.9 Hz, 1 H), 4.17-4.24 (m, 1 H), 4.05 (d, J = 6.9 Hz, 1 H), 3.79-3.87 (m, 1 H), 3.70 (s, 3 H), 2.90-2.96 (m, 1 H), 2.31-2.39 (m, 1 H), 1.99-2.13 (m, 3 H), 1.83-1.91 (m, 1 H), 0.78-0.90 (m, 18 H).
^{13}C NMR (100 MHz, $CD_3OD/CDCl_3 = 1:4$): δ 190.46, 176.03, 174.32, 173.30, 172.93, 164.17, 131.91, 130.03, 83.95, 82.19, 58.59, 58.21, 56.74, 54.93, 52.26, 37.01, 32.75, 31.29, 29.21, 26.78, 19.24, 19.11, 18.95, 18.10, 17.64, 15.41.
HRMS (ESI): *m/z* calcd for $C_{26}H_{41}O_8N_5SH^+$ $[M + H]^+$ 584.2749, found 584.2757.

Synthesis of syringolin A methyl ester, 52:

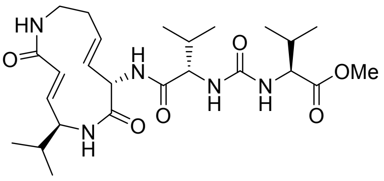

52

51 (20.0 mg, 34 μmol, 1 eq.) was dissolved under argon in trimethyl phosphite (2 mL) in a 10 mL flame-dried flask. The resulting mixture was refluxed for 3 hours at 130 °C. After concentration to dryness, the crude product was purified by flash column chromatography (10% methanol in dichloromethane) to yield **52**.
Yield: 13.1 mg (26 μmol, 76%) as a colorless solid.

Or, **49** (14 mg, 50 μmol, 1.1 eq.), **58** (11.6 mg, 46 μmol, 1 eq.), PyBop (30 mg, 56 μmol, 1.2 eq.) and HOAt (8 mg, 56 μmol, 1.2 eq.) were dissolved in *N,N*-dimethylformamide (1.0 mL) in a 10 mL flask. The solution was cooled to 0 °C and

N,*N*-diisopropylethylamine (16 µL, 92 µmol, 2 eq.) was added. The reaction was stirred for 40 minutes at room temperature. After concentration to dryness, the crude product was purified by flash column chromatography (10% methanol in dichloromethane) to yield **52**.

Yield: 22.2 mg (44 µmol, 95%) as a colorless solid.

TLC (8% methanol in dichloromethane)**:** R_f = 0.19.

HPLC (gradient 2): t_R = 6.84 min.

^{1}H NMR (500 MHz, d^6-DMSO): δ 8.04 (d, J = 7.2 Hz, 1 H), 8.00 (d, J = 8.7 Hz, 1 H), 7.44 (t, J = 7.1 Hz, 1 H), 6.68 (dd, J = 15.5, 5.5 Hz, 1 H), 6.42 (d, J = 8.8 Hz, 1 H), 6.22 (d, J = 9.1 Hz, 1 H), 6.09 (d, J = 15.5 Hz, 1 H), 5.60 (dt, J = 15.6, 7.7, 1 H), 5.41 (dd, J = 15.9, 7.7 Hz, 1 H), 4.86 (t, J = 7.4 Hz, 1 H), 4.00-4.11 (m, 3 H), 3.61 (s, 3 H), 3.10-3.24 (m, 2 H), 2.24-2.32 (m, 1 H), 1.86-2.02 (m, 3 H), 1.69-1.78 (m, 1 H), 0.95 (d, J = 6.7, 3 H), 0.90 (d, J = 6.7, 3 H), 0.82-0.87 (m, 9 H), 0.78 (d, J = 6.8, 3 H).

^{13}C NMR (125 MHz, d^6-DMSO): δ 190.46, 176.03, 174.32, 173.30, 172.93, 164.17, 131.91, 130.03, 83.95, 82.19, 58.59, 58.21, 56.74, 54.93, 52.26, 37.01, 32.75, 31.29, 29.21, 26.78, 19.24, 19.11, 18.95, 18.10, 17.64, 15.41.

HRMS (ESI): *m/z* calcd for $C_{25}H_{41}O_6N_5H^+$ $[M + H]^+$ 508.3130, found 508.3134.

Synthesis of syringolin A, 1:

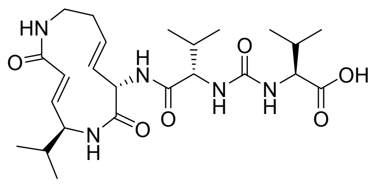

SylA, **1**

52 (8.0 mg, 16 µmol, 1 eq.) and aluminium trichloride (17.1 mg, 128 µmol, 8 eq.) were dissolved under argon in ethyl methyl sulfide (400 µL) in a 10 mL flame-dried flask. The resulting mixture was stirred for 1 hour at room temperature. After concentration to dryness, the crude product was purified by flash column chromatography (2% acetic acid + 15% methanol in dichloromethane) to yield syringolin A (SylA, **1**).

Yield: 7.3 mg (15 µmol, 92%) as a colorless solid.

Or, **52** (20.0 mg, 39.4 µmol, 1 eq.) and aluminium bromide (84 mg, 316 µmol, 8 eq.) were dissolved under argon in tetrahydrothiophene (2 mL) in a 10 mL flame-dried flask. The resulting mixture was stirred for 1 hour at room temperature. After concentration to dryness, the remaining residue was purified by preparative HPLC (0min/10%B → 10min/10%B → 30min/30%B → 50min/60%B → 60min/100%B → 80min/100%B) to yield syringolin A (SylA, **1**).

Yield: 16.3 mg (33.1 µmol, 84%) as a colorless solid.

TLC (2% acetic acid + 15% methanol in dichloromethane)**:** $R_f = 0.32$.

HPLC (gradient 2): $t_R = 6.13$ min.

^{1}H NMR (400 MHz, d^6-DMSO): δ 12.35 (br s, 1 H), 8.03 (d, J = 8.4 Hz, 1 H), 7.99 (d, J = 6.7 Hz, 1 H), 7.40-7.48 (m, 1 H), 6.68 (dd, J = 15.2, 4.3 Hz, 1 H), 6.32 (d, J = 8.9 Hz, 1 H), 6.25 (d, J = 9.0 Hz, 1 H), 6.10 (d, J = 15.4 Hz, 1 H), 5.59 (dt, J = 15.5, 7.1, 1 H), 5.40 (dd, J = 15.5, 7.5 Hz, 1 H), 4.82-4.88 (m, 1 H), 4.01-4.10 (m, 2 H), 3.97 (dd, J = 8.7, 4.7 Hz, 1 H), 3.07-3.25 (m, 2 H), 2.23-2.32 (m, 1 H), 1.86-2.03 (m, 3 H), 1.69-1.78 (m, 1 H), 0.94 (d, J = 6.2, 3 H), 0.90 (d, J = 6.3, 3 H), 0.80-0.88 (m, 9 H), 0.77 (d, J = 6.5, 3 H).

^{13}C NMR (100 MHz, d^6-DMSO): δ 174.00, 171.41, 168.88, 166.23, 157.62, 143.20, 133.04, 125.92, 121.50, 57.52, 57.36, 55.43, 53.57, 42.50, 34.98, 31.40, 31.07, 30.16, 19.72, 19.23, 19.19, 19.14, 17.60, 17.56.

HRMS (ESI): *m/z* calcd for $C_{24}H_{39}O_6N_5H^+$ $[M + H]^+$ 494.2973, found 494.2978.

Synthesis of compound 54:

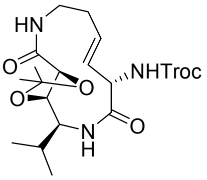

54

53 (166 mg, 510 µmol, 1 eq.) and sodium hydrogen carbonate (86 mg, 1.02 mmol, 2 eq.) were dissolved under argon in tetrahydrofurane (15 mL) in a 25 mL flame-dried flask. 2,2,2-Trichloroethyl chloroformate (76 µL, 560 µmol, 1.1 eq.) was added dropwise at 0 °C and the resulting mixture was stirred for further 90 minutes at room temperature. The solvents were removed *in vacuo* and the remaining residue was partitioned between a saturated ammonium chloride solution (50 mL) and dichloromethane (50 mL). The aqueous layer was extracted 3 more times with dichloromethane and the combined organic layers were finally dried over Na_2SO_4. After concentration to dryness, the crude product was purified by flash column chromatography (50% ethyl acetate in cyclohexane) to afford **54**.

Yield: 212 mg (423 μmol, 83%) as a colorless solid.
TLC (50% ethyl acetate in cyclohexane)**:** $R_f = 0.40$.
HPLC (gradient 2): $t_R = 9.32$ min.
^{1}H NMR (400 MHz, d^6-DMSO): δ 7.99 (d, J = 9.7 Hz, 1 H), 7.90 (d, J = 6.3 Hz, 1 H), 7.54 (d, J = 10.2 Hz, 1 H), 5.61 (ddd, J = 14.8, 11.2, 3.8 Hz, 1 H), 5.40 (dd, J = 15.1, 9.6 Hz, 1 H), 4.82 (d, J = 12.4 Hz, 1 H), 4.69 (d, J = 12.4 Hz, 1 H), 4.54 (dd, J = 9.6, 6.3 Hz, 1 H), 4.35 (dd, J = 10.5, 7.7 Hz 1 H), 3.82 (ddd, J = 10.4, 10.2, 3.4 Hz, 1 H), 3.73 (d, J = 7.6 Hz, 1 H), 3.66-3.77 (m, 1 H), 2.70-2.78 (m, 1 H), 2.22-2.30 (m, 1 H), 1.88-2.00 (m, 2 H), 1.33 (s, 3 H), 1.32 (s, 3 H), 0.86 (d, J = 6.9 Hz, 3 H), 0.79 (d, J = 6.9 Hz, 3 H).
^{13}C NMR (100 MHz, d^6-DMSO): δ 171.17, 167.69, 153.46, 130.41, 130.23, 109.63, 96.14, 79.82, 76.71, 73.32, 57.56, 55.11, 35.57, 32.32, 29.31, 26.73, 25.94, 19.44, 15.79.
HRMS (ESI): *m/z* calcd for $C_{19}H_{28}O_6N_3Cl_3H^+$ $[M + H]^+$ 500.1117, found 500.1113 and calcd for $C_{19}H_{28}O_6N_3Cl_2{}^{37}ClH^+$ $[M + H]^+$ 502.1087, found 502.1082.

Synthesis of compound 56:

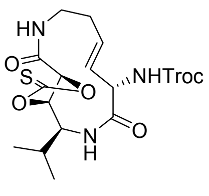

56

In a 10 mL vessel was placed **54** (20 mg, 40 μmol, 1 eq.), *p*-toluenesulfonic acid monohydrate (7.6 mg, 40 μmol, 1 eq.), methanol/water/tetrahydrofurane (2:2:1, 5 mL) and a magnetic stirring bar. The vessel was sealed with a septum, placed into the MW cavity, and locked with the pressure device. Constant microwave irradiation of 150 W as well as a simultaneous air-cooling (300 kPa, 45 Psi) were used during the entire reaction time (30 min, 140 °C, resulting reaction pressure 12 bar). After cooling to room temperature, the solvent was removed under reduced pressure to afford 18 mg (39 µmol, >98%) of the dihydroxyl intermediate **55** as a colorless solid. The product was pure enough to be used in the next step without further purification (intermediate characterization: HPLC (gradient 2): t_R = 7.45 min; HRMS (ESI): *m/z* calcd for $C_{16}H_{24}O_6N_3Cl_3H^+$ $[M + H]^+$ 460.0804, found 460.0802 and calcd for $C_{16}H_{24}O_6N_3Cl_2{}^{37}ClH^+$ $[M + H]^+$ 462.0774, found 462.0771).

After performing this reaction several times, all product fractions were pooled and the resulting residue of the dihydroxyl derivative **55** (124 mg, 269 µmol, 1 eq.) was dissolved under argon in tetrahydrofurane (80 mL) in a 250 mL flame-dried flask. To this solution was added 1,1'-thiocarbonyl diimidazole (480 mg, 2.69 mmol, 10 eq.) and 4-(dimethylamino)pyridine (329 mg, 2.69 mmol, 10 eq.). The resulting reaction mixture was heated to 80 °C and stirred at this temperature overnight. After cooling to room temperature, a small portion of silica gel was added and the solvent was removed under reduced pressure. The adsorbed crude product was purified by flash column chromatography (50% ethyl acetate in cyclohexane) to yield **56**.

Yield: 119 mg (237 µmol, 88%) as a colorless solid.

TLC (50% ethyl acetate in cyclohexane)**:** R_f = 0.30.

HPLC (gradient 2): t_R = 9.29 min.

^{1}H NMR (400 MHz, d^6-DMSO): δ 8.52 (d, J = 9.8 Hz, 1 H), 8.07 (d, J = 6.1 Hz, 1 H), 7.82 (d, J = 10.4 Hz, 1 H), 5.62 (ddd, J = 14.8, 11.1, 3.5 Hz, 1 H), 5.48 (dd, J = 15.2, 9.5 Hz, 1 H), 4.98 (dd, J = 10.5, 9.9 Hz, 1 H), 4.84 (d, J = 12.4 Hz, 1 H), 4.74 (d, J = 9.6 Hz, 1 H), 4.70 (d, J = 12.4 Hz, 1 H), 4.51 (dd, J = 9.4, 6.2 Hz, 1 H), 4.23 (ddd, J = 10.5, 10.4, 3.8 Hz, 1 H), 3.63-3.76 (m, 1 H), 2.90 (dd, J = 12.8, 4.6 Hz, 1 H), 2.29-2.36 (m, 1 H), 1.92-2.06 (m, 2 H), 0.90 (d, J = 6.9 Hz, 3 H), 0.84 (d, J = 6.8 Hz, 3 H).

^{13}C NMR (100 MHz, d^6-DMSO): δ 190.08, 171.56, 163.17, 153.59, 130.49, 130.36, 96.08, 83.69, 82.58, 73.37, 57.73, 53.56, 36.27, 31.84, 29.07, 19.06, 15.65.

HRMS (ESI): *m/z* calcd for $C_{17}H_{22}O_6N_3Cl_3SH^+$ $[M + H]^+$ 502.0368, found 502.0365 and calcd for $C_{17}H_{22}O_6N_3Cl_2{}^{37}ClSH^+$ $[M + H]^+$ 504.0338, found 504.0331.

Synthesis of compound 57:

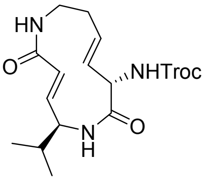

57

56 (70 mg, 139 μmol, 1 eq.) was dissolved under argon in trimethyl phosphite (1.0 mL) in a 10 mL flame-dried flask and refluxed in a pre-warmed oil bath at 130 °C for 2.5 hours. After concentration to dryness, the crude product was purified by flash column chromatography (6% methanol in dichloromethane) to yield **57**. Importantly, in order to assure high yields during this reaction, a minimal amount of trimethyl phosphite should be employed in the reaction, thereby facilitating precipitation of the desired product **57**.

Yield: 52 mg (122 μmol, 88%) as a colorless solid.
TLC (6% methanol in dichloromethane)**:** $R_f = 0.30$.
HPLC (gradient 2): $t_R = 7.79$ min.
^{1}H NMR (400 MHz, d^6-DMSO): δ 7.96-8.05 (m, 2 H), 7.45 (t, J = 7.1 Hz, 1 H), 6.69 (dd, J = 15.5, 5.5 Hz, 1 H), 6.08 (d, J = 15.6 Hz, 1 H), 5.66 (dt, J = 15.4, 7.7 Hz, 1 H), 5.38 (dd, J = 15.9, 7.9 Hz, 1 H), 4.82 (d, J = 12.4 Hz, 1 H), 4.75 (d, J = 12.3 Hz, 1 H), 4.67 (dd, J = 7.9, 7.7 Hz, 1 H), 4.03-4.11 (m, 1 H), 3.08-3.22 (m, 2 H), 2.26-2.35 (m, 1 H), 1.90-2.01 (m, 1 H), 1.69-1.79 (m, 1 H), 0.95 (d, J = 6.6 Hz, 3 H), 0.91 (d, J = 6.6 Hz, 3 H).
^{13}C NMR (100 MHz, d^6-DMSO): δ 168.97, 166.21, 153.91, 143.29, 133.53, 124.90, 121.56, 96.03, 73.48, 56.07, 55.50, 42.29, 35.07, 31.43, 19.70, 19.20.
HRMS (ESI): *m/z* calcd for $C_{16}H_{22}O_4N_3Cl_3H^+$ $[M + H]^+$ 426.0749, found 426.0748 and calcd for $C_{16}H_{22}O_4N_3Cl_2{}^{37}ClH^+$ $[M + H]^+$ 428.0719, found 428.0717.

Synthesis of 8*S*-Amino-5*S*-isopropyl-1,6-diaza-cyclododeca-3*E*,9*E*-diene-2,7-dione, 58:

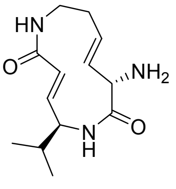

58

57 (34 mg, 81 µmol, 1 eq.) was dissolved in tetrahydrofurane (1 mL) in a 10 mL flask. Acetic acid was added (1 mL), followed by zinc powder (798 mg, 12.2 mmol, 150 eq.) which was added in portions over 30 minutes. After 3 hours of vigorous stirring, the mixture was filtered over a small plug of Celite and washed with ethyl acetate. After evaporation to dryness, **58** was obtained.

Yield: 20 mg (79 µmol, 98%) as a colorless solid.
TLC (1% triethylamine + 5% methanol in dichloromethane)**:** $R_f = 0.31$.
HPLC (gradient 2): $t_R = 2.06$ min.
^{1}H NMR (400 MHz, d^6-DMSO): δ 8.42 (d, J = 8.3 Hz, 1 H), 7.48 (t, J = 6.9 Hz, 1 H), 6.73 (dd, J = 15.5, 5.2 Hz, 1 H), 6.05 (d, J = 15.6 Hz, 1 H), 5.68 (dt, J = 15.8, 7.8 Hz, 1 H), 5.50 (d, J = 15.8, 7.5 Hz, 1 H), 4.30 (d, J = 7.4 Hz, 1 H), 4.10-4.17 (m, 1 H), 3.10-3.31 (m, 2 H), 2.27-2.37 (m, 1 H), 1.94-2.05 (m, 1 H), 1.70-1.80 (m, 1 H), 0.95 (d, J = 6.6 Hz, 3 H), 0.92 (d, J = 6.8 Hz, 3 H).
HRMS (ESI): *m/z* calcd for $C_{13}H_{21}O_2N_3H^+$ $[M + H]^+$ 252.1707, found 252.1708.

Synthesis of MRL, 61:

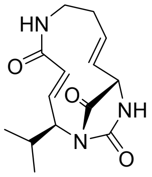

MRL, **61**

56 (66 mg, 130 µmol, 1 eq.) was dissolved under argon in trimethyl phosphite (5.0 mL) in a 10 mL flame-dried flask and refluxed at 150 °C for 2 hours. After concentration to dryness, the crude product was purified by flash column chromatography (6% methanol in dichloromethane) to yield **61**.

Yield: 17 mg (61 μmol, 47%) as colorless crystals.

TLC (10% methanol in dichloromethane)**:** $R_f = 0.46$.

HPLC (gradient 2): $t_R = 5.62$ min.

^{1}**H NMR** (400 MHz, d^6-DMSO): δ 8.34 (br s, 1 H), 7.41 (t, J = 6.7 Hz, 1 H), 6.74 (dd, J = 15.5, 5.5 Hz, 1 H), 5.91 (d, J = 15.4 Hz, 1 H), 5.31-5.44 (m, 1 H), 5.13-5.28 (m, 1 H), 4.58 (br s, 1 H), 3.84-3.93 (m, 1 H), 3.21-3.30 (m, 1 H), 3.10-3.20 (m, 1 H), 2.19-2.40 (m, 2 H), 1.91-2.04 (m, 1 H), 0.97 (d, J = 6.7 Hz, 3 H), 0.89 (d, J = 6.6 Hz, 3 H).

^{13}**C NMR** (100 MHz, d^6-DMSO): δ 168.67, 165.79, 157.92, 141.11, 129.94, 124.00, 123.84, 56.94, 56.61, 40.98, 34.75, 30.00, 19.80, 19.31.

HRMS (ESI): *m/z* calcd for $C_{14}H_{19}O_3N_3H^+$ $[M + H]^+$ 278.1499, found 278.1500.

Synthesis of 2*S*-[3-(1*S*-*tert*-Butoxycarbonyl-2-methyl-propyl)-ureido]-3-methyl-butyric acid methyl ester, 70:

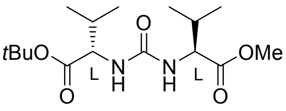

70

Methyl (*S*)-(–)-2-isocyanato-3-methylbutyrate **69** (431 μL, 3.00 mmol, 1 eq.) was dissolved under argon in dichloromethane (10 mL) in a 25 mL flame-dried flask. A solution of *tert*-butyl (L)-valine hydrochloride **16** (629 mg, 3.00 mmol, 1 eq.) and *N*,*N*-diisopropylethylamine (1.05 mL, 6.00 mmol, 2 eq.) in dichloromethane (5 mL) was added and the resulting mixture was stirred overnight at room temperature. The reaction was quenched by addition of a 20% aq. citric acid solution and the desired product was extracted with chloroform (2 × 20 mL). The combined organic layers were dried over Na_2SO_4, filtered and evaporated to dryness. The crude product was purified by flash column chromatography (15% ethyl acetate in cyclohexane) to yield **70**.

Yield: 892 mg (2.70 mmol, 90%) as colorless crystals.

TLC (25% ethyl acetate in cyclohexane)**:** $R_f = 0.21$.

HPLC (gradient 1): $t_R = 8.72$ min.

^{1}H NMR (400 MHz, $CDCl_3$): δ 5.17 (d, J = 8.8 Hz, 1 H), 5.14 (d, J = 9.2 Hz, 1 H), 4.41 (dd, J = 8.8, 4.8 Hz, 1 H), 4.29 (dd, J = 8.4, 4.4 Hz, 1 H), 3.73 (s, 3 H), 2.04-2.16 (m, 2 H), 1.46 (s, 9 H), 0.94 (d, J = 6.8 Hz, 3 H), 0.92 (d, J = 6.8 Hz, 3 H), 0.88 (d, J = 6.8 Hz , 3 H), 0.86 (d, J = 6.8 Hz, 3 H).

^{13}C NMR (100 MHz, $CDCl_3$): δ 173.94, 172.41, 157.48, 81.80, 58.45, 58.19, 52.13, 31.69, 31.48, 28.16, 19.10, 19.03, 17.86, 17.64.

HRMS (ESI): *m/z* calcd for $C_{16}H_{30}O_5N_2H^+$ $[M + H]^+$ 331.2228, found 331.2229.

Synthesis of 2*S*-[3-(1*R*-*tert*-Butoxycarbonyl-2-methyl-propyl)-ureido]-3-methyl-butyric acid methyl ester, 73:

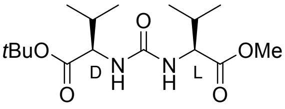

73

Methyl (S)-(–)-2-isocyanato-3-methylbutyrate **69** (144 µL, 1.0 mmol, 1 eq.) was dissolved under argon in dichloromethane (5 mL) in a 25 mL flame-dried flask. A solution of *tert*-butyl (D)-valine hydrochloride **72** (210 mg, 1.0 mmol, 1 eq.) and *N*,*N*-diisopropylethylamine (436 µL, 2.5 mmol, 2.5 eq.) in dichloromethane (5 mL) was added and the resulting mixture was stirred overnight at room temperature. The reaction was quenched by addition of a 20% aq. citric acid solution and the desired product was extracted with chloroform (2 × 20 mL). The combined organic layers were dried over Na_2SO_4, filtered and evaporated to dryness. The crude product was purified by flash column chromatography (15% ethyl acetate in cyclohexane) to yield **73**.

Yield: 299 mg (0.91 mmol, 91%) as a colorless solid.

TLC (25% ethyl acetate in cyclohexane)**:** $R_f = 0.22$.

HPLC (gradient 2): $t_R = 9.74$ min.

^{1}H NMR (400 MHz, $CDCl_3$): δ 5.15 (br s, 2 H), 4.37 (d, J = 5.2 Hz, 1 H), 4.26 (d, J = 4.7 Hz, 1 H), 3.72 (s, 3 H), 2.06-2.15 (m, 2 H), 1.46 (s, 9 H), 0.94 (d, J = 6.9 Hz, 6 H), 0.90 (d, J = 5.2 Hz, 3 H), 0.89 (d, J = 5.6 Hz, 3 H).

^{13}C NMR (100 MHz, $CDCl_3$): δ 173.55, 172.21, 157.41, 81.87, 58.62, 58.30, 52.08, 31.83, 31.67, 28.15, 19.01, 18.96, 17.96, 17.78.

HRMS (ESI): *m/z* calcd for $C_{16}H_{30}O_5N_2H^+$ $[M + H]^+$ 331.2228, found 331.2229.

Synthesis of 2*R*-[3-(1*S*-*tert*-Butoxycarbonyl-2-methyl-propyl)-ureido]-3-methyl-butyric acid methyl ester, 77:

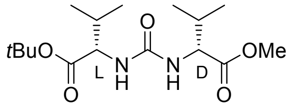

77

In a 10 mL flame-dried flask was dissolved triphosgene (110 mg, 370 μmol, 1.11 eq.) in dichloromethane (2 mL) under argon. To this solution was added dropwise a solution of *tert*-butyl (L)-valine hydrochloride **16** (210 mg, 1.0 mmol, 1 eq.) in dichloromethane (3.5 mL) and *N*,*N*-diisopropylethylamine (385 μL, 2.2 mmol, 2.2 eq.). The reaction was stirred for 5 minutes at room temperature. Then, a solution of methyl (D)-valine hydrochloride **76** (168 mg, 1.0 mmol, 1 eq.) in dichloromethane (2 mL) and *N*,*N*-diisopropylethylamine (385 μL, 2.2 mmol, 2.2 eq.) was added in one portion. The reaction was stirred for 10 minutes and then quenched with a 10% aq. $KHSO_4$ solution. The mixture was extracted once with ethyl acetate and the combined organic layers were washed with a 5% aq. $NaHCO_3$ solution, brine and dried over Na_2SO_4. After filtration and concentration to dryness the crude product was purified by flash column chromatography (30% ethyl acetate in cyclohexane) to afford **77**.

Yield: 98 mg (0.30 mmol, 30%) as a colorless solid.

TLC (25% ethyl acetate in cyclohexane)**:** $R_f = 0.22$.

HPLC (gradient 2): $t_R = 9.58$ min.

^{1}H NMR (400 MHz, $CDCl_3$): δ 5.27 (br s, 2 H), 4.38 (d, J = 5.1 Hz, 1 H), 4.27 (d, J = 4.7 Hz, 1 H), 3.71 (s, 3 H), 2.04-2.14 (m, 2 H), 1.45 (s, 9 H), 0.94 (d, J = 6.8 Hz, 6 H), 0.89 (d, J = 6.8 Hz, 3 H), 0.88 (d, J = 7.2 Hz, 3 H).

^{13}C NMR (100 MHz, $CDCl_3$): δ 173.65, 172.33, 157.34, 81.79, 58.51, 58.20, 52.06, 31.87, 31.71, 28.14, 19.01, 18.97, 17.96, 17.78.

HRMS (ESI): *m/z* calcd for $C_{16}H_{30}O_5N_2H^+$ $[M + H]^+$ 331.2228, found 331.2229.

Synthesis of 2*R*-[3-(1*R*-*tert*-Butoxycarbonyl-2-methyl-propyl)-ureido]-3-methyl-butyric acid methyl ester, 80:

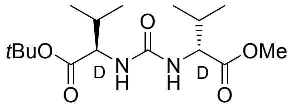

80

In a 10 mL flame-dried flask was dissolved triphosgene (110 mg, 370 µmol, 1.11 eq.) in dichloromethane (2 mL) under argon. To this solution was added dropwise a solution of *tert*-butyl (D)-valine hydrochloride **72** (210 mg, 1.0 mmol, 1 eq.) in dichloromethane (3.5 mL) and *N*,*N*-diisopropylethylamine (385 µL, 2.2 mmol, 2.2 eq.). The reaction was stirred for 5 minutes at room temperature. Then, a solution of methyl (D)-valine hydrochloride **76** (168 mg, 1.0 mmol, 1 eq.) in dichloromethane (2 mL) and *N*,*N*-diisopropylethylamine (385 µL, 2.2 mmol, 2.2 eq.) was added in one portion. The reaction was stirred for 10 minutes and then quenched with a 10% aq. $KHSO_4$ solution. The mixture was extracted once with ethyl acetate and the combined organic layers were washed with a 5% aq. $NaHCO_3$ solution, brine and dried over Na_2SO_4. After filtration and concentration to dryness the crude product was purified by flash column chromatography (30% ethyl acetate in cyclohexane) to afford **80**.

Yield: 250 mg (0.76 mmol, 76%) as a colorless solid.
TLC (25% ethyl acetate in cyclohexane)**:** $R_f = 0.22$.
HPLC (gradient 2): $t_R = 9.69$ min.
^{1}H NMR (400 MHz, $CDCl_3$): δ 5.21 (br s, 2 H), 4.40 (d, J = 4.9 Hz, 1 H), 4.29 (d, J = 4.5 Hz, 1 H), 3.73 (s, 3 H), 2.06-2.14 (m, 2 H), 1.46 (s, 9 H), 0.93 (d, J = 6.6 Hz, 3 H), 0.92 (d, J = 6.7 Hz, 3 H), 0.87 (d, J = 7.2 Hz, 3 H), 0.86 (d, J = 7.4 Hz, 3 H).
^{13}C NMR (100 MHz, $CDCl_3$): δ 173.94, 172.42, 157.63, 81.83, 58.54, 58.26, 52.13, 31.64, 31.45, 28.15, 19.08, 19.02, 17.88, 17.65.
HRMS (ESI): *m/z* calcd for $C_{16}H_{30}O_5N_2H^+$ $[M + H]^+$ 331.2228, found 331.2229.

Synthesis of 2*S*-[3-(1*S*-Methoxycarbonyl-2-methyl-propyl)-ureido]-3-methyl-butyric acid, 49:

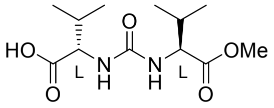

49

70 (892 mg, 2.70 mmol) was dissolved in formic acid (6 mL) in a 25 mL flask. Some drops of water were added and the mixture was stirred overnight. Evaporation to dryness, addition of toluene and re-evaporation yielded **49**.

Yield: 250 mg (0.76 mmol, 76%) as a colorless solid.
TLC (2% acetic acid + 78% ethyl acetate in cyclohexane)**:** $R_f = 0.51$.
HPLC (gradient 2): $t_R = 6.82$ min.
^{1}H NMR (400 MHz, CD_3OD): δ 4.85 (br s, 3 H), 4.20 (d, J = 5.2 Hz, 1 H), 4.19 (d, J = 4.8 Hz, 1 H), 3.71 (s, 3 H), 2.07-2.19 (m, 2 H), 0.98 (d, J = 6.8 Hz, 3 H), 0.97 (d, J = 6.8 Hz, 3 H), 0.94 (d, J = 6.8 Hz, 3 H), 0.92 (d, J = 6.8 Hz, 3 H).
^{13}C NMR (100 MHz, CD_3OD): δ 175.93, 174.76, 160.48, 59.57, 59.29, 32.09, 32.04, 19.64, 19.52, 18.03, 17.80.
HRMS (ESI): *m/z* calcd for $C_{12}H_{22}O_5N_2H^+$ $[M + H]^+$ 275.1602, found 275.1603.

Synthesis of 2*R*-[3-(1*S*-Methoxycarbonyl-2-methyl-propyl)-ureido]-3-methyl-butyric acid, 74:

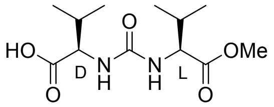

74

73 (299 mg, 0.91 mmol) was dissolved in formic acid (3 mL) in a 10 mL flask. Some drops of water were added and the mixture was stirred overnight. Evaporation to dryness, addition of toluene and re-evaporation yielded **74**.

Yield: 227 mg (0.83 mmol, 91%) as a colorless solid.
TLC (2% acetic acid + 58% ethyl acetate in cyclohexane)**:** $R_f = 0.40$.
HPLC (gradient 2): $t_R = 7.23$ min.

^{1}H NMR (400 MHz, CD_3OD): δ 4.22 (d, J = 5.7 Hz, 1 H), 4.21 (d, J = 5.6 Hz, 1 H), 3.71 (s, 3 H), 2.05-2.19 (m, 2 H), 0.98 (d, J = 6.9 Hz, 3 H), 0.96 (d, J = 6.9 Hz, 3 H), 0.93 (d, J = 7.0 Hz, 3 H), 0.92 (d, J = 7.0 Hz, 3 H).

^{13}C NMR (100 MHz, CD_3OD): δ 175.69, 174.60, 160.44, 59.50, 59.20, 52.31, 32.35, 32.25, 19.58, 19.47, 18.07, 17.85.

HRMS (ESI): *m/z* calcd for $C_{12}H_{22}O_5N_2H^+$ $[M + H]^+$ 275.1602, found 275.1603.

Synthesis of 2*S*-[3-(1*R*-Methoxycarbonyl-2-methyl-propyl)-ureido]-3-methyl-butyric acid, 78:

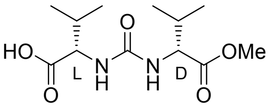

78

77 (73 mg, 0.22 mmol) was dissolved in formic acid (3 mL) in a 10 mL flask. Some drops of water were added and the mixture was stirred overnight. Evaporation to dryness, addition of toluene and re-evaporation yielded **78**.

Yield: 60 mg (0.22 mmol, >98%) as a colorless solid.

TLC (2% acetic acid + 58% ethyl acetate in cyclohexane)**:** $R_f = 0.40$.

HPLC (gradient 2): $t_R = 7.14$ min.

^{1}H NMR (400 MHz, CD_3OD): δ 4.22 (d, J = 5.4 Hz, 1 H), 4.21 (d, J = 5.1 Hz, 1 H), 3.71 (s, 3 H), 2.05-2.19 (m, 2 H), 0.98 (d, J = 6.9 Hz, 3 H), 0.96 (d, J = 6.9 Hz, 3 H), 0.93 (d, J = 6.9 Hz, 3 H), 0.92 (d, J = 6.9 Hz, 3 H).

^{13}C NMR (100 MHz, CD_3OD): δ 175.75, 174.60, 160.44, 59.51, 59.23, 52.31, 32.35, 32.26, 19.59, 19.47, 18.07, 17.86.

HRMS (ESI): *m/z* calcd for $C_{12}H_{22}O_5N_2H^+$ $[M + H]^+$ 275.1602, found 275.1603.

Synthesis of 2*R*-[3-(1*R*-Methoxycarbonyl-2-methyl-propyl)-ureido]-3-methyl-butyric acid, 81:

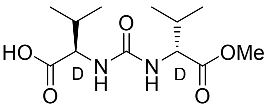

81

80 (250 mg, 0.76 mmol) was dissolved in formic acid (3 mL) in a 10 mL flask. Some drops of water were added and the mixture was stirred overnight. Evaporation to dryness, addition of toluene and re-evaporation yielded **81**.

Yield: 192 mg (0.70 mmol, 92%) as a colorless solid.
TLC (2% acetic acid + 58% ethyl acetate in cyclohexane)**:** $R_f = 0.33$.
HPLC (gradient 2): $t_R = 6.91$ min.
^{1}H NMR (400 MHz, CD_3OD): δ 4.21 (d, J = 4.5 Hz, 1 H), 4.20 (d, J = 4.4 Hz, 1 H), 3.71 (s, 3 H), 2.06-2.20 (m, 2 H), 0.98 (d, J = 6.9 Hz, 3 H), 0.97 (d, J = 6.9 Hz, 3 H), 0.94 (d, J = 7.2 Hz, 3 H), 0.92 (d, J = 7.2 Hz, 3 H).
^{13}C NMR (100 MHz, CD_3OD): δ 175.88, 174.75, 160.57, 59.59, 59.28, 52.31, 32.09, 32.03, 19.62, 19.51, 18.05, 17.82.
HRMS (ESI): *m/z* calcd for $C_{12}H_{22}O_5N_2H^+$ $[M + H]^+$ 275.1602, found 275.1603.

Synthesis of compound 82:

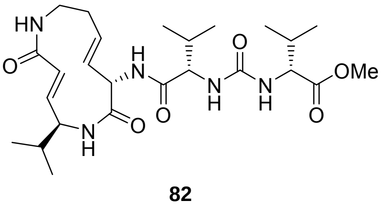

82

78 (7 mg, 25 μmol, 1.1 eq.), **58** (5.8 mg, 23 μmol, 1 eq.), PyBop (15 mg, 28 μmol, 1.2 eq.) and HOAt (4 mg, 28 μmol, 1.2 eq.) were dissolved in *N*,*N*-dimethylformamide (1.0 mL) in a 10 mL flask. The solution was cooled to 0 °C and *N*,*N*-diisopropylethylamine (8 μL, 46 μmol, 2 eq.) was added. The reaction was stirred for 40 minutes at room temperature. After concentration to dryness, the crude product was purified by flash column chromatography (10% methanol in dichloromethane) to yield **82**.

Yield: 10.1 mg (20 µmol, 87%) as a colorless solid.

TLC (8% methanol in dichloromethane)**:** $R_f = 0.30$.

HPLC (gradient 2): $t_R = 6.93$ min.

^{1}H NMR (500 MHz, d^6-DMSO): δ 8.10 (d, J = 7.0 Hz, 1 H), 8.01 (d, J = 8.2 Hz, 1 H), 7.43 (t, J = 6.9 Hz, 1 H), 6.68 (dd, J = 15.5, 5.4 Hz, 1 H), 6.51 (d, J = 8.9 Hz, 1 H), 6.27 (d, J = 9.2 Hz, 1 H), 6.10 (d, J = 15.5 Hz, 1 H), 5.55-5.64 (m, 1 H), 5.42 (dd, J = 16.0, 7.7 Hz, 1 H), 4.86-4.92 (m, 1 H), 4.05-4.12 (m, 3 H), 3.62 (s, 3 H), 3.09-3.24 (m, 2 H), 2.24-2.32 (m, 1 H), 1.85-2.02 (m, 3 H), 1.70-1.78 (m, 1 H), 0.95 (d, J = 6.6 Hz, 3 H), 0.91 (d, J = 6.6 Hz, 3 H), 0.85 (d, J = 6.9 Hz, 3 H), 0.83 (d, J = 6.5 Hz, 3 H), 0.82 (d, J = 6.5 Hz, 3 H), 0.77 (d, J = 6.8 Hz, 3 H).

^{13}C NMR (125 MHz, d^6-DMSO): δ 173.04, 171.33, 168.88, 166.20, 157.24, 143.12, 133.08, 125.81, 121.45, 57.45, 57.10, 55.42, 53.55, 51.43, 42.51, 34.98, 31.41, 31.36, 30.58, 19.70, 19.14, 19.09, 18.87, 17.64, 17.47.

HRMS (ESI): *m/z* calcd for $C_{25}H_{41}O_6N_5H^+$ $[M + H]^+$ 508.3130, found 508.3126.

Synthesis of compound 83:

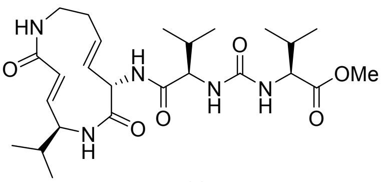

83

74 (7 mg, 25 µmol, 1.1 eq.), **58** (5.8 mg, 23 µmol, 1 eq.), PyBop (15 mg, 28 µmol, 1.2 eq.) and HOAt (4 mg, 28 µmol, 1.2 eq.) were dissolved in *N*,*N*-dimethylformamide (1.0 mL) in a 10 mL flask. The solution was cooled to 0 °C and *N*,*N*-diisopropylethylamine (8 µL, 46 µmol, 2 eq.) was added. The reaction was stirred for 40 minutes at room temperature. After concentration to dryness, the crude product was purified by flash column chromatography (10% methanol in dichloromethane) to yield **83**.

Yield: 9.6 mg (19 µmol, 76%) as a colorless solid.

TLC (8% methanol in dichloromethane)**:** $R_f = 0.30$.

HPLC (gradient 2): $t_R = 6.95$ min.

^{1}**H NMR** (500 MHz, d^6-DMSO): δ 8.16 (d, J = 7.5 Hz, 1 H), 8.00-8.06 (m, 1 H), 7.43 (t, J = 6.4 Hz, 1 H), 6.68 (dd, J = 15.5, 3.2 Hz, 1 H), 6.53 (d, J = 8.9 Hz, 1 H), 6.31 (d, J = 9.1 Hz, 1 H), 6.10 (d, J = 15.4 Hz, 1 H), 5.55-5.66 (m, 1 H), 5.34-5.42 (m, 1 H), 4.87-4.94 (m, 1 H), 4.16 (dd, J = 8.9, 5.6 Hz, 1 H), 4.05-4.12 (m, 2 H), 3.62 (s, 3 H), 3.09-3.22 (m, 2 H), 2.23-2.32 (m, 1 H), 1.84-2.02 (m, 3 H), 1.69-1.77 (m, 1 H), 0.89-0.97 (m, 6 H), 0.85 (d, J = 6.8 Hz, 3 H), 0.82 (d, J = 6.8 Hz, 3 H), 0.80 (d, J = 6.7 Hz, 3 H), 0.76 (d, J = 6.7 Hz, 3 H).

^{13}**C NMR** (125 MHz, d^6-DMSO): δ 173.02, 171.26, 169.02, 166.23, 157.26, 143.18, 132.97, 126.03, 121.49, 57.48, 57.06, 55.43, 53.64, 51.44, 42.61, 34.99, 31.58, 31.34, 30.58, 19.65, 19.19, 19.06, 18.89, 17.63, 17.42.

HRMS (ESI): *m/z* calcd for $C_{25}H_{41}O_6N_5H^+$ $[M + H]^+$ 508.3130, found 508.3127.

Synthesis of compound 84:

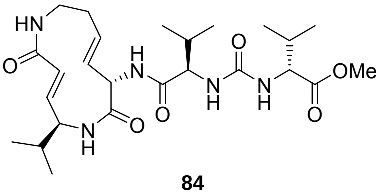

84

81 (7 mg, 25 µmol, 1.1 eq.), **58** (5.8 mg, 23 µmol, 1 eq.), PyBop (15 mg, 28 µmol, 1.2 eq.) and HOAt (4 mg, 28 µmol, 1.2 eq.) were dissolved in *N*,*N*-dimethylformamide (1.0 mL) in a 10 mL flask. The solution was cooled to 0 °C and *N*,*N*-diisopropylethylamine (8 µL, 46 µmol, 2 eq.) was added. The reaction was stirred for 40 minutes at room temperature. After concentration to dryness, the crude product was purified by flash column chromatography (10% methanol in dichloromethane) to yield **84**.

Yield: 12.0 mg (24 µmol, 95%) as a colorless solid.

TLC (8% methanol in dichloromethane)**:** $R_f = 0.21$.

HPLC (gradient 2): $t_R = 6.75$ min.

^{1}**H NMR** (500 MHz, d^6-DMSO): δ 8.00-8.12 (m, 2 H), 7.43 (t, J = 6.9 Hz, 1 H), 6.69 (dd, J = 15.4, 5.3 Hz, 1 H), 6.42 (d, J = 8.7 Hz, 1 H), 6.26 (d, J = 9.1 Hz, 1 H), 6.10 (d, J = 15.5 Hz, 1 H), 5.55-5.64 (m, 1 H), 5.34-5.42 (m, 1 H), 4.87-4.93 (m, 1 H), 4.12

(dd, J = 9.1, 5.6 Hz, 1 H), 4.05-4.11 (m, 1 H), 4.03 (dd, J = 8.7, 5.3 Hz, 1 H), 3.61 (s, 3 H), 3.09-3.24 (m, 2 H), 2.23-2.31 (m, 1 H), 1.84-2.01 (m, 3 H), 1.69-1.77 (m, 1 H), 0.95 (d, J = 6.6 Hz, 3 H), 0.91 (d, J = 6.6 Hz, 3 H), 0.86 (d, J = 6.8 Hz, 3 H), 0.84 (d, J = 6.9 Hz, 3 H), 0.80 (d, J = 6.7 Hz, 3 H), 0.77 (d, J = 6.8 Hz, 3 H).

^{13}C NMR (125 MHz, d^6-DMSO): δ 172.98, 171.24, 169.03, 166.25, 157.41, 143.20, 133.11, 126.03, 121.46, 57.82, 57.27, 55.44, 53.52, 51.37, 42.52, 34.98, 31.36, 30.18, 19.66, 19.19, 19.08, 19.02, 17.79, 17.44.

HRMS (ESI): *m/z* calcd for $C_{25}H_{41}O_6N_5H^+$ $[M + H]^+$ 508.3130, found 508.3127.

Synthesis of SylA-L-D, 85:

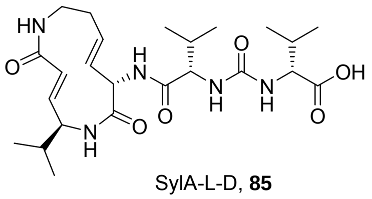

SylA-L-D, **85**

82 (10.0 mg, 19.7 µmol, 1 eq.) and aluminium bromide (42 mg, 158 µmol, 8 eq.) were dissolved under argon in tetrahydrothiophene (1 mL) in a 10 mL flame-dried flask. The resulting mixture was stirred for 1 hour at room temperature. After concentration to dryness, the remaining residue was purified by preparative HPLC (0min/10%B → 10min/10%B → 30min/30%B → 50min/60%B → 60min/100%B → 80min/100%B) to yield **85**.

Yield: 9.0 mg (18.3 µmol, 93%) as a colorless solid.

TLC (2% acetic acid + 15% methanol in dichloromethane)**:** $R_f = 0.40$.

HPLC (gradient 2): $t_R = 6.51$ min.

^{1}H NMR (500 MHz, d^6-DMSO): δ 12.43 (br s, 1 H), 8.07 (d, J = 6.6 Hz, 1 H), 8.00 (d, J = 8.5 Hz, 1 H), 7.43 (t, J = 6.7 Hz, 1 H), 6.68 (dd, J = 15.4, 4.9 Hz, 1 H), 6.40 (d, J = 9.1 Hz, 1 H), 6.28 (d, J = 8.9 Hz, 1 H), 6.10 (d, J = 15.6 Hz, 1 H), 5.60 (dt, J = 15.8, 7.2 Hz, 1 H), 5.42 (dd, J = 15.8, 8.1 Hz, 1 H), 4.88 (t, J = 6.6 Hz, 1 H), 4.05-4.12 (m, 2 H), 4.04 (dd, J = 8.2, 5.2 Hz, 1 H), 3.10-3.24 (m, 2 H), 2.24-2.31 (m, 1 H), 1.93-2.03 (m, 2 H), 1.85-1.93 (m, 1 H), 1.69-1.78 (m, 1 H), 0.95 (d, J = 6.4 Hz, 3 H), 0.90 (d, J =

6.4 Hz, 3 H), 0.85 (d, J = 6.8 Hz, 3 H), 0.83 (d, J = 6.4 Hz, 3 H), 0.82 (d, J = 6.4 Hz, 3 H), 0.77 (d, J = 6.5 Hz, 3 H).

^{13}C NMR (125 MHz, d^6-DMSO): δ 174.06, 171.52, 169.00, 166.26, 157.38, 143.26, 133.17, 125.73, 121.52, 57.15, 57.07, 55.41, 53.57, 42.52, 35.03, 31.52, 31.45, 30.57, 19.81, 19.21, 19.15, 19.11, 17.56, 17.44.

HRMS (ESI): *m/z* calcd for $C_{24}H_{39}O_6N_5H^+$ $[M + H]^+$ 494.2973, found 494.2969.

Synthesis of SylA-D-L, 86:

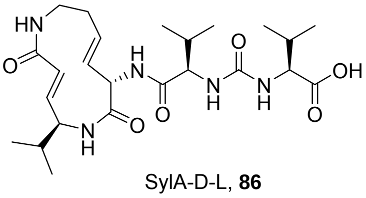

SylA-D-L, **86**

83 (9.0 mg, 17.7 μmol, 1 eq.) and aluminium bromide (38 mg, 142 μmol, 8 eq.) were dissolved under argon in tetrahydrothiophene (1 mL) in a 10 mL flame-dried flask. The resulting mixture was stirred for 1 hour at room temperature. After concentration to dryness, the remaining residue was purified by preparative HPLC (0min/10%B → 10min/10%B → 30min/30%B → 50min/60%B → 60min/100%B → 80min/100%B) to yield **86**.

Yield: 4.6 mg (9.3 μmol, 53%) as a colorless solid.

TLC (2% acetic acid + 15% methanol in dichloromethane)**:** $R_f = 0.40$.

HPLC (gradient 2): $t_R = 6.56$ min.

^{1}H NMR (500 MHz, d^6-DMSO): δ 12.39 (br s, 1 H), 8.12 (d, J = 7.8 Hz, 1 H), 8.05 (d, J = 8.7 Hz, 1 H), 7.43 (t, J = 6.9 Hz, 1 H), 6.69 (dd, J = 15.6, 5.3 Hz, 1 H), 6.42 (d, J = 9.0 Hz, 1 H), 6.32 (d, J = 9.0 Hz, 1 H), 6.10 (d, J = 15.5 Hz, 1 H), 5.62 (dt, J = 15.4, 7.6 Hz, 1 H), 5.37 (dd, J = 16.1, 7.7 Hz, 1 H), 4.92 (t, J = 7.6 Hz, 1 H), 4.16 (dd, J = 8.9, 5.5 Hz, 1 H), 4.06-4.12 (m, 1 H), 4.05 (dd, J = 8.9, 4.7 Hz, 1 H), 3.10-3.23 (m, 2 H), 2.24-2.31 (m, 1 H), 1.93-2.03 (m, 2 H), 1.84-1.92 (m, 1 H), 1.70-1.78 (m, 1 H), 0.95 (d, J = 6.6 Hz, 3 H), 0.91 (d, J = 6.6 Hz, 3 H), 0.86 (d, J = 6.7 Hz, 3 H), 0.82 (d, J = 6.8 Hz, 3 H), 0.80 (d, J = 6.8 Hz, 3 H), 0.76 (d, J = 6.8 Hz, 3 H).

^{13}C NMR (125 MHz, d^6-DMSO): δ 173.86, 171.34, 169.07, 166.19, 157.36, 143.21, 133.10, 125.83, 121.46, 57.20, 57.10, 55.44, 53.62, 42.50, 34.98, 31.56, 31.35, 30.53, 19.64, 19.19, 19.07, 19.03, 17.40.

HRMS (ESI): *m/z* calcd for $C_{24}H_{39}O_6N_5H^+$ $[M + H]^+$ 494.2973, found 494.2967.

Synthesis of SylA-D-D, 87:

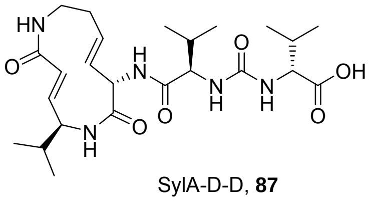

SylA-D-D, **87**

84 (11.8 mg, 23.2 μmol, 1 eq.) and aluminium bromide (50 mg, 186 μmol, 8 eq.) were dissolved under argon in tetrahydrothiophene (1 mL) in a 10 mL flame-dried flask. The resulting mixture was stirred for 1 hour at room temperature. After concentration to dryness, the remaining residue was purified by preparative HPLC (0min/10%B → 10min/10%B → 30min/30%B → 50min/60%B → 60min/100%B → 80min/100%B) to yield **87**.

Yield: 7.8 mg (15.8 μmol, 68%) as a colorless solid.

TLC (2% acetic acid + 15% methanol in dichloromethane)**:** $R_f = 0.35$.

HPLC (gradient 2): $t_R = 6.21$ min.

^{1}H NMR (600 MHz, d^6-DMSO): δ 8.03-8.10 (m, 2 H), 7.44 (br s, 1 H), 6.69 (dd, J = 15.2, 4.3 Hz, 1 H), 6.31 (d, J = 8.9 Hz, 1 H), 6.27 (d, J = 9.0 Hz, 1 H), 6.10 (d, J = 15.4 Hz, 1 H), 5.60 (dt, J = 15.7, 5.6 Hz, 1 H), 5.37 (dd, J = 15.5, 7.6 Hz, 1 H), 4.90 (t, J = 6.3 Hz, 1 H), 4.12 (dd, J = 8.1, 5.9 Hz, 1 H), 4.05-4.11 (m, 1 H), 3.98 (dd, J = 8.3, 4.8 Hz, 1 H), 3.10-3.24 (m, 2 H), 2.24-2.32 (m, 1 H), 1.92-2.02 (m, 2 H), 1.84-1.90 (m, 1 H), 1.70-1.77 (m, 1 H), 0.95 (d, J = 6.4 Hz, 3 H), 0.91 (d, J = 6.4 Hz, 3 H), 0.86 (d, J = 6.6 Hz, 3 H), 0.83 (d, J = 6.7 Hz, 3 H), 0.80 (d, J = 6.8 Hz, 3 H), 0.77 (d, J = 6.7 Hz, 3 H).

^{13}C NMR (150 MHz, d^6-DMSO): δ 174.09, 171.41, 169.08, 166.42, 157.64, 143.42, 133.15, 125.65, 121.34, 57.38, 57.21, 55.30, 53.47, 42.36, 34.80, 31.29, 31.20, 29.88, 19.93, 19.56, 18.97, 18.84, 17.78, 17.36.

HRMS (ESI): *m/z* calcd for $C_{24}H_{39}O_6N_5H^+$ $[M + H]^+$ 494.2973, found 494.2966.

Synthesis of 4*R*-*tert*-Butoxycarbonylamino-5-methyl-hexanoic acid methyl ester, 88:

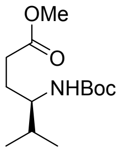

88

34 (756 mg, 2.94 mmol, 1 eq.) was dissolved in methanol (10 mL) in a 25 mL flask. To this solution was added 10%wt palladium/charcoal (157 mg, 0.15 mmol, 0.05 eq.) and the flask was flushed with hydrogen. The reaction was stirred overnight under hydrogen atmosphere. The mixture was filtered over a plug of Celite ® and washed with dichloromethane. Concentration to dryness afforded **88**.

Yield: 710 mg (2.73 mmol, 93%) as a colorless solid.
TLC (10% ethyl acetate in cyclohexane)**:** $R_f = 0.28$.
HPLC (gradient 2): $t_R = 10.04$ min.
^{1}H NMR (400 MHz, $CDCl_3$): δ 4.30 (d, J = 9.8 Hz, 1 H), 3.64 (s, 3 H), 3.35-3.45 (m, 1 H), 2.34 (t, J = 7.5 Hz, 2 H), 1.76-1.86 (m, 1 H), 1.62-1.72 (m, 1 H), 1.49-1.60 (m, 1 H), 1.40 (s, 9 H), 0.88 (d, J = 6.8 Hz, 3 H), 0.86 (d, J = 6.9 Hz, 3 H).
^{13}C NMR (100 MHz, $CDCl_3$): δ 174.28, 156.00, 78.99, 55.45, 51.63, 32.62, 31.26, 28.43, 27.68, 19.04, 17.84.
HRMS (ESI): *m/z* calcd for $C_{13}H_{25}O_4NH^+$ $[M + H]^+$ 260.1856, found 260.1857.

Synthesis of [1*R*-(2-But-3-enylcarbamoyl-ethyl)-2-methyl-propyl]-carbamic acid *tert*-butyl ester, 89:

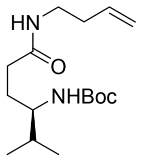

89

88 (702 mg, 2.71 mmol, 1 eq.) was dissolved in a mixture methanol/water (10:1, 16.5 mL) in a 25 mL flask. A solution of lithium hydroxide (341 mg, 8.13 mmol, 3 eq.) in water (3.5 mL) was slowly added at 0 °C and the solution was stirred for 30 minutes at room temperature. After evaporation of the solvent, the resulting solid was dissolved between a 10% aq. $KHSO_4$ solution and chloroform. The aqueous layer was extracted with chloroform and the combined organic layers were dried over Na_2SO_4, filtered and concentrated to dryness to afford 658 mg (2.68 mmol, 99%) of the free acid as a colorless solid (TLC (2% acetic acid + 30% ethyl acetate in cyclohexane): $R_f = 0.35$; HPLC (gradient 2): $t_R = 8.39$ min; HRMS (ESI): *m/z* calcd for $C_{12}H_{23}O_4NH^+$ $[M + H]^+$ 246.1700, found 246.1699).

The resulting acid (638 mg, 2.60 mmol, 1 eq.), 3-butenylamine hydrochloride (336 mg, 3.12 mmol, 1.2 eq.), and PyBop (2.03 g, 3.90 mmol, 1.5 eq.) were dissolved in dichloromethane (5 mL) in a 10 mL flask. *N*,*N*-Diisopropylethylamine (906 µL, 5.20 mmol, 2 eq.) was added at 0 °C and the resulting mixture was stirred overnight at room temperature. The reaction was stopped by quenching with a 20% aq. citric acid solution and the mixture was extracted with chloroform. The combined organic layers were washed with a 5% aq. $NaHCO_3$ solution, dried over Na_2SO_4, filtered and concentrated to dryness. The crude product was purified by flash column chromatography (30% ethyl acetate in cyclohexane) to afford **89**.

Yield: 720 mg (2.41 mmol, 93%) as a colorless solid.

TLC (35% ethyl acetate in cyclohexane)**:** $R_f = 0.35$.

HPLC (gradient 2): $t_R = 9.15$ min.

^{1}H NMR (400 MHz, $CDCl_3$): δ 6.29 (br s, 1 H), 5.77 (ddt, J = 17.0, 10.2, 6.8 Hz, 1 H), 5.02-5.12 (m, 2 H), 4.41 (d, J = 9.8 Hz, 1 H), 3.25-3.43 (m, 3 H), 2.10-2.30 (m, 4 H), 1.77-1.86 (m, 1 H), 1.63-1.72 (m, 1 H), 1.50-1.60 (m, 1 H), 1.42 (s, 9 H), 0.89 (d, J = 6.8 Hz, 3 H), 0.86 (d, J = 6.9 Hz, 3 H).

^{13}C NMR (100 MHz, $CDCl_3$): δ 173.08, 156.76, 135.50, 116.99, 79.29, 55.31, 38.67, 33.80, 32.66, 29.22, 28.47, 19.23, 17.82.

HRMS (ESI): *m/z* calcd for $C_{16}H_{30}O_3N_2H^+$ $[M + H]^+$ 299.2329, found 299.2325.

Synthesis of {1*S*-[1*R*-(2-But-3-enylcarbamoyl-ethyl)-2-methyl-propylcarbamoyl]-3-phenylselanyl-propyl}-carbamic acid *tert*-butyl ester, 90:

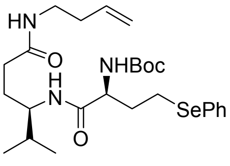

90

89 (700 mg, 2.35 mmol, 1 eq.) was dissolved in a mixture trifluoroacetic acid/dichloromethane (1:3, 10 mL) in a 25 mL flask. After 30 minutes, the mixture was evaporated to dryness to afford 653 mg (2.09 mmol, 89%) of the corresponding ammonium salts as a colorless solid (TLC (2% triethylamine + 50% ethyl acetate in cyclohexane): $R_f = 0.21$; HPLC (gradient 2): $t_R = 2.35$ min; HRMS (ESI): *m/z* calcd for $C_{11}H_{22}ON_2H^+$ $[M + H]^+$ 199.1805, found 199.1798).

The resulting ammonium (625 mg, 2.00 mmol, 1 eq.), acid **40** (932 mg, 2.60 mmol, 1.3 eq.), PyBop (1.56 g, 3.00 mmol, 1.5 eq.) and HOAt (409 mg, 3.00 mmol, 1.5 eq.) were dissolved in dichloromethane (10 mL) in a 25 mL flask. *N*,*N*-Diisopropylethylamine (697 µL, 4.00 mmol, 2 eq.) was added at 0 °C and the resulting mixture was stirred for 2 hours at room temperature. The reaction was stopped by quenching with a 20% aq. citric acid solution and the mixture was extracted with chloroform. The combined organic layers were washed with a 5% aq. $NaHCO_3$ solution, dried over Na_2SO_4, filtered and concentrated to dryness. The crude product was purified by flash column chromatography (50% ethyl acetate in cyclohexane) to afford **90**.

Yield: 867 mg (1.61 mmol, 81%) as a colorless solid.

TLC (60% ethyl acetate in cyclohexane)**:** $R_f = 0.37$.

HPLC (gradient 2): $t_R = 10.40$ min.

^{1}H NMR (400 MHz, $CDCl_3$): δ 7.46-7.51 (m, 2 H), 7.23-7.28 (m, 3 H), 6.36 (br s, 1 H), 6.20 (d, J = 9.6 Hz, 1 H), 5.76 (ddt, J = 17.0, 10.2, 6.8 Hz, 1 H), 5.13 (d, J = 7.7 Hz, 1 H), 5.02-5.11 (m, 2 H), 4.18 (td, J = 7.3, 6.5 Hz, 1 H), 3.65-3.73 (m, 1 H), 3.30-3.40 (m, 1 H), 3.18-3.28 (m, 1 H), 2.93 (t, J = 7.4 Hz, 2 H), 2.21-2.28 (m, 2 H), 2.11-

2.21 (m, 2 H), 1.93-2.09 (m, 2 H), 1.83-1.92 (m, 1 H), 1.64-1.75 (m, 1 H), 1.47-1.59 (m, 1 H), 1.43 (s, 9 H), 0.86 (d, J = 6.7 Hz, 3 H), 0.85 (d, J = 6.8 Hz, 3 H).

^{13}C NMR (100 MHz, $CDCl_3$): δ 172.91, 171.97, 155.85, 135.47, 132.90, 129.58, 129.30, 127.30, 117.00, 80.62, 55.06, 54.03, 38.78, 33.76, 33.37, 32.32, 28.68, 28.37, 23.77, 19.29, 17.87.

HRMS (ESI): *m/z* calcd for $C_{26}H_{41}O_4N_3SeH^+$ $[M + H]^+$ 540.2335, found 540.2327.

Synthesis of {1*S*-[1*R*-(2-But-3-enylcarbamoyl-ethyl)-2-methyl-propylcarbamoyl]-allyl}-carbamic acid *tert*-butyl ester, 91:

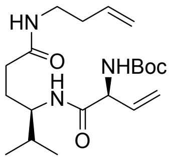

91

90 (847 mg, 1.57 mmol, 1 eq.) was dissolved in dichloromethane (80 mL) in a 250 mL flask. Hydrogen peroxide (30% in water, 10 mL) and *N*,*N*-diisopropylethylamine (10 mL) were added and the resulting mixture was heated to 50 °C for 3 hours. The reaction was quenched by addition of a saturated aq. $CuSO_4$ solution. Addition of ethyl acetate (50 mL) and a 10% aq. $KHSO_4$ solution (50 mL) generated a biphasic mixture which was separated in a funnel. The organic phase was washed with a 5% aq. $NaHCO_3$ solution (50 mL) and brine (50 mL), dried over Na_2SO_4, filtered and concentrated to dryness. The crude product was purified by flash column chromatography (60% ethyl acetate in cyclohexane) to afford **91**.

Yield: 437 mg (1.15 mmol, 73%) as a colorless solid.

TLC (60% ethyl acetate in cyclohexane)**:** $R_f = 0.19$.

HPLC (gradient 2): $t_R = 8.64$ min.

^{1}H NMR (400 MHz, $CDCl_3$): δ 6.28 (br s, 1 H), 6.11 (d, J = 9.5 Hz, 1 H), 5.92 (ddd, J = 17.0, 10.4, 6.5 Hz, 1 H), 5.77 (ddt, J = 17.0, 10.3, 6.8 Hz, 1 H), 5.38 (ddd, J = 17.2, 1.4, 0.7 Hz, 1 H), 5.30 (ddd, J = 10.3, 1.3, 0.8 Hz, 1 H), 5.27-5.31 (m, 1 H), 5.02-5.12 (m, 2 H), 4.54-4.62 (m, 1 H), 3.68-3.77 (m, 1 H), 3.31-3.42 (m, 1 H), 3.20-3.30 (m, 1

H), 2.23-2.30 (m, 2 H), 2.05-2.21 (m, 2 H), 1.84-1.95 (m, 1 H), 1.67-1.77 (m, 1 H), 1.52-1.62 (m, 1 H), 1.44 (s, 9 H), 0.89 (d, J = 6.7 Hz, 3 H), 0.87 (d, J = 6.7 Hz, 3 H).
^{13}C NMR (100 MHz, $CDCl_3$): δ 172.78, 170.48, 155.49, 135.50, 133.87, 118.35, 116.97, 80.54, 57.84, 54.19, 38.73, 33.81, 33.33, 32.43, 28.62, 28.38, 19.26, 17.99.
HRMS (ESI): *m/z* calcd for $C_{20}H_{35}O_4N_3H^+$ $[M + H]^+$ 382.2700, found 382.2704.

Synthesis of (5*R*-Isopropyl-2,7-dioxo-1,6diaza-cyclododec-9*E*-en-8*S*-yl)-carbamic acid *tert*-butyl ester, 92:

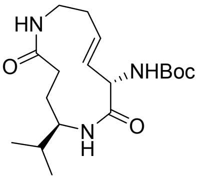

92

91 (260 mg, 682 µmol, 1 eq.) was dissolved under argon in toluene (340 mL) in a 500 mL flame-dried flask and heated to 90 °C. A solution of Grubbs' 2nd generation catalyst (87 mg, 102 µmol, 0.15 eq.) in toluene (25 mL) was added over 8 hours with a syringe pump to the preheated mixture. The resulting solution was stirred for further 10 hours at 90 °C. After concentration to dryness, the crude product was purified by flash column chromatography (70% ethyl acetate in cyclohexane) to afford **92**.

Yield: 105 mg (297 µmol, 44%) as a light brown solid.
TLC (80% ethyl acetate in cyclohexane)**:** $R_f = 0.19$.
HPLC (gradient 2): $t_R = 7.91$ min.
^{1}H NMR (400 MHz, $CDCl_3$): δ 5.99 (d, J = 7.5 Hz, 1 H), 5.76-5.86 (m, 1 H), 5.71 (d, J = 5.1 Hz, 1 H), 5.57 (d, J = 7.7 Hz, 1 H), 5.15 (ddd, J = 14.8, 9.7, 0.7 Hz, 1 H), 4.36-4.44 (m, 1 H), 3.89-4.02 (m, 1 H), 3.56-3.65 (m, 1 H), 2.79-2.87 (m, 1 H), 2.35-2.48 (m, 1 H), 2.09-2.21 (m, 1 H), 1.85-1.96 (m, 2 H), 1.75-1.84 (m, 1 H), 1.53-1.61 (m, 1 H), 1.41 (s, 9 H), 0.89 (d, J = 6.9 Hz, 3 H), 0.88 (d, J = 6.8 Hz, 3 H).
^{13}C NMR (100 MHz, $CDCl_3$): δ 174.25, 170.58, 154.87, 131.73, 130.62, 79.50, 57.52, 56.47, 37.54, 35.12, 32.99, 32.37, 28.46, 21.95, 18.63, 18.32.
HRMS (ESI): *m/z* calcd for $C_{18}H_{31}O_4N_3H^+$ $[M + H]^+$ 354.2387, found 354.2388.

Synthesis of 8*S*-Amino-5*R*-isopropyl-1,6-diaza-cyclododec-9*E*-ene-2,7-dione trifluoroacetic salts, 132:

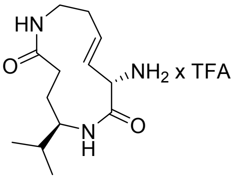

132

92 (50 mg, 141 µmol, 1 eq.) was dissolved in a mixture trifluoroacetic acid/dichloromethane (1:3, 3.5 mL) in a 10 mL flask. After 30 minutes, the mixture was evaporated to dryness to afford **132**.

Yield: 51 mg (138 µmol, >98%) as a colorless solid.
TLC (2% triethylamine + 5% methanol in dichloromethane)**:** $R_f = 0.34$.
HPLC (gradient 2): $t_R = 4.25$ min.
^{1}H NMR (400 MHz, CD_3OD): δ 6.93 (d, J = 8.8 Hz, 1 H), 6.03 (ddd, J = 15.3, 11.1, 4.4 Hz, 1 H), 5.37 (ddd, J = 15.1, 10.0, 0.8 Hz, 1 H), 4.38 (d, J = 10.0 Hz, 1 H), 3.87 (td, J = 13.7, 3.4 Hz, 1 H), 3.55-3.63 (m, 1 H), 2.88 (ddd, J = 13.6, 4.7, 2.2 Hz, 1 H), 2.35-2.50 (m, 2 H), 1.94-2.17 (m, 3 H), 1.74-1.83 (m, 1 H), 1.66 (ddd, J = 12.1, 7.7, 3.9 Hz, 1 H), 0.94 (d, J = 6.9 Hz, 6 H).
^{13}C NMR (100 MHz, CD_3OD): δ 175.98, 169.52, 138.05, 126.46, 58.24, 56.89, 37.84, 35.29, 34.38, 32.92, 23.76, 19.00, 18.93.
HRMS (ESI): *m/z* calcd for $C_{13}H_{23}O_2N_3H^+$ $[M + H]^+$ 254.1863, found 254.1863.

Synthesis of 2*S*-{3*S*-[1-(5*R*-Isopropyl-2,7-dioxo-1,6-diaza-cyclododec-9*E*-en-8*S*-ylcarbamoyl)-2-methyl-propyl]-ureido}-3-methyl-butyric acid methyl ester, 93:

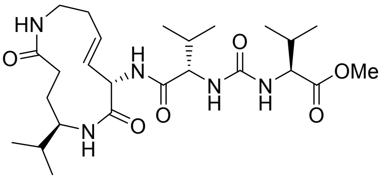

93

49 (16 mg, 57 µmol, 1.05 eq.), **132** (20 mg, 54 µmol, 1 eq.), PyBop (31 mg, 59 µmol, 1.1 eq.) and HOAt (8 mg, 59 µmol, 1.1 eq.) were dissolved in dichloromethane (5.0 mL) in a 10 mL flask. The solution was cooled to 0 °C and *N*,*N*-diisopropylethylamine (28 µL, 162 µmol, 3 eq.) was added. The reaction was stirred for 40 minutes at room temperature. After concentration to dryness, the crude product was purified by flash column chromatography (10% methanol in dichloromethane) and further precipitation in dichloromethane **93**.

Yield: 21 mg (41 µmol, 75%) as a colorless solid.
TLC (10% methanol in dichloromethane)**:** $R_f = 0.58$.
HPLC (gradient 2): $t_R = 7.42$ min.
^{1}H NMR (400 MHz, $CD_3OD/CDCl_3$ = 1:4): δ 5.77 (ddd, J = 15.2, 11.1, 3.9 Hz, 1 H), 5.19 (dd, J = 15.3, 9.6 Hz, 1 H), 4.62 (d, J = 9.8 Hz, 1 H), 4.21 (d, J = 5.0 Hz, 1 H), 4.00 (d, J = 6.2 Hz, 1 H), 3.83 (ddd, J = 13.4, 13.4, 3.6 Hz, 1 H), 3.68 (s, 3 H), 3.48-3.55 (m, 1 H), 2.75-2.82 (m, 1 H), 2.33-2.41 (m, 1 H), 2.26-2.33 (m, 1 H), 1.85-2.11 (m, 5 H), 1.66-1.73 (m, 1 H), 1.55-1.61 (m, 1 H), 0.91 (d, J = 6.7 Hz, 3 H), 0.90 (d, J = 6.8 Hz, 3 H), 0.84-0.88 (m, 12 H).
^{13}C NMR (100 MHz, $CD_3OD/CDCl_3$ = 1:4): δ 174.91, 174.18, 172.76, 171.74, 158.98, 133.16, 129.11, 59.26, 58.56, 57.14, 56.77, 37.39, 34.44, 33.49, 32.38, 31.47, 31.26, 29.95, 23.15, 19.33, 19.18, 18.82, 18.55, 17.72, 17.67.
HRMS (ESI): *m/z* calcd for $C_{25}H_{43}O_6N_5H^+$ $[M + H]^+$ 510.3286, found 510.3282.

Synthesis of 2*S*-{3*S*-[1-(5*R*-Isopropyl-2,7-dioxo-1,6-diaza-cyclododec-9*E*-en-8*S*-ylcarbamoyl)-2-methyl-propyl]-ureido}-3-methyl-butyric acid, 94 (SylA-Sat):

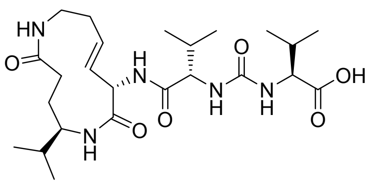

SylA-Sat, **94**

93 (21 mg, 41 µmol, 1 eq.) and aluminium chloride (55 mg, 410 µmol, 10 eq.) were dissolved under argon in ethanethiol/chloroform (3 mL, 1:1) in a 10 mL flame-dried flask. The resulting mixture was stirred for 1 hour at room temperature. After quenching the reaction with a 0.1 M solution of HCl, the mixture was concentrated to dryness and the remaining residue was purified by preparative HPLC (0min/10%B → 10min/10%B → 30min/30%B → 50min/60%B → 60min/100%B → 80min/100%B) to yield **94** (SylA-Sat).

Yield: 12.6 mg (25 µmol, 61%) as a colorless solid.
TLC (2% acetic acid + 15% methanol in dichloromethane)**:** $R_f = 0.42$.
HPLC (gradient 2): $t_R = 6.60$ min.
^{1}H NMR (400 MHz, d^6-DMSO): δ 12.39 (br s, 1 H), 7.86 (d, J = 6.5 Hz, 1 H), 7.54 (d, J = 8.4 Hz, 1 H), 6.65 (d, J = 9.3 Hz, 1 H), 6.31 (d, J = 8.8 Hz, 1 H), 6.27 (d, J = 8.9 Hz, 1 H), 5.66 (ddd, J = 15.0, 10.9, 3.8 Hz, 1 H), 5.20 (dd, J = 14.9, 9.8 Hz, 1 H), 4.62 (dd, J = 9.5, 6.6 Hz, 1 H), 3.95-4.03 (m, 2 H), 3.67-3.80 (m, 1 H), 3.39-3.50 (m, 1 H), 2.64-2.72 (m, 1 H), 2.16-2.27 (m, 2 H), 1.75-2.02 (m, 5 H), 1.54-1.64 (m, 1 H), 1.42-1.52 (m, 1 H), 0.75-0.89 (m, 18 H).
^{13}C NMR (100 MHz, d^6-DMSO): δ 174.08, 172.51, 170.90, 170.48, 157.63, 130.97, 129.88, 57.50, 57.43, 55.86, 55.20, 36.22, 33.75, 32.89, 31.71, 31.01, 30.24, 22.86, 19.26 (2 carbons), 18.93, 18.54, 17.62, 17.46.
HRMS (ESI): *m/z* calcd for $C_{24}H_{41}O_6N_5H^+$ $[M + H]^+$ 496.3130, found 496.3127.

Synthesis of Rh-SylA, 96:

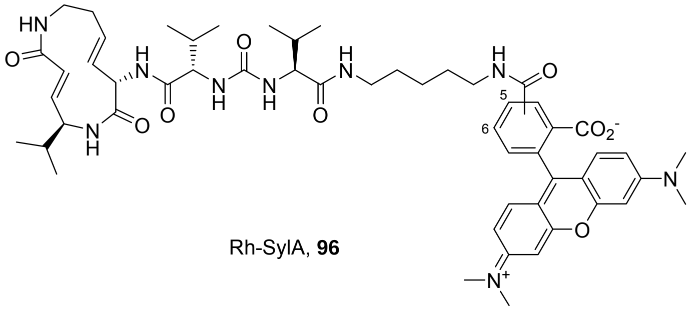

Rh-SylA, **96**

SylA (**1**) (7.85 mg, 15.9 µmol, 1 eq.) was dissolved in *N*,*N*-dimethylformamide (2 mL) in a 10 mL flask and cooled to 0 °C. A solution of a commercially available mixture of 5- and 6-rhodamine-amine **95** (30.7 mg, 55.7 µmol, 3.5 eq.), PyBop (24.8 mg, 47.7 µmol, 3 eq.), HOAt (6.5 mg, 47.7 µmol, 3 eq.) and *N*,*N*-diisopropylethylamine (13.9 µL, 79.5 µmol, 5 eq.) in *N*,*N*-dimethylformamide (1 mL) were added and the resulting mixture was stirred for 48 h at room temperature. After evaporation to dryness, the remaining residue was purified by preparative HPLC (0min/20%B → 10min/20%B → 20min/50%B → 50min/75%B → 70min/100%B → 80min/100%B) to yield **96** (Rh-SylA).

Yield: 1.42 mg (1.4 µmol, 9%) as a purple solid.
TLC (25% methanol in chloroform)**:** $R_f = 0.49$.
HPLC (gradient 2): $t_R = 6.78$ min.
^{1}H NMR (500 MHz, d^6-DMSO): δ 8.71-8.74 (m, 1 H), 8.17-8.21 (m, 2 H), 8.02 (d, J = 8.7 Hz, 1 H), 7.96 (s, 2 H), 7.91 (d, J = 6.9 Hz, 1 H), 7.84-7.87 (m, 1 H), 7.72-7.74 (m, 1 H), 7.62 (d, J = 7.5 Hz, 1 H), 7.41-7.47 (m, 2 H), 7.16-7.19 (m, 2 H), 7.11-7.13 (m, 1 H), 6.95-6.97 (m, 2 H), 6.69 (dd, J = 15.0, 5.7 Hz, 1 H), 6.25-6.31 (m, 2 H), 6.10 (d, J = 15.5 Hz, 1 H), 5.56-5.63 (m, 1 H), 5.38-5.44 (m, 1 H), 5.32-5.35 (m, 2 H), 4.84-4.88 (m, 1 H), 4.01-4.10 (m, 2 H), 3.91-3.96 (m, 1 H), 3.09-3.16 (m, 2 H), 3.00-3.06 (m, 4 H), 2.90 (s, 6 H), 2.74 (s, 6 H), 2.24-2.32 (m, 1 H), 1.94-2.04 (m, 3 H), 1.70-1.78 (m, 1 H), 1.44-1.60 (m, 5 H), 0.95 (d, J = 6.8 Hz , 3 H), 0.91 (d, J = 6.4 Hz, 3 H), 0.77-0.88 (m, 12 H).
HRMS (ESI): *m/z* calcd for $C_{54}H_{71}O_9N_9H^+$ $[M + H]^+$ 990.5448, found 990.5457.

Synthesis of compound 97:

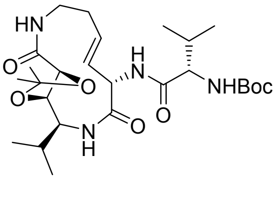

97

48 (61 mg, 188 µmol, 1 eq.), Boc-(L)-Val-OH (49 mg, 226 µmol, 1.2 eq.), HATU (107 mg, 282 µmol, 1.5 eq.) and HOAt (39 mg, 282 µmol, 1.5 eq.) were dissolved in dichloromethane/*N*,*N*-dimethylformamide (1:1, 3 mL) in a 10 mL flask. The solution was cooled to 0 °C and *N*,*N*-diisopropylethylamine (66 µL, 376 µmol, 2 eq.) was added. The reaction was stirred 1 hour at room temperature and concentrated to dryness. The crude product was purified by flash column chromatography (4% methanol in dichloromethane) to yield **97**.

Yield: 97 mg (185 mmol, 98%) as a colorless solid.

TLC (5% methanol in dichloromethane)**:** $R_f = 0.30$.

HPLC (gradient 2): $t_R = 8.85$ min.

^{1}H NMR (400 MHz, $CD_3OD/CDCl_3$ = 1:1): δ 7.94 (d, J = 7.1 Hz, ~1 H), 7.43 (d, J = 9.8 Hz, ~1 H), 5.66 (ddd, J = 14.9, 11.1, 3.9 Hz, 1 H), 5.34 (dd, J = 15.3, 9.7, 1 H), 4.77-4.82 (m, 1 H), 4.40 (dd, J = 10.3, 8.0 Hz, 1 H), 3.83-3.93 (m, 3 H), 3.79 (d, J = 7.9 Hz, 1 H), 2.84-2.90 (m, 1 H), 2.32-2.39 (m, 1 H), 1.98-2.10 (m, 3 H), 1.41 (s, 9 H), 1.40 (s, 3 H), 1.37 (s, 3 H), 0.85-0.93 (m, 12 H).

^{13}C NMR (100 MHz, $CD_3OD/CDCl_3$ = 1:1): δ 173.01, 170.12, 170.05, 157.14, 132.38, 130.48, 111.52, 81.00, 80.37, 77.41, 60.32, 57.37, 56.73, 37.04, 33.54, 31.76, 30.19, 28.57, 27.00, 26.31, 19.85, 19.45, 18.09, 15.82.

HRMS (ESI): *m/z* calcd for $C_{26}H_{44}O_7N_4H^+$ $[M + H]^+$ 525.3283, found 525.3278.

Synthesis of compound 98:

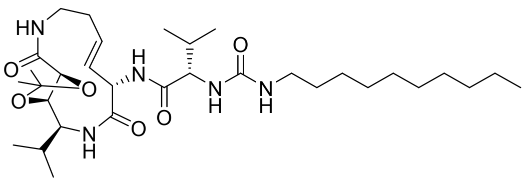

98

97 (56 mg, 107 µmol, 1 eq.) was dissolved in dichloromethane (375 µL) in a 10 mL flask. Trifluoroacetic acid (125 µL) was then added and the solution was stirred 30 min at room temperature and concentrated at room temperature to dryness. The resulting ammonium salts was pure enough to be used in the next step without further purification (intermediate characterization: HPLC (gradient 2): $t_R = 5.54$ min; HRMS (ESI): *m/z* calcd for $C_{21}H_{36}O_5N_4H^+$ $[M + H]^+$ 425.2759, found 425.2755).

The resulting ammonium salts were dissolved in dichloromethane (2 mL). *N*,*N*-diisopropylethylamine (37 µL, 214 µmol, 2 eq.) and decyl isocyanate (27 µL, 129 µmol, 1.2 eq.) were added. The reaction was stirred 1 hour at room temperature and concentrated to dryness. The crude product was purified by flash column chromatography (6% methanol in dichloromethane) to yield **98**.

Yield: 62 mg (102 µmol, 95%) as a colorless solid.

TLC (8% methanol in dichloromethane)**:** $R_f = 0.33$.

HPLC (gradient 2): $t_R = 11.25$ min.

^{1}H NMR (400 MHz, d^6-DMSO): δ 7.98 (d, J = 5.9 Hz, 1 H), 7.95 (d, J = 9.8 Hz, 1 H), 7.51 (d, J = 10.2 Hz, 1 H), 5.99-6.03 (m, 1 H), 5.87 (d, J = 9.3 Hz, 1 H), 5.58 (ddd, J = 15.0, 11.1, 4.0 Hz, 1 H), 5.35 (dd, J = 15.2, 9.6, 1 H), 4.66 (dd, J = 9.7, 6.0, 1 H), 4.33 (dd, J = 10.4, 7.7 Hz, 1 H), 4.02 (dd, J = 8.8, 5.5, 1 H), 3.81 (ddd, J = 10.4, 10.3, 3.4, 1 H), 3.73 (d, J = 7.6 Hz, 1 H), 3.65-3.74 (m, 1H), 2.90-2.97 (m, 2 H), 2.71-2.77 (m, 1 H), 2.23-2.29 (m, 1 H), 1.84-2.03 (m, 3 H), 1.33 (s, 3 H), 1.32 (s, 3 H), 1.21-1.28 (m, 16 H), 0.86 (t, J = 6.7 Hz, 1 H), 0.85 (d, J = 6.9 Hz, 1 H), 0.82 (d, J = 6.8 Hz, 1 H), 0.78 (d, J = 7.0 Hz, 1 H), 0.76 (d, J = 6.8 Hz, 1 H).

^{13}C NMR (100 MHz, d^6-DMSO): δ 171.22, 171.16, 167.71, 157.78, 131.19, 129.87, 109.64, 79.91, 76.83, 57.08, 55.99, 55.02, 53.57, 41.82, 35.63, 32.21, 31.26, 31.14, 29.94, 29.01, 28.92, 28.75, 28.66, 26.73, 26.33, 25.97, 22.06, 18.06, 17.53, 16.71, 15.81, 13.92.

HRMS (ESI): *m/z* calcd for $C_{32}H_{57}O_6N_5H^+$ $[M + H]^+$ 608.4382, found 608.4380.

Synthesis of 2*S*-(3-Decyl-ureido)-*N*-(5*S*-isopropyl-2,7-dioxo-1,6-diaza-cyclododeca-3*E*,9*E*-dien-8*S*-yl)-3-methyl-butyramide, 99 (SylA-LIP):

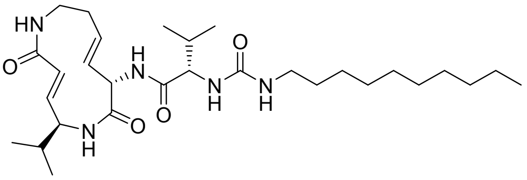

SylA-LIP, **99**

98 (25 mg, 41 µmol) was dissolved in formic acid/water/tetrahydrofurane (1:1.1, 10 mL) and the mixture was heated to 80°C overnight. After cooling, the solvents were removed under reduced pressure to afford 23 mg (40 µmol, >98%) of the dihydroxyl intermediate as a colorless solid. The product was pure enough to be used in the next step without further purification (intermediate characterization: HPLC (gradient 2): $t_R = 9.24$ min; HRMS (ESI): *m/z* calcd for $C_{29}H_{53}O_6N_5H^+$ $[M + H]^+$ 568.4069, found 568.4065).

The dihydroxyl derivative (16 mg, 29 µmol, 1 eq.) was dissolved under argon in tetrahydrofurane (5 mL) in a 100 mL flame-dried flask. To this solution was added thiocarbonyl diimidazole (52 mg, 290 µmol, 10 eq.) and 4-(dimethylamino)pyridine (35 mg, 290 µmol, 10 eq.). The resulting reaction mixture was heated to 80 °C and stirred at this temperature overnight. After cooling to room temperature, a small portion of silica gel was added and the solvent was removed under vacuo. The adsorbed crude product was purified by flash column chromatography (6% methanol in dichloromethane) to yield 12.5 mg (21 µmol, 73%) of the thiocarbonate derivative as a colorless solid. The product was pure enough to be used in the next step without further purification (intermediate characterization: HPLC (gradient 2): t_R = 11.15 min; HRMS (ESI): *m/z* calcd for $C_{30}H_{51}O_6N_5SH^+$ $[M + H]^+$ 610.3633, found 610.3631).

In a 10 mL vessel was placed the thiocarbonate derivative (5.4 mg, 8.8 µmol), trimethyl phosphite (300 µL) and a magnetic stirring bar. The vessel was sealed with a septum, placed into the MW cavity, and locked with the pressure device. Constant microwave irradiation of 250 W as well as a simultaneous air-cooling (300 kPa, 45 Psi) were used during the entire reaction time (15 min, 160 °C, resulting reaction pressure 2.5 bar). After concentration to dryness, the crude product was purified by flash column chromatography (9% methanol in dichloromethane) to yield **99** (SylA-LIP).

Yield: 3.0 mg (5.6 µmol, 64%) as a colorless solid.

TLC (10% methanol in dichloromethane)**:** R_f = 0.30.

HPLC (gradient 2): t_R = 9.81 min.

^{1}H NMR (400 MHz, d^6-DMSO): δ 7.99-8.03 (m, 2 H), 7.44 (t, J = 7.5 Hz, 1 H), 6.68 (dd, J = 15.4, 5.5 Hz, 1 H), 6.10 (d, J = 15.7 Hz, 1 H), 6.00-6.04 (m, 1 H), 5.90 (d, J = 9.0, 1 H), 5.60 (dt, J = 15.0, 7.7 Hz, 1 H), 5.41 (dd, J = 15.5, 7.8 Hz, 1 H), 4.86 (dd, J = 7.3, 7.3 Hz, 1 H), 4.03-4.10 (m, 2 H), 3.12-3.21 (m, 2 H), 2.92-2.98 (m, 2 H), 2.24-2.32 (m, 1 H), 1.94-2.01 (m, 1 H), 1.86-1.94 (m, 1 H), 1.69-1.78 (m, 1 H), 1.19-1.36 (m, 18H), 0.95 (d, J = 6.7, 3 H), 0.90 (d, J = 6.6, 3 H), 0.85 (t, J = 7.3 Hz, 3 H), 0.83 (d, J = 6.8, 3 H), 0.76 (d, J = 6.8, 3 H).

^{13}C NMR (125 MHz, d^6-DMSO): δ 170.24, 166.26, 162.92, 157.72, 142.45, 133.03, 125.19, 121.82, 57.33, 55.44, 52.98, 42.27, 33.95, 31.44, 31.27, 31.08, 29.95, 29.03, 28.94, 28.77, 28.68, 26.33, 22.07, 19.76, 19.28, 19.16, 17.59, 13.94.

HRMS (ESI): *m/z* calcd for $C_{29}H_{51}O_4N_5H^+$ $[M + H]^+$ 534.4014, found 534.4011.

Synthesis of Toluene-4-sulfonic acid 2-[2-(2-methoxy-ethoxy)-ethoxy]-ethyl ester, 103:

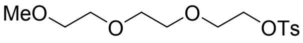

103

Triethylene glycol mono methyl ether **101** (314 μL, 2.0 mmol, 1 eq.) and triethylamine (416 μL, 3.0 mmol, 1.5 eq.) were dissolved in dry dichloromethane (5 mL) and the solution was cooled to 0 °C. A solution of tosyl chloride (382 mg, 2.0 mmol, 1 eq.) in dichloromethane (2 mL) was then added dropwise. The mixture was stirred for 2 hours at 0 °C and 30 minutes at room temperature. After addition of diethyl ether (5 mL) the resulting precipitate was filtered and the filtrate concentrated to dryness. The crude product was purified by flash column chromatography (diethyl ether) to afford **103**.

Yield: 481 mg (1.51 mmol, 76%) as a colorless oil.
TLC (50% diethyl ether in petroleum ether)**:** $R_f = 0.10$.
HPLC (gradient 2): $t_R = 8.68$ min.
^{1}H NMR (400 MHz, $CDCl_3$): δ 7.79 (d, J = 8.3 Hz, 2 H), 7.33 (d, J = 8.0 Hz, 2 H), 4.13-4.17 (m, 2 H) , 3.65-3.69 (m, 2 H), 3.57-3.62 (m, 6 H), 3.50-3.53 (m, 2 H), 3.36 (s, 3 H), 2.44 (s, 3 H).
^{13}C NMR (100 MHz, $CDCl_3$): δ 144.85, 132.98, 129.86, 128.02, 71.93, 70.77, 70.60, 70.58, 69.29, 68.70, 59.09, 21.70.
HRMS (ESI): *m/z* calcd for $C_{14}H_{22}O_6SH^+$ $[M + H]^+$ 319.1210, found 319.1212.

Synthesis of Toluene-4-sulfonic acid 2-(2-methoxy-ethoxy)-ethyl ester, 102:

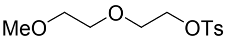

102

2-(2-methoxyethoxy)ethanol **100** (238 μL, 2.0 mmol, 1 eq.) and triethylamine (416 μL, 3.0 mmol, 1.5 eq.) were dissolved in dry dichloromethane (5 mL) and the solution was cooled to 0 °C. A solution of tosyl chloride (382 mg, 2.0 mmol, 1 eq.) in dichloromethane (2 mL) was then added dropwise. The mixture was stirred for 2 hours at 0 °C and 30 minutes at room temperature. After addition of diethyl ether (5 mL) the resulting precipitate was filtered and the filtrate concentrated to dryness. The crude product was purified by flash column chromatography (diethyl ether) to afford **102**.

Yield: 290 mg (1.05 mmol, 53%) as a colorless oil.
^{1}H NMR (400 MHz, $CDCl_3$): δ 7.79 (d, J = 8.3 Hz, 2 H), 7.33 (d, J = 8.1 Hz, 2 H), 4.14-4.18 (m, 2 H) , 3.66-3.70 (m, 2 H), 3.57 (dd, J = 5.6, 3.4 Hz, 2 H), 3.47 (dd, J = 5.6, 3.5 Hz, 2 H), 3.34 (s, 3 H), 2.44 (s, 3 H).
^{13}C NMR (100 MHz, $CDCl_3$): δ 144.87, 132.95, 129.86, 128.04, 71.84, 70.72, 69.28, 68.75, 59.11, 21.70.

Synthesis of 2-[2-(2-Methoxy-ethoxy)-ethoxy]-ethylamine, 105:

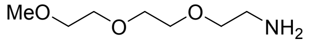

105

103 (117 mg, 365 μmol, 1 eq.) was dissolved in *N*,*N*-dimethylformamide (15 mL) and sodium azide (60 mg, 913 μmol, 2.5 eq.) was added. The flask was flushed with argon and the mixture stirred in a pre-warmed oil bath at 67 °C. After 10 hours, the resulting mixture was diluted with water (15 mL) and stirred further 30 minutes. The solution was poured in an Erlenmeyer flask containing ~ 15 mL ice. The cold mixture was extracted with diethyl ether (3 × 10 mL) and the combined organic layers were washed with water (2 × 5 mL). The organic layer was then dried over Na_2SO_4, filtered and the solvent was removed at room temperature. The crude product was used in the next step without further purification.

The crude azide was dissolved in diethyl ether (15 mL) and the solution cooled at 0 °C. Triphenyl phosphine (105 mg, 402 μmol, 1.1 eq.) was added and the mixture was stirred 1 hour at 0 °C and 1.5 hours at room temperature. The reaction was quenched with water (20 mL) and the mixture stirred vigorously for 4 hours. Toluene (15 mL) was added and the mixture was stirred overnight. After decantation, the layers were separated and the aqueous layer was extracted once with toluene. After concentration of the aqueous layer, the free amine **105** was obtained and used in the next step without further purification.

Yield: 49 mg (300 µmol, 82%) as a colorless oil.

^{1}H NMR (400 MHz, d^6-DMSO): δ 8.07 (br s, 2 H), 3.61 (t, J = 5.4 Hz, 2 H), 3.50-3.57 (m, 4 H), 3.41-3.45 (m, 4 H), 3.24 (s, 3 H), 2.90-2.97 (m, 2 H).

^{13}C NMR (100 MHz, d^6-DMSO): δ 71.21, 69.63, 69.56, 69.52, 66.56, 58.03, 38.41.

Synthesis of 2-(2-Methoxy-ethoxy)-ethylamine, 104:

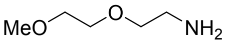

104

102 (100 mg, 365 µmol, 1 eq.) was dissolved in *N*,*N*-dimethylformamide (15 mL) and sodium azide (60 mg, 913 µmol, 2.5 eq.) were added. The flask was flushed with argon and the mixture stirred in a pre-warmed oil bath at 67 °C. After 10 hours the resulting mixture was diluted with water (15 mL) and stirred further 30 minutes. The solution was poured in an Erlenmeyer flask containing ~ 15 mL ice. The cold mixture was extracted with diethyl ether (3 × 10 mL) and the combined organic layers were washed with water (2 × 5 mL). The organic layer was then dried over Na_2SO_4, filtered and the solvent was removed at room temperature. The crude product was used in the next step without further purification.

The crude azide was dissolved in diethyl ether (15 mL) and the solution cooled at 0 °C. Triphenyl phosphine (105 mg, 402 µmol, 1.1 eq.) was added and the mixture was stirred 1 hour at 0 °C and 1.5 hours at room temperature. The reaction was quenched with water (20 mL) and the mixture stirred vigorously for 4 hours. Toluene (15 mL) was added and the mixture was stirred overnight. After decantation, the layers were separated and the aqueous layer was extracted once with toluene. After concentration of the aqueous layer, **104** was obtained and used in the next step without further purification.

Yield: 26 mg (215 µmol, 59%) as a colorless oil.

Synthesis of {2-[2-(2-Methoxy-ethoxy)-ethoxy]-ethyl}-carbamic acid 2,5-dioxo-pyrrolidin-1-yl ester, 106:

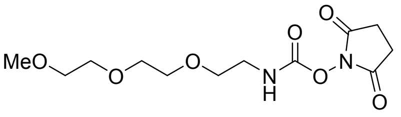

106

In a 10 mL flask, a solution of amine **105** (49 mg, 300 µmol, 1.0 eq.) in *N*,*N*-dimethylformamide (1.0 mL) was added dropwise to a solution of disuccinimidyl carbonate (154 mg, 600 µmol, 2.0 eq.) in *N*,*N*-dimethylformamide (2.0 mL). Triethylamine (84 µL, 600 µmol, 2.0 eq.) was then added dropwise and the mixture was stirred 90 minutes. The solvent was reduced to 1 mL by evaporation under reduced pressure and 1 N HCl (5 mL) was added. This mixture was extracted a mixture methanol/dichloromethane (1:4) and the organic layer was dried over Na_2SO_4, filtered and concentrated. The crude product **106** was used in the next step without further purification.

Synthesis of [1*S*-(5*S*-Isopropyl-2,7-dioxo-1,6-diaza-cyclododeca-3*E*,9*E*-dien-8*S*-ylcarbamoyl)-2-methyl-propyl]-carbamic acid *tert*-butyl ester, 133:

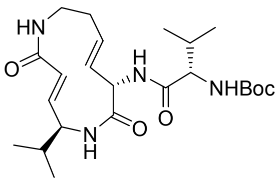

133

Boc-(L)-Valine (21 mg, 95 µmol, 1.2 eq.), **58** (20 mg, 79 µmol, 1 eq.), PyBop (62 mg, 119 µmol, 1.5 eq.) and HOAt (16 mg, 119 µmol, 1.5 eq.) were dissolved in *N*,*N*-dimethylformamide (1.5 mL) in a 10 mL flask. The solution was cooled to 0 °C and *N*,*N*-diisopropylethylamine (28 µL, 158 µmol, 2 eq.) was added. The reaction was stirred for 1 hour at room temperature. After concentration to dryness, the crude product was purified by flash column chromatography (6% methanol in dichloromethane) to yield **133**.

Yield: 34 mg (75 µmol, 95%) as a colorless solid.

TLC (6% methanol in dichloromethane)**:** $R_f = 0.30$.

HPLC (gradient 2): $t_R = 7.46$ min.

^{1}**H NMR** (400 MHz, d^6-DMSO): δ 8.04 (d, J = 8.6 Hz, 1 H), 7.90-7.96 (m, 1 H), 7.42-7.46 (m, 1 H), 6.70-6.74 (m, 1 H), 6.69 (dd, J = 15.5, 5.4 Hz, 1 H), 6.10 (d, J = 15.3 Hz, 1 H), 5.60 (dt, J = 15.6, 7.6 Hz, 1 H), 5.41 (dd, J = 15.8, 7.6 Hz, 1 H), 4.89 (dd, J = 7.6, 7.4 Hz, 1 H), 4.04-4.12 (m, 1 H), 3.82 (dd, J = 8.9, 7.1 Hz, 1 H), 3.10-3.22 (m, 2 H), 2.23-2.33 (m, 1 H), 1.87-2.02 (m, 2 H), 1.68-1.78 (m, 1 H), 1.37 (s, 9 H), 0.94 (d, J = 6.7 Hz, 3 H), 0.90 (d, J = 6.7 Hz, 3 H), 0.83 (d, J = 6.8 Hz, 3 H), 0.78 (d, J = 6.6 Hz, 3 H).

^{13}**C NMR** (100 MHz, d^6-DMSO): δ 170.80, 168.87, 166.24, 155.35, 143.21, 133.08, 126.00, 121.48, 77.99, 59.42, 55.48, 53.48, 42.56, 34.97, 31.41, 30.45, 28.15, 19.70, 19.19, 19.18, 18.00.

HRMS (ESI): *m/z* calcd for $C_{23}H_{38}O_5N_4H^+$ $[M + H]^+$ 451.2915, found 451.2912.

Synthesis of 2*S*-Amino-*N*-(5*S*-isopropyl-2,7-dioxo-1,6-diaza-cyclododeca-3*E*,9*E*-dien-8*S*-yl)-3-methyl-butyramide trifluoroacetic salts, 107:

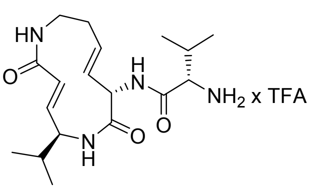

107

133 (34 mg, 75 µmol, 1 eq.) was dissolved in a mixture trifluoroacetic acid/dichloromethane (1:3, 1 mL) in a 10 mL flask. After 30 minutes, the mixture was evaporated to dryness to afford **107**.

Yield: 34 mg (73 µmol, 98%) as a colorless solid.

TLC (1% triethylamine + 5% methanol in dichloromethane)**:** $R_f = 0.31$.

HPLC (gradient 2): $t_R = 4.44$ min.

^{1}**H NMR** (400 MHz, d^6-DMSO): δ 8.64 (d, J = 6.8 Hz, 1 H), 8.14 (br s, 3 H), 7.47 (t, J = 6.9 Hz, 1 H), 6.69 (dd, J = 15.5, 5.2 Hz, 1 H), 6.10 (d, J = 15.3 Hz, 1 H), 5.65 (dt, J = 15.4, 7.7 Hz, 1 H), 5.45 (dd, J = 15.8, 7.8 Hz, 1 H), 4.94 (t, J = 7.3 Hz, 1 H), 4.05-4.13 (m, 1 H), 3.60-3.65 (m, 1 H), 3.10-3.27 (m, 2 H), 2.25-2.35 (m, 1 H), 1.94-2.09 (m, 2 H), 1.70-1.80 (m, 1 H), 0.88-0.98 (m, 12 H).

HRMS (ESI): *m/z* calcd for $C_{18}H_{30}O_3N_4H^+$ $[M + H]^+$ 351.2391, found 351.2391.

Synthesis of *N*-(5*S*-Isopropyl-2,7-dioxo-1,6-diaza-cyclododeca-3*E*,9*E*-dien-8*S*-yl)-2*S*-(3-{2-[2-(2-methoxy-ethoxy)-ethoxy]-ethyl}-ureido)-3-methyl-butyramide, 108 (SylA-PEG1):

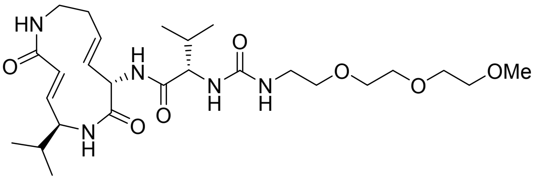

SylA-PEG1, **108**

106 (48 mg, 158 µmol, 8.0 eq.) and **107** (9.2 mg, 19.8 µmol, 1 eq.) were dissolved in *N*,*N*-dimethylformamide (0.5 mL) in a 10 mL flask. The solution was cooled to 0 °C and *N*,*N*-diisopropylethylamine (11 µL, 60 µmol, 3 eq.) was added. The reaction was stirred overnight at room temperature. After concentration to dryness, the remaining residue was purified by preparative HPLC (0min/15%B → 10min/15%B → 30min/50%B → 50min/75%B → 60min/100%B → 80min/100%B) to yield **108** (SylA-PEG1).

Yield: 7.28 mg (13,5 µmol, 68%) as a colorless solid.
TLC (10% methanol in dichloromethane)**:** $R_f = 0.21$.
HPLC (gradient 2): $t_R = 5.94$ min.
^{1}H NMR (500 MHz, d^6-DMSO): δ 7.96-8.03 (m, 2 H), 7.43 (t, J = 6.8 Hz, 1 H), 6.68 (dd, J = 15.5, 5.3 Hz, 1 H), 6.06-6.15 (m, 3 H), 5.60 (dt, J = 15.3, 7.6 Hz, 1 H), 5.42 (dd, J = 15.8, 7.7 Hz, 1 H), 4.86 (t, J = 7.2 Hz, 1 H), 4.02-4.12 (m, 2 H), 3.48-3.54 (m, 6 H), 3.41-3.45 (m, 2 H), 3.34-3.38 (m, 3 H), 3.24 (s, 3 H), 3.09-3.20 (m, 3 H), 2.24-2.32 (m, 1 H), 1.87-2.02 (m, 2 H), 1.69-1.78 (m, 1 H), 0.95 (d, J = 6.6 Hz, 3 H), 0.90 (d, J = 6.6 Hz, 3 H), 0.83 (d, J = 6.7 Hz, 3 H), 0.76 (d, J = 6.7 Hz, 3 H).
^{13}C NMR (125 MHz, d^6-DMSO): δ 171.40, 168.96, 166.29, 157.69, 142.93, 132.84, 125.80, 121.24, 71.19 (3 carbons), 69.91, 69.40, 57.78, 57.19, 55.24, 53.33, 42.32, 38.95, 34.75, 31.24, 30.79, 19.54, 18.98, 18.84, 17.44.
HRMS (ESI): *m/z* calcd for $C_{26}H_{45}O_7N_5H^+$ $[M + H]^+$ 540.3392, found 540.3388.

Synthesis of 2*S*-{3-[1*S*-(5*S*-Isopropyl-2,7-dioxo-1,6-diaza-cyclododeca-3*E*,9*E*-dien-8*S*-ylcarbamoyl)-2-methyl-propyl]-ureido}-*N*-[2-(2-methoxy-ethoxy)-ethyl]-3-methyl-butyramide, 109 (SylA-PEG2):

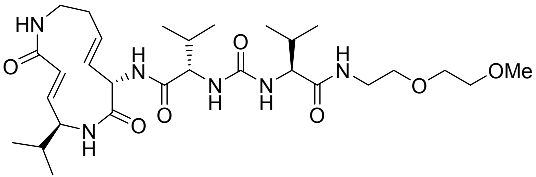

SylA-PEG2, **109**

SylA **1** (3.0 mg, 6.1 μmol, 1 eq.), **104** (1.1 mg, 9.2 μmol, 1.5 eq.), PyBop (3.8 mg, 7.3 μmol, 1.2 eq.) and HOAt (1.0 mg, 7.3 μmol, 1.2 eq.) were dissolved in *N*,*N*-dimethylformamide (1.0 mL) in a 10 mL flask. The solution was cooled to 0 °C and *N*,*N*-diisopropylethylamine (2.2 μL, 12.2 μmol, 2 eq.) was added. The reaction was stirred for 40 minutes at room temperature. After concentration to dryness, the remaining residue was purified by preparative HPLC (0min/15%B → 10min/15%B → 30min/50%B → 50min/75%B → 60min/100%B → 80min/100%B) to yield **109** (SylA-PEG2).

Yield: 2.87 mg (4.8 μmol, 79%) as a colorless solid.

TLC (10% methanol in dichloromethane)**:** $R_f = 0.20$.

HPLC (gradient 2): $t_R = 6.93$ min.

^{1}H NMR (500 MHz, d^6-DMSO): δ 8.34 (br s, 1 H), 8.08 (d, J = 8.1 Hz, 1 H), 7.89 (d, J = 7.1 Hz, 1 H), 7.42 (t, J = 6.5 Hz, 1 H), 6.70 (dd, J = 15.6, 5.4 Hz, 1 H), 6.29 (d, J = 8.5 Hz, 1 H), 6.27 (d, J = 9.1 Hz, 1 H), 6.07 (d, J = 15.3 Hz, 1 H), 5.56 (dt, J = 15.7, 7.8 Hz, 1 H), 5.40 (dd, J = 15.8, 7.9 Hz, 1 H), 4.81 (t, J = 7.3 Hz, 1 H), 4.01-4.05 (m, 1 H), 3.95-3.99 (m, 1 H), 3.88-3.92 (m, 1 H), 3.45-3.49 (m, 2 H), 3.39-3.41 (m, 2 H), 3.36-3.39 (m, 2 H), 3.21 (s, 3 H), 3.15-3.21 (m, 2 H), 3.07-3.11 (m, 2 H), 2.23-2.29 (m, 1 H), 1.89-1.98 (m, 2 H), 1.81-1.86 (m, 1 H), 1.68-1.74 (m, 1 H), 0.92 (d, J = 6.7 Hz, 3 H), 0.88 (d, J = 6.7 Hz, 3 H), 0.82 (d, J = 6.9 Hz, 3 H), 0.79 (d, J = 6.8 Hz, 3 H), 0.77 (d, J = 6.7 Hz, 3 H), 0.76 (d, J = 6.7 Hz, 3 H).

^{13}C NMR (125 MHz, d^6-DMSO): δ 172.66, 171.72, 169.47, 167.03, 157.92, 143.57, 133.68, 126.14, 121.40, 71.31, 69.42, 68.97, 58.21, 58.18, 57.77, 55.51, 53.72, 42.39, 42.02, 35.18, 31.79, 31.27, 30.84, 19.98, 19.26, 19.14, 17.70, 17.64.

HRMS (ESI): *m/z* calcd for $C_{29}H_{51}O_7N_6H^+$ $[M + H]^+$ 595.3814, found 595.3811.

Synthesis of Dodeca-2*E*,4*E*-dienoic acid ethyl ester, 111:

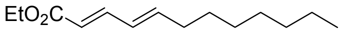

111

N,*N*-Diisopropylamine (212 µL, 1.5 mmol, 3 eq.) was dissolved under argon in tetrahydrofurane (2.5 mL) in a 25 mL flame-dried flask and cooled to -78 °C. To this solution was added slowly a solution of *n*-butyllithium (2.5 M./Hex, 400 µL, 1.0 mmol, 2 eq.). The mixture was stirred at -78 °C for 10 minutes and warmed to 0 °C for 10 minutes. After cooling again to -78 °C, (*E*)-triethyl 4-phosphonocrotonate **110** (272 mg, 1.0 mmol, 2 eq.) was added and stirred for 10 minutes. A solution of octanal (64 mg, 0.50 mmol, 1 eq.) in tetrahydrofurane (2 mL) was added and the mixture was slowly allowed to warm at room temperature over 2 hours. The reaction was quenched upon addition of a saturated aq. NH_4Cl solution. The mixture was extracted twice with a mixture of ethyl acetate/cyclohexane (1:1) and the combined organic layers were dried over Na_2SO_4, filtered and concentrated to dryness. The crude product was purified by flash column chromatography (2% ethyl acetate in cyclohexane) to afford **111**.

Yield: 68 mg (0.30 mmol, 61%) as a colorless solid.
TLC (5% ethyl acetate in cyclohexane)**:** $R_f = 0.31$.
HPLC (gradient 2): $t_R = 13.59$ min.
^{1}H NMR (400 MHz, $CDCl_3$): δ 7.25 (dd, J = 15.5, 10.0 Hz, 1 H), 6.07-6.20 (m, 2 H), 5.77 (d, J = 15.4 Hz, 1 H), 4.19 (q, J = 7.1 Hz, 2 H), 2.12-2.19 (m, 2 H) , 1.37-1.46 (m, 2 H), 1.28 (t, J = 7.1 Hz, 3 H), 1.24-1.33 (m, 8 H), 0.88 (t, J = 6.9 Hz, 3 H).
^{13}C NMR (100 MHz, $CDCl_3$): δ 167.39, 145.18, 144.82, 128.41, 119.24, 60.23, 33.08, 31.86, 29.22, 29.18, 28.81, 22.71, 14.40, 14.15.
HRMS (ESI): *m/z* calcd for $C_{14}H_{24}O_2H^+$ $[M + H]^+$ 225.1849, found 225.1848.

Synthesis of Dodeca-2*E*,4*E*-dienoic acid, 112:

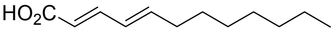

112

In a 10 mL flask was dissolved **111** (47 mg, 210 μmol, 1 eq.) in a mixture methanol/water/tetrahydrofurane (3:1:2, 3 mL) and cooled to 0 °C. To this solution was added slowly a solution of lithium hydroxide (15 mg, 630 μmol, 3 eq.) in water (0.5 mL). The mixture was then stirred overnight at room temperature and concentrated to dryness. The resulting solid was dissolved between a saturated aq. NH_4Cl solution and dichloromethane. The aqueous layer was extracted with dichloromethane and the combined organic layers were dried over Na_2SO_4, filtered and concentrated to dryness to afford **112**.

Yield: 34 mg (173 μmol, 82%) as a colorless solid.
TLC (1% acetic acid + 20% ethyl acetate in cyclohexane)**:** $R_f = 0.25$.
HPLC (gradient 2): $t_R = 11.36$ min.
^{1}H NMR (400 MHz, $CDCl_3$): δ 7.35 (ddd, J = 15.3, 7.0, 3.2 Hz, 1 H), 6.17-6.21 (m, 2 H), 5.78 (d, J = 15.2 Hz, 1 H), 2.14-2.21 (m, 2 H), 1.37-1.48 (m, 2 H), 1.23-1.35 (m, 8 H), 0.88 (t, J = 6.9 Hz, 3 H).
^{13}C NMR (100 MHz, $CDCl_3$): δ 172.90, 147.65, 146.40, 128.30, 118.31, 33.16, 31.85, 29.24, 29.17, 28.72, 22.72, 14.16.
HRMS (ESI): *m/z* calcd for $C_{12}H_{20}O_2H^+$ $[M + H]^+$ 197.1536, found 197.1536.

Synthesis of [2*R*-*tert*-Butoxy-1*S*-(5*S*-isopropyl-2,7-dioxo-1,6-diaza-cyclododeca-3*E*,9*E*-dien-8*S*-ylcarbamoyl)-propyl]-carbamic acid *tert*-butyl ester, 113:

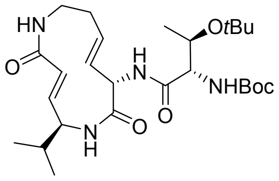

113

Boc-(L)-Thr(O^tBu)-OH (19 mg, 66 μmol, 1.2 eq.), **58** (17.9 mg, 55 μmol, 1 eq.), PyBop (43 mg, 82 μmol, 1.5 eq.) and HOAt (12 mg, 82 μmol, 1.5 eq.) were dissolved in *N*,*N*-dimethylformamide (2.0 mL) in a 10 mL flask. The solution was cooled to 0 °C and *N*,*N*-diisopropylethylamine (20 μL, 110 μmol, 2 eq.) was added. The reaction was stirred for 40 minutes at room temperature. After concentration to dryness, the crude product was purified by flash column chromatography (5% methanol in dichloromethane) to yield **113**.

Yield: 17.3 mg (34 µmol, 62%) as a colorless solid.
TLC (10% methanol in dichloromethane)**:** $R_f = 0.54$.
HPLC (gradient 2): $t_R = 8.56$ min.
^{1}H NMR (400 MHz, d^6-DMSO): δ 8.06-8.12 (m, 2 H), 7.45 (t, J = 7.1 Hz, 1 H), 6.68 (dd, J = 15.5, 5.5 Hz, 1 H), 6.14 (d, J = 9.3 Hz, 1 H), 6.10 (d, J = 15.5 Hz, 1 H), 5.61 (dt, J = 15.6, 7.8 Hz, 1 H), 5.42 (dd, J = 16.0, 7.7 Hz, 1 H), 4.94 (dd, J = 7.6, 7.6 Hz, 1 H), 4.05-4.12 (m, 1 H), 3.95 (dd, J = 9.2, 3.0 Hz, 1 H), 3.83-3.90 (m, 1 H), 3.08-3.23 (m, 2 H), 2.22-2.31 (m, 1 H), 1.90-2.04 (m, 1 H), 1.69-1.77 (m, 1 H), 1.39 (s, 9 H), 1.07 (s, 9 H), 1.02 (d, J = 6.1 Hz, 3 H), 0.93 (d, J = 6.7 Hz, 3 H), 0.91 (d, J = 6.7 Hz, 3 H).
^{13}C NMR (100 MHz, d^6-DMSO): δ 169.38, 168.70, 166.19, 155.10, 143.14, 132.94, 126.30, 121.46, 78.28, 73.41, 67.67, 58.95, 55.48, 53.30, 42.62, 34.90, 31.35, 28.09, 28.00, 19.66, 19.59, 19.20.
HRMS (ESI): *m/z* calcd for $C_{26}H_{44}O_6N_4H^+$ $[M + H]^+$ 509.3334, found 509.3332.

Synthesis of Dodeca-2*E*,4*E*-dienoic acid [2*R*-hydroxy-1*S*-(5*S*-isopropyl-2,7-dioxo-1,6-diaza-cyclododeca-3*E*,9*E*-dien-8*S*-ylcarbamoyl)-propyl]-amide, 114 (SylA-GlbA):

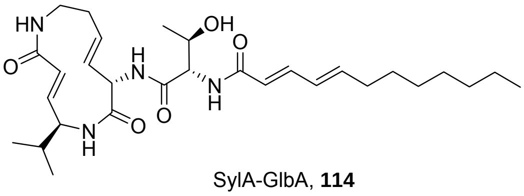

SylA-GlbA, **114**

In a 10 mL flask was dissolved **113** (14 mg, 27 µmol, 1 eq.) in a mixture of trifluoroacetic acid in dichloromethane (1:4, 1 mL). After 30 minutes, the mixture was concentrated to dryness and used in the next reaction without further purification (TLC (2% triethylamine + 15% methanol in dichloromethane): $R_f = 0.27$; HPLC (gradient 2): $t_R = 1.85$ min; HRMS (ESI): *m/z* calcd for $C_{17}H_{28}O_4N_4H^+$ $[M + H]^+$ 353.2183, found 353.2184).

The crude ammonium salts were dissolved in dichloromethane (1.5 mL) and acid **112** (7 mg, 33 µmol, 1.2 eq.), PyBop (22 mg, 41 µmol, 1.5 eq.), HOAt (6 mg, 41 µmol, 1.5 eq.) and *N*,*N*-diisopropylethylamine (20 µL, 110 µmol, 4 eq.) were added successively. The reaction was stirred overnight at room temperature. After concentration to dryness, the crude product was purified by preparative HPLC (0min/15%B → 10min/15%B → 30min/40%B → 50min/60%B → 60min/100%B → 80min/100%B) to yield **114**.

Yield: 3.55 mg (6.7 µmol, 25%) as a colorless solid.
TLC (2% acetic acid + 10% methanol in dichloromethane)**:** $R_f = 0.39$.
HPLC (gradient 2): $t_R = 9.30$ min.
^{1}H NMR (400 MHz, d^6-DMSO): δ 8.09 (d, J = 8.9 Hz, 1 H), 7.90 (d, J = 7.1 Hz, 1 H), 7.88 (d, J = 8.5 Hz, 1 H), 7.45 (t, J = 6.9 Hz, 1 H), 6.99 (dd, J = 15.0, 10.4 Hz, 1 H), 6.68 (dd, J = 15.4, 5.3 Hz, 1 H), 6.04-6.22 (m, 4 H), 5.59 (dt, J = 15.5, 7.6 Hz, 1 H), 5.43 (dd, J = 15.9, 7.4 Hz, 1 H), 4.89 (dd, J = 7.3, 7.3 Hz, 1 H), 4.35 (dd, J = 8.7, 4.3 Hz, 1 H), 4.04-4.11 (m, 1 H), 3.93-4.00 (m, 1 H), 3.09-3.25 (m, 2 H), 2.23-2.32 (m, 1 H), 2.09-2.16 (m, 2 H), 1.93-2.03 (m, 1 H), 1.68-1.78 (m, 1 H), 1.33-1.42 (m, 2 H), 1.22-1.30 (m, 8 H), 1.03 (d, J = 6.3 Hz, 3 H), 0.94 (d, J = 6.7 Hz, 3 H), 0.91 (d, J = 6.7 Hz, 3 H), 0.86 (t, J = 6.9 Hz, 3 H).
^{13}C NMR (150 MHz, d^6-DMSO): δ 169.70, 169.02, 166.32, 165.45, 143.27, 142.06, 139.70, 133.22, 128.56, 126.10, 123.08, 121.52, 66.82, 57.90, 55.56, 53.59, 42.58, 35.00, 32.23, 31.50, 31.21, 28.53, 28.48, 28.35, 22.06, 19.82, 19.75, 19.25, 13.95.
HRMS (ESI): *m/z* calcd for $C_{29}H_{46}O_5N_4H^+$ $[M + H]^+$ 531.3541, found 531.3535.

Synthesis of compound 122:

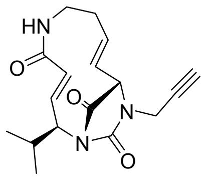

122

MRL **61** (15 mg, 54 µmol, 1 eq.) was dissolved in acetone (3.0 mL) in a 10 mL flame-dried flask. Then, K_2CO_3 (37 mg, 270 µmol, 5 eq.) and apropargyl bromide solution (80% in toluene, 32 µL, 324 µmol, 6 eq.) were added. The reaction was refluxed at

50 °C overnight and then quenched with a saturated aq. NH_4Cl solution. The mixture was extracted once with a mixture methanol/dichloromethane (1:20) and the combined organic layers were dried over Na_2SO_4. After filtration and concentration to dryness the crude product was purified by flash column chromatography (4% methanol in dichloromethane) and further re-crystalization in acetone yielded to **122**.

Yield: 14 mg (44 µmol, 82%) as colorless crystals.
TLC (10% methanol in dichloromethane)**:** $R_f = 0.81$.
HPLC (gradient 2): $t_R = 7.09$ min.
^{1}H NMR (500 MHz, d^6-DMSO): δ 7.41 (br s, 1 H), 6.73 (dd, J = 15.0, 4.1 Hz, 1 H), 5.99 (d, J = 15.0 Hz, 1 H), 5.22-5.39 (m, 2 H), 4.70 (br s, 1 H), 4.39 (dd, J = 18.0, 1.8 Hz, 1 H), 3.97 (d, J = 17.9 Hz, 1 H), 3.85-3.93 (m, 1 H), 3.34 (t, J = 2.4 Hz, 1 H), 3.26-3.33 (m, 1 H), 3.09-3.18 (m, 1 H), 2.29-2.40 (m, 1 H), 2.17-2.28 (m, 1 H), 1.92-2.04 (m, 1 H), 0.97 (d, J = 6.7 Hz, 3 H), 0.91 (d, J = 5.7 Hz, 3 H).
^{13}C NMR (125 MHz, d^6-DMSO): δ 166.76, 165.78, 155.98, 140.84, 131.27, 124.25, 120.55, 78.08, 75.49, 59.48, 58.02, 40.81, 34.64, 30.58, 30.26, 19.69, 19.28.
HRMS (ESI): *m/z* calcd for $C_{17}H_{21}O_3N_3H^+$ $[M + H]^+$ 316.1656, found 316.1657.

Synthesis of Toluene-4-sulfonic acid 5-*tert*-butoxycarbonylamino-pentyl ester, 134:

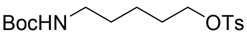

134

5-(Boc-amino)-1-pentanol **115** (509 µL, 2.5 mmol, 1 eq.) was dissolved in dichloromethane (5.0 mL) in a 25 mL flask. Then, triethylamine (520 µL, 3.75 mmol, 1.5 eq.) and a tosyl chloride solution (1 M in dichloromethane, 2.5 mL, 2.5 mmol, 1 eq.) were added slowly at 0 °C. The reaction was further stirred for 1 hour at room temperature and diethyl ether (10 mL) was added to the mixture. After filtration and concentration to dryness the crude product was purified by flash column chromatography (30% ethyl acetate in cyclohexane) to yield **134**.

Yield: 636 mg (1.78 mmol, 71%) as a colorless oil.

TLC (20% ethyl acetate in cyclohexane)**:** $R_f = 0.15$.

HPLC (gradient 2): $t_R = 10.55$ min.

^{1}H NMR (400 MHz, $CDCl_3$): δ 7.78 (d, J = 8.3 Hz, 2 H), 7.34 (dd, J = 8.6, 0.7 Hz, 2 H), 4.50 (br s, 1 H), 4.01 (t, J = 6.4 Hz, 2 H), 3.05 (t, J = 6.8 Hz, 2 H), 2.44 (s, 3 H), 1.61-1.69 (m, 2 H), 1.43 (s, 9 H), 1.38-1.44 (m, 2 H), 1.29-1.37 (m, 2 H).

^{13}C NMR (100 MHz, $CDCl_3$): δ 156.06, 144.79, 133.24, 129.91, 127.95, 79.28, 70.40, 40.33, 29.51, 28.57, 28.48, 22.74, 21.70.

HRMS (ESI): *m/z* calcd for $C_{17}H_{27}O_5NSH^+$ $[M + H]^+$ 358.1683, found 358.1682.

Synthesis of (5-Azido-pentyl)-carbamic acid *tert*-butyl ester, 116:

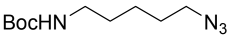

116

134 (200 mg, 560 µmol, 1 eq.) was dissolved in anhydrous *N*,*N*-dimethylformamide (25 mL) in a 50 mL flask and sodium azide (91 mg, 1.40 mmol, 2.5 eq.) was then added. After flushing the flask with argon, the reaction was lowered into an oil bath preheated to 65-68 °C and further stirred for 6 hours. At room temperature, the mixture was diluted with water (20 mL), further stirred for 30 minutes and poured in an Erlenmeyer flask containing ~ 20 mL of ice. The mixture was then extracted with diethyl ether (3 × 15 mL), the combined organic layers were washed with water (2 ×10 mL) and dried over Na_2SO_4. After filtration and concentration to dryness at room temperature, **116** was obtained. The product was pure enough to be used in the next step without further purification.

Yield: 114 mg (498 µmol, 89%) as a colorless oil.

HPLC (gradient 2): $t_R = 10.06$ min.

^{1}H NMR (400 MHz, $CDCl_3$): δ 4.53 (br s, 1 H), 3.26 (t, J = 6.9 Hz, 2 H), 3.10 (t, J = 6.9 Hz, 2 H), 1.56-1.64 (m, 2 H), 1.44-1.53 (m, 2 H), 1.43 (s, 9 H), 1.34-1.43 (m, 2 H).

^{13}C NMR (100 MHz, $CDCl_3$): δ 156.06, 79.27, 51.39, 40.49, 29.75, 28.59, 28.48, 24.01.

HRMS (ESI): *m/z* calcd for $C_{10}H_{20}O_2N_4H^+$ $[M + H]^+$ 229.1659, found 229.1660.

Synthesis of 5-Azido-pentylamine hydrochloride, 117:

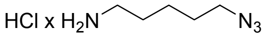

117

116 (114 mg, 498 µmol, 1 eq.) was dissolved in a hydrogen chloride solution (4 M in dioxane, 2.0 mL) and the reaction mixture was stirred for 90 minutes. After bubbling argon for 30 minutes, the solvent was evaporated at room temperature and the residual oil was lyophilized under high-vacuum to afford **117**. The product was pure enough to be used in the next step without further purification.

Yield: 80 mg (485 µmol, 97%) as a colorless solid.
HPLC (gradient 2): $t_R = 1.87$ min.
^{1}H NMR (400 MHz, CD_3OD): δ 3.34 (t, J = 6.7 Hz, 2 H), 2.94 (t, J = 7.6 Hz, 2 H), 1.60-1.74 (m, 4 H), 1.44-1.52 (m, 2 H).
^{13}C NMR (100 MHz, CD_3OD): δ 52.15, 40.60, 29.37, 28.12, 24.68.
HRMS (ESI): *m/z* calcd for $C_5H_{12}N_4H^+$ $[M + H]^+$ 129.1135, found 129.1132.

Synthesis of Biotin-(5-azido-pentyl)-amide, 121:

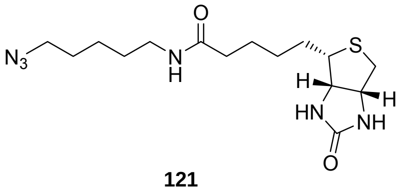

121

In a 10 mL flask, biotin **120** (40 mg, 164 µmol, 1 eq.), HATU (81 mg, 213 µmol, 1.3 eq.) and DMAP (6 mg, 49 µmol, 0.3 eq.) were dissolved in *N*,*N*-dimethylformamide (1 mL). The mixture was cooled to 0 °C and a solution of **117** (41 mg, 246 µmol, 1.5 eq.) and *N*,*N*-diisopropylethylamine (86 µL, 492 µmol, 3 eq.) in *N*,*N*-dimethylformamide (1 mL) was added. The reaction was stirred for 1 hour at room temperature and concentrated to dryness. The crude product was purified by flash column chromatography (8% methanol in dichloromethane) to afford **121**.

Yield: 48 mg (135 µmol, 82%) as a colorless solid.

TLC (10% methanol in dichloromethane)**:** $R_f = 0.34$.

HPLC (gradient 2): $t_R = 6.65$ min.

^{1}H NMR (400 MHz, $CD_3OD/CDCl_3$ = 1:1): δ 4.47 (dd, J = 7.8, 4.3 Hz, 1 H), 4.28 (dd, J = 7.9, 4.5 Hz, 1 H), 3.25 (t, J = 6.8 Hz, 2 H), 3.09-3.17 (m, 1 H), 2.89 (dd, J = 12.9, 5.0 Hz, 1 H), 2.70 (d, J = 12.8 Hz, 1 H), 2.16 (td, J = 7.2, 1.3 Hz, 2 H), 1.36-1.72 (m, 14 H).

^{13}C NMR (100 MHz, $CD_3OD/CDCl_3$ = 1:1): δ 175.21, 165.23, 62.87, 61.08, 56.51, 52.14, 41.12, 40.00, 36.61, 29.70, 29.32, 29.31, 29.01, 26.47, 24.88.

HRMS (ESI): *m/z* calcd for $C_{15}H_{26}O_2N_6SH^+$ $[M + H]^+$ 355.1911, found 355.1913.

Synthesis of Biot-MRL, 123:

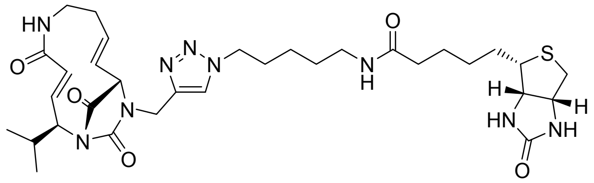

Biot-MRL, **123**

A catalyst solution was prepared by mixing $CuSO_4$ (4.0 mg, 15.8 μmol), ascorbic acid (11.1 mg, 63.2 μmol) and $NaHCO_3$ (5.3 mg, 63.2 μmol) in *tert*-butanol/water 2:1 (1 mL). In a 10 mL flask, **122** (5.0 mg, 15.8 μmol, 1 eq.) and **121** (6.2 mg, 17.4 μmol, 1.1 eq.) were dissolved in a mixture of *tert*-butanol/water 2:1 (3 mL) and ligand TBTA (0.8 mg, 1.6 μmol, 0.1 eq.) was added. To this mixture were then added 20 μL of the catalyst solution [$CuSO_4$ (0.02 eq.), ascorbic acid (0.08 eq.) and $NaHCO_3$ (0.08 eq.)]. The reaction was stirred overnight at room temperature. After concentration to dryness, the crude product was purified by preparative HPLC (0min/15%B → 10min/15%B → 30min/30%B → 50min/60%B → 60min/100%B → 80min/100%B) to yield **123** (Biot-MRL).

Yield: 10.0 mg (15.0 μmol, 95%) as a colorless solid.

TLC (15% methanol in dichloromethane)**:** $R_f = 0.20$.

HPLC (gradient 2): $t_R = 6.27$ min.

^{1}H NMR (400 MHz, d^6-DMSO): δ 8.11 (s, 1 H), 7.72 (t, J = 5.5 Hz, 1 H), 7.41 (br s, 1 H), 6.75 (dd, J = 15.4, 4.9 Hz, 1 H), 6.01 (d, J = 15.6 Hz, 1 H), 5.16-5.37 (m, 2 H), 4.88 (d, J = 15.7 Hz, 1 H), 4.57 (br s, 1 H), 4.28-4.33 (m, 3 H), 4.25 (d, J = 15.7 Hz, 1 H), 4.13 (dd, J = 7.8, 4.4 Hz, 1 H), 3.92 (br s, 1 H), 3.27-3.38 (m, 1 H), 3.06-3.18 (m, 2 H), 2.96-3.03 (m, 2 H), 2.82 (dd, J = 12.5, 5.1 Hz, 1 H), 2.57 (d, J = 12.4 Hz, 1 H), 2.28-2.38 (m, 1 H), 2.16-2.28 (m, 1 H), 2.03 (t, J = 7.4 Hz, 2 H), 1.91-2.03 (m, 1 H), 1.75-1.84 (m, 2 H), 1.55-1.66 (m, 1 H), 1.16-1.54 (m, 9 H), 0.97 (d, J = 6.7 Hz, 3 H), 0.90 (d, J = 6.1 Hz, 3 H).

HRMS (ESI): *m/z* calcd for $C_{32}H_{47}O_5N_9SH^+$ $[M + H]^+$ 670.3494, found 670.3490.

Synthesis of Rhodamine-(5-azido-pentyl)-amide, 119 (mixture of isomers):

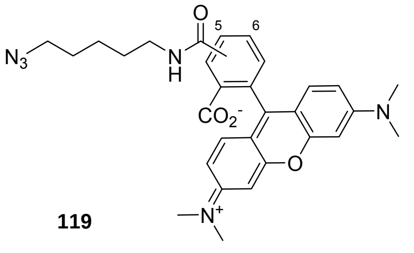

119

In a 10 mL flask, 5(6)-carboxytetramethylrhodamine *N*-succinimidyl ester **118** (25 mg, 47 µmol, 1 eq.) was dissolved in *N*,*N*-dimethylformamide (1 mL). The mixture was cooled to 0 °C and a solution of **117** (35 mg, 213 µmol, 4.5 eq.), DMAP (2 mg, 14 µmol, 0.3 eq.) and *N*,*N*-diisopropylethylamine (41 µL, 235 µmol, 5 eq.) in *N*,*N*-dimethylformamide (1 mL) was added. The reaction was stirred overnight at room temperature and concentrated to dryness. The crude product was purified by flash column chromatography (neutral alumina, 12% methanol in chloroform) to afford **119**.

Yield: 24 mg (5(6)-isomers mixture, 45 µmol, 96%) as a purple solid.

TLC (20% methanol in chloroform)**:** $R_f = 0.32$ and 0.42.

HPLC (gradient 2): $t_R = 7.17$ min.

^{1}H NMR (400 MHz, CD_3OD): δ 8.52 (br s, ½ H), 8.14 (d, J = 8.1 Hz, ½ H), 8.03-8.09 (m, 1 H), 7.72 (d, J = 1.3 Hz, ½ H), 7.37 (d, J = 7.9 Hz, ½ H), 7.24 (dd, J = 9.5, 2.2 Hz, 2 H), 7.01 (dt, J = 9.5, 2.6 Hz, 2 H), 6.90 (d, J = 2.3 Hz, 2 H), 3.47 (t, J = 7.0 Hz, 1 H), 3.38 (t, J = 7.3 Hz, 1 H), 3.27 (s, 12 H), 1.40-1.76 (m, 8 H).

HRMS (ESI): *m/z* calcd for $C_{30}H_{32}O_4N_6H^+$ $[M + H]^+$ 541.2558, found 541.2552.

Synthesis of Rh-MRL, 124 (mixture of isomers):

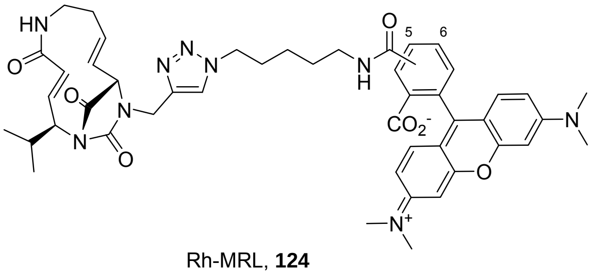

Rh-MRL, **124**

A catalyst solution was prepared by mixing $CuSO_4$ (4.0 mg, 15.8 µmol), ascorbic acid (11.1 mg, 63.2 µmol) and $NaHCO_3$ (5.3 mg, 63.2 µmol) in *tert*-butanol/water 2:1 (1 mL). In a 10 mL flask, **122** (5.0 mg, 15.8 µmol, 1 eq.) and **119** (9.4 mg, 17.4 µmol, 1.1 eq.) were dissolved in a mixture of *tert*-butanol/water 2:1 (3 mL) and ligand TBTA (0.8 mg, 1.6 µmol, 0.1 eq.) was added. To this mixture were then added 20 µL of the catalyst solution [$CuSO_4$ (0.02 eq.), ascorbic acid (0.08 eq.) and $NaHCO_3$ (0.08 eq.)]. The reaction was stirred overnight at room temperature. After concentration to dryness, the crude product was purified by preparative HPLC (0min/15%B → 10min/15%B → 30min/30%B → 50min/60%B → 60min/100%B → 80min/100%B) to yield **124** (Rh-MRL).

Yield: 10.2 mg (11.9 µmol, 75%) as a purple solid.

TLC (25% methanol in chloroform)**:** $R_f = 0.22$.

HPLC (gradient 2): $t_R = 6.87$ min.

^{1}H NMR (400 MHz, d^6-DMSO): δ 8.86 (t, J = 5.5 Hz, 1 H), 8.67 (d, J = 1.7 Hz, 1 H), 8.28 (dd, J = 7.9, 1.9 Hz, 1 H), 8.15 (s, 1 H), 7.57 (d, J = 8.0 Hz, 1 H), 7.41 (br s, 1 H), 7.03-7.11 (m, 4 H), 6.96-6.99 (m, 2 H), 6.74 (dd, J = 15.2, 4.6 Hz, 1 H), 6.00 (d, J = 15.6 Hz, 1 H), 5.16-5.36 (m, 2 H), 4.88 (d, J = 15.8 Hz, 1 H), 4.58 (br s, 1 H), 4.36 (t, J = 7.0 Hz, 2 H), 4.25 (d, J = 16.0 Hz, 1 H), 3.88-3.92 (m, 1 H), 3.29-3.35 (m, 3 H), 3.27 (s, 12 H), 3.08-3.17 (m, 1 H), 2.27-2.37 (m, 1 H), 2.16-2.26 (m, 1 H), 1.92-2.03 (m, 1 H), 1.79-1.91 (m, 2 H), 1.52-1.64 (m, 2 H), 1.27-1.37 (m, 2 H), 0.96 (d, J = 6.6 Hz, 3 H), 0.90 (d, J = 5.1 Hz, 3 H).

HRMS (ESI): *m/z* calcd for $C_{47}H_{53}O_7N_9H^+$ $[M + H]^+$ 856.4141, found 856.4142.

7. References and Notes

[1] (a) Pieterse, C. M. J.; Leon-Reyes, A.; van der Ent, S. and van Wees, S. C. M. *Nature Chem. Biol.* **2009**, *5*, 308–316; (b) Ma, W. W. and Adjei, A. A. *CA Cancer J. Clin.* **2009**, *59*, 111–133; (c) Whittleseya, K. J. and Shea, L. D. *Experiment. Neurol.* **2004**, *190*, 1–16; (d) MacRae, C. A. and Peterson, R. T. *Chem. Biol.* **2003**, *10*, 901–908; (e) Cho, C. H. and Nuttall, M. E. *Exp. Opin. Ther. Targ.* **2002**, *6*, 679–689.

[2] Kaiser**,** M.; Wetzel, S.; Kumar, K. and Waldmann, H. *Cell. Mol. Life Sci.* **2008**, *65*, 1186–1201.

[3] (a) Seifert, M. H. J. *Drug Discov. Tod.* **2009**, *14*, 562–569; (b) Andricopulo, A. D.; Salum, L. B. and Abraham, D. J. *Curr. Top. Med. Chem.* **2009**, *9*, 771–790; (c) de Kloe, G. E.; Bailey, D.; Leurs, R. and de Esch, I. J. P. *Drug Discov. Tod.* **2009**, *14*, 630–646.

[4] (a) Sieber, S. A.; Niessen, S.; Hoover, H. S. and Cravatt, B. F. *Nat. Chem. Biol.* **2006**, *2*, 274–281; (b) Adam, G. C.; Sorensen, E. J. and Cravatt, B. F. *Nature Biotech.* **2002**, *20***,** 805–809.

[5] Domagk, G. *Angew. Chem.* **1935**, *48*, 657–667.

[6] Newman, D.J.; Cragg, G.M. and Snader, K.M. *J. Nat. Prod.* **2003**, *66*, 1022–1037.

[7] Li, J. W.-H. and Vederas, J. C. *Science* **2009**, *325*, 161–165.

[8] Koehn, F. E. and Carter, G. T. *Nature* **2005**, *4*, 206–220.

[9] Simmons, T.L.; Andrianasolo, E.; McPhail, K.; Flatt, P. and Gerwick, W. H. *Mol. Cancer Ther.* **2005**, *4*, 333–342.

[10] Chin, Y.-W.; Balunas, M. J.; Chai, H. B. and Kinghorn, A. D. *Aaps* **2006**, *8*, 239–253.

[11] Kaschani, F. and van der Hoorn, R. A. L. *Curr. Opin. Chem. Biol.* **2007**, *11*, 88–98.

[12] Coux, O.; Tanaka, K. and Goldberg, A. L. *Annu. Rev. Biochem.* **1996**, *65*, 801–847.

[13] Baumeister, W.; Walz, J.; Zuhl, F. and Seemuller, E. *Cell* **1998**, *92*, 367–380.

[14] Groll, M.; Ditzel, L.; Löwe, J.; Stock, D.; Bochtler, M.; Bartunik, H. D. and Huber, R. *Nature*, **1997**, *386*, 463–471.

[15] Advanced information on the Nobel Prize in Chemistry, 6 October 2004.

[16] Murata, S.; Yashiroda, H. and Tanaka, K. *Nature Rev. Mol. Cell Biol.* **2009**, *10*, 104–115.

[17] Groll, M.; Berkers, C. R.; Ploegh, H. L. and Ovaa, H. *Structure* **2006**, *14*, 451–456.

[18] Honda, R.; Tanaka, H. and Yasuda, H. *FEBS Lett.* **1997**, *420*, 25–27.

[19] Scheffner, M.; Huibregtse, J. M.; Vierstra, R. D. and Howley, P. M. *Cell* **1993**, *75*, 495–505.

[20] Chen, Z.; Hagler, J.; Palombella, V. J.; Melandri, F.; Scherer, D.; Ballard, D. and Maniatis, T. *Genes Dev.* **1995**, *9*, 1586–1597.

[21] Goebl, M. G.; Yochem, J.; Jentsch, S.; McGrath, J. P.; Varshavsky, A. and Byers, B. *Science* **1988**, *241*, 1331–1335.

[22] Glotzer, M.; Murray, A. W. and Kirschner, M. W. *Nature* **1991**, *349*, 132–138.

[23] Nasmyth, K. *Annu. Rev. Genet.* **2001**, *35*, 673–745.

[24] Hershko, A. and Ciechanover, A. *Annu. Rev. Biochem.* **1998**, *67*, 425–479.

[25] Naujokat, C.; Fuchs, D. and Berges, C. *Biochim. Biophys. Acta* **2007**, *1773*, 1389–1397.

[26] Moore, B. S.; Eustquio, A. S. and McGlinchey, R. P. *Curr. Opin. Chem. Biol.* **2008**, *12*, 434–440.

[27] Sterz, J.; von Metzler, I.; Hahne, J.-C.; Lamottke, B.; Rademacher, J.; Heider, U.; Terpos, E. and Sezer, O. *Expert Opin. Invest. Drugs* **2008**, *17*, 879–895.

[28] Voorhees, P. M. and Orlowski, R. Z. *Annu. Rev. Pharmacol. Toxicol.* **2006**, *46*, 189–213.

[29] Kaiser, M.; Groll, M.; Siciliano, C.; Assfalg-Machleidt, I.; Weyher, E.; Kohno, J.; Milbradt, A. G.; Renner, C.; Huber, R. and Moroder, Luis *Chembiochem* **2004**, *5*, 1256–1266.

[30] Hines, J.; Groll, M.; Fahnestock, M. and Crews, C. M. *Chem. & Biol.* **2008**, *15*, 501–512.

[31] Nickeleit, I.; Zender, S.; Sasse, F.; Geffers, R.; Brandes, G.; Sörensen, I.; Steinmetz, H.; Kubicka, S.; Carlomagno, T.; Menche, D.; Gütgemann, I.; Buer, J.; Gossler, A.; Manns, M. P.; Kalesse, M.; Frank, R. and Malek, N. P. *Cancer Cell* **2008**, *14*, 23–35.

[32] Hassa, P.; Granado, J.; Freydl, E.; Wäspi, U. and Dudler, R. *MPMI* **2000**, *13*, 342–346.

[33] Wäspi, U.; Schweizer, P. and Dudler, R. *Plant Cell* **2001**, *13*, 153–161.

[34] Michel, K.; Abderhalden, O.; Bruggmann, R. and Dudler, R. *Plant Mol. Biol.* **2006**, *62*, 561–578.

[35] Coleman, C. S.; Rocetes, J. P.; Park, D. J.; Wallick, C. J.; Warn-Cramer, B. J.; Michel, K.; Dudler, R. and Bachmann, A. S. *Cell Prolif.* **2006**, *39*, 599–609.

[36] Groll, M.; Schellenberg, B.; Bachmann, A. S.; Archer, C. R.; Huber, R.; Powell, T. K.; Lindow, S.; Kaiser, M. and Dudler, R. *Nature* **2008**, *452*, 755–758.

[37] Schellenberg, B.; Bigler, L. and Dudler, R. *Environ. Microbiol.* **2007**, *9*, 1640–1650.

[38] Amrein, H.; Makart, S.; Granado, J.; Shakya, R.; Schneider-Pokorny, J. and Dudler, R. *Mol. Plant Microbe Interact.* **2004**, *17*, 90–97.

[39] Ramel, C.; Tobler, M.; Meyer, M.; Bigler, L.; Ebert, M. O.; Schellenberg, B. and Dudler, R. *BMC Biochem.* **2009**, *10*, 26–34.

[40] Imker, H. J.; Walsh, C. T. and Wuest, W. M. *J. Am. Chem. Soc.* **2009**, *131*, 18263–18265.

[41] Oka, M.; Nishiyama, Y.; Ohta, S.; Kamei, H.; Konishi, M.; Miyaki, T.; Oki, T. and Kawaguchi, H. *J. Antibiot. (Tokyo)* **1988**, *41*, 1331–1337.

[42] Gibson, S. E. and Lecci, C. *Angew. Chem.* **2006**, *118*, 1392–1405; *Angew. Chem. Int. Ed.* **2006**, *45*, 1364–1377.

[43] Driggers, E. M.; Hale, S. P.; Lee J. and Terrett, N. K. *Nature Rev.*, **2008**, *7*, 608–624.

[44] Wessjohann, L. A.; Ruijter, E.; Garcia-Rivera, D. and Brandt, W. *Mol. Diversity* **2005**, *9*, 171–186.

[45] Gradillas, A. and Perez-Castells, J. *Angew. Chem.* **2006**, *118*, 6232–6247; *Angew. Chem. Int. Ed.* **2006**, *45*, 6086–6101.

[46] Wessjohann, L. A. and Ruijter, E. *Mol. Divers.* **2005***,* *9*, 159–169.

[47] Gerbeleu, N. V. and Arion, V. B. in *Complex Formation and Stereochemistry of Coordination Compounds* (Ed.: Buslaev, Y.), Nova Science Publishers, New York, NY, USA, 1996, 133–204.

[48] Meutermans, W. D. F.; Bourne, G. T.; Golding, S. W.; Horton, D. A.; Campitelli, M. R.; Craik, D.; Scanlon, M. and Smythe, M. L. *Org. Lett.* **2003**, *5*, 2711–2714.

[49] Oka, M.; Yaginuma, K.; Numata, K.; Masataka, K. and Kawaguchi, H. *J. Antibiot. (Tokyo)* **1988**, *41*, 1338–1350.

[50] Schmidt, U.; Kleefeldt, A. and Mangold, R. *J. Chem. Soc., Chem. Commun.* **1992**, 1687–1689.

[51] Meng, Q. and Hesse, M. *Tetrahedron* **1991**, *41*, 6251–6264.

[52] Amrein, H.; Makart, S.; Granado, J.; Shakya, R.; Schneider-Pokorny, J. and Dudler, R. *Mol. Plant Microbe Interact.* **2004**, *17*, 90–97.

[53] Henkel, B; Zhang, L. and Bayer, E. *Liebigs Ann./Recueil* **1997**, 2161–2168.

[54] Majer, P. and Randad, R. S. *J. Org. Chem.* **1994**, *59*, 1937–1938.

[55] Shirota, O.; Nakanishi, K. and Berova, N. *Tetrahedron* **1999**, *55*, 13643–13658; Reginato, G.; Mordini, A.; Verrucci, M.; Degl'Innocenti, A. and Capperucci, A. *Tetrahedron: Asymmetry* **2000**, *11*, 3759–3768.

[56] Coleman, R. S. and Carpenter, A. J. *Tetrahedron Lett.* **1992**, *33*, 1697–1700.

[57] Johnson, W.S.; Werthemann, L.; Bartlett, W.R.; Brocksom, T.J.; Li, T.; Faulkner, D.J. and Petersen, M.R. *J. Am. Chem. Soc.* **1970**, *92*, 741–743.

[58] Trust, R. I. and Ireland, R. E. *Organic Synth. Coll. Vol. 6* **1988**, 606.

[59] De Kimpe, N.; Boeykens, M. and Tehrani, K. A. *J. Org. Chem.* **1994**, *59*, 8215–8219.

[60] Bal, B. S.; Childers, W. E. and Pinnick, H.W. *Tetrahedron* **1981**, *37*, 2091–2096.

[61] Just, G. and Grozinger, K. *Synthesis*, **1976**, 457–458.

[62] Fürstner, A. *Angew. Chem. Int. Ed.* **2000**, *39*, 3012–3043; Nicolaou, K. C.; Bulger, P. G. and Sarlah, D. *Angew. Chem. Int. Ed.* **2005**, *44*, 4490–4527.

[63] Berkowitz, D. B. and Smith, M. K. *Synthesis* **1996**, 39–41.

[64] Bartley, D. M. and Coward, J. K. *J. Org. Chem.* **2005**, *70*, 6757–6774.

[65] Dee, M. F. and Rosati, R. L. *Bioorg. Med. Chem. Lett.* **1995**, *5*, 949–952.

[66] Sakaitani, M. and Ohfune, Y. *J. Org. Chem.* **1990**, *55*, 870–876.

[67] Corey, E. J. and Winter, R. A. E. *J. Am. Chem. Soc.* **1963**, *85*, 2677–2678.

[68] Node, M.; Nishide, K.; Sai, M.; Fuji, K. and Fujita, E. *J. Org. Chem.* **1981**, *46*, 1991–1993.

[69] (a) Dressel, J.; Chasey, K. L. and Paquette, L. A. *J. Am. Chem. Soc.* **1988**, *110*, 5479–5489; (b) Tsuda, Y.; Sato, Y.; Kakimoto, K. and Kanemitsu, K. *Chem. Pharm. Bull.* **1992**, *40*, 1033–1036.

[70] Wadsworth, W. S., Jr. Organic Reactions (Hoboken, NJ, United States) **1977**, *25* Publisher: John Wiley & Sons, Inc.; (b) Waszkuć, W. and Janecki, T. *Org. Biomol. Chem.* **2003**, *1*, 2966–2972.

[71] (a) Bagley, M. C.; Davis, T.; Dix, M. C.; Widdowson, C. S. and Kipling, D. *Org. Biomol. Chem.* **2006**, *4*, 4158–4164; (b) Azad, S.; Kumamoto, K.; Uegaki, K.; Ichikawa, Y. and Kotsuki, H. *Tetrahedron Lett.* **2006**, *47*, 587–590.

[72] (a) Milne, H. B. and Kilday, W. D. *J. Org. Chem.* **1965**, *30*, 67–71; (b) Boeijen, A.; Kruijtzer, J. A. W. and Liskamp, R. M. J. *Bioorg. Med. Chem. Lett.* **1998**, *8*, 2375–2380.

[73] (a) Bigot, A.; Dau, M. E. T. H, and Zhu, J. *J. Org. Chem.* **1999**, *64*, 6283–6296; (b) Du, Y.; Creighton, C. J.; Yan, Z.; Gauthier, D. A.; Dahl, J. P.; Zhao, B.; Belkowski, S. M. and Reitz, A. B. *Bioorg. Med. Chem.* **2005**, *13*, 5936–5948.

[74] Weistheimer, F. H.; Huang, S. and Covitz, F. *J. Am. Chem. Soc.* **1988**, *110*, 181–185.

[75] Wäspi, U.; Blanc, D.; Winkler, T.; Rüedi, P. and Dudler, R. *MPMI* **1998**, *11*, 727–733.

[76] a) Bogyo, M. *Methods Enzymol.* **2005**, *399*, 609–622; b) Bogyo, M.; Shin, S.; McMaster, J. S. and Ploegh, H. L. *Chem. Biol.* **1998**, *5*, 307–320; c) Nazif, T. and Bogyo, M. *Proc. Natl. Acad. Sci. USA* **2001**, *98*, 2967–2972; d) Verdoes, M.; Florea, B. I.; Menendez-Benito, V.; Maynard, C. J.; Witte, M. D.; van der Linden, W. A.; van den Nieuwendijk, A. M. C. H.; Hofmann, T.; Berkers, C. R.; van Leeuwen, F. W. B.; Groothuis, T. A.; Leeuwenburg, M. A.; Ovaa, H.; Neefjes, J. J.; Filippov, D. V.; van der Marel, G. A.; Dantuma, N. P. and Overkleeft, H. S. *Chem. Biol.* **2006**, *13*, 1217–1226; e) Verdoes, M.; Hillaert, U.; Florea, B. I.; Sae-Heng, M.; Risseeuw, M. D.; Filippov, D. V.; van der Marel, G. A. and Overkleeft, H. S. *Bioorg. Med. Chem. Lett.* **2007**, *17*, 6169–6171.

[77] Speers, A. E.; Adam, G. C. and Cravatt, B. F. *J. Am. Chem. Soc.* **2003**, *125*, 4686–4687.

[78] a) Berkers, C. R.; Verdoes, M.; Lichtman, E.; Fiebiger, E.; Kessler, B. M.; Anderson, K. C.; Ploegh, H. L.; Ovaa, H. and Galardy, P. J. *Nat. Methods* **2005**, *2*, 357–362; b) Groll, M.; Berkers, C. R.; Ploegh, H. L. and Ovaa, H. *Structure* **2006**, *14*, 451–456.

[79] Groll, M.; Schellenberg, B.; Bachmann, A. S.; Archer, C. R.; Huber, R.; Powell, T. K.; Lindow, S.; Kaiser, M. and Dudler, R. *Nature* **2008**, *452*, 755–758.

[80] a) Hamidi, M.; Azadi, A. and Rafiei, P. *Drug Delivery* **2006**, *13*, 399–409; b) Greenwald, R. B.; Choe, Y. H.; McGuire, J. and Conover, C. D. *Adv. Drug Deliv. Rev.* **2003**, *55*, 217–250; c) Veronese, F. M. and Mero, A. *Biodrugs* **2008**, *22*, 315–329.

[81] Neumayer, D. A.; Belot, J. A.; Feezel, R. L.; Reedy, C.; Stern, C. L. and Marks, T. J. *Inorg. Chem*. **1998**, *37*, 5625–5633.

[82] Zhang, L.; Wu, Y. and Brunsveld, L. *Angew. Chem. Int. Ed.* **2007**, *46*, 1798–1802.

[83] Wang, Y.; Ma, J.; Cheon, H.-S. and Kishi, Y. *Angew. Chem. Int. Ed.* **2007**, *46*, 1333–1336.

[84] Speers, A. E.; Adam, G. C. and Cravatt, B. F. *J. Am. Chem. Soc.* **2003**, *125*, 4686–4687.

[85] Dieltiens, N.; Claeys, D. D. and Stevens, C. V. *J. Org. Chem.* **2006**, *71*, 3863–3868.

[86] Chan, T. R.; Hilgraf, R.; Sharpless, K. B. and Fokin, V. V. *Org. Lett.* **2004**, *6*, 2853–2855.

[87] Kaschani, F.; Gu, C.; Niessen, S.; Hoover, H.; Cravatt, B. F. and van der Hoorn, R. A. L. *Mol. Cell. Proteomics* **2009**, *8*, 1082–1093.

[88] Martin, M. and Schnarrenberger, C. *Curr. Genet.* **1997**, *32*, 1–18.

[89] Rius, S. P.; Casati, P.; Iglesias, A. A. and Gomez-Casati, D. F. *Plant Physiol.* **2008**, *148*, 1655–1667.

[90] (a) Foxall, D. L.; Brindle, K. M.; Campbell, I. D. and Simpson, R. J. *Biochim. Biophys. Acta* **1984**, *804*, 209–215; (b) Kim, H.; Deng, L.; Xiong, X.; Hunter, W. D.; Long, M. C. and Pirrung, M. C. *J. Med. Chem.* **2007**, *50*, 3423–3426.

[91] (a) Aronov, A. M.; Suresh, S.; Buckner, F. S.; Van Voorhis, W. C.; Verlinde, C. L. M. J., Opperdoes, F. R.; Hol, W. G. J. and Gelb, M. H. *Proc. Natl. Acad. Sci. USA* **1999**, *96*, 4273–4278; (b) Guido, R. V. C.; Oliva, G.; Montanari, C. A. and Andricopulo, A. D. *J. Chem. Inf. Model.* **2008**, *48*, 918–929; (c) Freitas, R. F.; Prokopczyk, I. M.; Zottis, A.; Oliva, G.; Andricopulo, A. D.; Trevisan, M. T. S.; Vilegas, W.; Silva, M. G. V. and Montanari, C. A. *Bioorg. Med. Chem.* **2009**, *17*, 2476–2482.

8. Abbreviations

Å	Ångström
Ac	Acetyl-
aq.	aqueous
Boc	*tert*-Butoxycarbonyl-
BuLi	Butyllithium
calcd	calculated
Cbz	Benzyloxycarbonyl-
Conv.	Conversion
COSY	Correlation spectroscopy
Da	Dalton
DCM	Dichloromethane
DIBAL-H	Diisobutylaluminium hydride
DIEA	*N*,*N*-Diisopropylethylamine
DMAP	4-(Dimethylamino)pyridine
DMF	*N*,*N*-Dimethylformamide
DMP	Dess-Martin Periodinane
DMSO	Dimethylsulfoxide
DPPA	Diphenylphosphorylazide
eq.	equivalent
ESI	Electron-spray ionization
Et	Ethyl-
Fm	9-Fluorenylmethyl-
HATU	*O*-(7-Azabenzotriazol-1-yl)-*N,N,N',N'*-tetramethyluronium hexafluorophosphate
HMBC	Heteronuclear multiple bond coherence
HPLC	High performance liquid chromatography
HOAt	1-Hydroxy-7-azabenzotriazole
HRMS	High resolution mass spectrometry
HSQC	Heteronuclear single quantum coherence
K_i’	Apparent constant of inhibition
LC-MS	Liquid chromatography – mass spectroscopy
M	mol/l
Me	Methyl-
MS	Mass spectroscopy
MW	Microwaves
N	normal
NMR	Nuclear magnetic resonance
PG	Protective group
Ph	Phenyl-
ppm	Parts per million
PPTS	Pyridinium *p*-toluenesulfonate
p-TSOH	*p*-toluenesulfonic acid
PyBop	(Benzotriazol-1-yl-oxy)-tripyrrolidinophosphonium hexafluorophosphate
n.a.	Not analyzed
n.d.	Not determined
®	Registered trademark
RCM	Ring closing metathesis
Rctn.	Reaction
R_f	Retension factor
rt	Room temperature
TBTA	Tris-[(1-benzyl-1H-1,2,3-triazol-4-yl) methyl]
*t*Bu	*tert*-Butyl-
TFA	Trifluoroacetic acid
THF	Tetrahydrofurane
TLC	Thin layer chromatography
TMSOTf	Trimethylsilyl trifluoromethansulfonate
TOCSY	Total correlation spectroscopy
Tol	Toluene
t_R	Retention time
Troc	2,2,2-trichloro ethoxycarbonyl-
Ts	*para*-toluene sulfonyl-
UV	Ultraviolet
wt	Wild type

9. Curriculum Vitae

Personal Data

Name	Jérôme Clerc
Date of birth	November 2, 1981
Place of birth	Rueil-Malmaison, France
Citizenship	French

Education background

10/2005-till present	**Doctoral work** under the supervision of **Prof. Dr. Herbert Waldmann** and **Dr. Markus Kaiser**, Chemical Genomics centre of the Max Planck Society, Dortmund, Germany "Synthetic and Structure-Activity Studies of the 20S Proteasome Inhibitor Syringolin A"
10/2004-06/2005	"**DEA de Chimie Organique Moléculaire et Supramoléculaire**" (equivalent to MSc) with honors in chemistry, Université Louis Pasteur, Strasbourg, France
10/2003-06/2004	"**Maitrise de Chimie**" (equivalent to MSc) with honors in chemistry, Faculté des Sciences et Techniques St Jérôme, Université Aix-Marseille III, France
10/2002-06/2003	"**Licence de Chimie**" (equivalent to BSc) with honors in chemistry, Faculté des Sciences et Techniques St Jérôme, Université Aix-Marseille III, France
09/2000-06/2002	"**DUT de Chimie**" (two-years university diploma) with honors in chemistry, Institut Universitaire de Technologie Paul Sabatier, Toulouse, France
2000	"**Baccalauréat**" (french A-levels school diploma) with honors in mathematics, physics and chemistry, Lycée Pierre d'Aragon, Muret, France

Scientific and industrial engagements	
10/2004-06/2005	Internship at the University Louis Pasteur, Strasbourg, France, under the supervision of **Dr. Frédéric Leroux** and in collaboration with **Lonza AG**. “Synthesis of new biaryl ligands for amination and Suzuki cross-coupling”
07/2004-09/2004	Voluntary internship at **BASF AG** at the Stabiliser and Inhibitor Department, Ludwigshafen, Germany, under the supervision of **Dr. Frank Hoefer**. “Development and test of new furan derivatives for polymers stabilization applications”
04/2004-06/2004	Internship at the University of Glasgow, Scotland, under the supervision of **Prof. Dr. David J. Procter**. “Samarium(II)-mediated cyclization reactions of γ,δ–unsaturated ketones”
07/2003-09/2003	Voluntary internship at **Bayer CropScience AG** at the Fungicides Research Department, Monheim, Germany, under the supervision of **Dr. Oliver Guth**. “Palladium-catalysed synthesis of heterocyclic active molecules using parallel synthetic method
04/2002-06/2002	Internship at the University St Jérôme, Marseille, France under the supervision of **Dr. Jacques Viala**. “Pauson-Khand reaction with acetylenic molecules”
Visited conferences	EMBL Conference on Chemical Biology, 8-11 October 2008, Heidelberg, Germany (with poster presentation)
	Eighth Tetrahedron Symposium, Challenges in Organic Chemistry, 26-29 June 2007, Berlin, Germany

10. List of publications and patents

10.1. *Publications*

1. Clerc, J.; Groll, M.; Illich, D. J.; Bachmann, A. S.; Huber, R.; Schellenberg, B.; Dudler, R. and Kaiser, M. “Synthetic and structural studies on Syringolin A and B reveal critical determinants of selectivity and potency of proteasome inhibition”. *Proceedings of the National Academy of Sciences of the United States of America* (*PNAS*), **2009**, *106*, 6507-6512.

2. Clerc, J.; Florea, B. I.; Kraus, M.; Groll, M.; Huber, R.; Bachmann, A. S.; Dudler, R.; Driessen, C.; Overkleeft, H. S.; Kaiser, M. “Syringolin A selectively labels the 20S proteasome in murine EL4 and wild-type and bortezomib-adapted leukaemic cell lines”. *Chembiochem*, **2009**, *10*, 2638-2643.

3. Archer, C. R.; Koomoa, D. L.; Mitsunaga, E. M.; Clerc, J.; Shimizu, M.; Kaiser, M.; Schellenberg, B.; Dulder, R. and Bachmann, A. “Syrbactin class proteasome inhibitor-induced apoptosis and autophagy occurs in association with p53 accumulation and Akt/PKB activation in neuroblastoma”. *Biochemical Pharmacology*, **2010**, in press.

4. Clerc, J.; Schellenberg, B.; Groll, M.; Bachmann, A. S.; Huber, R.; Dudler, R. and Kaiser, M. “Convergent synthesis and biological evaluation of syringolin A and derivatives as eukaryotic 20S proteasome inhibitors”. *European Journal of Organic Chemistry*, **2010**, in press.

10.2. *Patents*

1. Kaiser, M. and Clerc, J. (2008). Development of a synthesis of syringolin A and B and derivatives thereof. US 61/129,865.

2. Kaiser, M. and Clerc, J. (2009). Derivatives of syringolin A. EP09075018.3-2117.

11. Acknowledgements

I would like to express my sincerest thanks to the following people whose valuable assistance made possible the conclusion of this PhD work.

First I would like to thank my supervisor Prof. Herbert Waldmann for giving me the chance to work at the Chemical Genomics Centre on this fascinating project and for his constructive guidance.

My thanks also go to my direct supervisor Dr. Markus Kaiser. Interesting discussions, remarkable project vision and pleasant guidance have been my daily life during this work in his lab.

Special thanks go to the Kaiser group. Patrick, Rama, Zhe Ming, Timon, Philipp, Sabrina, Sara, Daniel and Julian; all contributed somehow to the accomplishment of this work.

I would like to thank also the Waldmann department, a fantastic team to perform great Science. A special attention goes to Frau Rose who achieves a talented organization of the administrative tasks.

I would like also to express my gratitude to the group of Renier van der Hoorn at the Max-Planck Institute for Plant Breading Research in Cologne. There, the invaluable help of Johana Misas and Izabella Kolodziejek contributed to introduce me to plant biology and fruitful discussions were also generously generated.

To finally thank all our collaborators, I would like to address many thanks to Prof. Robert Dudler and Barbara Schellenberg at the University of Zurich for the brilliant discussions and their work on the biological evaluation of my synthetic compounds in plant; Prof. Michael Groll and Prof. Robert Huber at the Technische Universität München for the co-crystallization experiments; and Dr. André Bachmann at the University of Hawaii and the groups of Prof. Overkleeft (University of Leiden) and Prof. Driessen (University of Tübingen) for the cell-based assays.

Also, I thank Damir Illich, who worked under my guidance for two months. Excellent discussions and a friendly collaboration rose up to establish the total synthesis of SylB and external accomplishments.

I would like to sincerely thank my good friends Dr. Robin Bon and Jorunn De Bruyn for their incomparable support and for being always here to motivate me.

My deepest gratitude goes to my family. *Je tiens à remercier toute ma famille et plus particulièrement mes parents, Elyane Clerc et Jean-Philippe Clerc, ainsi que ma sœur Mélanie, pour avoir toujours su me laisser faire mes propres choix et me donner la chance réaliser mes rêves. Je les remercie tous du fond du cœur pour leur soutien durant toutes ces années.*

Finally, I would like to express my greatest gratitude to my fiancée Marlene Krieg. You have given me the heart, the love and so much more to succeed in my work.